DECATIONIZED POLYPLEXES FOR TARGETED DELIVERY OF NUCLEIC ACIDS

from carrier design to *in vivo* evaluation

ISBN 978-90-393-6220-4

Cover design by Luís Novo.

Decationized polyplexes for targeted delivery of nucleic acids: from carrier design to *in vivo* evaluation

Gedekationiseerde polyplexen voor de gerichte afgifte van nucleïnezuren aan cellen: van ontwerp naar in vivo evaluatie

(met een samenvatting in het Nederlands)

Proefschrift

ter verkrijging van de graad van doctor aan de Universiteit Utrecht op gezag van de rector magnificus, prof. dr. G.J. van der Zwaan, ingevolge het besluit van het college voor promoties in het openbaar te verdedigen op maandag 20 oktober 2014 des middags te 2.30 uur

door

Luís Filipe Lima Novo

geboren op 16 mei 1985, te Viana do Castelo, Portugal

Promotor:	Prof. dr. Ir. W.E. Hennink
Copromotoren:	Dr. C.F. van Nostrum
	Dr. E. Mastrobattista

This thesis was (partly) accomplished with financial support from Fundação para a Ciência e a Tecnologia (FCT), the Portuguese Foundation for Science and Technology, grant SFRH/BD/47085/2008.

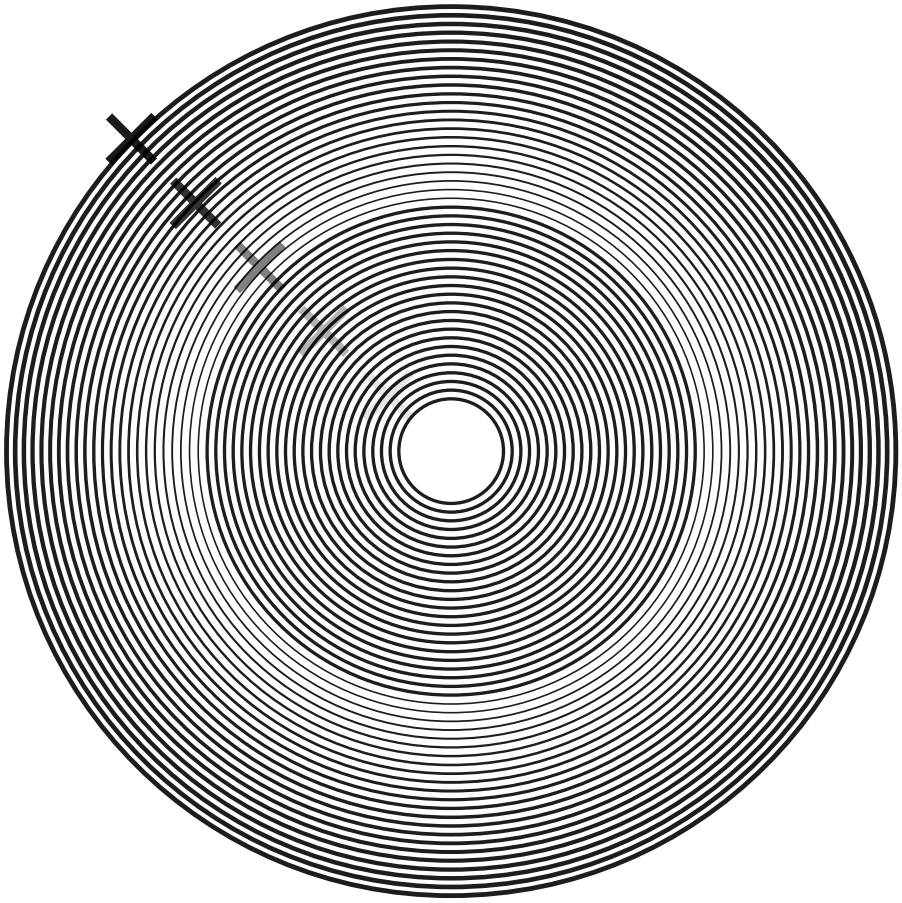

CONTENTS

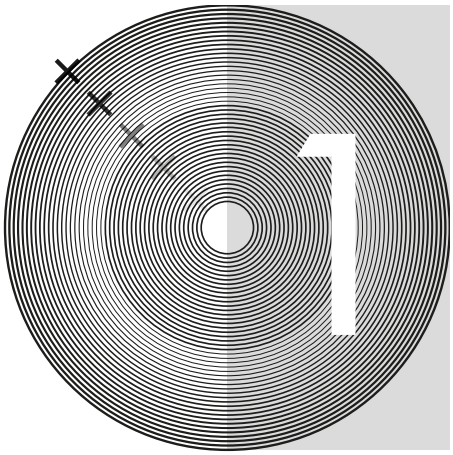

CHAPTER 1

General introduction

INTRODUCTION

1. Gene therapy

Gene therapy can be defined as the introduction of genetic material into target cells to obtain a therapeutic effect [1] by regulating, repairing, replacing, adding or deleting a genetic sequence [2]. Gene therapy aims to target specific activity at the transcriptional level with DNA by inducing gene expression or at the translational level with small interfering RNA (siRNA) by downregulating gene expression.

2. Applications

Gene therapy is considered a potential modality to treat or prevent intractable diseases with a genetic basis such as genetic disorders, degenerative diseases, infections, and cancer. Up to 2012, most of the clinical trials in gene therapy were focused on cancer treatment (around 64%). The applications aimed for treatment of several forms of cancer with expression of tumor-suppressor genes, immunotherapy or gene-directed enzyme pro-drug therapy (GDEPT). Following cancer treatment, monogenic disorders (e.g. cystic fibrosis, severe combined immunodeficiency (SCID)) were the second most prominent targets of gene therapy in clinical trials (9% of the trials). Cardiovascular gene therapy was the third most popular application for gene therapy (8% of the trials), aiming for therapeutic angiogenesis, myocardial protection, regeneration and repair. Gene therapy has also been studied for the treatment of infectious diseases (eg. HIV/AIDS), neurological diseases (e.g. Parkinson, Alzheimer, multiple sclerosis), rheumatoid arthritis, diabetes and as adjuvant therapy for organ transplantations [3, 4]. Another potential application of gene therapy is its use in tissue engineering and regenerative medicine [5].

3. Nucleic Acid Therapies

3.1. DNA-based therapies

DNA-based therapies generally use plasmid DNA (pDNA). pDNAs are produced in *Escherichia coli* cultures and consist of thousands of base pairs (~5000 bp). The aim of using pDNA as drug is to have it translated into therapeutic proteins, meaning that pDNA must be delivered into the nucleus of the target cell [6].

Such requirement is particularly problematic for treatment of slow or nondividing because disintegration of the nuclear membrane occurs only during cell division. pDNA contains all the required genetic sequences for plasmid production by replication in a prokaryotic cells and for the transcription of the therapeutic gene in eukaryotic cells. One of the great advantages of pDNA is that they can be easily engineered to include specific expression cassettes. For example, promoters, i.e. sequence where RNA polymerase II starts transcription, can be chosen for selective transcription in tissues or different cancer cell types. Other promoters allow on-demand transcription upon external stimuli, e.g. induction of hyperthermia (39-43 ºC) to achieve spatiotemporal controllable expression [7]. pDNA can be further engineered to be less immunogenic (e.g. by depletion of immunostimulatory CpG motifs that frequently occur in bacterial DNA [8]) and to possess long-term expression even when delivered via non-viral vectors [9].

As mentioned pDNA requires nuclear localization to be transcribed, which represents a serious hurdle to express a therapeutic protein in slow or nondividing cells. As alternative to pDNA, mRNA can be used for gene therapy purposes, especially for specific applications where from the therapeutic transient gene expression is sufficient, e.g. vaccination or immunotherapy. mRNA does not need to enter the nucleus to be translated into protein and can also be engineered, requiring more simple construct than pDNA and lacks bacterial sequences. However, in comparison to pDNA, mRNA is more susceptible for enzymatic degradation than pDNA [10, 11].

3.2. siRNA-based therapies

siRNA-based therapies use a synthetically prepared double-stranded RNA molecules of 21–23 bp long to induce (RNA interference) RNAi which inhibits target gene expression. The siRNA molecules bind to a multiprotein complex, located in the cytoplasm, to form a RNA-induced silencing complex (RISC). The complex formation results in degradation of mRNA complimentary to siRNA in the RISC. The use of siRNA, unlike pDNA, does not require nuclear delivery, and activated silencing can be observed for days in rapidly dividing cells and for weeks in nondividing cells [12, 13].

siRNA targets a single gene, which might not be sufficient for the treatment of a heterogenic disease such cancer, and therefore alternatively microRNA (miRNA)

can be used. miRNAs mechanism of action also requires the formation of RISC, however in contrast to siRNA, miRNA targets multiple sequences via imperfect pairing, which leads to simultaneous suppression of multiple target genes [14].

siRNA therapies are also shorter-lived than DNA-based counterparts because the RISC complex and residual siRNAs will eventually be degraded or lost during cell division. To overcome the transient nature of siRNA, DNA-vector-mediated mechanism can be used to induce RNAi, by expressing short hairpin RNAs (shRNAs) that can be converted into siRNA [15].

A schematic representation of the different gene delivery strategies can be found in Figure 1.

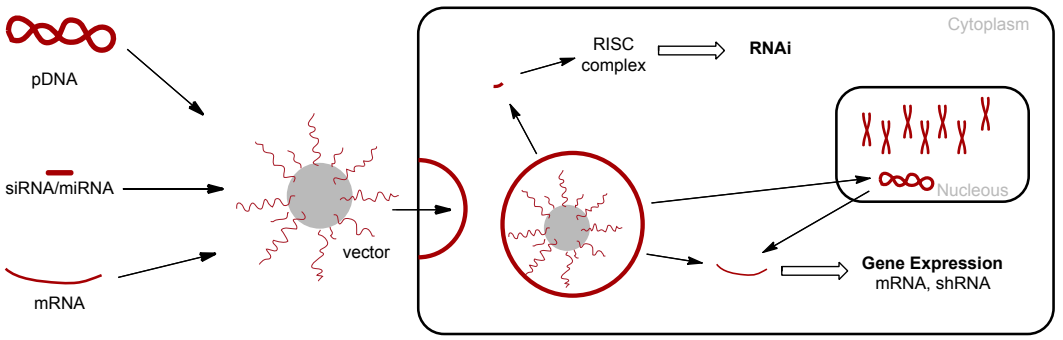

Figure 1. Schematic representation of the different nucleic acid therapies and intracellular site of action.

4. Gene delivery vectors

In order to target tissues that are difficult to access, nucleic acids should have long circulation kinetics. Application of targeted gene therapy intimately depends on the availability of safe and efficient delivery systems. Delivery systems are also essential because DNA or siRNA can easily degraded by nucleases present in the bloodstream and need to overcome several (extra- and intracellular) barriers to exert their therapeutic effect in the target cells [16].

4.1. Viral vectors

Natural viruses are highly efficient nucleic acid delivery vehicles. Virus have evolved to introduce foreign DNA (or RNA) into host cells. Consequently, initial research was focused engineered viral carriers. Viral vectors still remain the most frequently used delivery technology in clinical trials [4] and include retro-, lenti, adeno-, and adeno-associated viruses. Viral vectors are highly efficient, however, clinical studies have demonstrated their inherent risks such as possible severe immune reactions, cellular toxicity, lack of specificity and risk of insertional mutagenesis. Additional issues limiting their clinical application, including challenging large-scale production and restricted packaging capacity [17, 18]

4.2. Non-viral vectors

Non-viral synthetic vectors such as cationic lipids, polymers, dendrimers and peptides, are attractive alternatives to viral vectors due to their potential safety for clinical use and lower immunogenicity, relatively easy pharmaceutical preparation, and easy large-scale production [19], which have made non-viral vectors increasingly popular in clinical trials [4]. The major disadvantage of non-viral vectors is their relative low transfection efficiency when compared to viral vectors [20]. However, significant efforts have been made to improve the transfection efficiency of non-viral vectors.

5. Polymers for gene delivery

Synthetic polymers are interesting materials for gene delivery applications due to their almost unlimited chemical and structural flexibility, meaning that polymers can in principle be tuned to integrate the desirable functionalities to overcome specific biological barriers [21]. Furthermore, polymers can be easily prepared at low-cost and pharmaceutical grade and quantities. Typical examples of cationic polymers used for polyplex formation are shown in Figure 2 [22].

Nanosized particles, named polyplexes, can formed via the electrostatic interaction between negatively charged nucleic acids and cationic polymers (usually containing amine groups). Generally, complexes are formed after establishment of the optimal N/P ratio, where N represents amines of the polymer and P represents phosphates of the nucleic acid. Formation of small and stable polyplexes requires

an excess of amines, which results in a polyplex with overall positive charge. Formation of polyplexes is essential not only to protect the nucleic acids against enzymatic degradation but also to promote cellular uptake [21, 22].

In the case of pDNA, formation of polyplexes also leads condensation and collapsing of plasmids to form nanosized particles [23], into 10^{-3}-10^{-4} of the original volume with typical size of 100-200 nm [24].

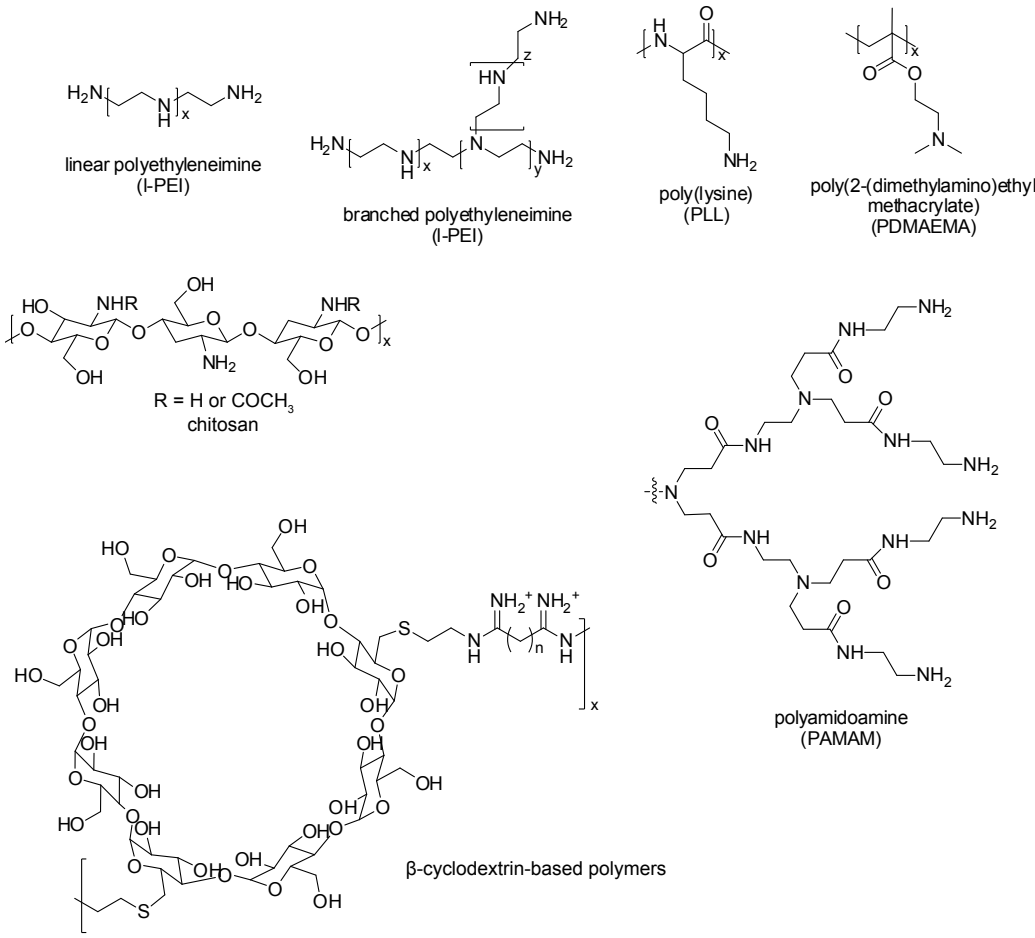

Figure 2. Chemical structures of commonly used cationic polymers in gene delivery [19, 22].

6. Polyplex requirements

6.1. Safety

Several cationic polymers such as polyethyleneimine (PEI) have demonstrated their efficiency as transfection agent *in vitro*. However, polyplexes based exclusively on cationic polymers can lead to significant toxicity *in vivo*. [25, 26]. Toxicity of these positively charged polyplexes arises firstly from their instability. Upon intravenous administration, polyplexes interact with negatively charged blood components (e.g. proteins, erythrocytes), which can lead the massive formation of aggregates, causing lung embolism or liver necrosis [25-27]. Furthermore, cationic polyplexes are associated with uncontrollable biodistribution and undesired off-targeting transfection [25-28], immunogenicity (e.g. complement activation) and blood coagulation [27, 29, 30]. The polyplex stability can be greatly improved by introducing hydrophilic polymers such poly(ethylene glycol) (PEG) or poly[*N*-(2-hydroxypropyl)methacrylamide] (pHPMA) on the surface of polyplexes. Such modification improves not only the colloidal stability and water solubility but also prevents aggregation and interaction with blood components by a steric repulsion effect [27, 31-33].

Safety issues are not only related to the lack of stability but are also a concern when polyplexes interact with the target cells. Polyplexes can induce toxicity at different levels within the cell. Excess polycations present in the polyplex formulations disrupt the cell membrane integrity [34-36], bind cellular polyanions such as receptors, enzymes, mRNA or genomic DNA, which greatly interferes on the cell homeostasis [37]. Additionally, polycations can deregulate the expression profile of the cells [38, 39] and can activate oncogenes and trigger apoptosis [40, 41]. The toxicity from polycation-based polyplexes is influenced by dose and exposure time [34, 42], as well as polymer properties (e.g. molecular weight and cationic charge density) [43, 44].

6.2. Biodegradability

Polyplexes should be preferably based on biodegradable polymers. Biodegradability aims to reduce acute polyplex cytotoxicity by limiting interaction with cellular negatively charged components and also the long-term toxicity, which is essential when multiple administration is required, by allowing efficient clearance of degradation products from the body. Furthermore, in the case of nondegradable

polymers, release of therapeutic nucleic acids from the particles, most likely, requires competitive binding of anionic components (e.g. genomic DNA, mRNA, and cytosolic proteins). By contrast, when biodegradable polymers are used, biodegradability is used as well as a tool for the dissociation of polyplexes and release of encapsulated DNA/RNA, which can lead to an improvement of the transfection efficiency as well [45, 46]. The ideal degradation profile should be rapid and/or environment-sensitive, which can be achieved by using pH and redox sensitive linkers in the polyplexes. Acid-labile imine [47] and acetal [48] linkers can be introduced into cationic polymers to allow degradation in acidic endosomes/lysosomes and disulfide linkers can be used to degrade in response intracellular reducing environment [46]. Labile linkers can be incorporated in the backbone [46, 49] or connected the cationic side-chains to the backbone [50, 51]. Some examples of biodegradable polymers can be found in Figure 3.

Biodegradable cationic polymers indeed show reduced cytotoxicity when compared to their non-degradable counterparts [45, 52]. However, biodegradability is not sufficient for a completely safe gene delivery system [53] and alternative approaches must be developed.

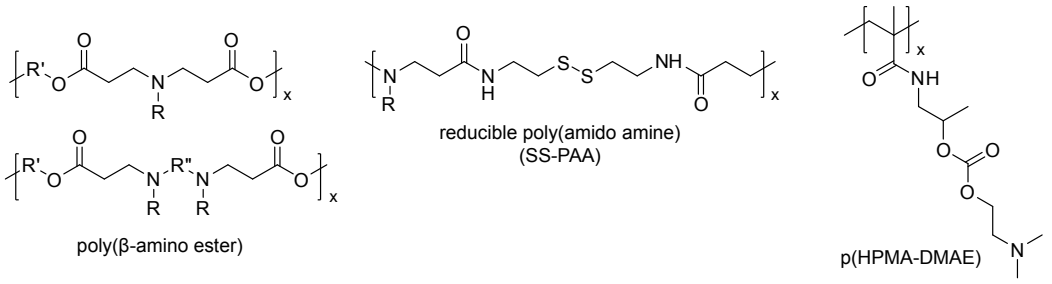

Figure 3. Chemical structures of some biodegradable cationic polymers for gene delivery [45].

6.3. Prolonged circulation time

Gene therapy can potentially achieve highly specific therapies upon systemic administration of polyplexes to target distant tissues. For targeted therapies, prolonged circulation time is the first requirement for *in vivo* efficiency of polyplexes. Nanomedicines are particularly interesting modalities to target tumors because, when they possess sufficient circulation time, tumor accumulation can be achieved due to the so-called enhanced permeability and retention (EPR). This phenomenon

occurs because of the permeable microvasculature and poor lymphatic drainage in solid tumors, allowing nanoparticles to extravasate into tumor microenvironment [54, 55]. Accumulation via the EPR effect, can occur only when polyplexes possess long circulating half-lives. Modification of polyplexes with PEG prevents not only formation of aggregations *in vivo*, but has also demonstrated to improve circulation time and to decrease polyplex capture in the mononuclear phagocyte system (MPS) [27, 33, 56]. However, due to excess of cationic charges, PEGylation of cationic polyplexes is insufficient to achieve prolonged blood circulation. Shielding with PEG cannot avoid unspecific cell binding in highly vascularized organs [57, 58], particularly in the liver where MPS system is located [33, 57, 59]. Consequently, current polyplex systems still lack the desired selectivity and accumulation in target tissues.

6.4. Stability and "smart" behavior

Another important feature of polyplexes for targeting applications is the ability to remain stable in circulation and in off-target sites, and the same time disassemble and release the nucleic acids when inside the target cells. This can be achieved by crosslinking the core of polyplexes using disulfides. Disulfide crosslinks stabilize the polyplex structure in the bloodstream, avoiding unwanted disassembly (e.g. by competition with negatively charged proteins in the blood), and can be rapidly cleaved in the intracellular reducing milieu [60-62]. Introduction of disulfide crosslinks into the PEG-stabilized polyplexes, have demonstrated to improve circulation time [63], as well as to improve tumor accumulation and efficiency upon systemic administration [64, 65].

6.7. Interaction with target tissue/cells

Ideally, polyplexes with prolonged circulation time also avoid interaction with nontarget cell. Only when a polyplex system possesses this property, cell specific targeting/interaction can be achieved by decorating the polyplex surface with the desired targeting ligands. Targeting ligands, will then maximize the binding to and uptake by target cells for cell specific transfection via receptor mediated endocytosis. Different targeting ligands have been identified to promote specific polyplex uptake [22], including peptides (eg. RGD [66]), antibodies (eg. anti-HER2 [67]) and vitamins (e.g. folate [68]) or sugars (eg. lactose [69]).

6.8 Overcoming subcellular barriers

After uptake, polyplexes face two major intracellular barriers to exert their therapeutic effect: endosomal escape (DNA and RNA therapeutics) and nuclear localization (DNA therapeutics). When polyplexes are taken up and internalized by endocytosis, they are directed into endosomal and lysosomal compartments. Therefore, the polyplexes need to escape these compartments before hydrolytic and enzymatic degradation occurs or before polyplexes are disposed via exocytosis [70-74]. Thus, endosomal escape ability is essential for polyplex efficiency. Polymers with endosomal escape ability have been developed over the years, including PEI [75] and derivatives, poly(amidoamine) [76], poly(histidine) [77], poly(*N*-(*N*-(2-aminoethyl)-2-aminoethyl)aspartamide) [PAsp(DET)] [78]. These polymers have in common the ability to become protonated at endosomal pH by possessing groups with a pKa value between physiological and lysosomal pH. In the case of PEI, it was suggested that endosomal escape occurs due to a “proton sponge effect”, in which amines in the polymer become increasingly protonated in the acidic environment of the endosomes, which causes an Cl^- influx resulting in an increase in osmotic pressure, eventually leading to burst of the endosome [75]. This effect might not be generally applicable to improve efficiency [79] but it is considered an important polyplex design property. Other strategies to improve polyplex endosomal escape include functionalization of polyplexes with endosomolytic peptides such the N-terminal segment of the HA-2 subunit of the haemagglutinin of the influenza virus (INF7), the histidine-rich variant of HA-2 (H5WYG), the pH-responsive KALA peptide or the bee venom derived peptide (melittin) [21, 80]. Other interesting strategies include the incorporation of pH sensitive polyacids [81], functionalization of peptides with chemical agents such as derivatives of chloroquine [82], a well-known agent to induce endosomal escape [83, 84], or introduction of photosensitisers in the polyplexes to allow light triggered disruption of endosomes at a specific wavelength [85].

Another particular barrier for the case of pDNA is the nuclear transport. The nuclear membrane allows the exclusive passage of small molecules through its pores. As mentioned, pDNA can enter the nucleus only when nuclear membrane breaks down during cell division, which makes transfection of slowly dividing cells very challenging. There have been reports that functionalization of non-viral vectors with nuclear localization signal (NLS) peptides [86, 87] or by functionalization with the trisaccharide maltotriose [88] may improve nuclear delivery and overcome this barrier.

AIM OF THE THESIS AND OUTLINE

The development polymeric gene delivery system with the adequate safety and efficiency has yet to be accomplished. Polymeric vectors based on polycations possess inherent toxicity that can affect the organism and the cells at many different levels. So far, the best approach consisted on switching towards biodegradable polymers which can only alleviated the toxicity issue. Another important requirement for the effective applicability of polymeric systems for targeted therapies is the ability to have prolonged blood circulation half-lives and low off-target accumulation. Stabilization of polyplex systems by shielding with PEG and by crosslinking have improved the biodistribution and stability of polyplexes, however, often such are rather marginal mainly because preparation of polyplexes requires an excess of cationic charges, which has a deep impact on the insufficient *in vivo* target tissue accumulation and transfection upon systemic administration. In this thesis we focused our efforts on the development of an alternative to conventional polycation-based polyplexes, in order to obtain a polymeric gene delivery system with absent toxicity and with improved targeting ability *in vivo*.

Given the significant disadvantages arising polycations, such system was developed to be based exclusively on biocompatible neutral polymers – **decationized polyplexes**. The development of these polyplexes is described in **Chapter 2**. The innovation of decationized polyplexes comes from the ability being based exclusively on neutral polymers, and yet, without compromising the ability to stability entrap pDNA. This was achieved by developing a method of polyplex preparation that relies on the transient presence of cationic charge to complex DNA for the formation of polyplexes. After complexation, polyplexes are stabilized by interchain disulfide crosslinks in the core of polyplexes, and the labile the cationic groups are removed by hydrolysis ('**decationization**'), to yield neutral polymer-based gene delivery system. The decationized polyplexes possessed intracellular triggered pDNA release, an excellent *in vitro* safety profile and very low degree of nonspecific uptake which is an important property to allow highly specific targeting. Consequently, in **Chapter 3** the optimization of decationized polyplexes by decorating them with a tumor targeting ligand (folate) to achieve cell specific uptake and transfection is described. In **Chapter 4** *in vivo* evaluation of decationized polyplexes is described, by focusing on the evaluation of potential toxicity and teratogenicity in zebrafish and on the evaluation of biodistribution and tumor accumulation of decationized polyplexes in a tumor-bearing mice model upon systemic administration. The decationized polyplexes developed have enormous

chemical and structural flexibility which makes them potential platforms for the application in different nucleic acids therapeutics. In **Chapter 5** the structural changes required for the application of targeted decationized polyplexes for siRNA delivery are described. Lastly, since decationized polyplexes lack the ability to overcome subcellular barriers, in **Chapter 6** introduction of functionalities required for effective endosomal escape are tested to potentially improve transfection efficiency of folate targeted decationized polyplexes for pDNA delivery. Chapter 7 summarizes the results and give directions for future research.

References

[1] R. Mulligan, The basic science of gene therapy, Science, 260 (1993) 926-932.

[2] T. Wirth, N. Parker, S. Ylä-Herttuala, History of gene therapy, Gene, 525 (2013) 162-169.

[3] C. Sheridan, Gene therapy finds its niche, Nat. Biotechnol., 29 (2011) 121-128.

[4] S.L. Ginn, I.E. Alexander, M.L. Edelstein, M.R. Abedi, J. Wixon, Gene therapy clinical trials worldwide to 2012 – an update, J. Gene Med., 15 (2013) 65-77.

[5] S. Worgall, R.G. Crystal, Chapter 34 - Gene Therapy, in: R. Lanza, R. Langer, J. Vacanti (Eds.) Principles of Tissue Engineering (Fourth Edition), Academic Press, Boston, 2014, pp. 657-686.

[6] C.W. Pouton, K.M. Wagstaff, D.M. Roth, G.W. Moseley, D.A. Jans, Targeted delivery to the nucleus, Adv. Drug Deliv. Rev., 59 (2007) 698-717.

[7] E.V.B. van Gaal, W.E. Hennink, D.J.A. Crommelin, E. Mastrobattista, Plasmid engineering for controlled and sustained gene expression for nonviral gene therapy, Pharm. Res., 23 (2006) 1053-1074.

[8] N.S. Yew, H. Zhao, I.H. Wu, A. Song, J.D. Tousignant, M. Przybylska, S.H. Cheng, Reduced inflammatory response to plasmid DNA vectors by elimination and inhibition of immunostimulatory CpG motifs, Mol. Ther., 1 (2000) 255-262.

[9] D.J. Glover, H.J. Lipps, D.A. Jans, Towards safe, non-viral therapeutic gene expression in humans, Nat. Rev. Genet., 6 (2005) 299-310.

[10] G. Tavernier, O. Andries, J. Demeester, N.N. Sanders, S.C. De Smedt, J. Rejman, mRNA as gene therapeutic: How to control protein expression, J. Control. Release, 150 (2011) 238-247.

[11] A. Yamamoto, M. Kormann, J. Rosenecker, C. Rudolph, Current prospects for mRNA gene delivery, Eur. J. Pharm. Biopharm., 71 (2009) 484-489.

[12] B.L. Davidson, P.B. McCray, Current prospects for RNA interference-based therapies, Nat. Rev. Genet., 12 (2011) 329-340.

[13] C. Scholz, E. Wagner, Therapeutic plasmid DNA versus siRNA delivery: Common and

different tasks for synthetic carriers, J. Control. Release, 161 (2012) 554-565.

[14] Y. Chen, D.-Y. Gao, L. Huang, In vivo delivery of miRNAs for cancer therapy: Challenges and strategies, Adv. Drug Deliv. Rev.

[15] D.D. Rao, J.S. Vorhies, N. Senzer, J. Nemunaitis, siRNA vs. shRNA: Similarities and differences, Adv. Drug Deliv. Rev., 61 (2009) 746-759.

[16] K. Miyata, N. Nishiyama, K. Kataoka, Rational design of smart supramolecular assemblies for gene delivery: chemical challenges in the creation of artificial viruses, Chem. Soc. Rev., 41 (2012) 2562-2574.

[17] C.E. Thomas, A. Ehrhardt, M.A. Kay, Progress and problems with the use of viral vectors for gene therapy, Nat. Rev. Genet., 4 (2003) 346-358.

[18] L.W. Seymour, A.J. Thrasher, Gene therapy matures in the clinic, Nat. Biotechnol., 30 (2012) 588-593.

[19] M.A. Mintzer, E.E. Simanek, Nonviral vectors for gene delivery, Chem. Rev., 109 (2008) 259-302.

[20] C.M. Varga, N.C. Tedford, M. Thomas, A.M. Klibanov, L.G. Griffith, D.A. Lauffenburger, Quantitative comparison of polyethylenimine formulations and adenoviral vectors in terms of intracellular gene delivery processes, Gene Ther, 12 (2005) 1023-1032.

[21] A. Aied, U. Greiser, A. Pandit, W. Wang, Polymer gene delivery: overcoming the obstacles, Drug Discovery Today, 18 (2013) 1090-1098.

[22] S.Y. Wong, J.M. Pelet, D. Putnam, Polymer systems for gene delivery—Past, present, and future, Progress in Polymer Science, 32 (2007) 799-837.

[23] A.V. Kabanov, V.A. Kabanov, DNA complexes with polycations for the delivery of genetic material into cells, Bioconjug. Chem., 6 (1995) 7-20.

[24] S. De Smedt, J. Demeester, W. Hennink, Cationic polymer based gene delivery systems, Pharm. Res., 17 (2000) 113-126.

[25] P. Chollet, M.C. Favrot, A. Hurbin, J.-L. Coll, Side-effects of a systemic injection of linear polyethylenimine–DNA complexes, J. Gene Med., 4 (2002) 84-91.

[26] C.M. Ward, M.L. Read, L.W. Seymour, Systemic circulation of poly(L-lysine)/DNA vectors is influenced by polycation molecular weight and type of DNA: differential circulation in mice and rats and the implications for human gene therapy, Blood, 97 (2001) 2221-2229.

[27] M. Ogris, S. Brunner, S. Schuller, R. Kircheis, E. Wagner, PEGylated DNA/transferrin-PEI complexes: reduced interaction with blood components, extended circulation in blood and potential for systemic gene delivery, Gene Ther., 6 (1999) 595-605.

[28] H.K. de Wolf, J. Luten, C.J. Snel, C. Oussoren, W.E. Hennink, G. Storm, In vivo tumor transfection mediated by polyplexes based on biodegradable poly(DMAEA)-phosphazene, J. Control. Release, 109 (2005) 275-287.

[29] R. Duncan, The dawning era of polymer therapeutics, Nat. Rev. Drug Discov., 2 (2003) 347-360.

[30] C.F. Jones, R.A. Campbell, A.E. Brooks, S. Assemi, S. Tadjiki, G. Thiagarajan, C.

Mulcock, A.S. Weyrich, B.D. Brooks, H. Ghandehari, D.W. Grainger, Cationic PAMAM dendrimers aggressively initiate blood clot formation, ACS Nano, 6 (2012) 9900-9910.

[31] D. Oupický, Č. Koňák, P.R. Dash, L.W. Seymour, K. Ulbrich, Effect of albumin and polyanion on the structure of DNA complexes with polycation containing hydrophilic nonionic block, Bioconjug. Chem., 10 (1999) 764-772.

[32] M. Glodde, S.R. Sirsi, G.J. Lutz, Physiochemical properties of low and high molecular weight poly(ethylene glycol)-grafted poly(ethylene imine) copolymers and heir complexes with oligonucleotides, Biomacromolecules, 7 (2005) 347-356.

[33] F.J. Verbaan, C. Oussoren, C.J. Snel, D.J.A. Crommelin, W.E. Hennink, G. Storm, Steric stabilization of poly(2-(dimethylamino)ethyl methacrylate)-based polyplexes mediates prolonged circulation and tumor targeting in mice, J. Gene Med., 6 (2004) 64-75.

[34] D. Fischer, Y. Li, B. Ahlemeyer, J. Krieglstein, T. Kissel, In vitro cytotoxicity testing of polycations: influence of polymer structure on cell viability and hemolysis, Biomaterials, 24 (2003) 1121-1131.

[35] S.M. Moghimi, P. Symonds, J.C. Murray, A.C. Hunter, G. Debska, A. Szewczyk, A two-stage poly(ethylenimine)-mediated cytotoxicity: implications for gene transfer/therapy, Mol. Ther., 11 (2005) 990-995.

[36] S. Choksakulnimitr, S. Masuda, H. Tokuda, Y. Takakura, M. Hashida, In vitro cytotoxicity of macromolecules in different cell culture systems, J. Control. Release, 34 (1995) 233-241.

[37] C. Lonez, M. Vandenbranden, J.-M. Ruysschaert, Cationic lipids activate intracellular signaling pathways, Adv. Drug Deliv. Rev., 64 (2012) 1749-1758.

[38] W.T. Godbey, K.K. Wu, A.G. Mikos, Poly(ethylenimine)-mediated gene delivery affects endothelial cell function and viability, Biomaterials, 22 (2001) 471-480.

[39] K. Masago, K. Itaka, N. Nishiyama, U.-i. Chung, K. Kataoka, Gene delivery with biocompatible cationic polymer: Pharmacogenomic analysis on cell bioactivity, Biomaterials, 28 (2007) 5169-5175.

[40] K. Regnström, E.G.E. Ragnarsson, M. Köping-Höggård, E. Torstensson, H. Nyblom, P. Artursson, PEI – a potent, but not harmless, mucosal immuno-stimulator of mixed T-helper cell response and FasL-mediated cell death in mice, Gene Ther., 10 (2003) 1575-1583.

[41] O.M. Merkel, A. Beyerle, B.M. Beckmann, M. Zheng, R.K. Hartmann, T. Stöger, T.H. Kissel, Polymer-related off-target effects in non-viral siRNA delivery, Biomaterials, 32 (2011) 2388-2398.

[42] S. Boeckle, K. von Gersdorff, S. van der Piepen, C. Culmsee, E. Wagner, M. Ogris, Purification of polyethylenimine polyplexes highlights the role of free polycations in gene transfer, J. Gene Med., 6 (2004) 1102-1111.

[43] K. Kunath, A. von Harpe, D. Fischer, H. Petersen, U. Bickel, K. Voigt, T. Kissel, Low-molecular-weight polyethylenimine as a non-viral vector for DNA delivery: comparison of physicochemical properties, transfection efficiency and in vivo distribution with high-molecular-weight polyethylenimine, J. Control. Release, 89 (2003) 113-125.

[44] E.V.B. van Gaal, R. van Eijk, R.S. Oosting, R.J. Kok, W.E. Hennink, D.J.A. Crommelin,

E. Mastrobattista, How to screen non-viral gene delivery systems in vitro?, J. Control. Release, 154 (2011) 218-232.

[45] J. Luten, C.F. van Nostrum, S.C. De Smedt, W.E. Hennink, Biodegradable polymers as non-viral carriers for plasmid DNA delivery, J. Control. Release, 126 (2008) 97-110.

[46] J.J. Green, R. Langer, D.G. Anderson, A Combinatorial polymer library approach yields insight into nonviral gene delivery, Acc. Chem. Res., 41 (2008) 749-759.

[47] Y.H. Kim, J.H. Park, M. Lee, Y.-H. Kim, T.G. Park, S.W. Kim, Polyethylenimine with acid-labile linkages as a biodegradable gene carrier, J. Control. Release, 103 (2005) 209-219.

[48] V. Knorr, V. Russ, L. Allmendinger, M. Ogris, E. Wagner, Acetal linked oligoethylenimines for use as pH-sensitive gene carriers, Bioconjug. Chem., 19 (2008) 1625-1634.

[49] C. Lin, Z. Zhong, M.C. Lok, X. Jiang, W.E. Hennink, J. Feijen, J.F.J. Engbersen, Novel bioreducible poly(amido amine)s for highly efficient gene delivery, Bioconjug. Chem., 18 (2006) 138-145.

[50] R.S. Burke, S.H. Pun, Synthesis and characterization of biodegradable HPMA-oligolysine copolymers for improved gene delivery, Bioconjug. Chem., 21 (2009) 140-150.

[51] A. Funhoff, C.F. van Nostrum, A. Janssen, M. Fens, D. Crommelin, W.E. Hennink, Polymer side-chain degradation as a tool to control the destabilization of polyplexes, Pharm. Res., 21 (2004) 170-176.

[52] J. Zhou, J. Liu, C.J. Cheng, T.R. Patel, C.E. Weller, J.M. Piepmeier, Z. Jiang, W.M. Saltzman, Biodegradable poly(amine-co-ester) terpolymers for targeted gene delivery, Nat. Mater., 11 (2012) 82-90.

[53] L. Parhamifar, A.K. Larsen, A.C. Hunter, T.L. Andresen, S.M. Moghimi, Polycation cytotoxicity: a delicate matter for nucleic acid therapy-focus on polyethylenimine, Soft Matter, 6 (2010) 4001-4009.

[54] H. Maeda, Tumor-selective delivery of macromolecular drugs via the EPR effect: Background and future prospects, Bioconjug. Chem., 21 (2010) 797-802.

[55] H. Maeda, J. Wu, T. Sawa, Y. Matsumura, K. Hori, Tumor vascular permeability and the EPR effect in macromolecular therapeutics: a review, J. Control. Release, 65 (2000) 271-284.

[56] M. Harada-Shiba, K. Yamauchi, A. Harada, I. Takamisawa, K. Shimokado, K. Kataoka, Polyion complex micelles as vectors in gene therapy – pharmacokinetics and in vivo gene transfer, Gene Ther., 9 (2002) 407-414.

[57] H.K. de Wolf, C.J. Snel, F.J. Verbaan, R.M. Schiffelers, W.E. Hennink, G. Storm, Effect of cationic carriers on the pharmacokinetics and tumor localization of nucleic acids after intravenous administration, Int. J. Pharm., 331 (2007) 167-175.

[58] D. Oupický, M. Ogris, K.A. Howard, P.R. Dash, K. Ulbrich, L.W. Seymour, Importance of lateral and steric stabilization of polyelectrolyte gene delivery vectors for extended systemic circulation, Mol. Ther., 5 (2002) 463-472.

[59] T. Merdan, K. Kunath, H. Petersen, U. Bakowsky, K.H. Voigt, J. Kopecek, T. Kissel,

PEGylation of poly(ethylene imine) affects stability of complexes with plasmid DNA under in vivo conditions in a dose-dependent manner after intravenous injection into mice, Bioconjug. Chem., 16 (2005) 785-792.

[60] M.H. Lee, Z. Yang, C.W. Lim, Y.H. Lee, S. Dongbang, C. Kang, J.S. Kim, Disulfide-cleavage-triggered chemosensors and their biological applications, Chem. Rev., 113 (2013) 5071-5109.

[61] F. Meng, W.E. Hennink, Z. Zhong, Reduction-sensitive polymers and bioconjugates for biomedical applications, Biomaterials, 30 (2009) 2180-2198.

[62] D.S. Manickam, J. Li, D.A. Putt, Q.-H. Zhou, C. Wu, L.H. Lash, D. Oupický, Effect of innate glutathione levels on activity of redox-responsive gene delivery vectors, J. Control. Release, 141 (2010) 77-84.

[63] D. Oupický, R.C. Carlisle, L.W. Seymour, Triggered intracellular activation of disulfide crosslinked polyelectrolyte gene delivery complexes with extended systemic circulation in vivo, Gene Ther., 8 (2001) 713-724.

[64] Y. Vachutinsky, M. Oba, K. Miyata, S. Hiki, M.R. Kano, N. Nishiyama, H. Koyama, K. Miyazono, K. Kataoka, Antiangiogenic gene therapy of experimental pancreatic tumor by sFlt-1 plasmid DNA carried by RGD-modified crosslinked polyplex micelles, J. Control. Release, 149 (2011) 51-57.

[65] R.J. Christie, Y. Matsumoto, K. Miyata, T. Nomoto, S. Fukushima, K. Osada, J. Halnaut, F. Pittella, H.J. Kim, N. Nishiyama, K. Kataoka, Targeted polymeric micelles for siRNA treatment of experimental cancer by intravenous injection, ACS Nano, 6 (2012) 5174-5189.

[66] Z. Ge, Q. Chen, K. Osada, X. Liu, T.A. Tockary, S. Uchida, A. Dirisala, T. Ishii, T. Nomoto, K. Toh, Y. Matsumoto, M. Oba, M.R. Kano, K. Itaka, K. Kataoka, Targeted gene delivery by polyplex micelles with crowded PEG palisade and cRGD moiety for systemic treatment of pancreatic tumors, Biomaterials, 35 (2014) 3416-3426.

[67] S.-J. Chiu, N.T. Ueno, R.J. Lee, Tumor-targeted gene delivery via anti-HER2 antibody (trastuzumab, Herceptin®) conjugated polyethylenimine, J. Control. Release, 97 (2004) 357-369.

[68] C. Dohmen, T. Frohlich, U. Lachelt, I. Rohl, H.-P. Vornlocher, P. Hadwiger, E. Wagner, Defined folate-PEG-siRNA conjugates for receptor-specific gene silencing, Mol. Ther. Nucleic Acids, 1 (2012) e7.

[69] M. Oishi, Y. Nagasaki, K. Itaka, N. Nishiyama, K. Kataoka, Lactosylated poly(ethylene glycol)-siRNA conjugate through acid-labile β-thiopropionate linkage to construct pH-sensitive polyion complex micelles achieving enhanced gene silencing in hepatoma cells, J. Am. Chem. Soc., 127 (2005) 1624-1625.

[70] M.A.E.M. Aa, U.S. Huth, S.Y. Häfele, R. Schubert, R.S. Oosting, E. Mastrobattista, W.E. Hennink, R. Peschka-Süss, G.A. Koning, D.J.A. Crommelin, Cellular uptake of cationic polymer-DNA complexes via caveolae plays a pivotal role in gene transfection in COS-7 cells, Pharm. Res., 24 (2007) 1590-1598.

[71] Z. Yang, G. Sahay, S. Sriadibhatla, A.V. Kabanov, Amphiphilic block copolymers enhance cellular uptake and nuclear entry of polyplex-delivered DNA, Bioconjug. Chem.,

19 (2008) 1987-1994.

[72] D. Vercauteren, J. Rejman, T.F. Martens, J. Demeester, S.C. De Smedt, K. Braeckmans, On the cellular processing of non-viral nanomedicines for nucleic acid delivery: Mechanisms and methods, J. Control. Release, 161 (2012) 566-581.

[73] Y. Wang, L. Huang, A window onto siRNA delivery, Nat. Biotechnol., 31 (2013) 611-612.

[74] L.K. Medina-Kauwe, J. Xie, S. Hamm-Alvarez, Intracellular trafficking of nonviral vectors, Gene Ther., 12 (2005) 1734-1751.

[75] O. Boussif, F. Lezoualc'h, M.A. Zanta, M.D. Mergny, D. Scherman, B. Demeneix, J.P. Behr, A versatile vector for gene and oligonucleotide transfer into cells in culture and in vivo: polyethylenimine, Proc. Natl. Acad. Sci. U.S.A., 92 (1995) 7297-7301.

[76] S. Richardson, P. Ferruti, R. Duncan, Poly(amidoamine)s as potential endosomolytic polymers: Evaluation in vitro and body distribution in normal and tumour-bearing animals, J. Drug Target., 6 (1999) 391-404.

[77] P. Midoux, C. Pichon, J.-J. Yaouanc, P.-A. Jaffrès, Chemical vectors for gene delivery: a current review on polymers, peptides and lipids containing histidine or imidazole as nucleic acids carriers, Br. J. Pharmacol., 157 (2009) 166-178.

[78] K. Miyata, M. Oba, M. Nakanishi, S. Fukushima, Y. Yamasaki, H. Koyama, N. Nishiyama, K. Kataoka, Polyplexes from poly(aspartamide) bearing 1,2-diaminoethane side chains induce pH-selective, endosomal membrane destabilization with amplified transfection and egligible cytotoxicity, J. Am. Chem. Soc., 130 (2008) 16287-16294.

[79] A.M. Funhoff, C.F. van Nostrum, G.A. Koning, N.M.E. Schuurmans-Nieuwenbroek, D.J.A. Crommelin, W.E. Hennink, Endosomal escape of polymeric gene delivery complexes is not always enhanced by polymers buffering at low pH, Biomacromolecules, 5 (2003) 32-39.

[80] J. Hoyer, I. Neundorf, Peptide vectors for the nonviral delivery of nucleic acids, Acc. Chem. Res., 45 (2012) 1048-1056.

[81] B.B. Lundy, A. Convertine, M. Miteva, P.S. Stayton, Neutral polymeric micelles for RNA delivery, Bioconjug. Chem., 24 (2013) 398-407.

[82] S.E. Andaloussi, T. Lehto, I. Mager, K. Rosenthal-Aizman, Oprea, II, O.E. Simonson, H. Sork, K. Ezzat, D.M. Copolovici, K. Kurrikoff, J.R. Viola, E.M. Zaghloul, R. Sillard, H.J. Johansson, F. Said Hassane, P. Guterstam, J. Suhorutsenko, P.M. Moreno, N. Oskolkov, J. Halldin, U. Tedebark, A. Metspalu, B. Lebleu, J. Lehtio, C.I. Smith, U. Langel, Design of a peptide-based vector, PepFect6, for efficient delivery of siRNA in cell culture and systemically in vivo, Nucleic Acids Res., 39 (2011) 3972-3987.

[83] M.A. Wolfert, L.W. Seymour, Chloroquine and amphipathic peptide helices show synergistic transfection in vitro, Gene Ther., 5 (1998) 409-414.

[84] J. Cheng, R. Zeidan, S. Mishra, A. Liu, S.H. Pun, R.P. Kulkarni, G.S. Jensen, N.C. Bellocq, M.E. Davis, Structure−function correlation of chloroquine and analogues as transgene expression enhancers in nonviral gene delivery, J. Med. Chem., 49 (2006) 6522-6531.

[85] T. Nomoto, S. Fukushima, M. Kumagai, K. Machitani, Arnida, Y. Matsumoto, M.

Oba, K. Miyata, K. Osada, N. Nishiyama, K. Kataoka, Three-layered polyplex micelle as a multifunctional nanocarrier platform for light-induced systemic gene transfer, Nat. Commun., 5 (2014).

[86] Q. Hu, J. Wang, J. Shen, M. Liu, X. Jin, G. Tang, P.K. Chu, Intracellular pathways and nuclear localization signal peptide-mediated gene transfection by cationic polymeric nanovectors, Biomaterials, 33 (2012) 1135-1145.

[87] W.-J. Yi, J. Yang, C. Li, H.-Y. Wang, C.-W. Liu, L. Tao, S.-X. Cheng, R.-X. Zhuo, X.-Z. Zhang, Enhanced nuclear import and transfection efficiency of TAT peptide-based gene delivery systems modified by additional nuclear localization signals, Bioconjug. Chem., 23 (2011) 125-134.

[88] H. Akita, T. Masuda, T. Nishio, K. Niikura, K. Ijiro, H. Harashima, Improving in vivo hepatic transfection activity by controlling intracellular trafficking: The function of GALA and maltotriose, Mol. Pharmaceutics, 8 (2011) 1436-1442.

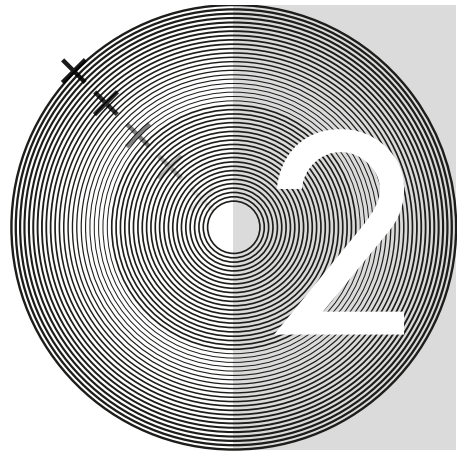

CHAPTER

Decationized crosslinked polyplexes for redox-triggered gene delivery

Luís Novo[a], Ethlinn V.B. van Gaal[b], Enrico Mastrobattista[a], Cornelus F. van Nostrum[a], Wim E. Hennink[a,*]

[a]Department of Pharmaceutics, Utrecht Institute for Pharmaceutical Sciences, Utrecht University, 3584 CG Utrecht, The Netherlands

[b]Cristal Delivery BV, Padualaan 8, 3584 CH Utrecht, The Netherlands

J. Control. Release, 169 (2013) 246-256.

Abstract

The clinical applicability of polymers as gene delivery systems depends not only on their efficiency, but also on their safety. The cytotoxicity of these systems remains a major issue, mainly due to their cationic nature. Therefore, it is highly preferable to have a system based on biocompatible neutral polymers, lacking polycations, without compromising the DNA condensing and protecting capacities. Here, we introduce a concept to obtain a neutral polymeric gene delivery system, through a 3-step process (charge-driven condensation; stabilization through disulfide crosslinking; polyplex decationization) to generate polyplexes with a core of disulfide crosslinked poly(hydroxypropyl methacrylamide) (pHPMA) in which plasmid DNA (pDNA) is entrapped and a shell of poly(ethylene glycol) (PEG). The resulting polyplexes combine beneficial features of high and stable DNA loading capacity, stealth behavior and reduced toxicity. The nanoparticles are designed to release the pDNA after cellular uptake through cleavage of disulfide crosslinks within the intracellular reducing environment. This was shown by forced introduction of the polyplexes into the cytosol of HeLa cells by electroporation, which resulted in a high level of expression of the reporter gene. Additionally, the decationized polyplexes showed no interference on the cellular cell viability or metabolic activity (even at high dose) and no complex-induced membrane destabilization. Furthermore, decationized polyplexes showed a low degree of nonspecific uptake, which is a highly favorable property for targeted therapy. Summarizing, the stabilized, decationized polyplexes presented here contribute to solve the high toxicity, low stability and lack of cellular/tissue specificity of cationic polymer-based gene delivery systems.

KEYWORDS Gene delivery, triggered release, polymer, biocompatibility, nanoparticle

1. INTRODUCTION

Successful *in vivo* gene therapy strongly depends on the availability of safe and efficient gene delivery vectors. Synthetic vectors based on cationic polymers are able to complex DNA via electrostatic interactions, to form nano-

sized particles ('polyplexes') capable of transfecting cells. Cationic polymers are of special interest because of their ease of preparation and upscaling, high DNA loading capacity and low immunogenicity, compared to biological vectors such as viruses. Their enormous flexibility in terms of chemical and structural design is also advantageous. Polyethylenimine (PEI) (and derivatives) has been a frequently investigated polymer, mainly due to its exceptional *in vitro* transfection properties [1]. However, its clinical applicability is significantly hampered by the high degree of toxicity for this polymer, observed both *in vitro* and *in vivo* [2, 3].

Biodegradable cationic polymers show reduced cytotoxicity as compared to their nondegradable counterparts [4, 5]. However, biodegradability alone is not sufficient for a completely safe gene delivery system [6], particularly when systemic administration is desired. *In vivo* toxicity is intimately related to the cationic nature of the polyplexes, leading to systemic and cellular toxicity. First, upon intravenous administration, cationic polyplexes can interact with negatively charged blood components (e.g. proteins, erythrocytes), followed by the formation of aggregates, leading to severe *in vivo* toxicity and reduced and uncontrollable biodistribution [7-10]. Furthermore, cationic polymers might induce immunogenicity and complement activation [2, 8]. These undesirable effects can only be partially prevented by shielding the surface charge of the particles, with for example poly(ethylene glycol) (PEG) [8, 11, 12]. Besides systemic toxicities, cytotoxic effects are also observed upon polyplex internalization. First of all, cationic polymers can interact with the cellular membrane compromising its integrity [13-15]. Furthermore, since polycations electrostatically bind and condense DNA, aspecific electrostatic binding to any kind of cellular polyanions (e.g. enzymes, mRNA or genomic DNA) results in changes of the cell homeostasis [16] by deregulating the expression profile of housekeeping genes [17, 18] or by inducing activation of oncogenes or genes involved in apoptosis [19]. Consequently, polycations can not only adversely affect the cell, but also the organism as a whole. The extent of cellular toxicity is directly related to polyplex dose and their time of exposure to the cells [13, 20]. Characteristics of cationic polyplex formulations such as polymer molecular weight, cationic charge density and the presence of free polymer also influence their cytotoxicity [21, 22].

Accordingly, we hypothesize that an ideal candidate for a safe synthetic gene delivery vector lacks polycations and is based on biocompatible neutral polymers. It is reasoned that a gene delivery system based on neutral polymers lacks the intra- and extracellular toxicity associated with the cationic nature of polyplexes. At

the same time, polyplexes should also have a stable and high loading capacity and allow a triggered and/or targeted DNA release. Consequently, a major challenge is to include all the previous properties in a system based on a neutral polymer.

In this paper a novel concept is presented to obtain a neutral polymeric gene delivery system through a 3-step process: charge-driven condensation, followed by stabilization through disulfide crosslinking and finally polyplex decationization. In order to prepare such polyplexes, the cationic block copolymer p(HPMA–DMAE-co-PDTEMA)-b-PEG (shortened pHDP-PEG) (Figure 1) is first complexed with pDNA, enabling efficient charge-driven condensation. Subsequently, interchain disulfide crosslinking of the polyplexes is induced via thiol exchange reaction with a dithiol (**1**). Finally, the dimethylaminoethanol (DMAE) cationic groups are removed by hydrolysis, at pH 8.5, of the carbonate ester bond linking the DMAE group to the pHPMA backbone (decationization). This procedure results in disulfide crosslinked p(HPMA-co-PDTEMA)-b-PEG (shortened pHP-PEG) based decationized polyplexes with pDNA stably entrapped in the core of disulfide crosslinked pHPMA and surrounded by a PEG shell (**2**) (Scheme 1). Consequently, the degradation product of such polyplexes are PEG and pHPMA, which are both have a good biocompatibility. The polyplexes are designed to be stable in the circulation through the crosslinked core and the stealth PEG corona for improved colloidal stability and circulation time *in vivo* [8, 11, 23] and to specifically disassemble and release the entrapped pDNA into the intracellular reducing environment by destabilization of its interchain disulfide crosslinked core [24-26].

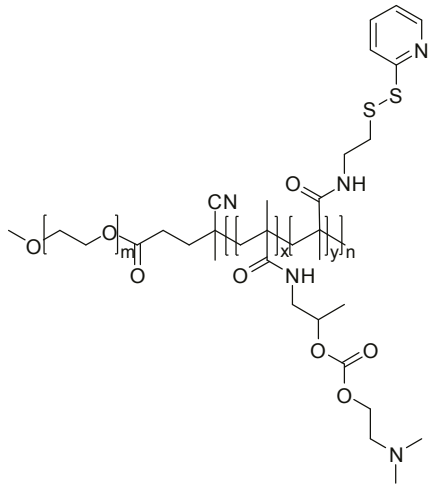

Figure 1. Chemical structure of the p(HPMA–DMAE-co-PDTEMA)-b-PEG block copolymers.

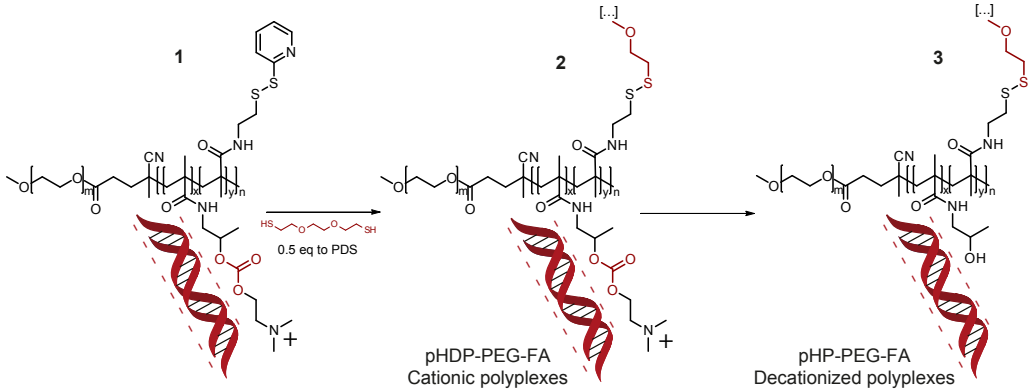

Scheme 1. Route for the preparation of interchain disulfide crosslinked pHDP-PEG based polyplexes.

2. MATERIALS AND METHODS

2.1. Materials

N-(2-Hydroxypropyl)methacrylamide (HPMAm) was obtained from Zentiva a. s. (Praha, Czech Republic). Acetonitrile (ACN), dichloromethane (DCM), ethylacetate (EtOAc), hexane and methanol were purchased from Biosolve (Valkenswaard, the Netherlands). Acetone was purchased from Merck (Darmstadt, Germany). The $(mPEG_{5000})_2$-ABCPA macroinitiator was synthesized as previously described [27]. pCMV_luc and pCMV_EGFP plasmids, encoding for firefly luciferase and enhanced green fluorescent protein (EGFP), respectively, with human cytomegalovirus promoter (CMV), were amplified with competent *E. coli* DH5α and purified with NucleoBond® **(**Macherey-Nagel, Bioke, Leiden, The Netherlands). pCMV_Luc was purchased from the Plasmid Factory (Bielefeld, Germany). pCMV_EGFP construction was described by van Gaal et al. [22]. Agarose MP was purchased from Roche Molecular Biochemicals (Mannheim, Germany). Exgen 500 (22 kDa, l-PEI) and 6× DNA Loading Dye were purchased from Fermentas (St. Leon-Roth, Germany). Human epithelial ovarian carcinoma cells (HeLa) were originally obtained from the American Type Culture Collection (ATCC) (Maryland, USA). Dulbecco's modification of Eagle's medium with 3.7 g/L sodium bicarbonate, 1 g/L l-glucose, l-glutamine (DMEM), RPMI 1640, phosphate buffered saline (PBS), fetal bovine serum (FBS), antibiotics/antimycotics (penicillin, streptomycin sulphate, amphotericin B and trypsin/EDTA 10× were purchased from PAA

Laboratories GmbH (Pasching, Austria). Luciferase assay system and CytoTox-ONE Homogeneous Membrane Integrity Assay kits were obtained from Promega (Leiden, The Netherlands). Micro BCA Protein Assay kit was purchased from Pierce (Etten-Leur, The Netherlands). LabelIT Cy5 Nucleic Acid Labeling Kit was purchased from Mirus Bio (Madison, WI, USA). All other chemicals and reagents were obtained from Sigma-Aldrich (Zwijndrecht, The Netherlands).

2.2. Monomer synthesis

2.2.1. Synthesis of Carbonic Acid 2-Dimethylamino-ethyl Ester 1-Methyl-2-(2-Methacryloylamino)-Ethyl Ester (HPMA–DMAE)

HPMA–DMAE was synthesized according to a previously described method by Funhoff et al. [28], with some changes. The first step of the synthesis is the activation of *N*'*N*'-dimethylaminoethanol (DMAE) by 1,1'-carbonyldiimidazole (CDI). Briefly, DMAE (10 mL, 100 mmol) was added dropwise to CDI (20.6 g, 127 mmol) dissolved in 200 mL of DCM, while stirring vigorously under a nitrogen flow. The reaction was allowed to proceed for 1 h at room temperature. Next, the crude product was washed 3 times with 80 mL of water and dried over anhydrous $MgSO_4$. Subsequently, DCM was evaporated by rotary evaporation and a colorless oil was obtained (DMAE-CI). Yield: 12.3 g, 67%. ^{1}H NMR ($CDCl_3$): δ (ppm) 2.31 (s, 6H), 2.71 (t, 2H), 4.50 (t, 2H), 7.06 (s, 1H), 7.42 (s, 1H), 8.14 (s, 1H). The second step of the synthesis comprises the reaction between DMAE-CI and HPMA. Firstly, DMAE-CI (12.3 g, 67 mmol) was dissolved in 120 mL of DCM. Next, a solution of HPMA (11.5 g, 80.8 mmol) in 120 mL of DCM was added to the DMAE-CI solution. Hydroquinone monomethyl ether (~5 mg) was added to the mixture in order to prevent premature polymerization. The mixture was stirred for 5 days at room temperature under a nitrogen atmosphere and the solvent was evaporated by rotary evaporation. A colorless oil was obtained (HPMA–DMAE, HPMA, imidazole, hydroquinone monomethylether). The inhibitor and unreacted HPMA were removed from the crude product by flash column chromatography (VersaPak® Silica Cartridge 40×150 mm). In detail, the column was washed with acetone/hexane 10/90 (v/v) and the crude product dissolved in 5 mL of acetone/hexane 50/50 (v/v) was applied on the column. Inhibitor and HPMA were eluted with acetone/hexane 90/10 (v/v). HPMA–DMAE and part of imidazole were eluted with acetone/methanol 90/10. The retention times of HPMA–DMAE and imidazole were very similar. Since imidazole does not interfere with the polymerization of

HPMA–DMAE, fractions containing imidazole were also collected. Imidazole fractions were monitored using Pauly's reagent [29], which allowed to collect a small fraction of pure HPMA–DMAE. After drying the product, a colorless oil was obtained.

The ratio between HPMA–DMAE and imidazole in the product was determined using standards of pure HPMA–DMAE with Waters Acquity UPLC™ system with an ACQUITY UPLC HSS T3 Column, 2.1x30 mm, 1.8 µm equipped with a UV detector. A mobile phase gradient, from 100% of eluent A (100/0.1% H_2O/perchloric acid) to 60% of B (5/95/0.1 H_2O/acetonitrile/perchloric acid) in 3 min was used. The yield of HPMA–DMAE was: 4.87 g, 67% (10 g of purified crude product). ^{1}H NMR ($CDCl_3$): δ (ppm) 1.29 (d, 3H), 1.96 (s, 3H), 2.27 (s, 6H), 2.58 (t, 2H), 3.7–3.3 (m, 2H), 4.23 (m, 2H), 5.34 (s, 1H), 4.90 (m, 1H), 5.34 (s, 1H), 5.68 (s, 1H), 6.27 (bs, 1H).

2.2.2.1. Synthesis of 2-(Pyridyldithio)-Ethylamine Hydrochloride (PDTEA•HCl)

PDTEA•HCl was synthesized based on a method previously described by Zugates et al. and Ebright et al. [30, 31]. Briefly, 2,2'-dipyridyl disulfide (8.815 g, 40 mmol) was dissolved in 41.6 mL of methanol containing 1.6 mL of glacial acetic acid (28 mmol). Subsequently, a solution of 2-mercaptoethylamine hydrochloride (2-MEA) (2.288 g, 20 mmol) in 17.5 mL of methanol was added dropwise over a period of 30 min, in order keep low concentrations of free thiols in solution [32]. The reaction mixture was kept under N_2 to minimize oxidation of the thiol groups and after 48 h, the solvent was evaporated by rotary evaporation, yielding a yellow oil. The product was washed with 100 mL of cold diethyl ether and redissolved in 20 mL of methanol. The procedure was repeated 6 times. A white powder was obtained. Yield: 3.34 g, 75%. ^{1}H NMR (D_2O): δ (ppm) 3.12 (t, 2H), 3.36 (t, 2H), 7.35 (m, 1H), 7.76 (m, 1H), 7.86 (m, 1H), 8.48 (m, 1H).

2.2.2.2. Synthesis of N-[2-(2-Pyridyldithio)]ethyl Methacrylamide (PDTEMA)

The synthesis of PDTEMA was performed under Schotten-Baumann reaction conditions. In detail, PDTEA•HCl (1.5 g, 6.73 mmol) was dissolved in 7 mL of reverse osmosis (RO) water. A solution of methacryloyl chloride (0.79 mL, 8.08 mmol) in 27 mL of DCM was added to the PDTEA•HCl solution and the formed 2 phase system was stirred vigorously at 0 °C for 30 min. Hydroquinone monoethyether (~ 5 mg) was added, in order to prevent premature polymerization. Next, 8.1 mL of 2 M

NaOH solution was added dropwise to the 2 phase system over a period of 30 min, while the temperature was kept at 0 °C. The reaction mixture was subsequently stirred for 2 h at room temperature. Thereafter, the water phase was discarded and the organic phase, containing the product, was washed with 10 mL of 0.1 M HCl (2 times) and 0.1 M NaOH (3 times). Finally, the DCM solution was dried over $MgSO_4$ and the solvent was removed by rotary evaporation.

The obtained crude product was purified by flash column chromatography (VersaPak® Silica Cartridge 40×75 mm). The column was washed with EtOAc/hexane 10/90 (v/v) and the crude product was dissolved in 5 mL EtOAc/hexane 50/50 (v/v) and then applied onto the column. The column was eluted with a gradient of EtOAc/hexane 50/50-70/30 (v/v). The fractions containing only PDTEMA (determined by TLC monitoring) were collected and white crystals were obtained after evaporation of the solvent (Yield: 0.742 g, 2.92 mmol, 43%). The identity of PDTEMA was assessed by NMR analysis: ^{1}H NMR ($CDCl_3$): δ (ppm) 2.03 (s, 3H), 2.94 (t, 2H), 3.60 (m, 2H), 5.38 (s, 1H), 5.81 (s, 1H), 7.14 (m, 1H), 7.46-7.65 (m+bs, 3H), 8.47 (m, 1H).

The purity of the monomer was further assessed by UPLC using a similar method as described for HPMA–DMAE (section 2.2.1).

2.3. Synthesis of p(HPMA–DMAE-co-PDTEMA)-b-PEG and p(HPMA–DMAE)-b-PEG

Free radical polymerization using $(mPEG_{5000})_2$-ABCPA as macroinitiator was performed to synthesize p(HPMA–DMAE-co-PDTEMA)-b-PEG (pHDP-PEG). The synthesis and characterization of the $(mPEG_{5000})_2$-ABCPA macroinitiator was performed based on the methods previously described [27, 33]. The polymers were synthesized using a monomer to initiator ratio (M/I) of 400. Different molar feed ratios of HPMA–DMAE and PDTEMA were used; 100/0 (pHD-PEG), 95/5, 90/10 and 85/15 (pHDP-PEG). In detail, 600 mg of a crude mixture of HPMA–DMAE and imidazole (528.8 mg, 2.0 mmol HPMA–DMAE) and 52.6 mg of $(mPEG_{5000})_2$-ABCPA (HPMA–DMAE/PDTEMA 100/0), 55.4 mg $(mPEG_{5000})_2$-ABCPA and 27.8 mg (0.11 mmol) PDTEMA (HPMA–DMAE/PDTEMA 95/5), 58.5 mg $(mPEG_{5000})_2$-ABCPA and 58.8 mg (0.23 mmol) PDTEMA (HPMA–DMAE/PDTEMA 90/10) or 61.9 mg $(mPEG_{5000})_2$-ABCPA and 93.3 mg (0.36 mmol) PDTEMA (HPMA–DMAE/PDTEMA 85/15) were dissolved in ACN (300 mg/mL) in flasks sealed with rubber

septa and subjected to vacuum-N_2 cycles. The polymerization was carried at 70 °C for 24 h. Next, the ACN solutions were transferred into dialysis tubes (molecular weight cutoff (MWCO) 12-14 kDa) and the polymers were extensively dialyzed against 10 mM NH_4Ac buffer pH 5.0 for 3 days at 4 °C. In the last dialysis cycle the ionic strength of the buffer was changed to 5 mM. The polymer was collected by freeze drying.

2.4. ^{1}H NMR characterization of the polymers

The copolymer composition of the different pHDP-PEGs was determined by ^{1}H NMR analysis performed with a Gemini 300 MHz spectrometer (Varian Associates Inc., NMR Instruments, Palo Alto, CA) in DMSO-d6. The ratio HPMA–DMAE/PDTEMA was determined by comparison of the integrals at δ 4.6 ppm (bs, $CH_2C\underline{H}CH_3O$, HPMA–DMAE) and the integral at δ8.5 ppm (bs, pyridyl group proton, PDTEMA) ($\int\delta_{4.6}/\int\delta_{8.5}$). The integral ratios between δ4.2 ppm (bs, $OC\underline{H_2}CH_2$), HPMA–DMAE) and δ4.6 ppm (bs, $CH_2C\underline{H}CH_3O$, HPMA–DMAE) were used to verify if the integrity of the carbonate ester bond between HPMA and the DMAE side group was preserved during polymerization and purification.

Number average molecular weight (M_n) of the polymers was determined according to equation (1).

$$M_n = (\int\delta_{4.6} \times M_{HPMA–DMAE} + \int\delta_{8.5} \times M_{PDTEMA})/(\int\delta_{3.5}/448) + 5000 \text{ (g/mol)} \quad (1)$$

where, $\int\delta_{3.5}$, $\int\delta_{4.6}$ and $\int\delta_{8.5}$ are the integrals at 3.5, 4.6, and 8.5 ppm, respectively. $M_{HPMA–DMAE}$ and M_{PDTEMA} are the molar masses of HPMA–DMAE and PDTEMA, respectively. The number of protons for the 5 kDa PEG block, this is $\int\delta_{3.5,}$ was set to 448.

2.5. UV spectroscopy characterization of the polymers

UV spectroscopy was performed on Shimadzu UV-2450 UV/VIS spectrophotometer (‘s-Hertogenbosch, The Netherlands) to quantify the molarity of thiol reactive pyridyl disulfide (PDS) groups per weight of polymer. Polymer stock solutions of 1 mg/mL in 20 mM HEPES pH 7.4 were prepared. Next, 10 µL of a freshly prepared DTT solution (100 mM) was added and after 15 min the UV absorbance at 343 nm was measured to determine the release of 2-mercaptopyridine (2-MP)

[34]. Quantification was done using a calibration curve with 2-MP standards. UV spectra of the polymers (200-400 nm) were determined before and after addition of DTT.

2.6. Gel permeation chromatography (GPC) characterization of the polymers

The molecular weights of the synthesized polymers were determined by GPC analysis using a Viscotek-GPCmax (Viscotek, Oss, The Netherlands) light scattering/viscosimetric detection system, using a Shodex OHPak SB-806 or SB-804 8.0x300 mm columns in series with a Shodex OHPak SB-G 6.0x50 mm guard column and 0.3 M NaOAc pH 4.4 as eluent [35]. The flow rate was 0.7 mL/min and the run time was 50 min. Data from the laser photometer (λ = 670 nm) (right (90°) and low (7°) angle light scattering), refractive index detector (RI) and viscosity detector were integrated using OmniSEC software to calculate the number and weight average molecular weight (M_n, M_w) and polydispersity index (PDI). Besides, UV detection at 280 nm, specific for the PDS group, was also applied [34]. Pullulan (M_n=170 kDa, M_w=178 kDa, Viscotek Benelux (Oss, the Netherlands)) was used for calibration.

2.7. Polyplex preparation

2.7.1. Complexation

Polyplexes were prepared by mixing 100 µL of polymer solutions in 20 mM Tris-HCl pH 8.5 buffer (e.g. 0.6-0.7 mg/mL for pHDP-PEG 85/15 at N/P=4) with 200 µL (75 µg/mL) of pDNA (pCMV-luc or pCMV-EGFP) solutions in the same buffer, to a yield a final pDNA concentration of 50 µg/mL. The polyplexes were incubated for 10 min at room temperature.

When higher concentrations of the polyplex dispersions were required, the pDNA and polymer concentrations were increased, and volume ratios were kept constant.

2.7.2. Crosslinking

After polyplex formation (section 2.7.1) for 10 min, polyplexes were crosslinked by addition of 3,6-dioxa-1,8-octane-dithiol (DODT) crosslinker solution (0.5 mg/mL in mQ H_2O) corresponding to one molar equivalent of DODT thiol groups to PDS

groups of the polymer. The DODT amounts were dependent on the molarity of PDS groups per weight of polymer (determined as mentioned in section 2.5, shown in Table 1) and N/P of the polyplexes. The DODT solution was added to the polyplexes in 3 steps, separated by 15 min. Particle crosslink efficiency was monitored by UV-spectroscopy by determining the molarity of 2-MP released upon crosslinking and compared with the expected released amount from the free polymer.

2.7.3. Decationization

After crosslinking, the polyplex dispersions were incubated at 37 °C, keeping the polyplexes in the buffer of preparation (20 mM Tris-HCl pH 8.5), to hydrolyze the DMAE groups from the polymers. After 6 h hydrolysis, the ionic strength and pH were adjusted to physiological conditions (150 mM, pH 7.4), by addition of 37.5 µL of 200 mM HEPES (1.3 M NaCl, pH 6.5) and mQ H_2O to a final volume of 375 µL, corresponding to a pDNA concentration of 40 µg/m. When purification of the polyplexes was needed (e.g. in vitro assays), polyplex preparation buffer was exchanged to HEPES buffered saline (HBS; 20 mM HEPES, 150 mM NaCl, pH 7.4) by ultrafiltration with vivaspin tubes (MWCO 100 kDa).

2.8. Particle size determination

The size of the polyplexes was measured with Dynamic Light Scattering (DLS) on an ALV CGS-3 system (Malvern Instruments, Malvern, UK) equipped with a JDS Uniphase 22 mW He-Ne laser operating at 632.8 nm, an optical fiber-based detector, a digital LV/LSE-5003 correlator with temperature controller set at 25 °C or 37 °C. Measurements were performed HBS (20 mM HEPES, 150 mM NaCl, pH 7.4) at a pDNA concentration of 10 µg/mL.

2.9. Zeta potential determination

The zeta potential (ζ) of the polyplexes was measured using a Malvern Zetasizer Nano-Z (Malvern Instruments, Malvern, UK) with universal ZEN 1002 ‘dip’ cells and DTS (Nano) software (version 4.20) at 25 °C or 37 °C. Polyplex zeta-potential measurements were performed in 20 mM HEPES pH 7.4 at a pDNA concentration of 10 µg/mL.

2.10. ^{1}H NMR analysis of pHDP-PEG based polyplexes

In order to establish the minimum time needed to hydrolyze the DMAE groups, crosslinked pHDP-PEG 85/15 based polyplexes (N/P=8) were prepared in 20 mM Tris-HCl buffered D_2O pD 8.5. The ^{1}H NMR spectrum was determined 30 min after polyplex preparation. A second spectrum (to the same sample) was determined after incubation of the sample for 6 h at 37 °C. Polyplex preparation was done using the procedure described in section 2.7, however, a final concentration of 150 µg/mL pDNA was used and no purification of the polyplexes was performed. Spectra were taken at 25 °C using 256 scans.

2.11. Polyplex stability

2.11.1. Polyplex properties and stability determined by DLS and zetasizer

Polyplex properties and stability during hydrolysis of DMAE groups were determined by continuous DLS (Z-average, scattered light intensity (SLI), PDI) and zetasizer (ζ-potential) measurements at 37 °C in 20 mM Tris-HCl pH 8.5. pHDP-PEG 85/15 polyplexes (crosslinked (DLS and zetasizer) and non-crosslinked (DLS)) were prepared with N/P=4 at pDNA concentration of 50 µg/mL. Next, the concentration was adjusted to a pDNA concentration of 10 µg/mL, with 20 mM Tris-HCl pH 8.5. Data were collected at regular time points of 30 min.

2.11.2. Gel Retardation Assay

Polyplex (in)stability was studied by addition of dithiothreitol (DTT) (as reducing agent) and/or heparin (as counter polyanion). Two microliters of DTT (250 mM) and/or 0.4 µL heparin sodium salt (50 mg/mL) were added to 25 µL of polyplex dispersion in HBS (40 µg/mL of pDNA). Next, the sample volume was adjusted to 50 µL with HBS, yielding a final pDNA concentration of 20 µg/mL, 10 mM DTT and 0.4 µg/µL heparin. After 7 h incubation time at 37 °C, 20 µL of the sample was mixed with 4 µL 6× DNA Loading Dye, loaded into 0.8% agarose gel in Tris-acetate-EDTA (TAE) buffer containing 0.5 µg/mL ethidium bromide and run at 120 V for 40 min. pDNA was detected using a Gel Doc™ XR+ system (BioRad Laboratories Inc., Hercules, CA) with Image Lab software.

2.12. *In vitro* transfection and cytotoxicity studies

In vitro studies were performed based on the methods previously described by van Gaal et al. [22]. In detail, HeLa cells were cultured in DMEM supplemented with antibiotics/antimycotics and 10% FBS. Cells were maintained at 37 °C in a 5% CO_2 humidified air atmosphere.

For Luciferase and XTT assays 5,000 HeLa cells/well were seeded into 96-well plates 24 h prior to transfection. For uptake analysis, 30,000 cells/well were seeded into 24-well culture plates.

Immediately prior to transfection, the culture medium was replaced with DMEM supplemented with 12.5% FBS with or without 125 µM chloroquine. Next, 25 µL (96-well plate) or 150 µL (24-well plate) of polyplex dispersions containing 10, 40 or 150 µg/mL of pDNA was added per well. After 24 h incubation time, the culture medium was replaced with fresh DMEM containing 10% FBS. Cells were additionally incubated for 24 h and analyzed. Polyplexes based on Exgen 500 have high transfection activities in vitro in different cell lines, also in the presence of serum [22, 36]. Consequently, this polymer was used as control and polyplexes were prepared according to the manufacturer's protocol at N/P=6; a detailed description of particle size and zeta potential for ExGen 500 can be found elsewhere [22]).

Luciferase expression assay was performed 48 h after transfection. Cells were washed with 100 µL of cold PBS and lysed with 50 µL of lysis buffer (Reporter Lysis Buffer 5× (Promega), diluted in mQ H_2O). A freeze-thaw cycle was performed by incubating cells for 1 h at -80 °C. Next, 5 µL of cell lysate was mixed with 25 µL of Luciferase Assay Reagent (Promega), after 2 s luminescence was measured for 10 s using a FLUOstar OPTIMA microplate, equipped with a luminescence light guide (BMG LabTech, Germany). The obtained luciferase activity was normalized to the amount of protein in the lysates determined by the Micro BCA Protein Assay Reagent Kit (Pierce). Results are expressed as relative light units (RLU) per µg of cellular protein.

In parallel with the luciferase expression assay, cell viability was determined using the XTT colorimetric assay which determines the cellular metabolic activity. Two hours before performing the XTT assay, the medium was refreshed and 2 h later, 50 µL of a freshly prepared XTT solution (25 µM *N*-methyl dibenzopyrazine methylsulfate (PMS) and 1 mg/mL 2,3-bis(2-methoxy-4-nitro-5-sulfophenyl)-2*H*-tetrazolium-5-carboxanilide (XTT) in plain RPMI 1640 medium) was added per

well. Next, the cells were incubated for 1 h at 37 °C in a CO_2-incubator. Absorbance was measured at 490 nm with a reference wavelength of 655 nm. Cell viability is expressed as relative metabolic activity normalized against cells cultured with HBS without polyplex dispersions.

2.13. LDH assay

The polyplex capability to interfere on the membrane integrity was analyzed by CytoTox-ONE kits, which determines the lactate dehydrogenase (LDH) release from cells after exposure of polyplex samples. The assays were performed using a 96-well plate, where 5,000 HeLa cells were plated 24 h before treatment. Immediately after sample addition, the culture medium was replaced with DMEM supplemented with 12.5% FBS. Next, 25 µL of polyplex dispersions containing 40 µg/mL of pDNA was added per well. After 24 h incubation time, LDH activity was determined according to the manufacturer's protocol.

2.14. Cellular uptake of polyplexes

pDNA was labeled with Cy5 according to the manufacturer's protocol using a Label IT Nucleic Acid Labeling Kit and polyplexes were prepared as described in section 2.7 (final pDNA concentration 10 µg/mL). Polyplexes were incubated with the HeLa cells for 1, 4 and 24 h and washed 3 times (PBS, glycine buffer (0.2 M glycine, 0.15 M NaCl, pH 3), and PBS). The degree of cellular uptake (Cy5-positive cells) was determined by flow cytometry (see section 2.16).

2.15. Electroporation assisted transfection

Firstly, a 1×10^6 cells/mL of a suspension of HeLa cells was prepared in PBS and kept on ice. Decationized crosslinked polyplexes (N/P=16) or naked pDNA (pCMV_EGFP) were prepared with a final pDNA concentration of 40 µg/mL in HBS. Fifty microlitres (2 µg of pDNA) of the samples was added to 200 µL of cell suspension (200,000 cells). Next, the samples were transferred into Electroporation Cuvettes Plus 640 4mm gap (BTX, San Diego, USA), and the electroporation was performed at 250 V for 10 ms (Electro Square Porator ECM830 with Safety Stand 630B, BTX, San Diego, USA). Immediately after electroporation, the cell suspension

was added to 750 µL DMEM supplemented with 13.3% FBS and 600 µL of cell suspension was plated into a 24-well plate. After overnight incubation, the medium was refreshed with DMEM supplemented with 10% FBS. EGFP expression of each sample was determined by flow cytometry, 48 h after electroporation.

2.16. Flow cytometry

The cell samples from 24 well plate (sections 2.14 & 2.15) were washed, trypsinized (50 µL Trypsin/EDTA 1×) and resuspended in DMEM supplemented with 10% FBS (150 µL) to inactivate trypsin. The cells were subsequently transferred into a round bottom 96-well plate and centrifuged for 5 min at 250 ×g at 4 °C. After medium removal, the cells were resuspended in 100 µL phosphate-buffered albumin (PBA; 1% w/v albumin in PBS) and fixed with 100 µL of 10% formalin. Samples were analyzed by flow cytometry on a FACSCantoII (Becton and Dickinson, Mountain View, CA, USA) equipped with a 488 nm 20 mW Solid State diode laser and a 633 nm 20 mW He–Ne laser. 10,000 Cell events were recorded per sample to determine Cy-5 positive cells (APC channel) or EGFP expression (FITC channel).

3. RESULTS AND DISCUSSION

3.1. Synthesis of HPMA–DMAE

The synthesis of HPMA–DMAE was performed by reaction of CDI activated DMAE with (Scheme S1), followed by column chromatographic purification. The synthesis approach was slightly modified from the route previously described by Funhoff et al. [28]. HPMA–DMAE was obtained in a relatively good yield (67%) and purity (undetected inhibitor in ^{1}H NMR and UPLC).

3.2. Synthesis of PDTEMA

PDTEMA was synthesized in a two-step route. First, 2,2'-dipyridyl disulfide reacted cysteamine hydrochloric to yield PDTEA•HCl, as previously described by Zugates et al. [31]. The second step of the reaction to yield PDTEMA, was

performed by methacrylation of PDTEA•HCl in a two-phase system of chloroform and an aqueous solution of NaOH (Scheme S2). The product was obtained in a yield of 43% and very good purity as evidenced from ^{1}H NMR and UPLC analysis.

3.3. Synthesis and characterization of p(HPMA–DMAE-co-PDTEMA)-b-PEG

HPMA–DMAE was randomly copolymerized with PDTEMA using a 5 kDa PEG bi-functionalized azo macroinitiator ((mPEG5000)$_2$-ABCPA) [27] to yield p(HPMA–DMAE-co-PDTEMA)-b-PEG (yield 40-45%). Different feed ratios of HPMA–DMAE/PDTEMA (100/0, 95/15, 90/10, 85/15) were used (Scheme S3). HPMA was chosen as monomer for the second block of the polymer, mainly because of the safety profile of pHPMA and since it is a methacrylamide monomer, it can be easily polymerized via radical polymerization with a PEG macroinitiator. Furthermore, direct functionalization of the HPMA monomer into HPMA–DMAE, directly gives the desired decationizable polymer without necessity of post-functionalization. PDTEMA, being also a methacrylamide monomer, can be randomly copolymerized with HPMA. The PDS functionality of the PDTEMA monomer allows an efficient and mild crosslinking reaction to yield the interchain disulfide crosslinks in the core of the polyplexes.

The block copolymer compositions were determined by ^{1}H NMR and UV spectroscopy. The molar ratio of HPMA–DMAE/PDTEMA in the polymers was determined using NMR analysis by comparing the integrals at δ 4.6 ppm (methylene proton of HPMA) and at δ 8.5 ppm (aromatic proton of PDTEMA) as shown in Figure S1 for pHDP-PEG 85/15. Table 1 gives an overview of the polymer molecular weights and compositions as determined by ^{1}H NMR, GPC and UV spectroscopy. This table shows that the HPMA–DMAE/PDTEMA copolymer compositions, obtained by NMR, were very close to feed and that the molarity of the PDS groups per weight of polymer (PDS/polymer) determined by NMR were close to the values obtained by UV spectroscopy. Table 1 also shows the absolute molecular weights of the synthesized polymers as determined by GPC using a combination of light scattering and viscometry detection. The table shows that with increasing PDTEMA in the feed, an increase in both M_n and M_w was clearly observed. It is known that disulfides can act as chain transfer agents during free-radical polymerization [37] and therefore the observed increasing M_n and M_w with increasing amount of PDTEMA might be ascribed to branching. It is important to note that side reactions during polymerization were not considerable

(did not result in crosslinking), since all polymers were highly soluble in aqueous solutions and able to form nanosized particles (no aggregates were detected in DLS measurements). Table 1 also shows that M_n values determined by GPC are higher than those calculated by NMR and reported in Table 1. These differences are reasonable since termination by recombination of two active chain ends, either main chain or multiple branches, or by reaction of an active chain with an initiator radical would lead in average to more than one PEG block per polymer chain, and M_n based on NMR is calculated assuming only one PEG block per polymer chain.

Table 1. Characteristics of the synthesized pHDP-PEG as determined by ^{1}H NMR, GPC (light scattering and viscometry detection) and UV spectroscopy. [a]Determined by 1H NMR spectroscopy. [b]Determined by GPC. [c]Determined by UV spectroscopy. Results are expressed as mean±SD (n=3).

				HPMA–DMAE/PDTEMA			
Polymer	M_n (kDa)[a]	M_n (kDa)[b]	M_w/M_n[b]	Feed (%mol/%mol)	Copolymer (%mol/%mol)[a]	PDS/Polymer (nmol/mg)[a]	PDS/Polymer (nmol/mg)[c]
pHDP-PEG 85/15	27.0	254	1.2	85/15	87/13	420	342±1
pHDP-PEG 90/10	23.8	77	1.7	90/10	91/9	274	208±2
pHDP-PEG 95/5	24.9	52	2.0	95/5	95/5	154	107±2
pHD-PEG	20.6	27	1.8	100/0	n.d.	n.d.	n.d.

3.4. Preparation and characterization of disulfide crosslinked decationized polyplexes

Polyplex preparation, characterization and *in vitro* tests were performed with pHDP-PEG 85/15, which allows the formation of polyplexes with the highest crosslinking density. This polymer contains approximately one crosslinking point (PDTEMA) per 7 cationic units (HPMA–DMAE) and on the average 11.4 PDTEMA units per polymer molecule.

Polyplexes of pHDP-PEG and pDNA were formed in 20 mM Tris-HCl pH 8.5. This pH was selected because it is below the pK_a of HPMA–DMAE (9.5 [28]) and therefore results in almost full protonation of the polymer and allows a fast hydrolysis of the carbonate ester bond linking the cationic DMAE side group with the HPMA backbone (half-life of 10-11 h at pH 7.4 and 37 °C [28, 38]). Furthermore, the kinetics of polyplex crosslinking via thiol-disulfide exchange reaction between

the thiol groups from the dithiol DODT and PDS groups from PDTEMA is faster in this pH, when compared to a crosslinking reaction at pH 7.4. The size (and size distribution) of the polyplexes throughout the 3-step preparation process (Scheme 1) was evaluated by DLS (Table 2). Polyplexes prepared at N/P=4 gave small and stable polyplexes with highest *in vitro* transfection activity (Supporting Information). Polyplexes formed by complexation at pH 8.5 had a diameter of 120±4 nm and a PDI of 0.127±0.042. These polyplexes were subsequently crosslinked by addition of the dithiol compound (DODT), at a molar equivalent of thiol groups to the PDS groups of the polymer. Crosslinking was monitored by UV-spectroscopy analysis (measuring the release of 2-MP) and showed that ~95% of the PDS groups was released, indicating efficient crosslinking. Polyplex properties (size and PDI) were not significantly changed after the crosslinking reaction (Table 2). Before and after crosslinking, the polyplexes possessed positive zeta potentials close to 10 mV, which is significantly lower than the surface charge of polyplexes based on the corresponding homopolymer pHPMA–DMAE (+20 mV) [3, 28], and can be ascribed to the surface charge shielding of the polyplexes by the PEG corona.

Table 2. Particle z-average diameter (Z-avg) and polydispersity index (PDI) determined by DLS and particle charge (ζ Pot) determined by zeta-potential measurements of different pHDP-PEG based polyplexes, at different stages of preparation. Prepared at N/P=4 and a pDNA concentration of 50 μg/mL in 20 mM Tris-HCl pH 8.5. Results are expressed as mean±SD (n=3).

Polyplexes	DLS		Zetasizer
	Z-avg (nm)	PDI	ζ Pot (mV)
Before crosslinking	120±4	0.127±0.042	11.4±1.6
After crosslinking	122±6	0.156±0.023	10.1±2.3
After decationization	128±7	0.202±0.084	-4.9±1.9

Decationization was performed by incubation of the crosslinked polyplexes at 37 °C and pH 8.5 for 6 h to trigger hydrolysis of the cationic DMAE groups. During this procedure, the size slightly increased from 122±6 nm to 128±7 nm. Importantly, the surface charge of decationized polyplexes decreased from +10.1±2.3 mV to -4.9±1.9 mV, confirming loss of the cationic DMAE groups from the polyplexes. The kinetics of positive surface charge loss of the disulfide crosslinked polyplexes during decationization is shown in Figure S2, demonstrating a fast decrease in surface charge overtime. After 20 h of hydrolysis, the polyplexes have a negative

zeta-potential (-20 mV) which can likely be ascribed to the negative charge of the polyplex core due to the presence of DNA, which is not fully shielded by the PEG-corona. On the other hand and in contrast to disulfide crosslinked polyplexes, when non-crosslinked polyplexes were incubated at pH 8.5 and 37 °C a rapid increase in polyplex size and scattered light intensity was observed after 5 h of incubation of the polyplexes. Further, the intensity of scattered light started to decrease at this time point, as result of disappearance of the particles (Figure S4a), because of loss of the complexation ability of the polymer as a result of DMAE side group hydrolysis, finally resulting in polyplex destabilization [28]. Importantly, crosslinked polyplexes kept a relatively stable size (and PDI) and intensity of the scattered light for 24 h (Figure S4b), proving that particles are hydrolytically stable and again demonstrating that the integrity was preserved by covalent disulfide crosslinks between the polymer chains. Decationized polyplexes obtained upon incubation of pHDP-PEG polyplexes for 6 h at pH 8.5 and 37 °C had a slight negative zeta-potential (-5 mV). In literature, many papers have been published in which it has shown that nanoparticles with a negative zeta-potential have excellent circulation behavior upon iv administration [39-44]. Also, the clinically applied liposomal formulation of doxorubicin that has a half-time in humans of 90 h [45] has a negative zeta-potential [46].

The carbonate ester bonds linking the DMAE groups to the pHPMA backbone are much more hydrolytically sensitive than the ester bond that connects the PEG block to the pHDP block (half-life of 34 h at pH 8.5 and 37 °C) [28, 47]. Nevertheless, prolonged incubation at pH 8.5 and 37 °C might result in co-hydrolysis of the ester bond connecting the two blocks, leading to unwanted loss of PEG chains. Consequently, establishment of the minimum hydrolysis time for the DMAE group hydrolysis was crucial. The rate of hydrolysis of the carbonate ester bond connecting the cationic DMAE groups to the pHPMA backbone can be determined directly by ^{1}H NMR through the disappearance of the peak at δ4.2 ppm ($OC\underline{H_2}CH_2$), which is ascribed to the DMAE group [28]. Based on the previously determined half-life of the carbonate ester bond at pH 7.4 and 37 °C (10-11 h) [28, 38]. It is calculated that ~6 h incubation at pH 8.5 and 37 °C will result in an extent of hydrolysis of >99%. Indeed, this is confirmed in Figure 2, since specific signal of the DMAE group at δ4.2 ppm was hardly detectable after incubation of disulfide crosslinked pHDP-PEG 85/15 polyplexes for 6 h at pH 8.5 and 37 °C. The core of the polyplexes consists of pHPMA and DNA, which are both hydrophilic polymers, assuring good accessibility for water molecules. Our results show a high efficiency

of the crosslinking reaction (~95%) meaning that the water-soluble crosslinker can indeed easily access the core of the polyplexes.

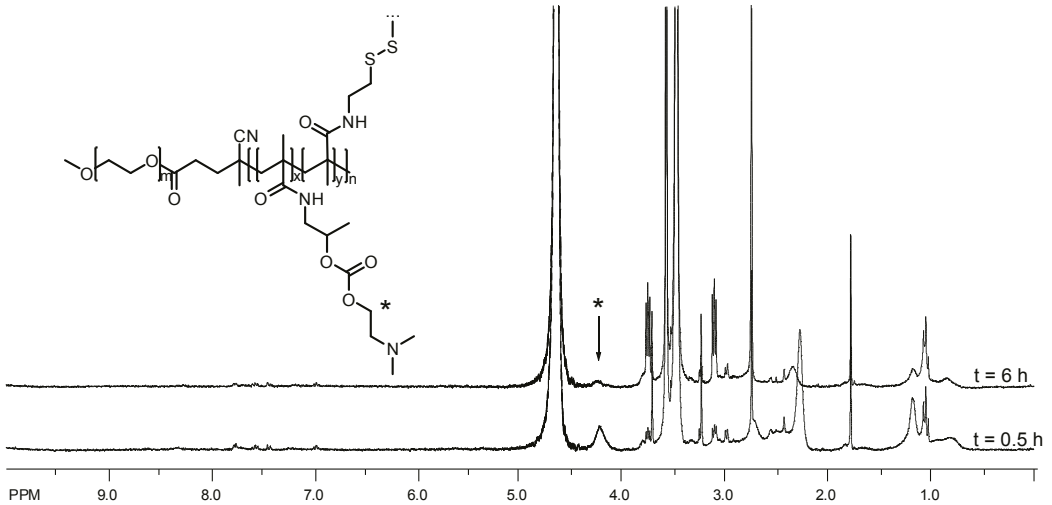

Figure 2. ^{1}H NMR spectra of disulfide crosslinked pHDP-PEG based polyplexes 30 min and 6 h after incubation at 37 °C in D_2O buffered with 20 mM Tris-HCl pD 8.5.

3.5. Stability of disulfide crosslinked pHDP-PEG polyplexes

The (in)stability of polyplexes before and after decationization was studied by an agarose gel retardation assay (Figure 3). Both cationic and decationized polyplexes exposed to only HBS buffer for 7 h, did not show release of pDNA (lanes 2), demonstrating that after decationization pDNA remained fully entrapped in the crosslinked core of the polyplexes, as conventional polyplexes. DLS stability studies showed that the size (and PDI) of polyplexes remained unchanged for at least 24 h. When polyplexes were exposed to DTT (lanes 3) (mimicking the intracellular reductive environment), pDNA release was only observed for the decationized polyplexes and not for the cationic polyplexes. After cleavage of the polyplex crosslinks by reduction with DTT, the cationic polyplexes maintained the electrostatic interactions with pDNA and the polyplexes are preserved. On the other hand, decationized polyplexes destabilized and released pDNA upon exposure to DTT, because of lack of interactions of the remaining neutral polymer formed after hydrolysis of the DMAE side groups with pDNA. Further, disulfide crosslinked polyplexes (both cationic and decationized) treated with an excess

of the negatively charged macromolecule heparin, which has been shown to destabilize non-crosslinked polyplexes [48, 49], did not show release of pDNA (lanes 4), confirming successful stabilization through disulfide cross-linking. This is an important observation since polyplex destabilization by polyanions has been reported to occur in both extracellular and intracellular media [50], and interchain disulfide crosslinks are expected to protect against destabilization from polyanions, present in the circulation and extracellular environment [24, 51, 52]. This observation also demonstrates a high and stable DNA loading capacity of decationized polyplexes. By using an N/P=4, a quantitative complexation was obtained after decationization. When crosslinks were cleaved by DTT and, at the same time, polyplexes were exposed to an excess of heparin, pDNA release was observed (lanes 5).

To further prove extensive hydrolysis of DMAE groups and explain the release of pDNA from the decationized pHD-PEG upon incubation with only 10 mM DTT (lane 3), polyplexes were prepared with the same properties as used in the gel retardation assay, followed by continuous DLS size measurement in the presence of 10 mM DTT in HBS at 37 °C (Figure S4a). In a parallel experiment, samples were collected from the polyplex suspension at different time points of hydrolysis and loaded into an agarose gel to access the release of pDNA from the polyplexes in time (Figure S4b). Figure S4a shows that immediately after addition of DTT the scattered light intensity rapidly decreases, even though the average size also shows fast increase. This clearly reveals that the great majority of polyplexes disassembled, due to the lack of electrostatic interactions, and due to a continuous cleavage of the disulfide network, which is supported by a continuous increase in the release of pDNA in both open circular and supercoiled form, as shown in Figure S4b. After, 7 h incubation with DTT, the light scattering signal is close to zero, showing that the great majority of the polyplexes were dissociated. At the same time, the formation of some aggregates is observed. Assuming that at least 1% of the HPMA monomers still contain the DMAE group, and because these aggregates contain a very high local concentration of polymer, some interactions between pDNA and polymer are expected. On the other hand, it has been reported that PEG induces DNA precipitation [53] or even condensation and particle formation [54]. In conclusion, it is expected that aggregates formed contain the remaining pDNA, and it is shown in the gel retardation assay (Figure 3) that heparin is needed to completely extract the remaining fully functional pDNA. The behavior of decationized polyplexes is in great contrast with the cationic polyplexes, which

show an increase in size and scattered light intensity, due to some degree of hydrolysis followed by hydration of the core over 7 h of incubation with 10 mM DTT in HBS at 37 °C (Figure S5). Furthermore, no release of pDNA is observed as shown in Figure 3 (lane 3).

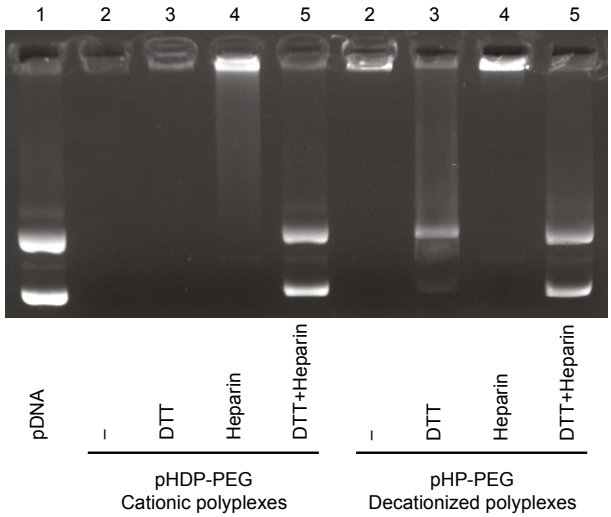

Figure 3. Agarose gel retardation assay of cationic polyplexes and disulfide crosslinked pHDP-PEG polyplexes after incubation for 6 h in 20 mM Tris-HCl pH 8.5 at 37 ºC (decationized polyplexes) and comparison with polyplexes not subjected to hydrolysis (cationic polyplexes), Lane 1, naked pDNA; lane 2, sample without any destabilization agent; lane 3, sample treated with 10 mM DTT; lane 4, sample exposed to heparin; lane 5, sample exposed to 10 mM DTT and heparin.

3.6. *In vitro* evaluation of polyplexes

The cytotoxicity and transfection efficiency of the disulfide crosslinked decationized (pHP-PEG) and cationic (pHDP-PEG) polyplexes was evaluated in HeLa cells in the presence of serum. Firstly, the cytotoxicity assay of the polyplexes was generally evaluated by an XTT assay (Figure 4). This assay shows that a high metabolic activity was found for the cells incubated with pHP-PEG and pHDP-PEG based polyplexes at all pDNA doses tested, including a very high dose of 3 µg pDNA per well. At this dose, cells treated with linear PEI showed no metabolic activity above the background. Neutral Red assay (Supporting Information Figure S10) was performed to determine the number of viable cells, showing that both

pHP-PEG and pHDP-PEG did not affect cell viability, which confirms the results obtained by XTT. In the case of ExGen the lowest pDNA dose did not lead to a decrease in the number of viable cells, however higher doses showed a significant decrease in cell viability.

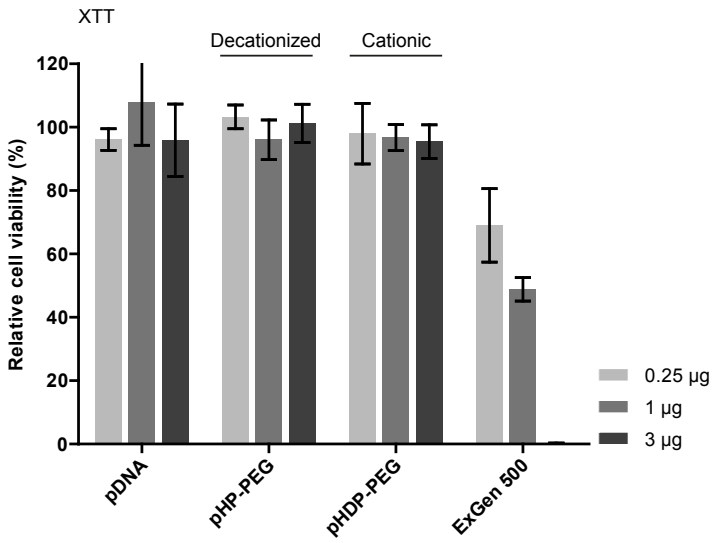

Figure 4. Effect of pDNA dose (0.25, 1 and 3 µg of pDNA/well) on cell viability, determined by XTT assay, for the different polyplexes (pHP-PEG and pHDP-PEG N/P=4). HeLa cells were transfected in the presence of 10% serum. Results are expressed as mean±SD (n=3).

The cytoxicity of the different formulations was also studied using the LDH release assay (Figure 5) which is indicative for cellular membrane destabilizing capability of the polyplexes, giving more insights in the cytocompatibility of the polyplexes. The detected enzymatic activity of released LDH from the cells upon incubation with both cationic and decationized polyplexes was at the same level as naked pDNA, whereas ExGen 500 showed significantly higher LDH release, again pointing to a good cytocompatibility of the pHP-PEG and pHDP-PEG polyplexes and a high cytotoxicity of the PEI-based systems.

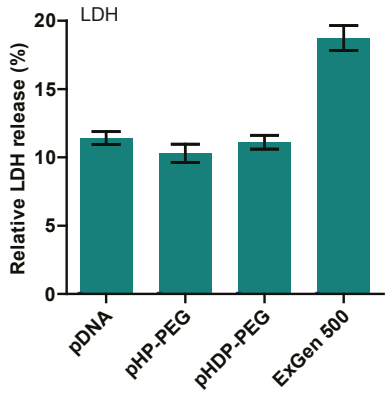

Figure 5. Relative LDH release from HeLa cells upon their incubation with the different polyplexes (1 μg pDNA/well; pHP-PEG and pHDP-PEG N/P=4) in the presence of 10% serum. Results are expressed as mean±SD (n=6).

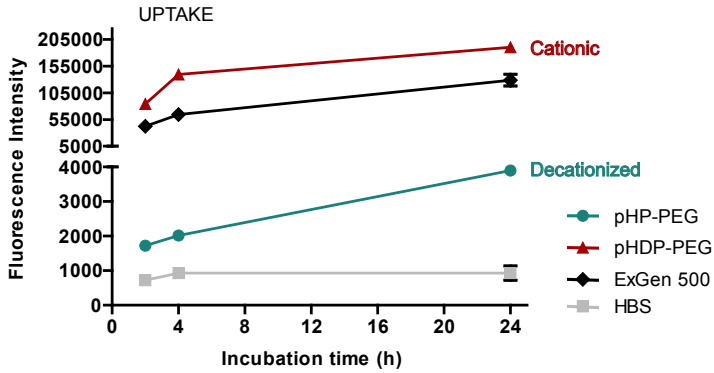

Figure 6. Degree of cellular uptake of Cy5-labelled pDNA-based polyplexes in HeLa cells, depending on the incubation time of HeLa cells in time the polyplexes (2, 4 and 24 h), determined by flow cytometry (0,25 μg pDNA/well; pHP-PEG and pHDP-PEG N/P=4). Results are expressed as mean±SD (n=3).

Uptake studies of Cy5-labeled pDNA containing polyplexes by HeLa cells are shown in Figure 6. After incubation with the polyplexes, the cells were subjected to an acid wash (0.2 M glycine, 0.15 M NaCl, pH 3) to remove cell-surface adsorbed polyplexes [55]. Results showed that the extent of uptake for decationized polyplexes was more than 50-fold lower than for the cationic pHDP-PEG based systems, which showed a high degree of uptake (in the same order of ExGen), as previously also observed for other PEG shielded cationic polyplexes [56, 57].

It has been suggested that for nontargeted cationic polyplexes, cell uptake occurs firstly by electrostatic interaction with membrane anionic components [58-60], explaining the differences in uptake degree between cationic and decationized polyplexes. Furthermore, the low degree of nonspecific uptake of the decationized pHP-PEG polyplexes confirms their stealth behavior, which allows these polyplexes to be used for specific cellular uptake using polyplexes decorated with a suitable targeting ligand.

The high cytocompatibility obtained for the extensively taken up cationic pHDP-PEG polyplexes was expected since polyplexes based on pHPMA–DMAE have been previously studied, both *in vivo* (after local administration) and *in vitro* (in the absence of serum) showing very good biocompatibility [3, 28]. The lack of cytotoxicity of the pHPMA–DMAE based polyplexes is partly attributed to its biodegradable character, showing a relatively fast hydrolysis at physiological conditions. But, as shown in the uptake study, the cationic polyplexes show a high degree of nonspecific uptake, which makes them unsuitable for the application we aim for our system: targeted therapy upon systemic administration. Further, in many studies it has been shown that cationic polyplexes show cellular cytotoxicity, pointing to a need of neutral systems.

The efficiency of the polyplexes to induce transgene expression was firstly evaluated by a luciferase transfection assay (Figure 7) for polyplexes prepared at N/P=4, in the presence of serum as well in the absence and presence of chloroquine, a known endosomal disruptive agent [61]. Figure 7 shows that decationized polyplexes induced an approximately order of magnitude lower luciferase expression, as compared to polyplexes containing cationic DMAE groups in the presence of chloroquine. Differences in transfection level between cationic pHDP-PEG and decationized pHP-PEG polyplexes can be explained by different degrees of cellular uptake, as shown Figure 6. Figure 7 also shows that the presence of chloroquine induced transfection levels that were at least one order of magnitude higher than those in its absence, for both pHDP-PEG and pHP-PEG polyplexes. Compared to linear PEI in its optimal formulation (ExGen 500, N/P=6) [22], pHDP-PEG and pHP-PEG derived polyplexes showed lower efficiency, however, significant levels were observed. At the highest pDNA dose the cationic polyplexes in the presence of chloroquine showed a transfection level at the same order of magnitude of polyplexes based on linear PEI in its optimal formulation.

Polyplexes are known to end up in acidic vacuoles after cellular uptake, and therefore endosomal escape of polyplexes before digestion in lysosomes is an important step for efficient transfection [58, 60, 62, 63]. Chloroquine is known to induce endosome disruption [61], leading to an increase of the transfection of the polyplexes lacking endosomal escaping functionalities. Consequently, the lower degree of gene expression of cells exposed to the decationized polyplexes can be explained by their limited endosomal escape properties in combination with their low extent of uptake.

A second cell line (the A549 lung cancer cell line) was also tested to evaluate the transfection efficiency of the different polyplexes (Figure S11). pHDP-PEG and pHP-PEG polyplexes were prepared at N/P=4 and transfection was performed in the presence of 10% FBS. Both pHP-PEG and pHDP-PEG polyplexes showed a similar transfection pattern as observed for HeLa cells. However, it should be noted that a significant transfection level was obtained even in the absence of chloroquine and at the highest pDNA dose, pHDP-PEG polyplexes show an even higher transfection activity than ExGen 500 systems. Further, chloroquine induces higher transfection, however at a lower level, when compared to the improvement observed for HeLa cells. This probably occurs because the chloroquine concentration is not the optimal for this cell line.

Importantly, in sharp contrast to ExGen (Figure 7) and other cationic polymer-based polyplexes [20, 64], decationized polyplexes transfection levels increased with increasing pDNA dose. Increased pDNA doses for ExGen polyplexes ultimately lead to substantial decrease in transfection, which is intimately related to the toxicity of the formulations [22]. Increasing transfection levels by increasing pDNA dose for the pHP-PEG and pHDP-PEG formulations can be therefore explained by their undetected/low cytotoxicity as shown with XTT and LDH assays.

To force the introduction of pHP-PEG polyplexes into the cells and to overcome also their low endosomal escape, electroporation of HeLa cells in the presence of polyplexes was performed. Interestingly, flow cytometry (Figure 8) showed similar percentage HeLa cells expressing enhanced green fluorescent protein (EGFP) after electroporation in the presence of either naked pDNA (positive control) or pHP-PEG polyplexes. This demonstrates that decationized pHP-PEG based polyplexes are indeed able to successfully induce transgene expression once efficiently introduced into the cells. Moreover, these results also show that interchain disulfide crosslinks are indeed cleaved intracellularly due to the

presence of relatively high concentration of intracellular glutathione, resulting in similar expression levels as naked pDNA.

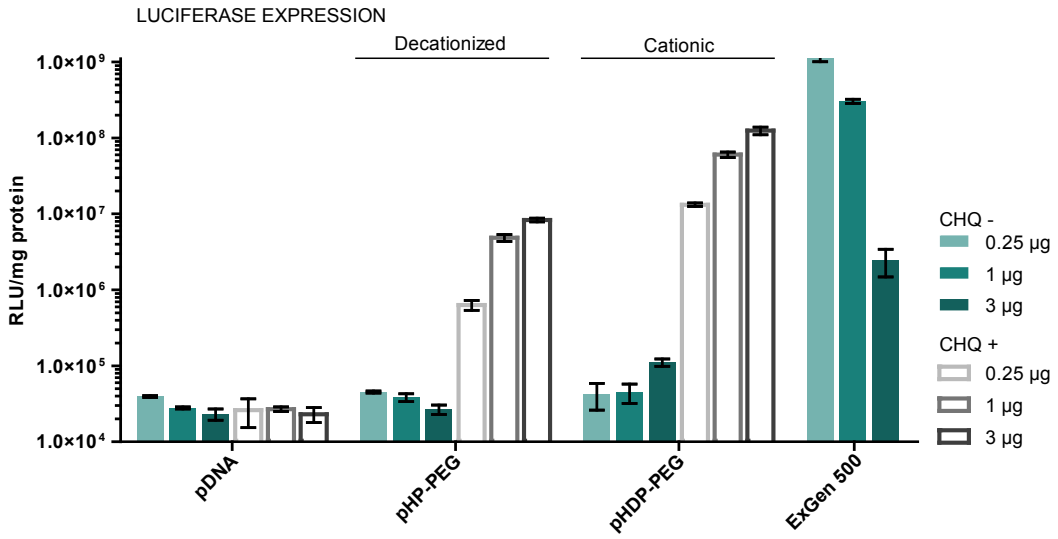

Figure 7. Effect of pDNA dose (0.25, 1 and 3 µg of pDNA/well) and absence (CHQ -) or presence (CHQ +) of chloroquine on luciferase expression levels for the different polyplexes (pHP-PEG and pHDP-PEG N/P=4). HeLa cells were transfected in the presence of 10% serum. Results are expressed as mean±SD (n=3).

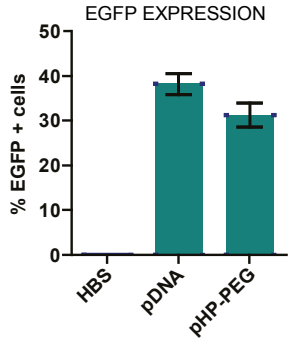

Figure 8. Percentage of EGFP positive HeLa cells analyzed by flow cytometry, upon electroporation of naked EGFP-encoding pDNA or EGFP-encoding pDNA pHP-PEG (N/P=16) based polyplexes (2 µg pDNA/200,000 cells) Results are expressed as mean±SD (n=3).

4. CONCLUSION

The present study describes the preparation, characterization and *in vitro* testing of decationized disulfide crosslinked p(HPMA-co-PDTEMA)-b-PEG polyplexes. The combination of exploiting the efficient charge-driven condensation followed by crosslinking stabilization and finally removal (decationization) of the unnecessary cationic charge, results in neutral polymer-based polyplexes after condensation of the pDNA. The inherent toxicity related to the excess of polycations that are required to stabilize conventional polymeric gene delivery systems can, in this way, be overcome. The results show that these polyplexes based on neutral polymers show several important and distinctive features: 1. High pDNA entrapment not based on charge interactions between polymer and pDNA; 2. Excellent stability of intact particles in extracellular environment (the polyplexes exhibited a stable profile in saline solutions as well as in the presence of polyanions); 3. Triggered release of therapeutic payload upon polyplex crosslink destabilization inside the cells; 4. Excellent safety profile (no cytotoxicity was observed even at the highest dose investigated); 5. Very low degree of nonspecific uptake, when compared to cationic polyplexes, which is favorable for a targeted therapy upon intravenous administration, since low nonspecific uptake is required to direct the system exclusively to targeted sites; 6. Despite the relatively low uptake of nontargeted polyplexes, successful transgene expression was observed (electroporation results confirms the efficiency of these systems once efficiently internalized).

Efficiency of decationized polyplexes is expected to be further increased through higher dosing (possible because of its safety profile) and due to their high chemical and structural flexibility the system is a platform for further optimizations. Introduction of targeting ligands, to improve cellular recognition and internalization, and incorporation of endosomal escaping functionalities, are feasible possibilities to greatly improve its efficiency and make this system a safe and efficient gene delivery vector for targeted therapy after systemic administration.

APPENDIX A. Supporting Information

Methods S1 and S2, Supplemental Schemes S1-3 and Supplemental Figures S1-11 can be found in Supporting Information.

Acknowledgement

L. Novo is financially supported by Fundação para a Ciência e a Tecnologia (FCT), the Portuguese Foundation for Science and Technology, grant SFRH/BD/47085/2008.

References

[1] O. Boussif, F. Lezoualc'h, M.A. Zanta, M.D. Mergny, D. Scherman, B. Demeneix, J.P. Behr, A versatile vector for gene and oligonucleotide transfer into cells in culture and in vivo: polyethylenimine, Proc. Natl. Acad. Sci. U.S.A., 92 (1995) 7297-7301.

[2] R. Duncan, The dawning era of polymer therapeutics, Nat. Rev. Drug Discov., 2 (2003) 347-360.

[3] H.K. de Wolf, J. Luten, C.J. Snel, G. Storm, W.E. Hennink, Biodegradable, cationic methacrylamide-based polymers for gene delivery to ovarian cancer cells in mice, Mol. Pharmaceutics, 5 (2008) 349-357.

[4] J. Luten, C.F. van Nostrum, S.C. De Smedt, W.E. Hennink, Biodegradable polymers as non-viral carriers for plasmid DNA delivery, J. Control. Release, 126 (2008) 97-110.

[5] J. Zhou, J. Liu, C.J. Cheng, T.R. Patel, C.E. Weller, J.M. Piepmeier, Z. Jiang, W.M. Saltzman, Biodegradable poly(amine-co-ester) terpolymers for targeted gene delivery, Nat. Mater., 11 (2012) 82-90.

[6] L. Parhamifar, A.K. Larsen, A.C. Hunter, T.L. Andresen, S.M. Moghimi, Polycation cytotoxicity: a delicate matter for nucleic acid therapy-focus on polyethylenimine, Soft Matter, 6 (2010) 4001-4009.

[7] P. Chollet, M.C. Favrot, A. Hurbin, J.-L. Coll, Side-effects of a systemic injection of linear polyethylenimine–DNA complexes, J. Gene Med., 4 (2002) 84-91.

[8] M. Ogris, S. Brunner, S. Schuller, R. Kircheis, E. Wagner, PEGylated DNA/transferrin-PEI complexes: reduced interaction with blood components, extended circulation in blood and potential for systemic gene delivery, Gene Ther., 6 (1999) 595-605.

[9] C.M. Ward, M.L. Read, L.W. Seymour, Systemic circulation of poly(L-lysine)/DNA vectors is influenced by polycation molecular weight and type of DNA: differential circulation in mice and rats and the implications for human gene therapy, Blood, 97 (2001) 2221-2229.

[10] H.K. de Wolf, J. Luten, C.J. Snel, C. Oussoren, W.E. Hennink, G. Storm, In vivo tumor transfection mediated by polyplexes based on biodegradable poly(DMAEA)-phosphazene, J. Control. Release, 109 (2005) 275-287.

[11] F.J. Verbaan, C. Oussoren, C.J. Snel, D.J.A. Crommelin, W.E. Hennink, G. Storm, Steric stabilization of poly(2-(dimethylamino)ethyl methacrylate)-based polyplexes mediates prolonged circulation and tumor targeting in mice, J. Gene Med., 6 (2004) 64-75.

[12] B. Ballarín-González, K.A. Howard, Polycation-based nanoparticle delivery of RNAi therapeutics: Adverse effects and solutions, Adv. Drug Deliv. Rev., (2012).

[13] D. Fischer, Y. Li, B. Ahlemeyer, J. Krieglstein, T. Kissel, In vitro cytotoxicity testing of

polycations: influence of polymer structure on cell viability and hemolysis, Biomaterials, 24 (2003) 1121-1131.

[14] S.M. Moghimi, P. Symonds, J.C. Murray, A.C. Hunter, G. Debska, A. Szewczyk, A two-stage poly(ethylenimine)-mediated cytotoxicity: implications for gene transfer/therapy, Mol. Ther., 11 (2005) 990-995.

[15] S. Choksakulnimitr, S. Masuda, H. Tokuda, Y. Takakura, M. Hashida, In vitro cytotoxicity of macromolecules in different cell culture systems, J. Control. Release, 34 (1995) 233-241.

[16] C. Lonez, M. Vandenbranden, J.-M. Ruysschaert, Cationic lipids activate intracellular signaling pathways, Adv. Drug Deliv. Rev., 64 (2012) 1749-1758.

[17] W.T. Godbey, K.K. Wu, A.G. Mikos, Poly(ethylenimine)-mediated gene delivery affects endothelial cell function and viability, Biomaterials, 22 (2001) 471-480.

[18] K. Masago, K. Itaka, N. Nishiyama, U.-i. Chung, K. Kataoka, Gene delivery with biocompatible cationic polymer: Pharmacogenomic analysis on cell bioactivity, Biomaterials, 28 (2007) 5169-5175.

[19] K. Regnström, E.G.E. Ragnarsson, M. Köping-Höggård, E. Torstensson, H. Nyblom, P. Artursson, PEI – a potent, but not harmless, mucosal immuno-stimulator of mixed T-helper cell response and FasL-mediated cell death in mice, Gene Ther., 10 (2003) 1575-1583.

[20] S. Boeckle, K. von Gersdorff, S. van der Piepen, C. Culmsee, E. Wagner, M. Ogris, Purification of polyethylenimine polyplexes highlights the role of free polycations in gene transfer, J. Gene Med., 6 (2004) 1102-1111.

[21] K. Kunath, A. von Harpe, D. Fischer, H. Petersen, U. Bickel, K. Voigt, T. Kissel, Low-molecular-weight polyethylenimine as a non-viral vector for DNA delivery: comparison of physicochemical properties, transfection efficiency and in vivo distribution with high-molecular-weight polyethylenimine, J. Control. Release, 89 (2003) 113-125.

[22] E.V.B. van Gaal, R. van Eijk, R.S. Oosting, R.J. Kok, W.E. Hennink, D.J.A. Crommelin, E. Mastrobattista, How to screen non-viral gene delivery systems in vitro?, J. Control. Release, 154 (2011) 218-232.

[23] G. Storm, S.O. Belliot, T. Daemen, D.D. Lasic, Surface modification of nanoparticles to oppose uptake by the mononuclear phagocyte system, Adv. Drug Deliv. Rev., 17 (1995) 31-48.

[24] F. Meng, W.E. Hennink, Z. Zhong, Reduction-sensitive polymers and bioconjugates for biomedical applications, Biomaterials, 30 (2009) 2180-2198.

[25] C. Lin, Z. Zhong, M.C. Lok, X. Jiang, W.E. Hennink, J. Feijen, J.F.J. Engbersen, Linear poly(amido amine)s with secondary and tertiary amino groups and variable amounts of disulfide linkages: Synthesis and in vitro gene transfer properties, J. Control. Release, 116 (2006) 130-137.

[26] K. Miyata, Y. Kakizawa, N. Nishiyama, A. Harada, Y. Yamasaki, H. Koyama, K. Kataoka, Block catiomer polyplexes with regulated densities of charge and disulfide cross-linking directed to enhance gene expression, J. Am. Chem. Soc., 126 (2004) 2355-2361.

[27] D. Neradovic, C.F. van Nostrum, W.E. Hennink, Thermoresponsive polymeric

micelles with controlled instability based on hydrolytically sensitive N-isopropylacrylamide copolymers, Macromolecules, 34 (2001) 7589-7591.

[28] A. Funhoff, C.F. van Nostrum, A. Janssen, M. Fens, D. Crommelin, W.E. Hennink, Polymer side-chain degradation as a tool to control the destabilization of polyplexes, Pharm. Res., 21 (2004) 170-176.

[29] M. Kinuta, N. Masuoka, K. Yao, J. Ohta, S. Yoshida, S. Futani, T. Ubuka, S-[2-Carboxy-1-(1H-imidazol-4-yl)ethyl]cysteine in normal human urine, Amino Acids, 1 (1991) 259-262.

[30] Y.W. Ebright, Y. Chen, P.S. Pendergrast, R.H. Ebright, Incorporation of an EDTA-metal complex at a rationally selected site within a protein: application to EDTA-iron DNA affinity cleaving with catabolite gene activator protein (CAP) and Cro, Biochemistry, 31 (1992) 10664-10670.

[31] G.T. Zugates, D.G. Anderson, S.R. Little, I.E.B. Lawhorn, R. Langer, Synthesis of poly(β-amino ester)s with thiol-reactive side chains for DNA delivery, J. Am. Chem. Soc., 128 (2006) 12726-12734.

[32] L. Field, T.F. Parsons, D.E. Pearson, Organic Disulfides and Related Substances. XVIII. Synthesis and Disproportionation of 2-(Aryldithio)ethylamine Hydrochlorides1a,b, J. Org. Chem., 31 (1966) 3550-3555.

[33] M. Talelli, C.J.F. Rijcken, S. Oliveira, R. van der Meel, P.M.P. van Bergen en Henegouwen, T. Lammers, C.F. van Nostrum, G. Storm, W.E. Hennink, Nanobody – Shell functionalized thermosensitive core-crosslinked polymeric micelles for active drug targeting, J. Control. Release, 151 (2011) 183-192.

[34] D.R. Grassetti, J.F. Murray, Determination of sulfhydryl groups with 2,2'- or 4,4'-dithiodipyridine, Arch. Biochem. Biophys., 119 (1967) 41-49.

[35] X. Jiang, A. van der Horst, M. van Steenbergen, N. Akeroyd, C. van Nostrum, P. Schoenmakers, W. Hennink, Molar-mass characterization of cationic polymers for gene delivery by aqueous size-exclusion chromatography, Pharm. Res., 23 (2006) 595-603.

[36] C.L. Gebhart, A.V. Kabanov, Evaluation of polyplexes as gene transfer agents, J. Control. Release, 73 (2001) 401-416.

[37] S. Harrisson, T.P. Davis, R.A. Evans, E. Rizzardo, Substituent effects on the chain-transfer behavior of 7-methylene-2-methyl-1,5-dithiacyclooctane in the presence of disulfides and thiols, J. Polym. Sci. A Polym. Chem., 40 (2002) 4421-4425.

[38] J. Luten, N. Akeroyd, A. Funhoff, M.C. Lok, H. Talsma, W.E. Hennink, Methacrylamide Polymers with Hydrolysis-Sensitive Cationic Side Groups as Degradable Gene Carriers, Bioconjug. Chem., 17 (2006) 1077-1084.

[39] Y.-P. Li, Y.-Y. Pei, X.-Y. Zhang, Z.-H. Gu, Z.-H. Zhou, W.-F. Yuan, J.-J. Zhou, J.-H. Zhu, X.-J. Gao, PEGylated PLGA nanoparticles as protein carriers: synthesis, preparation and biodistribution in rats, J. Control. Release, 71 (2001) 203-211.

[40] S.H. Jung, D.H. Lim, S.H. Jung, J.E. Lee, K.-S. Jeong, H. Seong, B.C. Shin, Amphotericin B-entrapping lipid nanoparticles and their in vitro and in vivo characteristics, Eur. J. Pharm. Sci., 37 (2009) 313-320.

[41] B. Shi, C. Fang, Y. Pei, Stealth PEG-PHDCA niosomes: Effects of chain length of PEG

and particle size on niosomes surface properties, in vitro drug release, phagocytic uptake, in vivo pharmacokinetics and antitumor activity, J. Pharm. Sci., 95 (2006) 1873-1887.

[42] B. Shi, C. Fang, M.X. You, Y. Zhang, S. Fu, Y. Pei, Stealth MePEG-PCL micelles: effects of polymer composition on micelle physicochemical characteristics, in vitro drug release, in vivo pharmacokinetics in rats and biodistribution in S180 tumor bearing mice, Colloid and Polymer Science, 283 (2005) 954-967.

[43] T.S. Levchenko, R. Rammohan, A.N. Lukyanov, K.R. Whiteman, V.P. Torchilin, Liposome clearance in mice: the effect of a separate and combined presence of surface charge and polymer coating, Int. J. Pharm., 240 (2002) 95-102.

[44] J.S. Lee, M. Ankone, E. Pieters, R.M. Schiffelers, W.E. Hennink, J. Feijen, Circulation kinetics and biodistribution of dual-labeled polymersomes with modulated surface charge in tumor-bearing mice: Comparison with stealth liposomes, J. Control. Release, 155 (2011) 282-288.

[45] Y. Barenholz, Doxil® — The first FDA-approved nano-drug: Lessons learned, J. Control. Release, 160 (2012) 117-134.

[46] O. Garbuzenko, S. Zalipsky, M. Qazen, Y. Barenholz, Electrostatics of PEGylated Micelles and Liposomes Containing Charged and Neutral Lipopolymers, Langmuir, 21 (2005) 2560-2568.

[47] D. Neradovic, M.J. van Steenbergen, L. Vansteelant, Y.J. Meijer, C.F. van Nostrum, W.E. Hennink, Degradation Mechanism and Kinetics of Thermosensitive Polyacrylamides Containing Lactic Acid Side Chains, Macromolecules, 36 (2003) 7491-7498.

[48] D.S. Manickam, J. Li, D.A. Putt, Q.-H. Zhou, C. Wu, L.H. Lash, D. Oupický, Effect of innate glutathione levels on activity of redox-responsive gene delivery vectors, J. Control. Release, 141 (2010) 77-84.

[49] M. Neu, O. Germershaus, S. Mao, K.-H. Voigt, M. Behe, T. Kissel, Crosslinked nanocarriers based upon poly(ethylene imine) for systemic plasmid delivery: In vitro characterization and in vivo studies in mice, J. Control. Release, 118 (2007) 370-380.

[50] D. Oupický, R.C. Carlisle, L.W. Seymour, Triggered intracellular activation of disulfide crosslinked polyelectrolyte gene delivery complexes with extended systemic circulation in vivo, Gene Ther., 8 (2001) 713-724.

[51] N. Nishiyama, K. Kataoka, R. Satchi-Fainaro, R. Duncan, Nanostructured Devices Based on Block Copolymer Assemblies for Drug Delivery: Designing Structures for Enhanced Drug Function Polymer Therapeutics II, in, Springer Berlin / Heidelberg, 2006, pp. 67-101.

[52] M. Ruponen, S. Ylä-Herttuala, A. Urtti, Interactions of polymeric and liposomal gene delivery systems with extracellular glycosaminoglycans: physicochemical and transfection studies, Biochim. Biophys. Acta, 1415 (1999) 331-341.

[53] J.T. Lis, R. Schleif, Size fractionation of double-stranded DNA by precipitation with polyethylene glycol, Nucleic Acids Res., 2 (1975) 383-390.

[54] E. Froehlich, J.S. Mandeville, D. Arnold, L. Kreplak, H.A. Tajmir-Riahi, PEG and mPEG–Anthracene Induce DNA Condensation and Particle Formation, The Journal of Physical Chemistry B, 115 (2011) 9873-9879.

[55] S. Kameyama, M. Horie, T. Kikuchi, T. Omura, A. Tadokoro, T. Takeuchi, I. Nakase, Y. Sugiura, S. Futaki, Acid wash in determining cellular uptake of Fab/cell-permeating peptide conjugates, Biopolymers, 88 (2007) 98-107.

[56] K. Itaka, K. Yamauchi, A. Harada, K. Nakamura, H. Kawaguchi, K. Kataoka, Polyion complex micelles from plasmid DNA and poly(ethylene glycol)-poly(-lysine) block copolymer as serum-tolerable polyplex system: physicochemical properties of micelles relevant to gene transfection efficiency, Biomaterials, 24 (2003) 4495-4506.

[57] K. Miyata, S. Fukushima, N. Nishiyama, Y. Yamasaki, K. Kataoka, PEG-based block catiomers possessing DNA anchoring and endosomal escaping functions to form polyplex micelles with improved stability and high transfection efficacy, J. Control. Release, 122 (2007) 252-260.

[58] M.A. Mintzer, E.E. Simanek, Nonviral vectors for gene delivery, Chem. Rev., 109 (2008) 259-302.

[59] K.A. Mislick, J.D. Baldeschwieler, Evidence for the role of proteoglycans in cation-mediated gene transfer, Proc. Natl. Acad. Sci. U.S.A., 93 (1996) 12349-12354.

[60] D. Vercauteren, J. Rejman, T.F. Martens, J. Demeester, S.C. De Smedt, K. Braeckmans, On the cellular processing of non-viral nanomedicines for nucleic acid delivery: Mechanisms and methods, J. Control. Release, 161 (2012) 566-581.

[61] M.A. Wolfert, L.W. Seymour, Chloroquine and amphipathic peptide helices show synergistic transfection in vitro, Gene Ther., 5 (1998) 409-414.

[62] M.A.E.M. Aa, U.S. Huth, S.Y. Häfele, R. Schubert, R.S. Oosting, E. Mastrobattista, W.E. Hennink, R. Peschka-Süss, G.A. Koning, D.J.A. Crommelin, Cellular uptake of cationic polymer-DNA complexes via caveolae plays a pivotal role in gene transfection in COS-7 cells, Pharm. Res., 24 (2007) 1590-1598.

[63] Z. Yang, G. Sahay, S. Sriadibhatla, A.V. Kabanov, Amphiphilic block copolymers enhance cellular uptake and nuclear entry of polyplex-delivered DNA, Bioconjug. Chem., 19 (2008) 1987-1994.

[64] P. van de Wetering, J.Y. Cherng, H. Talsma, D.J.A. Crommelin, W.E. Hennink, 2-(dimethylamino)ethyl methacrylate based (co)polymers as gene transfer agents, J. Control. Release, 53 (1998) 145-153.

APPENDIX A.

SUPPORTING INFORMATION

Methods

S1. Neutral Red assay

Cell viability was determined using the Neutral Red assay using the In Vitro Toxicology Assay Kit, Neutral Red-based (Sigma-Aldrich) following the supplier's protocol. The assay measures the amount of living cells, based on the principle that viable cells take up the dye by active transport and incorporate the dye into lysosomes, whereas nonviable cells will not take up the dye. Transfection followed the procedure described in section 2.12. The cell viability was accessed 48 h after transfection, firstly by adding 10 µL of 0.33% Neutral Red solution (filtered over a 0.2 µm filter before use) per well. Next, the cells were incubated for 2 h at 37 °C in a CO_2-incubator. After incubation, the medium was carefully removed and cells were quickly rinsed with 100 µL of Neutral Red Assay Fixative. After removal of the fixative, the dye was solubilized by incubating the cells at room temperature with 100 µL of Neutral Red Assay Solubilization Solution. Subsequently, the plates were gently stirred and the absorbance was measured at 540 nm with a reference wavelength of 690 nm. Cell viability is expressed as relative number of viable cells normalized against cells cultured with HBS without polyplex dispersions.

S2. A549 in vitro transfection

A549 human lung epithelial carcinoma cell line cells were cultured in was cultured in Ham's F-12 Nutrient Mixture (F-12) (PAA Laboratories GmbH, Pasching, Austria) supplemented with antibiotics/antimycotics and 10% FBS. Cells were maintained at 37 °C in a 5% CO_2 humidified air atmosphere.

For Luciferase transfection assay, 6,000 A549 cells/well were seeded into 96-well plates. Transfection followed the procedure described in section 2.12.

Supporting Schemes and Figures

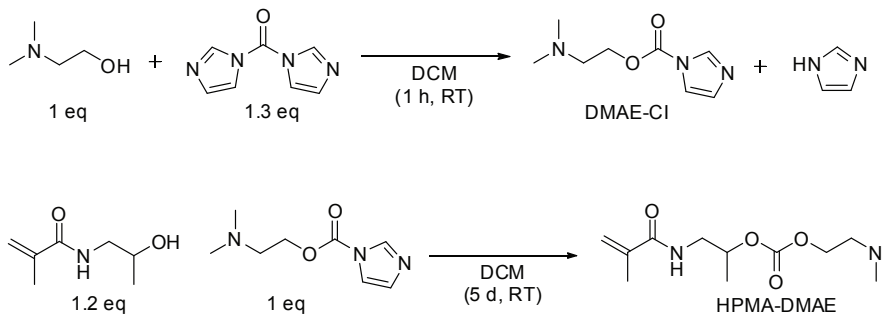

Scheme S1. Two-step synthesis of HPMA–DMAE.

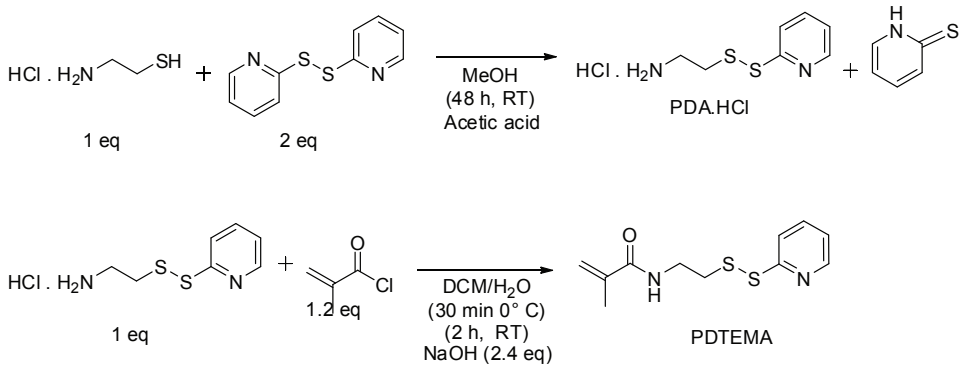

Scheme S2. Two-step synthesis of PDTEMA.

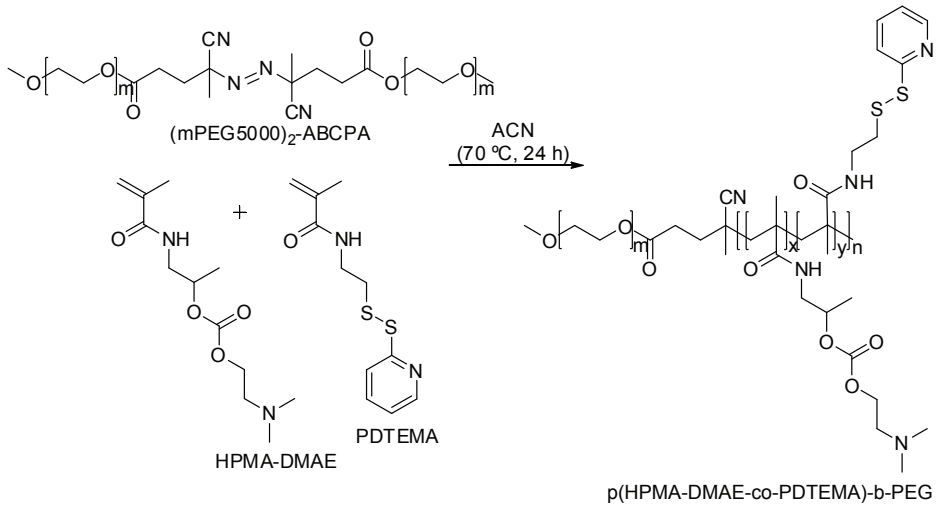

Scheme S3. Synthesis of p(HPMA–DMAE-co-PDTEMA)-b-PEG using $(mPEG_{5000})_2$-ABCPA macroinitiator.

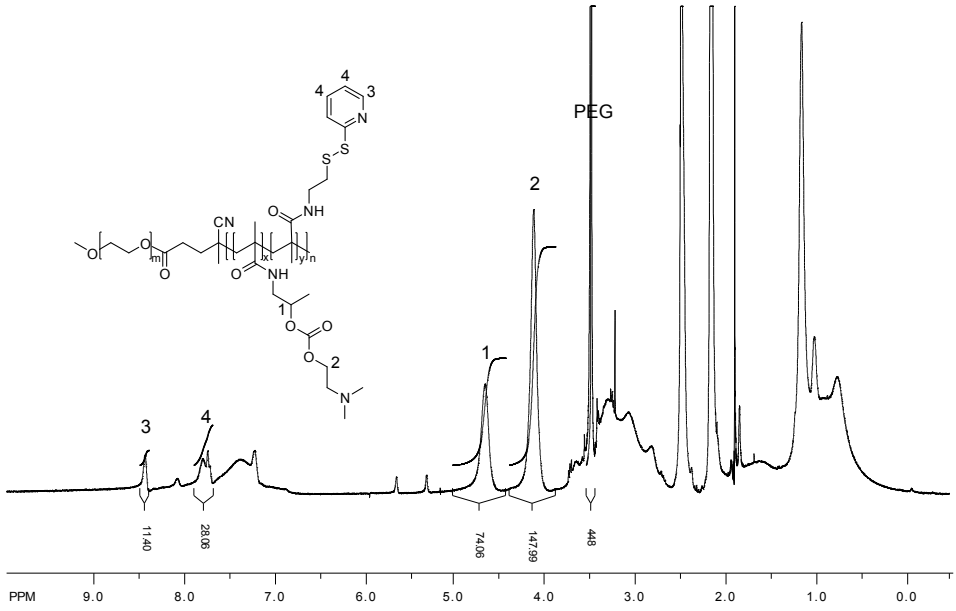

Figure S1. ^{1}H NMR spectrum of pHDP-PEG 85/15 in DMSO-d6.

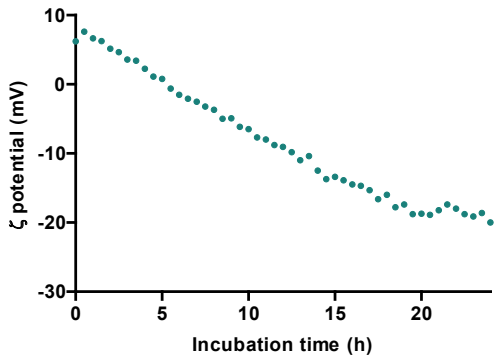

Figure S2. ζ potential of disulfide crosslinked pHDP-PEG 85/15 polyplexes upon incubation in Tris-HCl pH 8.5 at 37 ºC.

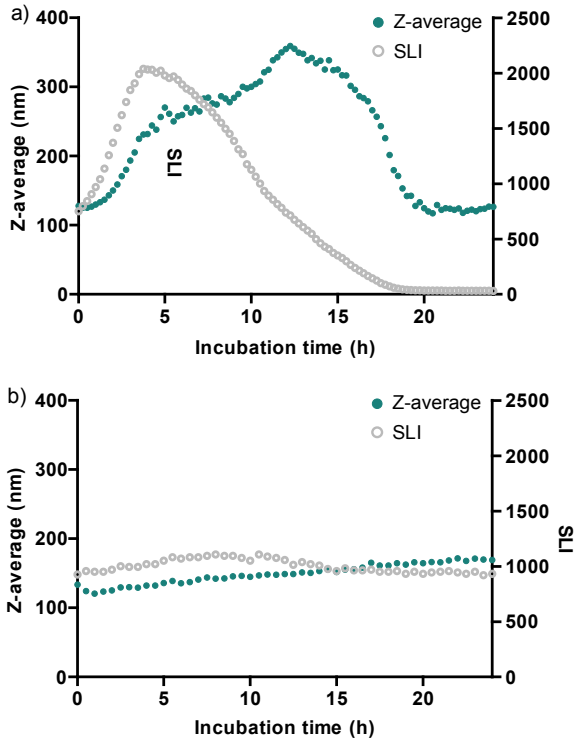

Figure S3. Particle size and scattered light intensity (SLI) given by DLS of non-crosslinked (a) and disulfide crosslinked (b) pHDP-PEG 85/15 polyplexes upon incubation in Tris-HCl pH 8.5 at 37 ºC.

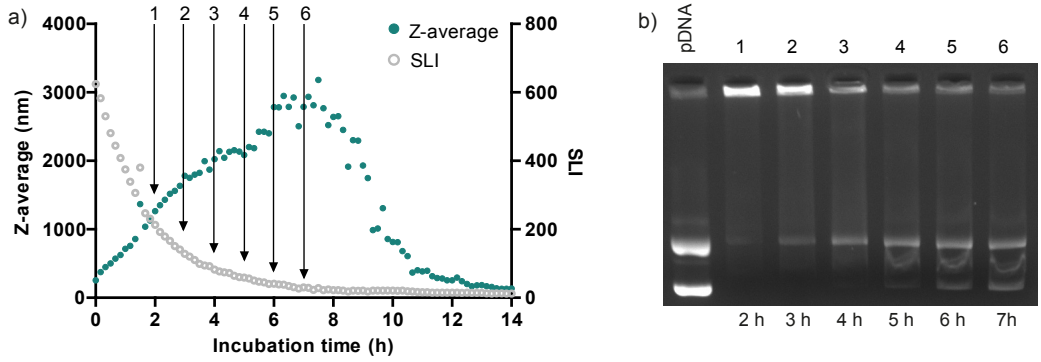

Figure S4. (a) Particle size and scattered light intensity (SLI) given by DLS of pHP-PEG decationized polyplexes upon incubation with 10 mM DTT in HBS at 37 °C (a) Agarose gel retardation assay of pHD-PEG decationized polyplexes upon incubation for incubation time points with 10 mM DTT in HBS at 37 °C, Lane 1, 2 h; lanes 2, 3 h; lane 3, 4 h; lane 4, 5 h; lane 5, 6 h; lane 6, 7 h.

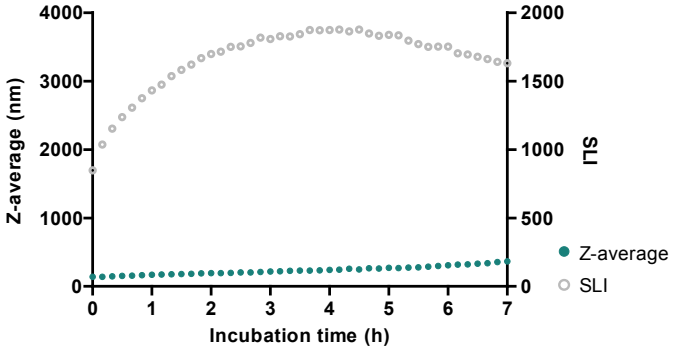

Figure S5. Particle size and scattered light intensity (SLI) given by DLS of pHDP-PEG cationic polyplexes upon incubation with 10 mM DTT in HBS at 37 °C.

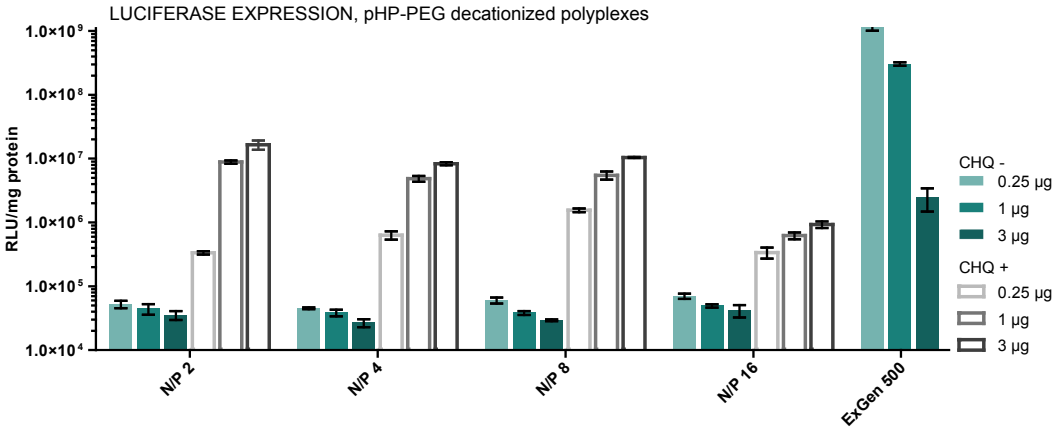

Figure S6. Effect of dose (0.25, 1 and 3 µg of pDNA/well), starting N/P ratio and absence (CHQ -) or presence (CHQ +) of chloroquine on luciferase expression levels for the different pHP-PEG 85/15 decationized crosslinked polyplexes. HeLa cells were transfected in the presence of 10% serum. Results are expressed as mean±SD (n=3).

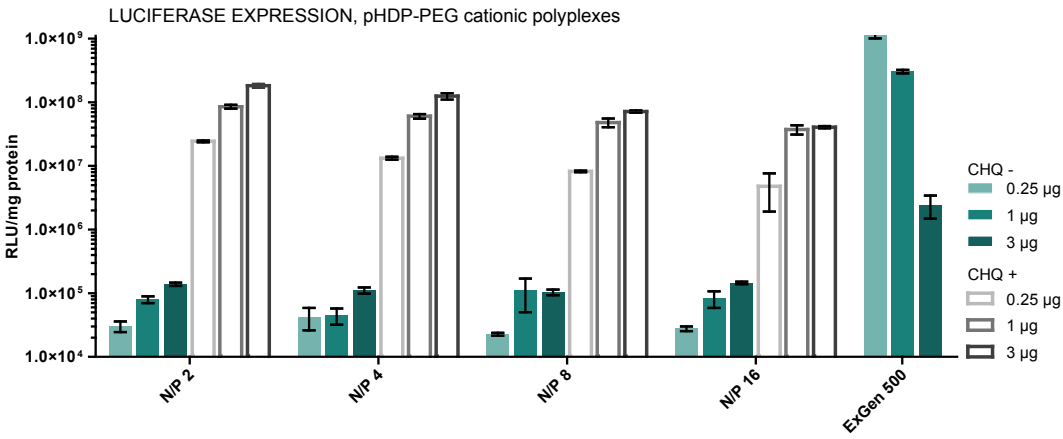

Figure S7. Effect of dose (0.25, 1 and 3 µg of pDNA/well), N/P ratio and absence (CHQ -) or presence (CHQ +) of chloroquine on luciferase expression levels for the different pHDP-PEG cationic crosslinked polyplexes. HeLa cells were transfected in the presence of 10% serum. Results are expressed as mean±SD (n=3).

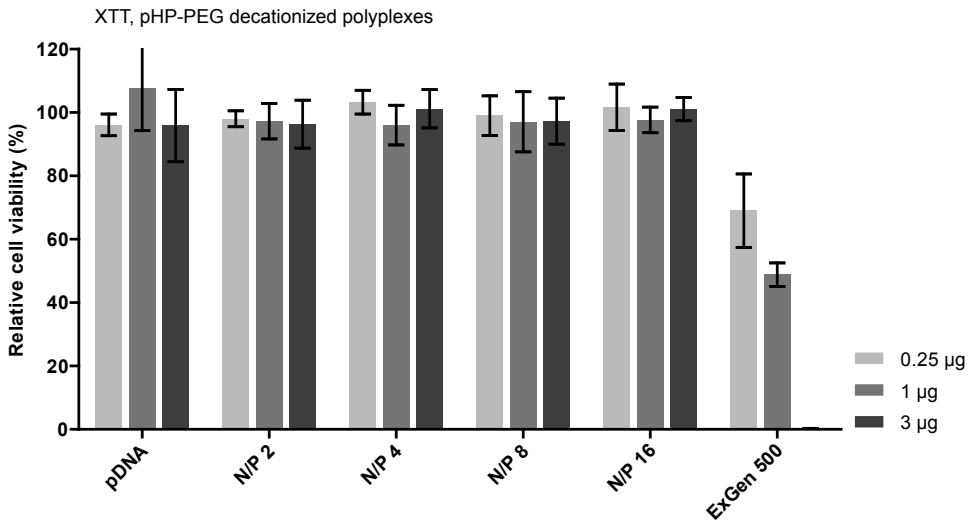

Figure S8. Effect of pDNA dose (0.25, 1 and 3 µg of pDNA/well) and starting N/P ratio on cell viability, determined by XTT assay, for the different pHP-PEG decationized crosslinked polyplexes. HeLa cells were transfected in the presence of 10% serum. Results are expressed as mean±SD (n=3).

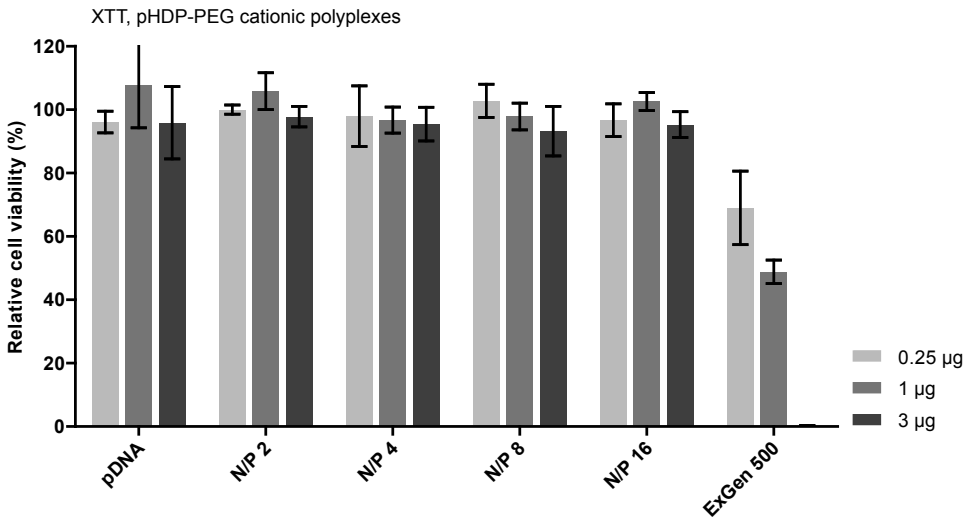

Figure S9. Effect of pDNA dose (0.25, 1 and 3 µg of pDNA/well) and N/P ratio on cell viability, determined by XTT assay, for the different pHDP-PEG cationic crosslinked polyplexes. HeLa cells were transfected in the presence of 10% serum. Results are expressed as mean±SD (n=3).

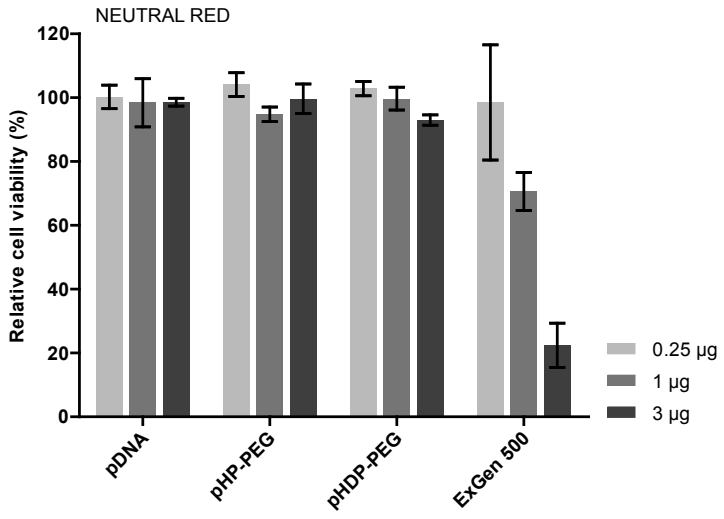

Figure S10. Effect of pDNA dose (0.25, 1 and 3 µg of pDNA/well) on cell viability, determined by Neutral Red assay, for different polyplexes (pHP-PEG, pHDP-PEG N/P=4 and ExGen 500). HeLa cells were transfected in the presence of 10% serum. Results are expressed as mean±SD (n=3).

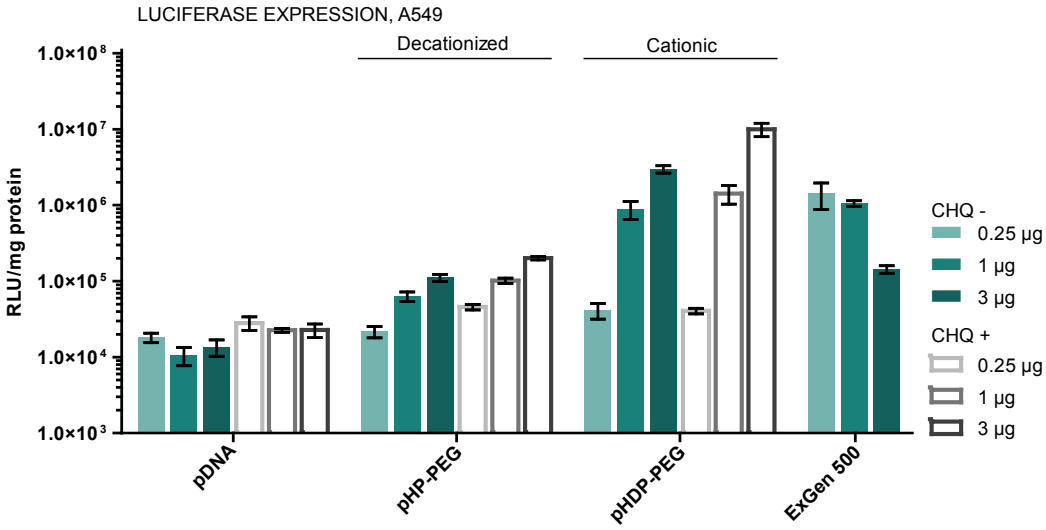

Figure S11. Effect of pDNA dose (0.25, 1 and 3 µg of pDNA/well) and absence (CHQ -) or presence (CHQ +) of chloroquine on luciferase expression levels for the different polyplexes (pHP-PEG and pHDP-PEG N/P=4). A549 cells were transfected in the presence of 10% serum. Results are expressed as mean±SD (n=3).

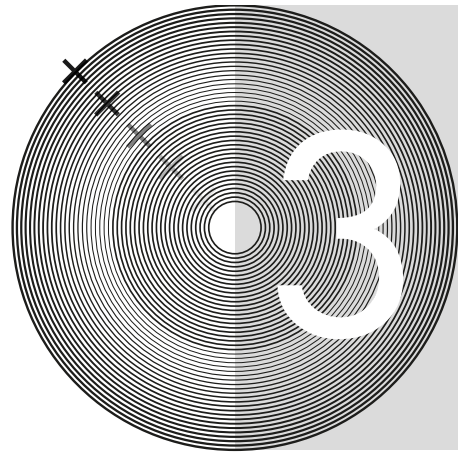

CHAPTER

Targeted decationized polyplexes for cell specific gene delivery

Luís Novo[a], Enrico Mastrobattista[a], Cornelus F. van Nostrum[a], Wim E. Hennink[a,*]

[a] Department of Pharmaceutics, Utrecht Institute for Pharmaceutical Sciences, Utrecht University, 3584 CG Utrecht, The Netherlands

Bioconjug. Chem., 25 (2014) 802-812.

Abstract

Decationized polyplexes have previously shown unique features, especially regarding their excellent cytocompatibility and very low degree of non-specific cellular uptake. In the present study, targeted disulfide crosslinked decationized polyplexes were composed of a core of disulfide crosslinked poly(hydroxypropyl methacrylamide) (pHPMA) stably entrapping plasmid DNA (pDNA) and a shell of poly(ethylene glycol) (PEG) decorated with folate molecules. Folate was used as targeting ligand because of its high binding affinity to its receptor, which is overexpressed in many tumors. Studies using folate receptor overexpressing cell lines (HeLa and OVCAR-3) showed significantly higher cell uptake for the folate-targeted decationized polyplexes, when compared to their non-targeted counterparts. On the contrary, for a non-expressing folate receptor cell line (A549) similar uptake was observed for both targeted and non-targeted decationized polyplexes. Transfection studies using OVCAR-3 cells showed higher transfection efficiency for folate-targeted polyplexes, because of improved cellular uptake. Simultaneously, introduction of targeting moiety on polyplexes did not affect their good cytocompatibilty. The results reported in this paper demonstrate that coupling of folate to decationized polyplexes generates a potential system for targeted gene delivery.

KEYWORDS Gene delivery, triggered release, polymer, biocompatibility, targeting

1. INTRODUCTION

Gene therapy is a highly promising modality for the treatment of many disorders with a genetic basis, including cancer [1]. The applicability of gene therapy relies on the emergence of gene delivery vectors with *in vivo* safety and effectiveness. Serious disadvantages are however associated with viral vectors when applied in patients, including insertional mutagenesis and immunogenicity [1, 2]. Therefore non-viral gene delivery systems based on e.g. cationic polymers, peptides or lipids have been developed and investigated as a safer alternatives for viral vectors [3-9].

Cationic polymers are of particular interest since they can easily interact with

the negatively charged DNA to form nanosized particles (polyplexes). However, the cationic surface charge of such systems leads to toxicity both *in vivo* [10, 11] and in cell cultures [12]. A major challenge of non-viral vectors is therefore the development of systems suitable for systemic applications. In order to target their site of action (e.g. a tumor), the polyplexes should firstly possess long circulation and stability to reach the target tissue and extravasate in the tissue leaky vasculature, referred to as the enhanced permeation and retention (EPR) effect [13, 14]. Only, after sufficient accumulation internalization of the vectors can occur [15]. Often, polycation based systems, even when shielded with hydrophilic polymers such as PEG, lead to insufficient improvements on the circulation times and tumor accumulation [16-18]. After interaction with the target cells, polyplexes should induce efficient transgene expression, and at the same time, reduce the risk of interference with cell homeostasis to a minimum level.

In a previous paper we reported on decationized polyplexes [19] that unlike conventional polymeric gene delivery systems, are based on noncharged and hydrophilic polymers. Structurally, the polyplexes possess a core of disulfide crosslinked pHPMA, surrounded by a PEG shell. Cationic charges are present on the polymers during complex formation with DNA, but are subsequently removed by hydrolysis leaving a hydrophilic disulfide crosslinked polyplex. These decationized polyplexes show a high and stable DNA loading, based exclusively on physical entrapment in the disulfide crosslinked core, and excellent cytocompatibility. We further demonstrated that pDNA is released from the polyplexes triggered by intracellular reducing environment that results in cleavage of disulfide crosslinks [20, 21]. Importantly, the decationized polyplexes showed a low degree of nonspecific uptake, which on the one hand reduced significantly their efficiency when compared to their cationic counterparts, but on the other hand, is a highly favorable property for targeted therapy upon local or intravenous administration. Incorporation of a targeting ligand on the decationized polyplexes could lead not only to significantly increased cellular binding and internalization, required for efficient transfection, but also to create a gene delivery system with high specificity as compared to conventional polyplexes.

Folic acid (FA) selectively binds with high affinity to its receptor, the folate receptor (FR), which is overexpressed in many tumor types including metastatic forms, while having limited expression in normal tissues [22]. Due to its particular anatomic distribution, expressed in apical plasma membrane of the polarized cells, FR is normally inaccessible via the blood stream in normal tissues, however, loss

of epithelial cell polarity, observed in tumors, makes the FR accessible from the circulation [23, 24]. Drug delivery systems conjugated to FA bind to FR on the cell surface and are subsequently internalized *via* receptor mediated endocytosis. Accordingly, folic acid is a suitable targeting ligand for tumor-specific targeted drug and gene delivery upon systemic administration [22, 25, 26].

In this study, we exploited the advantageous property of the very low degree of nonspecific cellular uptake of decationized polyplexes together with the folic acid targeting ability to design a polymeric gene delivery vector with high targeting specificity for FA overexpressing cells.

2. MATERIALS AND METHODS

2.1. Materials

N-(2-hydroxypropyl)methacrylamide (HPMAm) was obtained from Zentiva a.s. (Prague, Czech Republic). Carbonic acid 2-dimethylamino-ethyl ester 1-methyl-2-(2-methacryloylamino)-ethyl ester (HPMA–DMAE) and *N*-[2-(2-pyridyldithio)]ethyl methacrylamide (PDTEMA) were synthesized as previously described [19]. NH_2-PEG-OH (M_w 5000 Da) was obtained from NOF corporation (Kyoto, Japan). pCMV_Luc plasmid, encoding for firefly luciferase, with human cytomegalovirus promoter (CMV), was amplified with competent *E. coli* DH5α and purified with NucleoBond® (Macherey-Nagel, Bioke, Leiden, The Netherlands). pCMV_Luc was purchased from the Plasmid Factory (Bielefeld, Germany). Agarose MP was purchased from Roche Molecular Biochemicals (Mannheim, Germany). Exgen 500 (22 kDa, l-PEI) and 6× DNA Loading Dye were purchased from Fermentas (St. Leon-Roth, Germany). HeLa (human epithelial ovarian carcinoma cell line), OVCAR-3 (ovarian carcinoma cell line) and A549 (human lung epithelial carcinoma cell line) cells were obtained from the American Type Culture Collection (ATCC) (Maryland, USA). Dulbecco's Modified Eagle Medium with 3.7 g/L sodium bicarbonate, 1 g/L l-glucose, l-glutamine (DMEM), RPMI 1640, Ham's F-12 Nutrient Mixture (F-12), phosphate buffered saline (PBS), fetal bovine serum (FBS), antibiotics/antimycotics (penicillin, streptomycin sulphate, amphotericin B) and trypsin/EDTA 10× were purchased from PAA Laboratories GmbH (Pasching, Austria). Folate free RPMI-1640 medium and dialyzed FBS was purchased from Gibco (Breda, The Netherlands).

Luciferase assay kit and QuantiLum® recombinant luciferase were obtained from Promega (Leiden, The Netherlands). (2,4,6-Trinitrobenzene sulfonic acid) (TNBSA) and Micro BCA Protein Assay kits were purchased from Pierce (Etten-Leur, The Netherlands). LabelIT Cy5 Nucleic Acid Labeling Kit was purchased from Mirus Bio (Madison, WI, USA). All other chemicals and reagents were obtained from Sigma-Aldrich (Zwijndrecht, The Netherlands).

2.2. Synthesis of FA-NHS

FA-NHS was prepared according to previously described procedures, with small changes [27, 28]. Folic acid (FA) (1g, 2.27 mmol) was dissolved in 15 mL DMSO at 40 ºC. Next, the solution was cooled to room temperature and 4-dimethylaminopyridine (DMAP) (0.056 g, 0.45 mmol) and *N*hydroxysuccinimide (NHS) (0.523 g, 4.54 mmol) were added. After dissolution of both compounds, *N,N'*-dicyclohexylcarbodiimide (DCC) (0.468 g, 2.27 mmol) was slowly added to the reaction mixture under vigorous stirring. The reaction mixture was kept in the dark for 24 h under an N_2 atmosphere. The solution was consecutively filtered to remove precipitated dicyclohexylurea (DCU), followed by precipitation of FA-NHS in a mixture of ether/acetone 85/15 (500 mL). The precipitated product was washed and collected by filtration. The product was further dried in a vacuum oven for 2 days.

2.3. Synthesis of (FA-PEG$_2$-ABCPA)

The synthesis of (FA-PEG$_2$-ABCPA) was performed in 3 major steps (Scheme 1).

2.3.1. Boc protection of NH$_2$-PEG-OH

NH_2-PEG-OH (5000 Da) (1 g, 0.20 mmol) was dissolved in 10 mL DCM. Next, di-tert-butyl dicarbonate (t-Boc) (87.3 mg, 0.40 mmol) was added to the solution. The reaction mixture was stirred for 24 h under an N_2 atmosphere. Next, DCM was partially evaporated under reduced pressure and the obtained product (Boc-NH-PEG-OH) was precipitated in 50 mL diethyl ether. The product was dissolved in DCM and precipitated diethyl ether (3 times).

2.3.2. Synthesis of (Boc-NH-PEG)$_2$-ABCPA

The synthesis and characterization of (Boc-NH-PEG)$_2$-ABCPA was based on the (mPEG)$_2$ABCPA macroinitiator synthesis as previously described [29, 30], with some modifications. Boc-NH-PEG-OH (1020.2 mg, 0.2 mmol) was introduced into a round bottomed-flask and dried overnight in a vacuum oven. After dissolution of PEG in 7 mL of DCM, 1 mL of 0.1 M 4,4′-azobis(4-cyanovaleric acid) (ABCPA) solution (0.10 mmol) in DCM/THF (1/1 v/v) was added to the PEG solution. Next, 1 mL of 0.03 M 4-(dimethylamino)pyridinium 4-toluenesulfonate (DPTS) solution in DCM (0.03 mmol) was added to the mixture and 1 mL THF was added to adjust the PEG concentration to ~100 mg/mL. The mixture was cooled on ice, and 1 mL 0.3 M DCC solution (0.3 mmol) in DCM/THF (1/1 v/v) was slowly added. The reaction was carried at room temperature for 48 h under an N_2 atmosphere. The formed DCU was removed by centrifugation, followed by filtration through a 0.2 µm nylon filter. The product (Boc-NH-PEG)$_2$-ABCPA was further purified by precipitation in diethyl ether , followed by dissolution in DCM and precipitated in diethyl ether (2 times).

2.3.2. Deprotection of (Boc-NH-PEG)$_2$-ABCPA

(Boc-NH-PEG)$_2$-ABCPA (200 mg, 19.1 µmol) was deprotected in 2 mL DCM/TFA 1/1 (v/v) mixture for 4 h at room temperature. Next, the solvent was partially evaporated under reduced pressure and the product (TFA·NH$_2$-PEG)$_2$-ABCPA was precipitated in diethyl ether, followed by dissolution in DCM and precipitated in diethyl ether (3 times).

2.3.3. Synthesis of (FA-PEG)$_2$-ABCPA

FA-NHS (48.46 mg, 90 µmol) was dissolved in 1.5 mL DMSO and 21 µL of triethylamine (150 µmol) was subsequently added. Next, a solution of (TFA·NH$_2$-PEG)$_2$-ABCPA (154.2 mg, 15 µmol) in 1.5 mL DMSO was slowly added to this reaction mixture. The reaction was allowed to proceed for 36 h under an N_2 atmosphere in the dark. The product was purified by dialysis against DMSO for 24 h (MWCO 6000-8000 Da), followed by a gradual exchange of the dialysis medium to 2 mM NaOAc pH 5. The purified product was filtered over a 0.2 µm nylon filter and freeze-dried.

2.4. Synthesis of pHDP-PEG-FA and pHDP-PEG

Free radical polymerization using $(FA\text{-}PEG)_2$-ABCPA or $(Boc\text{-}NH\text{-}PEG)_2$-ABCPA as macroinitiator was performed to synthesize p(HPMA–DMAE-co-PDTEMA)-b-PEG-FA (pHDP-PEG-FA) or p(HPMA–DMAE-co-PDTEMA)-b-PEG-Boc (pHDP-PEG), respectively. The polymers were synthesized using a HPMA–DMAE-to-initiator ratio (M/I) of 200 (mol/mol). The feed ratio HPMA–DMAE/PDTEMA was 1/0.2 (mol/mol). The polymerization was carried at 70 ºC for 24 h in DMSO under an N_2 atmosphere, using 2.5 µmol macroinitiator and monomer concentration of 1 M. After polymerization, the polymers were precipitated in diethyl ether, dialyzed against 5 mM NH_4OAc buffer pH 5.0 for 3 days at 4 °C (MWCO 6000-8000) and collected by freeze-drying.

2.5. Polymer characterization

2.5.1. Gel permeation chromatography (GPC) characterization of the polymers

Analysis of the $(FA\text{-}PEG)_2$-ABCPA macroinitiator was performed using a Waters System (Waters Associates Inc., Milford, MA) with refractive index (RI) and UV detector using two serial Plgel 5 µm MIXED-D columns (Polymer Laboratories) and DMF containing 10 mM LiCl as eluent. The flow rate was 0.7 mL/min (50 min run time) and the temperature was 40 °C [31]. The molecular weights of the synthesized polymers were determined by GPC analysis using a Viscotek-GPCmax (Viscotek, Oss, The Netherlands) light scattering/viscosimetric detection system, firstly by determining the dn/dc of the different polymers and subsequently by using two Ultrahydrogel 1000 7.8×300 mm in series with Ultrahydrogel 6×40 guard column and 0.3 M NaOAc pH 4.4 as eluent [32]. The flow rate was 0.7 mL/min (run time was 50 min) and the temperature was 30 °C. Data from the laser photometer (λ = 670 nm) (right (90°) and low (7°) angle light scattering), RI and viscosity detector were integrated using OmniSEC software to calculate the number and weight average molecular weight (M_n, M_w) and polydispersity index (PDI; (M_w/M_n). Besides, UV detection at 280 nm, specific for the pyridyl disulfide (PDS) group, was also applied [33]. PEO (M_n=18.1 kDa, M_w=18.9 kDa, Malvern (Worcestershire, UK)) was used for calibration.

2.5.2. ^{1}H NMR characterization of the polymers

The copolymer composition of the different polymers dissolved in DMSO-d6 was determined by ^{1}H NMR analysis performed using a Gemini 300 MHz spectrometer (Varian Associates Inc., NMR Instruments, Palo Alto, CA). The copolymer composition and its M_n were determined as previously described [19].

2.6. Preparation of decationized polyplexes

The preparation of decationized polyplexes was essentially performed as previously described (Scheme 2) [19]. Briefly, to prepare a dispersion of 50 µg/mL pDNA polyplexes, 100 µL of polymer solutions in 20 mM Tris-HCl pH 8.5 buffer (pHDP-PEG (nontargeted) or pHDP-PEG-FA (folate targeted)) at N/P=4 (N, molarity of protonable amines from polymer; P, molarity of negatively charged phosphates from pDNA)) were mixed with 200 µL pDNA (75 µg/mL). After 10 min at room temperature, polyplexes were crosslinked by addition of 3,6-dioxa-1,8-octane-dithiol (DODT) corresponding with a molar equivalent of DODT thiol groups to PDS groups of the polymer.

Polyplexes were decationized by incubation of the polyplex dispersions at 37 °C and pH 8.5 for 6 h, to hydrolyze the cationic dimethylaminoethanol (DMAE) groups from the polymers [19]. Next, the ionic strength and pH were adjusted to physiological conditions (150 mM, pH 7.4). Given the fact that the side products from cross-linking and decationization, (2mercaptopyridine and DMAE) possess high cellular tolerance, as previously demonstrated [19, 34, 35] polyplexes were directly used without purification procedures.

2.7. Dynamic Light Scattering (DLS)

The size of the polyplexes was measured by DLS using an ALV CGS-3 system (Malvern Instruments, Malvern, UK) equipped with a JDS Uniphase 22 mW He-Ne laser operating at 632.8 nm, an optical fiber-based detector, a digital LV/LSE-5003 correlator with temperature controller set at 25 °C. Measurements were performed in HBS (20 mM HEPES, 150 mM NaCl, pH 7.4) at a final pDNA polyplex concentration of 20 µg/mL.

2.8. Zeta potential

Zeta potential of the polyplexes was determined using a Malvern Zetasizer Nano-Z (Malvern Instruments, Malvern, UK) with universal ZEN 1002 'dip' cells and DTS (Nano) software (version 4.20) at 25 °C. Zeta-potential measurements were performed in 20 mM HEPES at pH 7.4 at a final pDNA polyplex concentration of 20 μg/mL.

2.9. Gel Retardation Assay

Decationized pHP-PEG-FA and cationic pHDP-PEG-FA polyplexes were prepared at N/P=4 and subsequently incubated with 10 mM dithiothreitol (DTT) (as reducing agent) at 37 ºC. At specific incubation time points, samples of 20 μL polyplex dispersion in HEPES buffered saline (HBS) (20 μg/mL of pDNA) were collected. Samples were then mixed with 4 μL 6× DNA Loading Dye and loaded into 0.8% agarose gel in Tris-acetate-EDTA (TAE) buffer containing 0.5 μg/mL ethidium bromide and run at 120 V for 40 min. pDNA was detected using a Gel Doc™ XR+ system (BioRad Laboratories Inc., Hercules, CA) with Image Lab software.

2.10. Cell culture

HeLa cells (FR +; folate receptor positive cells) were cultured in DMEM supplemented with antibiotics/antimycotics and 10% FBS. OVCAR-3 cells (FR +) were cultured in RPMI 1640 supplemented with antibiotics/antimycotics, bovine insulin (0.01 mg/mL), sodium pyruvate (1 mM) and 20% FBS. A549 cells (FR –; folate receptor negative cells) were cultured in Ham's F12 supplemented with antibiotics/antimycotics and 10% FBS. Cells were maintained at 37 °C in a 5% CO_2 humidified air atmosphere. All in vitro experiments were performed in the presence of 20% serum at every stage of the *in vitro* experimental set-up.

2.11. Cellular uptake of polyplexes

For uptake studies, 30,000 HeLa, 90,000 OVCAR-3 or 36,000 A549 cells/well were seeded into 24-well culture plates. pDNA was labeled with Cy5 according to the manufacturer's protocol using a Label IT Nucleic Acid Labeling Kit and polyplexes were prepared at a final pDNA concentration of 10 μg/mL, containing

10 wt% labeled pDNA. Polyplexes were incubated with HeLa, OVCAR-3 or A549 cells for 2 h at 37 °C in the presence of serum (10% FBS for HeLa and A549 cells, 20% FBS for OVCAR-3 cells) and washed 3 times (PBS, glycine buffer (0.2 M glycine, 0.15 M NaCl, pH 3), and PBS). Glycine buffer was used to remove adsorbed particles on the surface of the cells [36]. The degree of cellular uptake (Cy5-positive cells) was determined by flow cytometry.

2.12. Flow cytometry

The cells adhering to the well plate were washed, trypsinized (50 µL 1× trypsin/EDTA) and resuspended in FBS supplemented medium (150 µL). The cells were subsequently transferred into a round bottom 96-well plate and centrifuged for 5 min at 250 ×g and 4 °C. After medium removal, the cells were resuspended in 100 µL phosphate-buffered albumin (PBA; 1% w/v albumin in PBS) and fixed with 100 µL of 10% formalin. Samples were analyzed by flow cytometry using a FACSCantoII (Becton and Dickinson, Mountain View, CA, USA) equipped with a 488 nm 20 mW Solid State diode laser and a 633 nm 20 mW He–Ne laser. A number of 10,000 cell events were recorded per sample to determine the degree of uptake for Cy-5 positive cells (APC channel). Statistical analyses were performed with the software GraphPad Prism 5 (GraphPad Software Inc., La Jolla, California, USA)

2.13 Polyplex transfection efficiency

The transfection efficiency of the different polyplex formulations was determined by luciferase assay essentially as described by van Gaal et al. [37] OVCAR-3 cells were plated into 96-well plates 48 h prior to transfection (15,000 cells per well). Before addition of the polyplex dispersions to the cells, the culture medium was replaced by folate-free RPMI 1640 supplemented with 25% dialyzed FBS, 250 µM chloroquine with or without 1.25 mM folic acid. Next, 25 µL of polyplex dispersions containing 120 µg/mL or 200 µg/mL of pDNA were added per well and the plates were immediately placed on ice for 4 h. Next, cells were washed 3× with PBS and folate-free RPMI 1640 supplemented with 20% FBS, 200 µM chloroquine and with or without 1 mM folic acid was added to the cells. Cells were incubated for 24 h at 37 ºC and the culture medium was replaced with fresh RPMI containing 20% FBS. Cells were additionally incubated for 24 h. Polyplexes based on Exgen 500 at N/

P=6 were used as positive control [37].

Luciferase expression assay was performed 48 h after transfection. Cells were washed with 100 µL of cold PBS and lysed with 50 µL of lysis buffer (Reporter Lysis Buffer 5× (Promega), diluted in mQ H_2O). A freeze-thaw cycle was performed by incubating the cells for 1 h at 80 °C. Next, 10 µL of cell lysate was mixed with 50 µL of Luciferase Assay Reagent (Promega), after 2 sec luminescence was measured for 10 sec using a FLUOstar OPTIMA microplate, equipped with a luminescence light guide (BMG LabTech, Germany). The obtained luciferase activity was normalized to the amount of protein in the lysates, determined by Micro BCA Protein Assay. Results are expressed as relative light units (RLU) per mg of cellular protein. RLU were quantified using QuantiLum recombinant luciferase standards (1×10^2-1×10^6 pg) in 10 µL 1× Reporter Lysis Buffer containing 1 mg/mL bovine serum albumin (BSA), following the suppliers recommendation. Linear regression was performed with GraphPad Prism 5. Statistical analyses were performed with the software GraphPad Prism 5.

2.14. XTT assay

Cell viability was analyzed using the XTT assay which determines the metabolic activity of HeLa cells upon incubation with polyplex dispersions. HeLa cells were seeded 24 h prior to transfection into 96-well plates (5,000 HeLa cells/well). Immediately prior to transfection, the culture medium was replaced with DMEM supplemented with 12.5% FBS. Next, samples of 25 µL polyplex dispersions containing 10, 40 or 150 µg/mL of pDNA were added per well. Medium was replaced after 24h and the XTT assay was performed 48 h after transfection. Two hours before performing the XTT assay, the medium was refreshed. After adding 50 µL of a freshly prepared XTT solution (25 µM *N*-methyl dibenzopyrazine methylsulfate (PMS) and 1 mg/mL 2,3-bis(2-methoxy-4-nitro-5-sulfophenyl)-2H-tetrazolium-5-carboxanilide (XTT) in plain RPMI 1640 medium) per well, the cells were incubated for 1 h at 37 °C in a CO_2-incubator. Next, absorbance was measured at 490 nm with a reference wavelength of 655 nm. Cell viability is expressed as relative metabolic activity normalized against cells cultured with HBS without polyplex dispersions.

3. RESULTS AND DISCUSSION

3.1. Synthesis of pHDP-PEG with terminal folate moiety

To obtain prepare folate targeted decationized polyplexes, a protocol to synthesize a folate-PEG (Mw 5000 Da) bi-functionalized azo macronitiator ((FA-PEG)$_2$-ABCPA) was developed, based on the synthesis of mPEG$_2$-ABCPA previously described by Neradovic et al. [29]. The rationale behind this route is that the (FA-PEG)$_2$-ABCPA will initiate free radical polymerization to form block copolymers with a folate functionality at the distal PEG end (Scheme 3). Consequently, the folic acid can be coupled to the macroinitiator, to allow a straightforward approach to obtain folic acid functionalized polymers that can be used for polyplex preparation, without the need of post-modification procedures.

The synthesis of (FA-PEG)$_2$-ABCPA (Scheme 1) starts with Boc protection of the primary amine (a) of the commercially available NH$_2$-PEG-OH. ^{1}H NMR analysis showed quantitative protection (^{1}H NMR (CDCl3) δ (ppm) 1.4 (9H, Boc)) and primary amines were not detected using the TNBSA assay. Next, Boc-NH-PEG-OH was coupled to ABCPA via DCC coupling (b). GPC analysis of the product (Figure 1) showed a bimodal distribution, corresponding to a mixture of PEG bi-functionalized ABCPA (10 kDa) and unreacted BocPEGOH or PEG mono-functionalized ABCPA (5 kDa). The ratio between 10 kDa and 5 kDa products was 77%/23%. The third step of the reaction scheme was the Boc deprotection with TFA, generating the TFA salt form of (NH$_2$-PEG)$_2$-ABCPA (c). ^{1}H NMR analysis showed the complete disappearance of the Boc signal at δ1.4 ppm and the TNBSA assay showed that the mol/mol ratio of primary amines to PEG chains was close to 1. Additionally, the GPC chromatogram showed that the ratio between 10 kDa and 5 kDa co-products was retained. The last step of the synthesis was the reaction between NHS activated folic acid (FA-NHS) and the deprotected (TFA·NH$_2$PEG)$_2$ABCPA (d). The reaction was done under anhydrous conditions to avoid hydrolysis of FA-NHS and using a molar excess of FA-NHS to NH$_2$ groups from the macroinitiator to limit possible aminolysis of the ester bond that links the PEG chain and ABCPA.

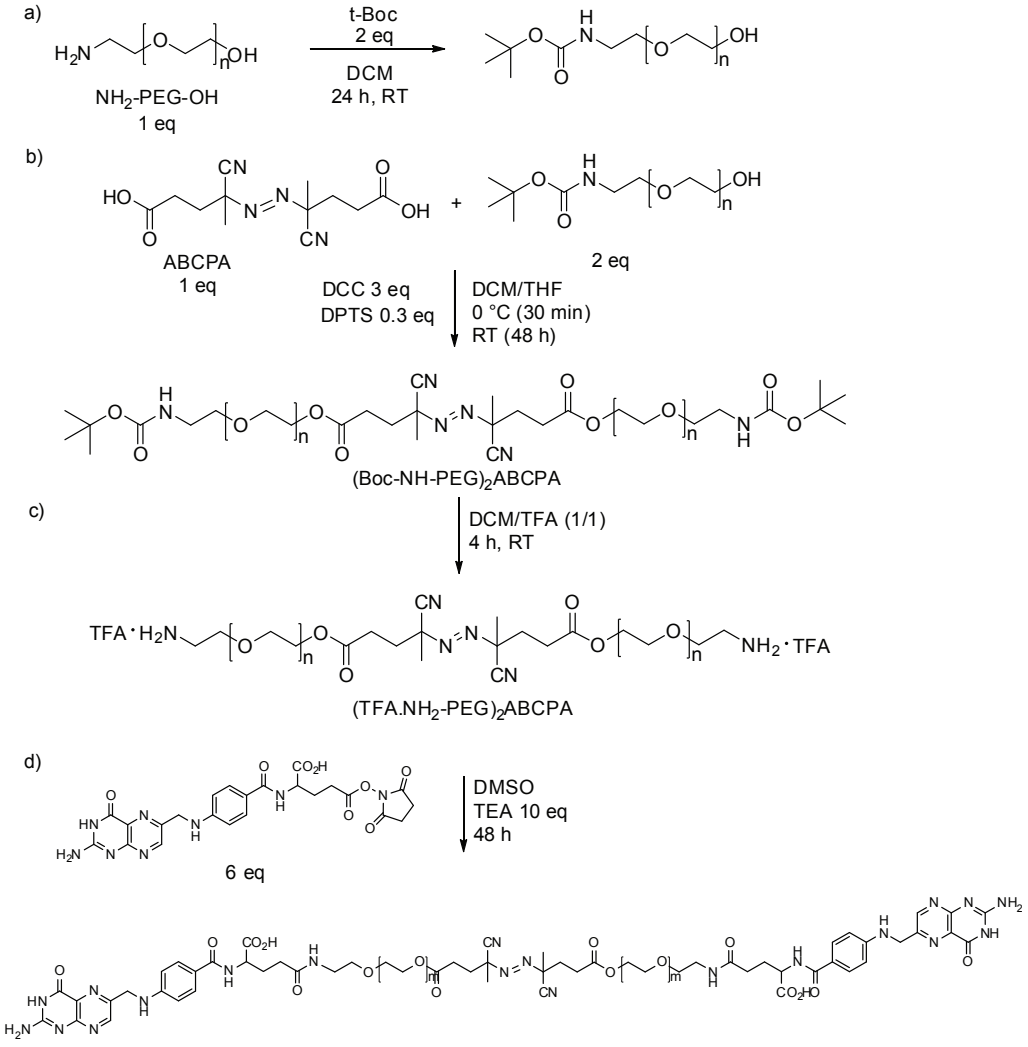

Scheme 1. Synthesis route of $(FA\text{-}PEG)_2$-ABCPA.

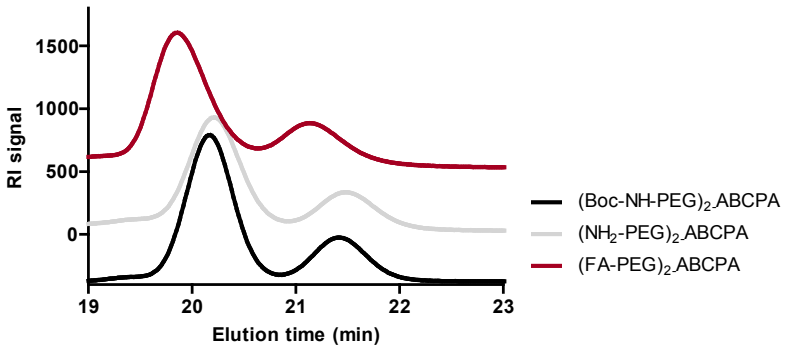

Figure 1. GPC chromatograms (RI signal) of (Boc-NH-PEG)$_2$-ABCPA, (NH_2-PEG)$_2$-ABCPA and (FA-PEG)$_2$-ABCPA.

To determine the coupling efficiency of folic acid to NH_2 groups in the macroinitiator, ^{1}H NMR was used to compare the integral values of the specific signal of folic acid with the integral values of the specific signal of PEG (Figure 2), which showed that approximately one mol of folic acid was coupled to one mol of PEG chains. The GPC chromatogram of the (FAPEG)$_2$ABCPA shows again that the ratio of 10 kDa and 5 kDa co-products was retained and that the excess of FA-NHS was removed by dialysis (Figure 3). The ^{1}H NMR and GPC results demonstrate that the applied synthetic route results lead to the formation of the aimed product, namely PEG bi-functionalized macroinitiator with coupled folic acid moiety.

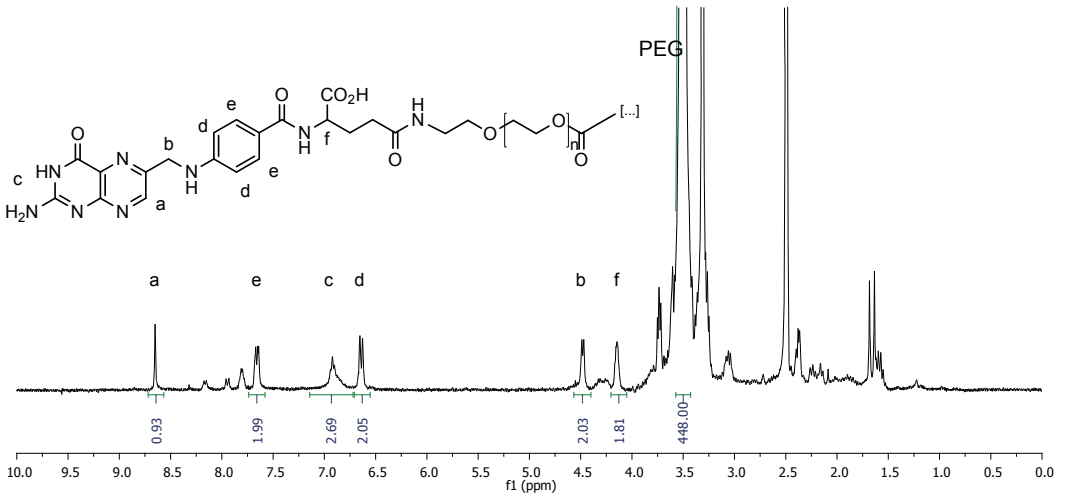

Figure 2. ^{1}NMR spectrum of (FA-PEG)$_2$-ABCPA in DMSO.

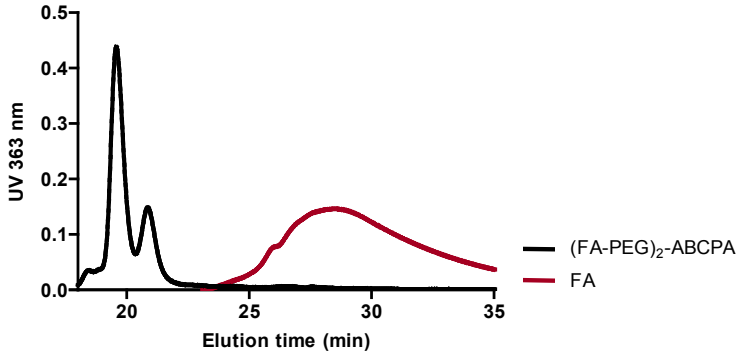

Figure 3. GPC chromatograms (UV signal at 363 nm) of $(FA\text{-}PEG)_2$-ABCPA and free folic acid (FA).

Free radical polymerization of HPMA–DMAE with PDTEMA using $(FA\text{-}PEG)_2$-ABCPA as macroinitiator resulted in the formation of pHDP-PEG-FA. A second polymer was prepared using the $(Boc\text{-}PEG)_2$-ABCPA, which was used to prepare nontargeted polyplexes (pHDP-PEG) (Scheme 3). The yield of both polymerizations was close to 50%, which suggests that the incorporation of folic acid molecule in the PEG_2-ABCPA macroinitiator did not affect the copolymerization reaction.

The cationic HPMA–DMAE monomer was incorporated in the copolymer to allow pDNA complexation by electrostatic interactions. Hydrolysis of the DMAE cationic groups[38] after interchain disulfide crosslinking yielded decationized polyplexes based on the hydrophilic PEG and pHPMA polymers. The PDTEMA monomer, also a methacryamide monomer, was chosen because it contains a PDS functionality, which allows interchain disulfide crosslinking reaction in the core of the polyplexes using the dithiol DODT.

The block copolymer compositions were determined by ^1H NMR and UV spectroscopy [19] (Table 1). As previously shown, the copolymer composition as determined by NMR analysis was close to the feed ratio of HPMA–DMAE/PDTEMA. Both polymers pHDP-PEG-FA and pHDP-PEG had similar M_n as determined by NMR analysis. UV spectroscopy showed that the molarity of PDS groups per weight of polymer was similar for both polymers. GPC results indicated that polymer characteristics, such as M_w, PDI and dn/dc, are similar for both polymers. Using the polymer characterization data. It can be calculated that the synthesized polymers contained approximately one disulfide crosslinking point (PDTEMA) per 6.5 cationic units (HPMA–DMAE).

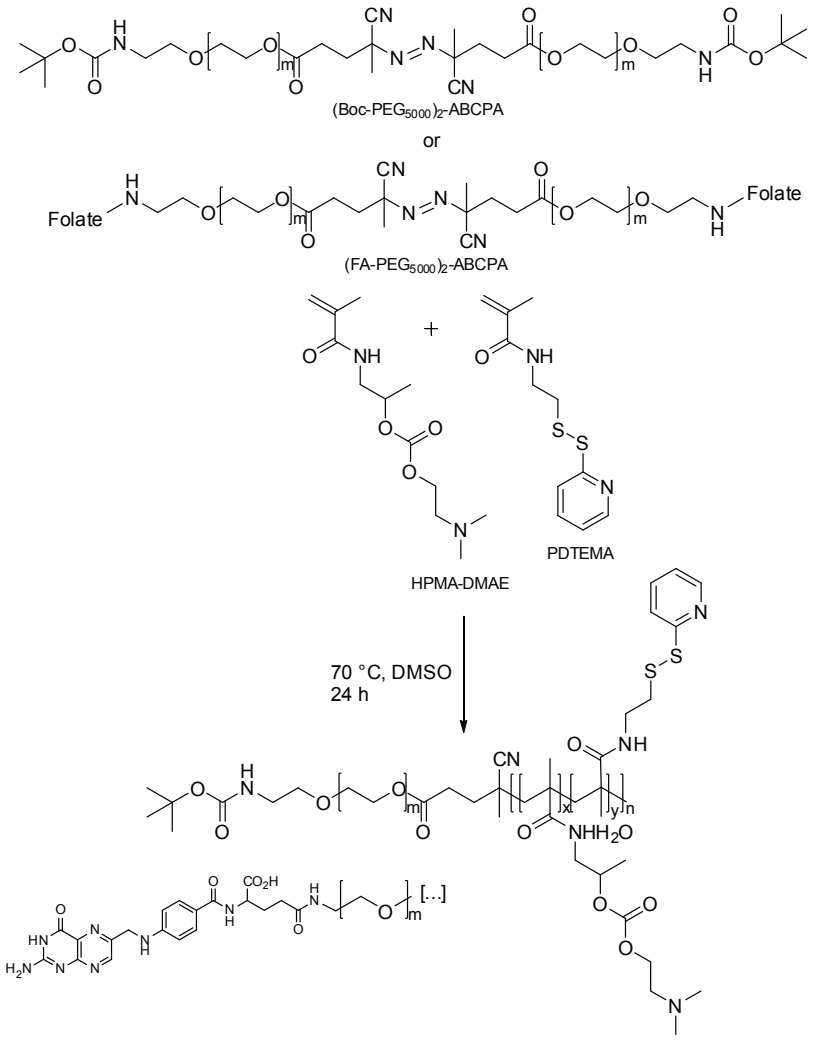

Scheme 3. Synthesis of pHDP-PEG-FA and pHDP-PEG.

Table 1. Overview of the characteristics of the synthesized pHDP-PEG-FA and pHDP-PEG as determined by GPC, ^{1}H NMR and UV spectroscopy.

Polymer	GPC			NMR			UV
	M_n (kDa)	PDI	dn/dc	M_n (kDa)	Feed HPMA–DMAE/PDTEMA	Polymer HPMA–DMAE/PDTEMA	$nmol_{PDS}/mg_{polymer}$
pHDP-PEG-FA	116.6	1.4	0.18	43.3	1/0.2	1/0.16	295±9
pHDP-PEG	119.9	1.5	0.17	43.9	1/0.2	1/0.15	305±2

3.2. Preparation and stability of pHDP-PEG(-FA) polyplexes

Polyplexes of pHDP-PEG and pHDP-PEG-FA were formed through the 3-step process as schematically shown in Scheme 2 and as also reported in our previous work [19]. The preparation of FA-targeted decationized polyplexes started with the synthesis of the cationic block copolymer p(HPMA–DMAE-co-PDTEMA-b-PEG-FA (pHDP-PEG-FA), which contains FA at the PEG distal end. The block copolymer was subsequently used to complex pDNA via electrostatic interactions and interchain disulfide crosslinking of the polyplexes was performed via thiol–disulfide exchange reaction between a short dithiol (DODT) and the PDS groups of the PDTEMA units present in the polymer backbone. In order to achieve polyplex core-crosslinking DODT was added at a molar equivalent of thiol groups to the PDS groups of the polymer. Structural stabilization and pDNA entrapment occurred due to the interchain disulfide crosslinks in the pHPMA–DMAE core. Decationization was performed by removal of the DMAE cationic side groups linked to the HPMA backbone via carbonate ester bond at pH 8.5, to form p(HPMAco-PDTEMA)-b-PEG-FA (pHP-PEG-FA) decationized polyplexes, containing the folate moiety at their PEG shell.

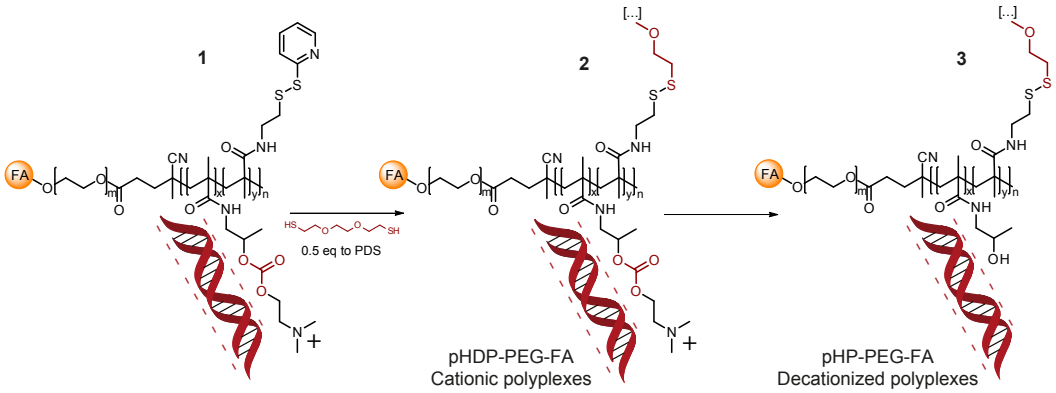

Scheme 2. Route for the preparation of interchain disulfide crosslinked pHP-PEG-FA decationized polyplexes, through a 3-step process: 1. charge-driven condensation; 2. stabilization through disulfide crosslinking; 3. polyplex decationization (adapted from Novo et al. [19]).

The biophysical properties of both pHDP-PEG and pHDP-PEG-FA polyplexes obtained by DLS and zeta potential measurements are given in Table 2. Polyplexes were firstly prepared by complexing the polymer with pDNA at an N/P=4 which ratio was selected because it was shown in our previous study that the pHDP-PEG particles prepared at this N/P had best biophysical and *in vitro* transfection properties [19]. Both polymers formed nanosized polyplexes with a diameter of 127±5 nm for pHDP-PEG cationic polyplexes and 142±8 nm for pHDP-PEG-FA cationic polyplexes. Also, both polyplexes showed a positive zeta potential, however, the zeta potential of the pHDP-PEG-FA cationic polyplexes (+6.5±1.4 mV) was slightly lower than that observed for the pHDP-PEG polyplexes (+10.2±3.1). This difference in zeta potential has been previously observed for folate conjugated polyplexes [27, 39] and is ascribed to of the presence of carboxylic acid groups of folate at the shell of the polyplexes which are negatively charged at pH 7 and therefore lower the zeta potential of the particles. After cross-linking, removal of DMAE cationic groups from the polyplexes was performed by incubation of the polyplex dispersions at pH 8.5 and 37 ºC for 6 h to yield pHP-PEG decationized polyplexes with and without FA groups. DLS results showed that after decationization the polyplex diameter slightly increased from 142±8 to 152±8 nm for pHP-PEG-FA decationized polyplexes and from 127±5 to 132±8 nm for pHP-PEG. Most likely, loss of electrostatic interactions between the polymer and pDNA resulted in hydration and slight swelling of the polyplex core.

Importantly, the zeta potentials of the polyplexes dropped from slightly positive to negative values after decationization (-12.4±0.6 mV for pHP-PEG-FA and -5.3±1.5 mV for pHP-PEG polyplexes). The change in the zeta potential upon decationization procedure is due to the loss of the cationic DMAE groups from the pHDP core. Again, a lower zeta potential was observed for the folate targeted polyplexes, therefore, after decationization the folic acid groups are most likely present on the surface of the polyplexes.

When pHP-PEG-FA decationized polyplexes were incubated in the presence of a reductive agent (10 mM DTT) (Figure 4) and subjected to a gel retardation assay, release of pDNA was observed (Figure 4a), whereas for their cationic counterparts, pDNA remained stably encapsulated in the polyplexes (Figure 4b). This confirms the redox triggered release previously observed for pHP-PEG decationized polyplexes [19].

Tables 2a and 2b. Particle z-average diameter (Z-avg) and polydispersity index (PDI) determined by DLS and particle charge (ζ Pot) determined by zeta potential measurements of pHDP-PEG-FA (a) and pHDP-PEG (b) based polyplexes, at different stages of preparation. Polyplexes were prepared at N/P=4 and a pDNA concentration of 50 µg/mL. Results are expressed as mean±SD (n=3).

a) pHDP-PEG-FA

Polyplexes	DLS		Zetasizer
	Z-ave (nm)	PDI	ζ Pot (mV)
After crosslinking	142±8	0.130±0.046	6.5±1.4
After decationization	152±8	0.099±0.011	-12.4±0.6

b) pHDP-PEG

Polyplexes	DLS		Zetasizer
	Z-ave (nm)	PDI	ζ Pot (mV)
After crosslinking	127±5	0.162±0.028	10.2±3.1
After decationization	132±8	0.190±0.064	-5.3±1.5

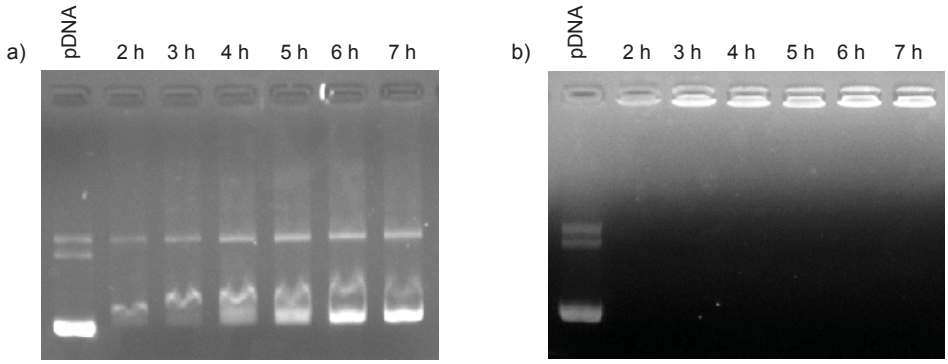

Figure 4. Agarose gel retardation assay of pHP-PEG-FA decationized (a) and pHDP-PEG-FA cationic (b) polyplexes upon incubation with 10 mM DTT in HBS at 37 °C, for 2 h; 3 h; 4 h; 5 h; 6 h; 7 h.

3.3. In vitro evaluation of the pHP-PEG-FA decationized polyplexes in cell cultures

The cellular uptake of pHP-PEG (decationized), pHP-PEG-FA (targeted and decationized) and pHDP-PEG (cationic) polyplexes was evaluated, in the presence of serum, in two folate overexpressing cell lines, HeLa (Figure 5a) and OVCAR-3 (Figure 5b) and in a folate nonexpressing cell line A549 (Figure 5c) [40]. The polyplexes were prepared at low concentration with Cy5 labeled pDNA and the degree of uptake was accessed by flow cytometry shortly 2 h after incubation with the cells at 37 ºC. In the case of the folate overexpressing cell lines, the pHP-PEG-FA targeted decationized polyplexes were taken up by cells to a much higher extent (a factor 3-4) than the pHP-PEG nontargeted decationzed polyplexes. In the case of A549 cell line, the pHP-PEG-FA decationized polyplexes had an almost insignificant degree of uptake, and even lower than pHP-PEG decationized polyplexes. The observed relatively lower uptake in the case of the targeted formulation is probably due to a more negative zeta potential observed in pHP-PEG-FA decationized polyplexes that further reduces the possibility of nonspecific interaction with cells. These results clearly show that the high uptake of pHP-PEG-FA decationized polyplexes by the folate receptor overexpressing cell lines, HeLa and OVCAR3, is due to the presence of folate moieties on the surface of the polyplexes and not due to small differences in their biophysical properties. It should be stressed again, that pHDP-PEG nontargeted cationic polyplexes showed a very high degree of uptake in the cell lines tested, once more confirming that polyplexes based on polycations, even when PEGylated, are not suitable for a targeted therapy because specific uptake via the receptor that matches the used targeting ligand is most likely overruled by the high degree of nonspecific uptake.

Transfection efficiency of the decationized polyplexes with and without FA was evaluated using polyplexes of an N/P=4 and at pDNA dose of 3 and 5 μg per well. The transfection efficiency of the FA-decorated and control polyplexes in OVCAR-3 (FR +) cells was studied in the absence of folic acid (medium and serum) [41]. As control transfection was also evaluated in folate saturated medium (1 mM). Folate-targeted nanoparticles or conjugates are known to interact with high affinity to the folate receptor of the cells and internalized by receptor-mediated endocytosis [42]. The polyplexes which end up in endosomes after cellular uptake, need to escape from the endosomes before lysosomal digestion occurs [3, 43-45]. pHP-PEG based polyplexes do not possess endosomal escape functionalities [19], and therefore chloroquine, a known agent to induce endosomal escape [46], was

added to the transfection medium. As positive control ExGen 500 (l-PEI) based polyplexes were used [37].

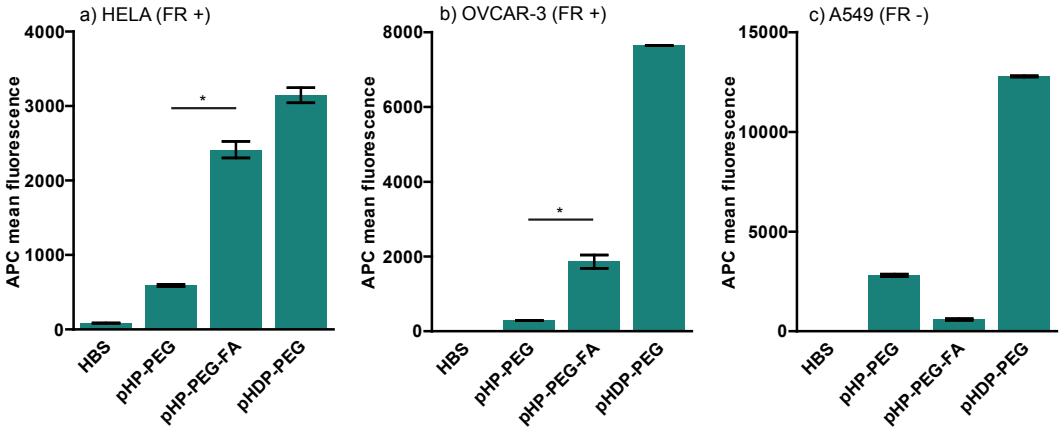

Figure 5. Mean fluorescence intensity per cell after different Cy5-pDNA polyplexes were incubated with HeLa cells (FR +) (a), OVCAR-3 cells (FR +) (b) and A549 (FR -) (c) for 2 h at 37 ºC (pDNA dose was 10 µg/mL, 10%wt Cy5 pDNA). Results are expressed as mean±SD (n=3). *p<0.01 (t-test).

The polyplexes were firstly incubated with the cells for 4 h at 5 °C, allowing binding of polyplexes to the cells and minimizing artifact effects on transfection such nonspecific cell binding due to particle sedimentation and/or excessive contact time of the polyplexes with the cells. Subsequently, medium containing polyplexes which have not interacted with the cells were washed away and the cells were incubated at 37 °C to allow active internalization of the polyplexes firmly interacting with the cells. Polyplexes were added to the cells in a relatively high dose to maximize the number of specific polyplex interactions per cell. Figure 6 shows that pHP-PEG-FA targeted polyplexes exhibit a transfection level in OVCAR3 close to ExGen. More importantly, increasing dose is not detrimental for transfection, emphasizing the safety of a neural polymer based system. It should be noted, that transfection levels of pHP-PEG-FA decationized polyplexes are relatively low when compared to previously shown transfection levels of ExGen in its optimal transfection conditions [37]. However, in the same set-up conditions, where nonspecific internalization is minimized, PEI polyplexes had comparable transfection efficiency to pHP-PEG-FA decationized polyplexes. Often transfection levels of PEI are unrealistic since they arise from significant aggregation in biological media. Aggregation of

PEI formulations (>500 nm) is known to be one of the key factors for its high transfection efficiency in vitro [37].

Figure 6 also shows that when the same cells were transfected with folate-decorated polyplexes in folate saturated medium, the transfection was completely blocked. On the other hand, the transfection levels of cells incubated with nontargeted polyplexes did not decrease in folate saturated medium, which was particularly evident for the highest pDNA dose (5 μg). These results reveal that the decrease in transfection for pHP-PEG-FA decationized polyplexes in folate saturated medium is due to saturation of the folate receptors with free folate making them inaccessible for interaction with the folate-decorated polyplexes. In folate saturated medium, some degree of transfection was observed for pHP-PEG decationized polyplexes, in contrast to nontargeted pHP-PEG-FA particles, in which no detectable luciferase expression was observed at both pDNA doses. This result is in accordance with the uptake observed for folate nonexpressing cell line A549 (Figure 2c), where nonspecific uptake is higher for nontargeted polyplexes. The low degree of transfection observed for pHP-PEG decationized polyplexes, is also in accordance with the findings previously observed in HeLa and A549 [19], where the lack of cellular uptake greatly contributed for low transfection efficiency.

In the absence of folic acid in the medium, the difference in transfection activity between targeted pHP-PEG-FA and nontargeted pHP-PEG decationized polyplexes is close to one order of magnitude higher for the targeted systems. Several reports have shown the improvement of transfection efficiency by folate targeting of polyplexes [47-49] and our results are in line with these findings. In the case of our system, folate targeting triggers transfection with very high specificity for target cells. Furthermore, Salvati et al. [50] reported that targeting specificity can be lost by unspecific interactions with components from biological fluids with nanoparticles, the lack of cationic charges in the decationized polyplexes is expected to further reduce the occurrence of unspecific interactions, improving in this way the targeting specificity.

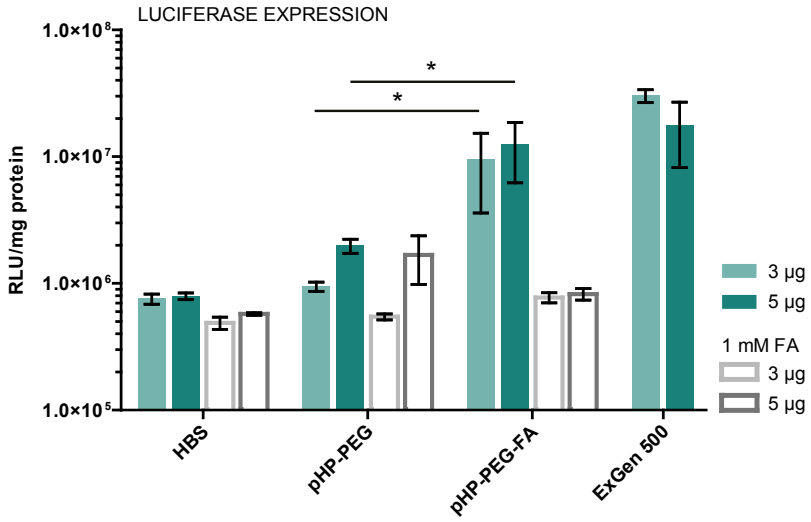

Figure 6. Effect of pDNA dose (3 and 5 µg of pDNA/well; final FA concentration is 2.26 µM and 3.37 µM, respectively) and on luciferase expression levels of OVCAR-3 cells (FR +) incubated with different decationized polyplexes (N/P=4, pHP-PEG and pHP-PEG-FA). OVCAR-3 cells were incubated with polyplex dispersions at 5 ºC, followed by removal of unbound polyplexes, and incubated at 37 ºC for 4 h for transfection. Polyplexes were prepared with an N/P=4. A RLU is unit equivalent to 0.52 pg of luciferase (r^2=0,99, n=3). Results are expressed as mean±SD (n=4). *p<0.05 (t-test).

The cytotoxicity of targeted pHP-PEG decationized polyplexes was evaluated using the XTT assay and compared with that of nontargeted pHP-PEG and cationic nontargeted pHDP-PEG polyplexes. Polyplexes were prepared at an N/P=4 and tested at different pDNA doses (0.25, 1 and 3 µg pDNA per well, Figure 7) and incubated HeLa cells for 24 h. This figure shows that a high metabolic activity was found for the cells incubated with both targeted and nontargeted polyplexes. The outcome of the study reveals that even after extensive uptake of the decationized polyplexes, metabolic activity of the cells was not affected, confirming the safety profile that was previously found for nontargeted decationized systems in HeLa cells [19].

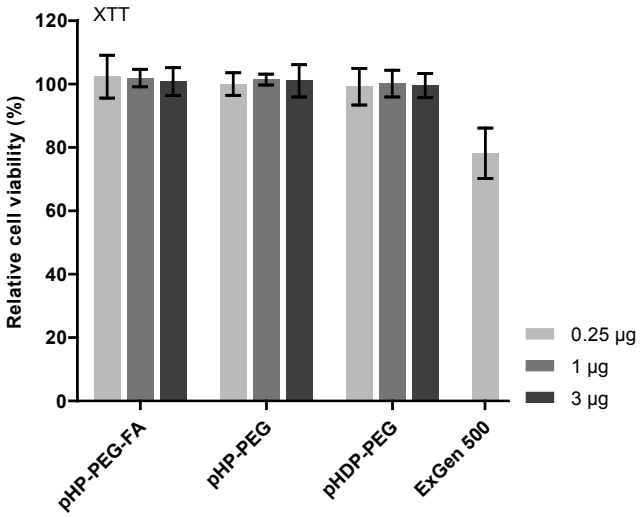

Figure 7. Effect of pDNA dose (0.25, 1 and 3 µg of pDNA/well) on cell viability of HeLa cells (FR +) for the different polyplexes (pHP-PEG, pHP-PEG-FA and pHDP-PEG). HeLa cells were transfected in the presence of 10% serum. Polyplexes were prepared with a starting N/P=4 and incubated with the cells for 24h at 37 ºC. Results are expressed as mean±SD (n=3).

4. CONCLUSION

Folate targeted polyplexes based on the hydrophilic and noncharged pHP-PEG polymer were prepared using the cationic pHDP-PEG-FA polymer as precursor. The introduction of the folate targeting units at the surface of decationized polyplexes did not alter significantly their properties like triggered release under intracellular-mimicking reducing conditions, polyplex biophysical properties or the safety profile of this system. Importantly, uptake of FA targeted decationized polyplexes by folate receptor overexpressing cell lines, HeLa and OVCAR-3, was significantly higher when compared to its nontargeted counterpart. Oppositely, uptake studies with the folate receptor negative cell line, A549, showed a slightly lower uptake for targeted polyplexes. In line with the uptake studies, transfection efficiency determined using OVCAR-3 showed striking differences between pHP-PEG-FA targeted and pHP-PEG nontargeted decationized polyplexes. When the medium was saturated with free folic acid the transfection activity of targeted polyplexes was lowered to the level of the nontargeted system.

The results presented in this paper demonstrate that the introduction of folic acid moiety at the surface of decationized polyplexes allow the preparation of a targetable polyplex formulation that is highly promising for site-specific gene therapy after intravenous administration.

Acknowledgement

L. Novo is financially supported by Fundação para a Ciência e a Tecnologia (FCT), the Portuguese Foundation for Science and Technology, grant SFRH/BD/47085/2008.

References

[1] L.W. Seymour, A.J. Thrasher, Gene therapy matures in the clinic, Nat. Biotechnol., 30 (2012) 588-593.

[2] C.E. Thomas, A. Ehrhardt, M.A. Kay, Progress and problems with the use of viral vectors for gene therapy, Nat. Rev. Genet., 4 (2003) 346-358.

[3] M.A. Mintzer, E.E. Simanek, Nonviral vectors for gene delivery, Chem. Rev., 109 (2008) 259-302.

[4] W. Li, F.C. Szoka, Jr., Lipid-based nanoparticles for nucleic acid delivery, Pharm. Res., 24 (2007) 438-449.

[5] J. Luten, C.F. van Nostrum, S.C. De Smedt, W.E. Hennink, Biodegradable polymers as non-viral carriers for plasmid DNA delivery, J. Control. Release, 126 (2008) 97-110.

[6] S.Y. Wong, J.M. Pelet, D. Putnam, Polymer systems for gene delivery—Past, present, and future, Progress in Polymer Science, 32 (2007) 799-837.

[7] E. Mastrobattista, M.A.E.M. van der Aa, W.E. Hennink, D.J.A. Crommelin, Artificial viruses: a nanotechnological approach to gene delivery, Nat. Rev. Drug Discov., 5 (2006) 115-121.

[8] A. Yousefi, G. Storm, R. Schiffelers, E. Mastrobattista, Trends in polymeric delivery of nucleic acids to tumors, J. Control. Release, 170 (2013) 209-218.

[9] P. Midoux, C. Pichon, J.-J. Yaouanc, P.-A. Jaffrès, Chemical vectors for gene delivery: a current review on polymers, peptides and lipids containing histidine or imidazole as nucleic acids carriers, Br. J. Pharmacol., 157 (2009) 166-178.

[10] P. Chollet, M.C. Favrot, A. Hurbin, J.-L. Coll, Side-effects of a systemic injection of linear polyethylenimine–DNA complexes, J. Gene Med., 4 (2002) 84-91.

[11] C.M. Ward, M.L. Read, L.W. Seymour, Systemic circulation of poly(L-lysine)/DNA vectors is influenced by polycation molecular weight and type of DNA: differential circulation in mice and rats and the implications for human gene therapy, Blood, 97 (2001) 2221-2229.

[12] S.M. Moghimi, P. Symonds, J.C. Murray, A.C. Hunter, G. Debska, A. Szewczyk, A two-

stage poly(ethylenimine)-mediated cytotoxicity: implications for gene transfer/therapy, Mol. Ther., 11 (2005) 990-995.

[13] H. Maeda, Tumor-selective delivery of macromolecular drugs via the EPR effect: Background and future prospects, Bioconjug. Chem., 21 (2010) 797-802.

[14] J. Fang, H. Nakamura, H. Maeda, The EPR effect: Unique features of tumor blood vessels for drug delivery, factors involved, and limitations and augmentation of the effect, Adv. Drug Deliv. Rev., 63 (2011) 136-151.

[15] Y.H. Bae, K. Park, Targeted drug delivery to tumors: Myths, reality and possibility, J. Control. Release, 153 (2011) 198-205.

[16] F.J. Verbaan, C. Oussoren, C.J. Snel, D.J.A. Crommelin, W.E. Hennink, G. Storm, Steric stabilization of poly(2-(dimethylamino)ethyl methacrylate)-based polyplexes mediates prolonged circulation and tumor targeting in mice, J. Gene Med., 6 (2004) 64-75.

[17] M. Ogris, S. Brunner, S. Schuller, R. Kircheis, E. Wagner, PEGylated DNA/transferrin-PEI complexes: reduced interaction with blood components, extended circulation in blood and potential for systemic gene delivery, Gene Ther., 6 (1999) 595-605.

[18] M. Harada-Shiba, K. Yamauchi, A. Harada, I. Takamisawa, K. Shimokado, K. Kataoka, Polyion complex micelles as vectors in gene therapy – pharmacokinetics and in vivo gene transfer, Gene Ther., 9 (2002) 407-414.

[19] L. Novo, E.V.B. van Gaal, E. Mastrobattista, C.F. van Nostrum, W.E. Hennink, Decationized crosslinked polyplexes for redox-triggered gene delivery, J. Control. Release, 169 (2013) 246-256.

[20] M.H. Lee, Z. Yang, C.W. Lim, Y.H. Lee, S. Dongbang, C. Kang, J.S. Kim, Disulfide-cleavage-triggered chemosensors and their biological applications, Chem. Rev., 113 (2013) 5071-5109.

[21] F. Meng, W.E. Hennink, Z. Zhong, Reduction-sensitive polymers and bioconjugates for biomedical applications, Biomaterials, 30 (2009) 2180-2198.

[22] A.R. Hilgenbrink, P.S. Low, Folate receptor-mediated drug targeting: From therapeutics to diagnostics, J. Pharm. Sci., 94 (2005) 2135-2146.

[23] L. Teng, J. Xie, L. Teng, R.J. Lee, Clinical translation of folate receptor-targeted therapeutics, Expert Opin. Drug Deliv., 9 (2012) 901-908.

[24] Y. Lu, P.S. Low, Folate-mediated delivery of macromolecular anticancer therapeutic agents, Adv. Drug Deliv. Rev., 54 (2002) 675-693.

[25] Y. Lu, P.S. Low, Folate-mediated delivery of macromolecular anticancer therapeutic agents, Adv. Drug Deliv. Rev., 64, Supplement (2012) 342-352.

[26] C. Dohmen, D. Edinger, T. Fröhlich, L. Schreiner, U. Lächelt, C. Troiber, J. Rädler, P. Hadwiger, H.-P. Vornlocher, E. Wagner, Nanosized multifunctional polyplexes for receptor-mediated siRNA delivery, ACS Nano, 6 (2012) 5198-5208.

[27] J.H. van Steenis, E.M. van Maarseveen, F.J. Verbaan, R. Verrijk, D.J.A. Crommelin, G. Storm, W.E. Hennink, Preparation and characterization of folate-targeted pEG-coated pDMAEMA-based polyplexes, J. Control. Release, 87 (2003) 167-176.

[28] J.M. Benns, A. Maheshwari, D.Y. Furgeson, R.I. Mahato, S.W. Kim, Folate-PEG-folate-graft-polyethylenimine-based gene delivery, J. Drug Target., 9 (2001) 123-139.

[29] D. Neradovic, C.F. van Nostrum, W.E. Hennink, Thermoresponsive polymeric micelles with controlled instability based on hydrolytically sensitive N-isopropylacrylamide copolymers, Macromolecules, 34 (2001) 7589-7591.

[30] M. Talelli, C.J.F. Rijcken, S. Oliveira, R. van der Meel, P.M.P. van Bergen en Henegouwen, T. Lammers, C.F. van Nostrum, G. Storm, W.E. Hennink, Nanobody – Shell functionalized thermosensitive core-crosslinked polymeric micelles for active drug targeting, J. Control. Release, 151 (2011) 183-192.

[31] O. Soga, C.F. van Nostrum, A. Ramzi, T. Visser, F. Soulimani, P.M. Frederik, P.H.H. Bomans, W.E. Hennink, Physicochemical characterization of degradable thermosensitive polymeric micelles, Langmuir, 20 (2004) 9388-9395.

[32] X. Jiang, A. van der Horst, M. van Steenbergen, N. Akeroyd, C. van Nostrum, P. Schoenmakers, W. Hennink, Molar-mass characterization of cationic polymers for gene delivery by aqueous size-exclusion chromatography, Pharm. Res., 23 (2006) 595-603.

[33] D.R. Grassetti, J.F. Murray, Determination of sulfhydryl groups with 2,2'- or 4,4'-dithiodipyridine, Arch. Biochem. Biophys., 119 (1967) 41-49.

[34] G.T. Zugates, D.G. Anderson, S.R. Little, I.E.B. Lawhorn, R. Langer, Synthesis of poly(β-amino ester)s with thiol-reactive side chains for DNA delivery, J. Am. Chem. Soc., 128 (2006) 12726-12734.

[35] J.-H. Ryu, R.T. Chacko, S. Jiwpanich, S. Bickerton, R.P. Babu, S. Thayumanavan, Self-cross-linked polymer nanogels: A versatile nanoscopic drug delivery platform, J. Am. Chem. Soc., 132 (2010) 17227-17235.

[36] S. Kameyama, M. Horie, T. Kikuchi, T. Omura, A. Tadokoro, T. Takeuchi, I. Nakase, Y. Sugiura, S. Futaki, Acid wash in determining cellular uptake of Fab/cell-permeating peptide conjugates, Biopolymers, 88 (2007) 98-107.

[37] E.V.B. van Gaal, R. van Eijk, R.S. Oosting, R.J. Kok, W.E. Hennink, D.J.A. Crommelin, E. Mastrobattista, How to screen non-viral gene delivery systems in vitro?, J. Control. Release, 154 (2011) 218-232.

[38] A. Funhoff, C.F. van Nostrum, A. Janssen, M. Fens, D. Crommelin, W.E. Hennink, Polymer side-chain degradation as a tool to control the destabilization of polyplexes, Pharm. Res., 21 (2004) 170-176.

[39] J. Luten, M.J. van Steenbergen, M.C. Lok, A.M. de Graaff, C.F. van Nostrum, H. Talsma, W.E. Hennink, Degradable PEG-folate coated poly(DMAEA-co-BA)phosphazene-based polyplexes exhibit receptor-specific gene expression, Eur. J. Pharm. Sci., 33 (2008) 241-251.

[40] I.G. Campbell, T.A. Jones, W.D. Foulkes, J. Trowsdale, Folate-binding protein is a marker for ovarian cancer, Cancer Res., 51 (1991) 5329-5338.

[41] K.A. Mislick, J.D. Baldeschwieler, J.F. Kayyem, T.J. Meade, Transfection of folate-polylysine DNA complexes: Evidence for lysosomal delivery, Bioconjug. Chem., 6 (1995) 512-515.

[42] X. Zhao, H. Li, R.J. Lee, Targeted drug delivery via folate receptors, Expert Opin. Drug Deliv., 5 (2008) 309-319.

[43] M.A.E.M. Aa, U.S. Huth, S.Y. Häfele, R. Schubert, R.S. Oosting, E. Mastrobattista, W.E. Hennink, R. Peschka-Süss, G.A. Koning, D.J.A. Crommelin, Cellular uptake of cationic polymer-DNA complexes via caveolae plays a pivotal role in gene transfection in COS-7 cells, Pharm. Res., 24 (2007) 1590-1598.

[44] Z. Yang, G. Sahay, S. Sriadibhatla, A.V. Kabanov, Amphiphilic block copolymers enhance cellular uptake and nuclear entry of polyplex-delivered DNA, Bioconjug. Chem., 19 (2008) 1987-1994.

[45] D. Vercauteren, J. Rejman, T.F. Martens, J. Demeester, S.C. De Smedt, K. Braeckmans, On the cellular processing of non-viral nanomedicines for nucleic acid delivery: Mechanisms and methods, J. Control. Release, 161 (2012) 566-581.

[46] M.A. Wolfert, L.W. Seymour, Chloroquine and amphipathic peptide helices show synergistic transfection in vitro, Gene Ther., 5 (1998) 409-414.

[47] L. Liu, M. Zheng, T. Renette, T. Kissel, Modular synthesis of folate conjugated ternary copolymers: polyethylenimine-graft-polycaprolactone-block-poly(ethylene glycol)-folate for targeted gene delivery, Bioconjug. Chem., 23 (2012) 1211-1220.

[48] C. Dohmen, T. Frohlich, U. Lachelt, I. Rohl, H.-P. Vornlocher, P. Hadwiger, E. Wagner, Defined folate-PEG-siRNA conjugates for receptor-specific gene silencing, Mol. Ther. Nucleic Acids, 1 (2012) e7.

[49] F. Zhao, H. Yin, Z. Zhang, J. Li, Folic acid modified cationic γ-cyclodextrin-oligoethylenimine star polymer with bioreducible disulfide linker for efficient targeted gene delivery, Biomacromolecules, 14 (2013) 476-484.

[50] A. Salvati, A.S. Pitek, M.P. Monopoli, K. Prapainop, F.B. Bombelli, D.R. Hristov, P.M. Kelly, C. Aberg, E. Mahon, K.A. Dawson, Transferrin-functionalized nanoparticles lose their targeting capabilities when a biomolecule corona adsorbs on the surface, Nat. Nanotechnol., 8 (2013) 137-143.

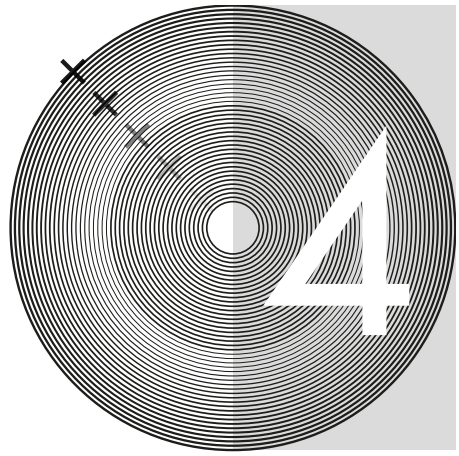

CHAPTER

Decationized polyplexes as stable and safe carrier systems for improved biodistribution in systemic gene therapy

Luís Novo[a,1], Larissa Y. Rizzo[b,1], Susanne K. Golombek[b], George R. Dakwar[c], Bo Lou[a], Katrien Remaut[c], Enrico Mastrobattista[a], Cornelus F. van Nostrum[a], Wilhelm Jahnen-Dechent[d], Fabian Kiessling[b], Kevin Braeckmans[c,f], Twan Lammers[a,b,e], Wim E. Hennink[a]*

[a]Department of Pharmaceutics, Utrecht Institute for Pharmaceutical Sciences, Utrecht University, 3584 CG Utrecht, The Netherlands

[b]Nanomedicines and Theranostics, Department for Experimental Molecular Imaging, University Hospital RWTH Aachen, Pauwelsstrasse 30, 52074 Aachen, Germany

[c]Laboratory for General Biochemistry and Physical Pharmacy, Faculty of Pharmacy, Ghent University, Ghent Research Group on Nanomedicines, Harelbekestraat 72, 9000 Ghent, Belgium

[d]Helmholtz Institute for Biomedical Engineering, Biointerface Laboratory, RWTH Aachen University, Aachen, Germany

[f]Centre for Nano– and Biophotonics, Ghent University, Harelbekestraat 72, 9000 Ghent, Belgium

[e]Department of Targeted Therapeutics, MIRA Institute for Biomedical Technology and Technical Medicine, University of Twente, Enschede, The Netherlands

[1]Authors contributed equally to this work

Accepted for publication in Journal of Controlled Release

Abstract

Many polycation-based gene delivery vectors show high transfection *in vitro*, but their cationic nature generally leads to significant toxicity and poor *in vivo* performance which significantly hampers their clinical applicability. Unlike conventional polycation-based systems, decationized polyplexes are based on hydrophilic and neutral polymers. They are obtained by a 3-step process: charge-driven condensation followed by disulfide crosslinking stabilization and finally polyplex decationization. They consist of a disulfide-crosslinked poly(hydroxypropyl methacrylamide) (pHPMA) core stably entrapping plasmid DNA (pDNA), surrounded by a shell of poly(ethylene glycol) (PEG). In the present paper the applicability of decationized polyplexes for systemic administration was evaluated. Cy5-labeled decationized polyplexes were evaluated for stability in plasma by fluorescence single particle tracking (fSPT), which technique showed stable size distribution for 48 h unlike its cationic counterpart. Upon the incubation of the polymers used for the formation of polyplexes with HUVEC cells, MTT assay showed excellent cytocompatibility of the neutral polymers. The safety was further demonstrated by a remarkable low teratogenicity and mortality activity of the polymers in a zebrafish assay, in great contrast with their cationic counterpart. Near-infrared (NIR) dye-labeled polyplexes were evaluated for biodistribution and tumor accumulation by noninvasive optical imaging when administered systemically in tumor bearing mice. Decationized polyplexes exhibited an increased circulation time and higher tumor accumulation, when compared to their cationic precursors. Histology of tumors sections showed that decationized polyplexes induced reporter transgene expression *in vivo*. In conclusion, decationized polyplexes are a platform for safer polymeric vectors with improved biodistribution properties when systemically administered.

KEYWORDS Gene delivery, polymer, nanoparticle, biocompatibility, biodistribution, EPR

1. INTRODUCTION

Gene therapy has generated great interest to be used as a therapeutic tool to solve unmet medical needs [1, 2] and relies on the development of safe and efficient

vectors. Non-viral vectors, such as cationic polymers, lipids and peptides, have been investigated in depth because of their flexibility and easiness of preparation when compared to viral vectors [3-9].

Polyplexes are normally formed by adding an excess of polycations to pDNA to yield positively charged and small-sized polyplexes which can, however, lead to significant toxicity *in vivo* [10, 11]. Toxicity of polycation-based vectors was especially evident for the "first-generation" homopolymer systems. Upon intravenous administration, cationic polyplexes show great instability *in vivo*, since they interact with negatively charged blood components (e.g. proteins, erythrocytes), followed by the formation of aggregates, leading to severe *in vivo* toxicity (lung embolism and/or liver necrosis) and uncontrollable biodistribution and off-targeting transfection [10-12]. Furthermore, cationic polymers/dendrimers might induce immunogenicity, complement activation and even blood coagulation [12-14].

Several strategies have been proposed and investigated to improve the *in vivo* behavior of polyplexes. Coating of polycation-based systems with PEG, effectively avoids the formation of aggregates and reduces protein binding, resulting in improvements of the circulation kinetics and tumor accumulation *in vivo* [12, 15, 16]. Another strategy to improve polyplex stability consists of the incorporation of disulfide crosslinks into the polyplex core. Disulfide crosslinks stabilize the polyplex structure in the bloodstream, avoiding unwanted disassembly in circulation, but these bonds can be rapidly cleaved in the intracellular reducing milieu [17-19]. *In vivo*, introduction of disulfide crosslinks, has demonstrated to improve circulation kinetics [20], as well as to improve tumor accumulation and transfection upon systemic administration [21]. However, further improvements on the blood circulation kinetics and biodistribution are of utmost importance to achieve the desired selective accumulation into target tissues. Even when shielded with PEG, the cationic groups of conventional polyplexes can also lead to unspecific cell binding in highly vascularized organs and, consequently, to poor *in vivo* biodistribution and insufficient blood circulation half-life [22, 23].

The major challenge for the clinical applicability of polymeric vectors is to achieve therapeutic efficacy with minimal toxicity and side effects upon systemic administration. Toxicity arising from polycations occurs not only on the systemic level but also at the cellular basis. Introduction of biodegradability into cationic polymers leads to the development of safer systems [5, 24]. However, during the development of new gene delivery polymer, toxicity is measured with cell

viability assays in limited concentrations and exposure times, likely leading to underestimation of the toxicity problem. Toxicity is a complex process and requires deeper analysis at both acute and long term basis. When cationic polyplexes are taken up by cells, they will firstly compromise the cell membrane integrity [25-27]. Polycations can also disrupt the cell homeostasis by interaction with cellular polyanions (e.g. cell receptors, enzymes, mRNA or genomic DNA) [28]. Polycations can change the genomic expression profile [29-31] and induce the activation of oncogenes or even apoptosis [26, 32]. Such consequences are directly related to the polycationic nature of synthetic vectors and have a substantial impact on the safety of such systems. Accordingly, neutral polymer based systems are a logical step to obtain not only to improve blood circulation kinetics and biodistribution but also to accomplish the necessary safety requirements.

In previous the work the development of decationized polyplexes was reported [33, 34]. These polyplexes constitute of a core of disulfide-crosslinked pHPMA, surrounded by a PEG shell. Complexation with DNA to form polyplexes occurs by the transient presence of cationic charge in the core of the polyplexes. After structure stabilization by interchain disulfide crosslinking, the cationic groups are removed by hydrolysis, leading to a disulfide crosslinked polyplex based on a neutral polymer. As a result, entrapment of pDNA is exclusively based on disulfide crosslinks, providing an intracellularly triggered release mechanism. This means that pDNA release from decationized polyplexes occurs exclusively in a reducing environment, such as the intracellular milieu [17-19]. Importantly, the decationized polyplexes, in contrast to their cationic precursor, showed a low degree of nonspecific uptake, which is thought to be an important advantage for improved blood circulation and higher target tissue accumulation exploiting the enhanced permeation and retention (EPR) effect [35].

In this study, we evaluated the stability, safety and *in vivo* biodistribution as well as the ability of decationized polyplexes for tumor targeting applications. The stability in biological fluids was evaluated by fSPT [36], as well as the safety by the teratogenicity and mortality potential in zebrafish embryo assay in parallel with cytotoxicity tests *in vitro* [37], and biodistribution and tumor accumulation in a A431 tumor-bearing mice by noninvasive optical imaging based on the combination micro-computed tomography (μCT) and fluorescence molecular tomography (FMT) [38]. Finally, transgene expression was also assessed by histological analysis of tumor cryosections.

2. MATERIALS AND METHODS

2.1. Materials

N-hydroxysuccinimide (NHS) ester functionalized dyes Cyanine5 NHS ester (Cy5-NHS) and Cyanine7 NHS ester (Cy7-NHS) were obtained from Lumiprobe (Hannover, Germany). Carbonyldiimidazole (CDI) activation of *N,N*'-dimethylaminoethanol (DMAE) was performed as previously described to yield DMAE-CI [39]. *N*-[2-(2-pyridyldithio)]ethyl methacrylamide (PDTEMA) was synthesized as previously described [33]. *N*-(3-aminopropyl)methacrylamide hydrochloride (APMA) was obtained from Polysciences (Eppelheim, Germany). The synthesis and characterization of $(mPEG)_2$ABCPA (4,4'-azobis(4-cyanovaleric acid)) macroinitiator were done as previously described [40, 41]. 2,4,6-Trinitrobenzene sulfonic acid (TNBSA) was obtained from ThermoScientific (Etten-Leur,The Netherlands). pCMV_EGFP plasmid, encoding for enhanced green fluorescent protein (EGFP) with human cytomegalovirus promoter (CMV), was amplified with competent *E. coli* DH5α and purified with NucleoBond® **(**Macherey-Nagel, Bioke, Leiden, The Netherlands). pCMV_EGFP construction was described by van Gaal et al. [42]. MTT Cell Proliferation Kit (3-(4,5-dimethylthiazol-2-yl)-2,5-diphenyl tetrazolium bromide) was purchased from Roche (Basel, Switzerland). Zebrafish medium was prepared in-house [37]. All other chemicals and reagents were obtained from Sigma-Aldrich (Zwijndrecht, The Netherlands). The following buffer systems were used: 4-(2-hydroxyethyl)-1-piperazineethanesulfonic acid (HEPES) for buffering at pH 6.8–8.2; 3-[[1,3-dihydroxy-2-(hydroxymethyl)propan-2-yl]amino]propane-1-sulfonic acid (TAPS) for buffering at pH pH 7.7–9.1.

2.2. Polymer synthesis

2.2.1 Synthesis of p(HPMA-co-PDTEMA-co-APMA)-b-PEG

Free radical polymerization using 5 kDa PEG bi-functionalized azo macroinitiator $(PEG)_2$-ABCPA was performed to synthesize p(HPMA-co-PDTEMA-co-APMA)-b-PEG (Scheme 1). The polymers were synthesized using a monomer to initiator ratio (M/I) of 220 (mol/mol). The feed ratio HPMA/PDTEMA/APMA was 1/0.2/0.01 (mol/mol/mol). The polymerization was carried at 70 °C for 24 h in DMSO under an N_2 atmosphere, using 5 µmol macroinitiator and a monomer concentration of 0.4 M. After polymerization, the obtained product was precipitated in diethyl ether and collected by centrifugation. After removing ether under vacuum, the product was

dissolved in 2.5 mM NH_4OAc pH 5 buffer and dialyzed for 2 days at 4 °C (MWCO 6000−8000 Da) against the same buffer. Finally, the product was collected by freeze-drying.

Unreacted PEG was removed by precipitation in cold EtOH (5 mg/mL of solids) followed by centrifugation and filtration over a 0.2 µm filter. The product, solubilized in EtOH, was collected after EtOH evaporation, dissolution in water and freeze-drying.

2.2.2. Synthesis of p(HPMA–DMAE-co-PDTEMA-co-Cy5/Cy7)-b-PEG

Firstly, a solution of p(HPMA-co-PDTEMA-co-APMA)-b-PEG·TFA) (M_w = 44.1 kDa; 10 mg, 46.75 nmol NH_2/mg polymer, 1 eq.) was prepared in 100 µL of DMSO. Next, the polymer solution was slowly added to a 0.01 M Cy7-NHS or Cy5-NHS solution in 93.5 µL of DMSO (935 nmol, 2 eq), containing 2.3 µmol (5 eq.) of triethylamine (Scheme 2). The reaction was performed for 36 h (in the dark) under stirring and N_2 atmosphere.

To determine the coupling efficiency, the crude product was diluted to a final polymer concentration of 1 mg/mL in DMF containing 10 mM LiCl and analyzed by GPC equipped with a UV detector set at 646 nm for Cy5 and 700 nm for Cy7 detection. The coupling efficiency was determined by analyzing the area under the curve (AUC) of the polymer and unreacted dye peaks. AUC was determined using GraphPad Prism 5 (GraphPad Software Inc., La Jolla, California, USA).

A 1 M of DMAE-CI solution in DMSO (451.5 µmol), corresponding to a 10-fold excess to HPMA reactive groups of the polymer, was added to the reaction mixture. The reaction was performed at room temperature for 24h, in the dark and N_2 atmosphere to yield p(HPMA–DMAE-co-PDTEMA-co-Cy5/Cy7)-b-PEG (Scheme 2). After completion of the reaction, 1 M of acetic acid was added to adjust the pH 5. Removal of free dye was performed by dialysis against a mixture of EtOH/water 10 mM NH_4Ac pH 5 (50/50) for 2 days. The polymer was collected by freeze-drying after buffer exchange to 5 mM NH_4Ac pH 5 and desalting using PD-10 (GE Healthcare Life Sciences) columns following supplier's protocol.

2.2.3. Preparation of p(HPMA-co-PDTEMA)-b-PEG

To prepare p(HPMA-co-PDTEMA)-b-PEG (pHP-PEG), 5 mg of p(HPMA–

DMAE-co-PDTEMA)-b-PEG (pHDP-PEG) was dissolved in 2.5 mL 10 mM HEPES 10 mM TAPS pH 8.5 buffer and hydrolyzed for 6 h at 37 ºC. After hydrolysis the polymer was purified with a PD10 column following supplier's protocol and collected by freeze-drying.

2.3. ^{1}H NMR characterization of the polymers

The composition of the polymers was determined by ^{1}H NMR analysis performed with a 400 MHz Agilent 400-MR NMR spectrometer (Agilent Technologies, Santa Clara, USA) in DMSOd6. The ratio HPMA/PDTEMA was determined by comparison of the integrals at δ 4.6 ppm (bs, CH_2CHCH_3O, HPMA) and the integral at δ8.5 ppm (bs, pyridyl group proton, PDTEMA) ($\int\delta_{4.6}/\int\delta_{8.5}$). The integral ratios between δ4.2 ppm (bs, OCH_2CH_2), HPMA–DMAE) and δ4.6 ppm (bs, CH_2CHCH_3O, HPMA–DMAE) were used to verify reaction between DMAE-CI and hydroxyl groups in the polymer from HPMA.

The number average molecular weight (M_n) of the polymers was determined according to equation (1).

$$M_n = (\int\delta_{4.6} \times M(_{HPMA}/_{HPMA-DMAE} + \int\delta_{8.5} \times M_{PDTEMA})/(\int\delta_{3.5}/448) + 5000 \text{ (g/mol)} \quad (1)$$

where, $\int\delta_{3.5}$, $\int\delta_{4.6}$ and $\int\delta_{8.5}$ are the integrals at 3.5, 4.6, and 8.5 ppm, respectively. $M_{HPMA,}$ $M_{HPMA-DMAE}$ and M_{PDTEMA} are the molar masses of HPMA, HPMA–DMAE and PDTEMA, respectively. The number of protons for the 5000 Da PEG block, at $\int\delta_{3.5,}$ was set at 448.

2.4. UV spectroscopy characterization of the polymers

UV spectroscopy was performed on a Shimadzu UV-2450 UV/VIS spectrophotometer ('s-Hertogenbosch, The Netherlands) to quantify the molarity of thiol reactive pyridyl disulfide (PDS) groups per weight of polymer. Polymer stock solutions of 1 mg/mL were prepared in 20 mM HEPES pH 7.4 containing 50 mM of tris(2-carboxyethyl)phosphine (TCEP). After incubation for 1 h at 37 ºC the UV absorbance at 343 nm was measured to determine the released 2-mercaptopyridine (2-MP) [43]. Quantification was performed using a calibration curve with 2-MP standards.

To quantify the molarity of dye Cy7 or Cy5 per weight of polymer, polymer stocks

of 1 mg/mL in DMSO were prepared and the UV absorbance was measured at 646 nm for pHDP-Cy5-PEG or 750 nm for pHDP-Cy7-PEG. The quantification was done using a calibration curve of dye standards in DMSO.

2.5. TNBSA assay

In order to determine the molarity of free primary amines in p(HPMA-co-PDTEMA-co-APMA)-b-PEG, the TNBSA assay was performed [44]. Polymer solutions were prepared at 1 mg/mL in 0.1M sodium bicarbonate buffer (pH 8.5) using glycine standards. The amine content was determined by detecting the absorbance at 420 nm.

2.6. Gel permeation chromatography (GPC) characterization of the polymers

GPC analysis of the polymers was performed using a Waters System (Waters Associates Inc., Milford, MA) with refractive index (RI) and UV detector using two serial Plgel 5 µm MIXED-D columns (Polymer Laboratories) and DMF containing 10 mM LiCl as eluent. The flow rate was 1 mL/min (30 min run time) and the temperature was 60 °C. The average molecular weight (M_n), weight average molecular weight (M_w) and polydispersity (PDI, M_w/M_n) were determined by calibration with a series PEG calibration standards of different molecular weights and with narrow molecular weight distribution.

2.7. Preparation of decationized polyplexes

The preparation of Cy5/Cy7-labeled decationized polyplexes was adapted from the method previously described (Scheme 3) [33]. In order to prepare a high concentrated polyplex dispersion 400 µg/mL pDNA, 80 µL of aqueous solution of pHDP-PEG was mixed with 160 µL of pDNA (pCMV_EGFP) (600 µg/mL) in 10 mM HEPES 10 mM TAPS pH 8.5 buffer containing 5% glucose. The amount of polymer added to the pDNA solution corresponded to N/P=4 (N, molarity of positively charged amines from polymer; P, molarity of negatively charged phosphates from pDNA). Subsequently, the formed polyplexes were crosslinked by the addition of dithiothreitol (DTT) corresponding with a half molar equivalent to PDS groups of the polymer, in order to induce self-crosslinking of the polyplexes [45] for 1 h at pH 8.5 at room temperature.

To prepare decationized pHP-PEG polyplexes, the cationic DMAE side groups were removed by hydrolysis by the incubation of the polyplex dispersions at 37 °C in 10 mM HEPES 10 mM TAPS, pH 8.5 for 6 h [33]. Next, the pH of the dispersion was adjusted to pH 7.4. For cationic pHDP-PEG polyplexes the pH was adjusted to pH 7.4 immediately after the completion of the crosslinking step. When polyplexes needed to be stored for long periods, the pH of the dispersions was adjusted to pH 5 and the dispersions were stored at 0-5 ºC, with the pH being readjusted to pH 7.4 immediately before use. Comparative studies were always performed by dividing the same batch of polyplexes into pHDP-PEG cationic and pHP-PEG decationized polyplexes. Given the fact that the side products from cross-linking and decationization (2-mercaptopyridine and DMAE) have a high cellular tolerance [33, 45, 46], the polyplexes were directly used without purification procedures.

2.8. Particle size and zeta potential determination

The size of the polyplexes was measured with DLS on an ALV CGS-3 system (Malvern Instruments, Malvern, UK) equipped with a JDS Uniphase 22 mW He–Ne laser operating at 632.8 nm, an optical fiber-based detector, a digital LV/LSE-5003 correlator with temperature controller set at 25 °C or 37 °C. Measurements were performed in HBS (20 mM HEPES, 150 mM NaCl, pH 7.4) at a pDNA concentration of 40 μg/mL.

Size distribution and polydispersity of the polyplexes were also determined by nanoparticle tracking analysis (NTA) measurements on a NanoSight LM10SH (NanoSight, Amesbury, United Kingdom), equipped with a sample chamber with a 532-nm laser. Polyplexes were diluted in phosphate buffered saline (PBS) to a concentration of 0.1 μg/mL pDNA and measured for 160 s with manual shutter and gain adjustments. The captured videos were analyzed by the NTA 2.0 image analysis software (NanoSight, Amesbury, UK). The detection threshold was set to 2 and the minimum track length to 10. The mode and mean size and SD values were obtained by the NTA software.

The zeta potential (ζ) of the polyplexes was measured using a Malvern Zetasizer Nano-Z (Malvern Instruments, Malvern, UK) with universal ZEN 1002 ‘dip’ cells and DTS (Nano) software (version 4.20) at 25 °C. Zeta potential measurements were performed in 20 mM HEPES pH 7.4 at a pDNA concentration of 10 μg/mL.

2.9. Stability using fluorescence single particle tracking (fSPT)

fSPT was performed to measure the stability of the cationic pHDP-PEG polyplexes and decationized pHP-PEG polyplexes in full human plasma. fSPT is a fluorescence microscopy technique that uses wide-field and a fast and sensitive CCD camera to record movies of diffusing particles in biofluids. These movies are analyzed using in-house developed software, to obtain size distributions as previously described [36].

fSPT measurements were performed as follows: a volume of 5 µL of sample of Cy5-labeled polyplex dispersion in HEPES buffer (20 mM pH 7.4) or in fresh plasma (10 µg/mL final pDNA concentration) was placed between a microscope slide and cover glass with double-sided adhesive sticker, following incubation for different time points at 37 °C. Both the objective and the sample were kept at 37 °C during the measurements using an objective heater (Bioptechs, Butler, USA) and a sample heater (Linkam, Surrey, U.K.). Videos were recorded with the NIS Elements software (Nikon) driving the EMCCD camera (Cascade II:512, Roper Scientific, AZ, USA) and a TE2000 inverted microscope equipped with a 100_ NA1.4 oil immersion lens (Nikon). To convert SPT diffusion measurements to size distributions, the viscosity of human plasma at 37 °C was set to 1.35 cP [36]. Human plasma was obtained from a healthy donor at UMC Utrecht. Blood was collected in EDTA tubes which were cooled on ice and subsequently centrifuged at 4 ºC, 2000 ×g for 10 min and plasma was isolated and stored at -80 ºC.

2.10. Cell Culture

HUVEC (human umbilical vein endothelial) cells were obtained from human umbilical cords and cultured in Endopan 3 (E3) medium (Pan Biotech, Germany), supplemented with 1% penicillin/streptomycin. A431 epidermoid carcinoma cells (ATCC) were cultured in Dulbecco's modified Eagle's Medium (DMEM; Gibco, Invitrogen, Germany), supplemented with 10% fetal bovine serum (FBS) (Invitrogen, Germany) and with 1% penicillin/streptomycin. Cell lines were kept at 37 °C and 5% CO2, in a humidified atmosphere.

2.11. MTT assay

The cell viability upon incubation with decationized pHP-PEG and cationic

pHDP-PEG polymers was evaluated via MTT assay, which measures the cellular metabolic activity of the cells. HUVECs were seeded into 96-well plates: 12,000 cells were seeded per well for 24 h test and 1950 cells per well were seeded for the 72 h test. After 24 h, the medium was refreshed and 30 µL of polymer samples in PBS was added to each well corresponding to a final concentration of 0.01–3 mg/mL also containing 12% FBS. After 24 h or 72 h, the MTT assay (Roche) was performed according to manufacturer's protocol. First, cells were washed with 200 µL PBS and 100 µL of cell culture medium was added per well. Next, MTT labeling reagent was added to a final concentration of 0.5 mg/mL. After 4 h at 37 ºC and 5% CO_2, the medium was discarded and 100 µL of DMSO was added per well to dissolve the formed formazan crystals. The plate was protected from light and formazan crystals were dissolved overnight at room temperature. The supernatants (100 µL) were then transferred into another 96-well plate and the absorbance was measured at 570 nm using reference wavelength of 690 nm.

2.12. *In vivo* toxicity using the zebrafish embryo assay

The *in vivo* toxicity of decationized pHP-PEG and cationic pHDP-PEG polymers was evaluated using the zebrafish (*Danio rerio*) embryo assay based on the method previously described in detail by Rizzo et al. [37]. In short, fertilized eggs were transferred into round-bottom 96-well plates (16-cell stadium, 1 egg per well). Polymers were diluted in fish medium corresponding to polymer concentrations ranging from 0.1 to 3 mg/mL. As positive control, branched polyethylenimine (b-PEI) 25 kDa was tested at 0.1 mg/mL. The development and survival of the zebrafish embryos was evaluated for 72 h every 24 h post-fertilization using a Leica DMI 6000B inverted microscope.

2.13. Animal experiments

CD-1 nude female mice were fed with chlorophyll-free food pellets and water *ad libitum*. Mice were housed in ventilated cages and clinically controlled rooms and atmosphere. CD-1 nude mice were inoculated with A431 tumor cells (4×10^6 cells/100 µL) subcutaneously into the left flank 15 days before experiment, which lead to the development of A431 tumor xenografts with an approximate size of 6–7 mm in width.

Decationized pHP-PEG polyplexes (group 1, n=3 and cationic pHDP-PEG

polyplexes (group 2, n=3) were tested for their *in vivo* biodistribution and tumor accumulation. Polyplex dispersions labeled with Cy7 were injected (80 µL, 32 µg pDNA, 2.5 nmol Cy7) into mice via tail vein under anesthesia. Immediately after sample injection, µCT (Tomoscope DUO; CT Imaging, Erlangen, Germany) and 3D FMT imaging (FMT2500; PerkinElmer), were performed essentially as previously described [38]. Briefly, mice were placed in a multi-modal imaging cassette under anesthesia (2% of isoflurane) to be firstly scanned in a µCT. Images with an isotropic voxel size of 35 µm were reconstructed using a modified Feldkamp algorithm with a smooth kernel. Immediately after µCT procedure, the animals were placed into the FMT docking station under 2% isoflurane anesthesia. The excitation wavelength channel was set to 750 nm. Whole body images of the mice were captured using FRI to allow the definition of the region of interest (ROI) and 3D scans were performed. µCT and 3D FMT images were collected 15 min, 4 h, 24 h and 48 h post-injection.

The obtained µCT and FMT scans were fused. Based on the µCT data, liver, kidneys, lungs, heart, bladder and tumor were segmented, using an Imalytics Research Workstation software (Philips Technologie GmbH Innovative Technologies, Aachen, Germany). FMT reconstructed signals were overlapped onto respective organ-segmented µCT images, and the amount accumulated Cy7 in these organs was quantified. The percentage injected dose (% ID) was calculated based on the quantification obtained for each segmented organ and normalized to the organ volume. In parallel to the imaging protocol, blood and urine samples were also collected at relevant time 2 min, 15 min, 1 h and 4 h for blood and 1 h, 4 h and 24 h for urine collection.

2.15. *Ex vivo* analysis

Mice were injected intravenously with rhodamine-labeled lectin (Vector Laboratories, Ltd., UK), for staining of blood vessels, 15 min before sacrifice and 48h after sample injection. Tumors, liver, spleen, heart, lungs, uterus, intestines, muscle and skin were collected, weighted and analyzed by 2D Fluorescence reflectance imaging (FRI) at the FMT at the 750 nm channel. Tumors were preserved in Tissue-Tek® O.C.T™ compound (Sakura, The Netherlands) at -80 °C for immunohistochemistry.

2.16. Histological analysis

Histological staining was performed to analyze the Cy7-labeled polyplex accumulation in tumors. Simultaneously, EGFP expression in the tissue was evaluated in order to determine the degree of transfection for both decationized pHP-PEG and cationic pHDP-PEG polyplexes. Frozen 8 µm sections were prepared, where blood vessels were previously stained by rhodamine-lectin perfusion. Sections were mounted using Mowiol and fluorescence microscopy imaging was performed using an Axio Imager M2 microscope and a high-resolution AxioCam MRm Rev.3 camera, at magnification 40×. Images of 3 independent sections per animal were further post-processed using AxioVision Rel 4.8 software (Carl Zeiss Microimaging GmbH, Göttingen, Germany) and analyzed for Cy7 signal (polyplex accumulation) and EGFP signal (transfection efficiency).

2.17. Statistical analysis

Statistical analysis for comparison between means was performed with the software GraphPad Prism 5 (GraphPad Software Inc., La Jolla, California, USA) and a two-tailed paired Student's t-test was used, where $p<0.05$ was considered to represent statistical significance.

3. RESULTS AND DISCUSSION

3.1. Synthesis of fluorescently labeled p(HPMA–DMAE-co-PDTEMA)-b-PEG

The stability evaluation by fSPT and the *in vivo* evaluation by 3D-FMT of decationized polyplexes required the synthesis of Cy5- and Cy7-labeled pHDP-PEG. which was performed in 3 steps (Scheme 1). First, p(HPMA-co-PDTEMA-co-APMA)-b-PEG was synthesized via free-radical polymerization of HPMA, PDTEMA and APMA using $mPEG)_2$-ABCPA as a PEG_{5000} bi-functionalized azo macronitiator [40] (Scheme 1). The yield of polymerization was close to 75%. The results of the analysis of the polymer by ^{1}H NMR (Figure 1), GPC and TNBSA assay are given in Table 1. The different monomers were incorporated in the polymer close to the feed ratio. The M_n calculated by ^{1}H NMR (44.0 kDa) is in good agreement with GPC (34.4 kDa, PDI=1.6). The incorporation of PDTEMA was confirmed by UV, and a value of 821±43 nmol per mg of polymer was found, which is very close to

the value calculated by NMR (863 nmol per mg of polymer; thus around 40 units of PDTEMA were present per polymer chain). The TNBSA assay showed that approximately 2 units APMA per polymer chain were present.

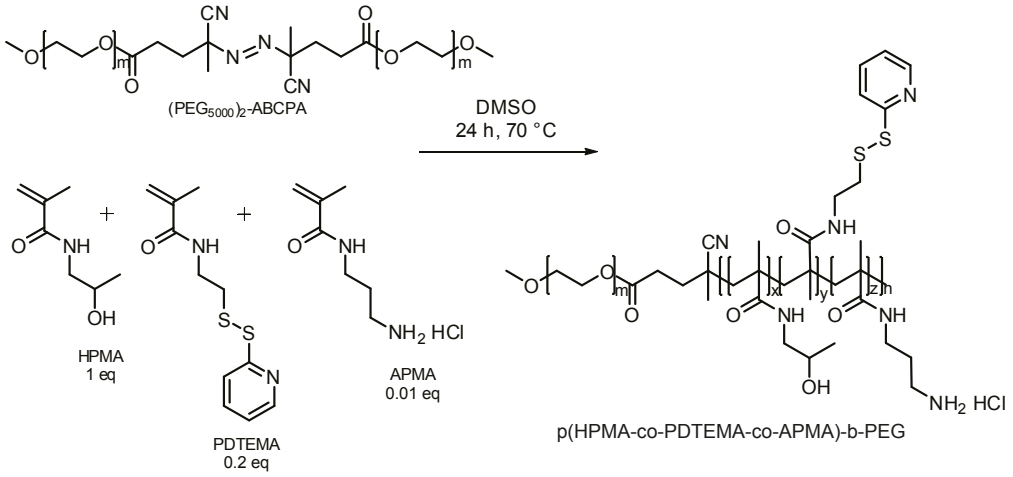

Scheme 1. Synthesis of p(HPMA-co-PDTEMA-co-APMA)-b-PEG, by free-radical polymerization of HPMA, PDTEMA and APMA using ($(mPEG_{5000})_2$-ABCPA) macroinitiator.

Table 1. p(HPMA-co-PDTEMA-co-APMA)-b-PEG characteristics as determined by GPC, ^{1}H NMR, UV spectroscopy and TNBSA assay.

GPC		NMR		NMR, TNBSA	UV
M_n (kDa)	PDI	M_n (kDa)	Feed HPMA–DMAE/PDTEMA/APMA	Polymer HPMA–DMAE/PDTEMA/APMA	$nmol_{PDS}/mg_{polymer}$
34.4	1.6	44.0	1/0.20/0.01	1/0.19/0.01	821.0±43.3

NHS-functionalized dyes were conjugated to p(HPMA-co-PDTEMA-co-APMA)-b-PEG by reaction with the primary amines of APMA for 36 h using a 2 molar excess of reactive dyes (Scheme 2). After reaction, the crude product was analyzed with GPC, and the coupling efficiency was determined by GPC analysis of the AUC of the polymer and unreacted dye peaks (detection at 646 nm (Cy5 coupling) or 700 nm (Cy7 coupling)). The obtained chromatograms revealed that the AUC for each peak was close to 50% for both reactions, demonstrating that the amine groups of the polymers were quantitatively modified with dye molecules. Figure 2a shows the GPC chromatogram of the crude product from Cy7 coupling reaction. In the third step, the crude product (e.g. p(HPMA-co-PDTEMA-co-(Cy5/Cy7)-b-PEG) was reacted with DMAE-CI (Scheme 2) to yield the cationic polymer p(HPMA–DMAE-

co-PDTEMA-co-(Cy5/Cy7)-b-PEG. After purification of the polymer by extensive dialysis, ^{1}H NMR (Figure 1) showed that the integral ratio between peaks at δ4.2 ppm (bs, $OC\underline{H}_2CH_2$), HPMA–DMAE) and δ4.6 ppm (bs, $CH_2C\underline{H}CH_3O$, HPMA–DMAE) was close to 2, confirming a quantitative reaction of the OH groups of HPMA with DMAE-CI. GPC analysis of the final purified products showed complete removal of the unreacted dyes for both Cy5- and Cy7-labeled polymer (e.g. Figure 2b for Cy7-labeled polymer). The modification of HPMA groups with the cationic DMAE groups after dye coupling was chosen over the direct polymerization of HPMA–DMAE monomer [33, 34] because of the incompatibility of the carbonate ester bond in HPMA–DMAE with primary amines.

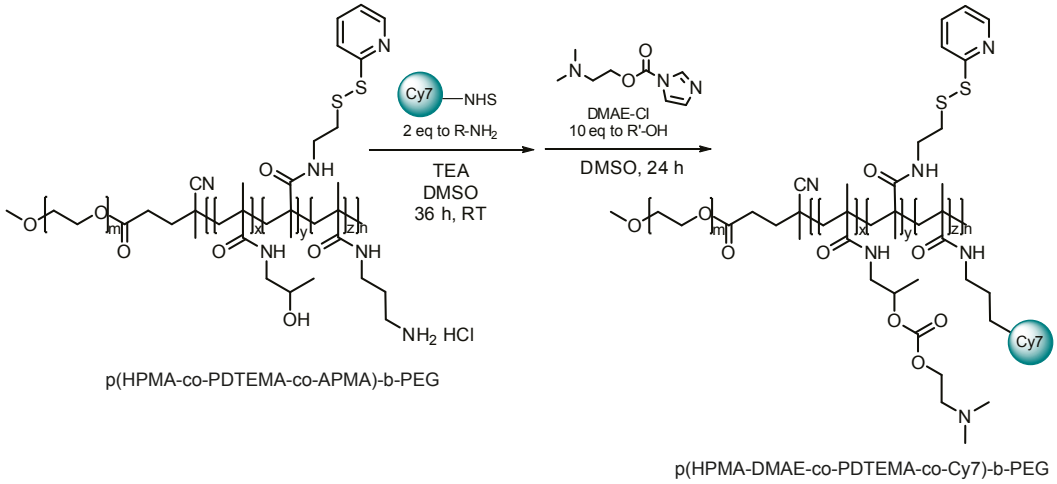

Scheme 2. Synthesis of p(HPMA–DMAE-co-PDTEMA-co-Cy7)-b-PEG, by sequential coupling of Cy-7NHS and DMAE-CI to p(HPMA-co-PDTEMA-co-APMA)-b-PEG.

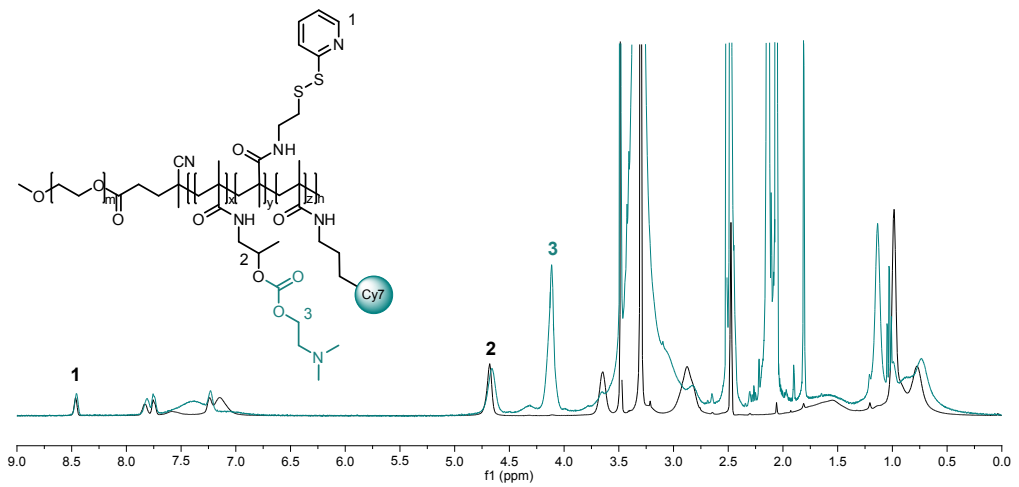

Figure 1. [1]NMR spectra of p(HPMA-co-PDTEMA-co-APMA) and p(HPMA–DMAE-co-PDTEMA-co-Cy7)-b-PEG in DMSO.

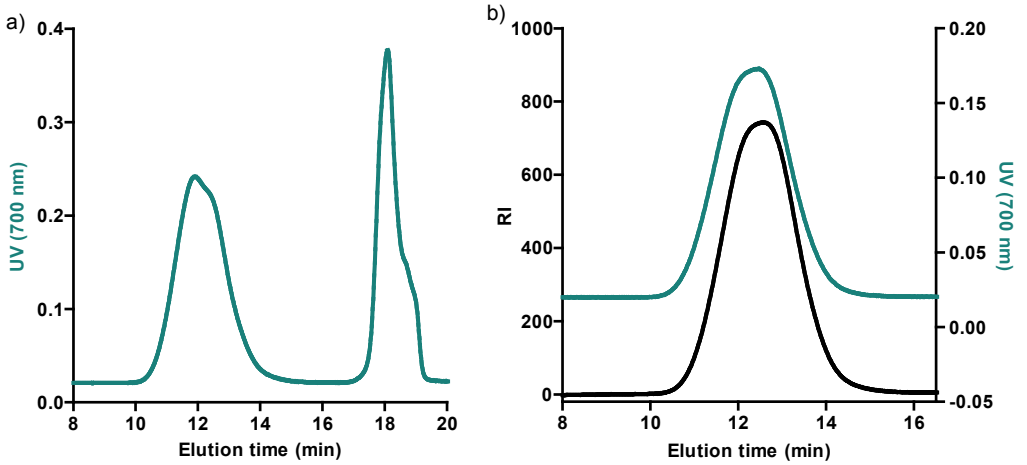

Figure 2. GPC chromatograms (a) UV detection at 700 nm of the crude product from coupling of Cy7NHS to p(HPMA-co-PDTEMA-co-APMA)-b-PEG, using a 2 molar equivalent excess of Cy7-NHS to primary amines in the polymer. (b) Refractive index signal (RI) and UV signal at 700 nm of the final purified p(HPMA–DMAEcoPDTEMAcoCy7)-b-PEG polymer.

3.2. Preparation of fluorescently labeled decationized pHP-PEG polyplexes

Polyplexes of pHP-PEG were formed through the 3-step process [33, 34] (Scheme 3). The preparation of Cy5 or Cy 7-labeled decationized polyplexes

started with the complexation of the cationic block copolymer p(HPMA–DMAE-co-PDTEMA-co-Cy5/Cy7)-b-PEG (pHDP-PEG) with pDNA via electrostatic interactions. The interchain disulfide crosslinking of the polyplexes was performed via thiol-disulfide exchange reaction by the addition of DTT corresponding to a 50% molar equivalent of the PDS groups of the polymer, to induce self-crosslinking of the polyplexes [45], yielding cationic pHDP-PEG polyplexes. To obtain decationized polyplexes from cationic precursors, decationization was performed by the removal of the DMAE cationic side groups linked via carbonate ester bond to the HPMA backbone at pH 8.5 for 6.5 h. This process yields p(HPMA-co-PDTEMA-co-Cy5/Cy7)-b-PEG (pHP-PEG) decationized polyplexes. The structural stabilization and pDNA entrapment was solely dependent on the interchain disulfide crosslinks in the pHPMA–DMAE core.

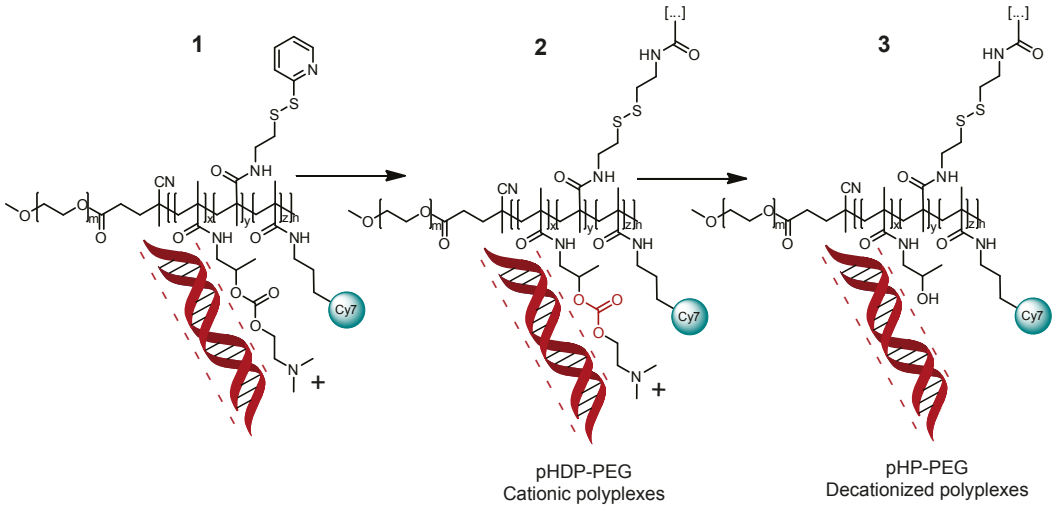

Scheme 3. Route for the preparation of interchain disulfide-crosslinked decationized polyplexes, through a 3-step process: 1. charge-driven condensation with nucleic acids; 2. stabilization through disulfide crosslinking; 3. decationization of cationic pHDP-PEG polyplexes, resulting in decationized pHP-PEG polyplexes (adapted from [33]).

An overview of the biophysical properties of both the decationized pHP-PEG and cationic pHDP-PEG polyplexes by DLS and zeta potential measurements is shown in Table 2. Polyplexes were prepared by complexing the polymer with pDNA at an optimal N/P=4 regarding their biophysical and *in vitro* transfection properties [33]. Firstly, pHDP-PEG formed nanosized particles with a diameter of 140±5 nm and a

positive zeta potential of +11±3. After decationization, pHP-PEG polyplexes had a size of 142±8 nm and a slightly negative zeta potential of -4±2 mV. The decrease in zeta potential, from cationic to decationized arises from the loss of the cationic DMAE groups from the pHDP and from the entrapped pDNA in the core [33]. The loss of electrostatic interactions between the polymer and pDNA potentially leads to some hydration and thus slight swelling of the polyplex core, however by using a zero-length crosslinking agent such as DTT, this effect is limited. Size is a particularly critical property for the biodistribution of nanoparticles [47], however, here this variable is ruled out by evaluation polyplexes of very similar size.

Both decationized pHP-PEG and cationic pHDP-PEG polyplexes were complementarily analyzed by NTA, a technique that allows the simultaneous analysis of individual particles in a suspension and gives information of the true size distribution (Figure 3) [48]. Similarly to the DLS results, decationized polyplexes and cationic polyplexes showed comparable average sizes (around 145-150 nm). Importantly, the size distribution measured by NTA displayed similar distribution profiles: for both particles, when prepared at high concentration for *in vivo* applications (400 µg/mL), around 90% of the polyplexes had a size below 210 nm. Size and charge measurements demonstrate that introduction of cyanine fluorophores and preparation of polyplexes at high concentration did not affect significantly the polyplexes properties [33, 34].

Table 2. Particle z-average diameter (Z-avg) and polydispersity index (PDI) determined by DLS, and particle charge (ζ Pot) determined by zeta potential measurements, of decationized pHP-PEG and cationic pHDP-PEG polyplexes. Results are expressed as mean±SD (n=3).

Polyplexes	DLS		Zetasizer
	Z-ave (nm)	PDI	ζ Pot (mV)
pHP-PEG	142±8	0.20±0.01	-4±2
pHDP-PEG	140±5	0.19±0.01	11±3

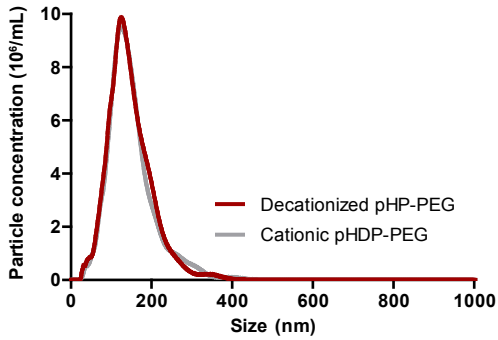

Figure 3. Decationized pHP-PEG and cationic pHDP-PEG polyplexes size distribution determined by NTA in PBS at 25 ºC.

3.3. Stability of decationized pHP-PEG polyplexes in human plasma

The stability of cationic pHDP-PEG and decationized pHP-PEG Cy5-labeled was evaluated by incubation at 37 ºC in human plasma. The size distribution of the polyplexes in plasma was determined by fSPT and compared to the distributions obtained when polyplexes were diluted in HEPES buffer pH 7.4 (Figure 4). The method is based on single particle tracking analysis of fluorescent particles which allows the determination of precise size distributions in media with intrinsic light scattering such as undiluted biological fluids [36]. The fSPT technique is especially important to gain information on the possible aggregation of nanoparticles. When Cy5-labeled polyplexes, both cationic and decationized, were measured in HEPES buffer by fSPT, comparable size distributions to the ones obtained by DLS and NTA were observed. The distribution was relatively narrow, with a peak around 200 nm. When the cationic pHDP-PEG polyplexes were incubated in human plasma for 1 h, a clear change in the distribution profile was observed and a higher average size (~300 nm) as well as polyplexes with >400 nm in diameter were clearly detected. Upon incubation for 48 h, the average size (560 nm) and the population of polyplexes with diameter >400 nm were increased. The instability detected for crosslinked cationic polyplexes likely occurs due to insufficient shielding of the positive charge of the polyplexes by PEG and consequent interaction of polyplexes with negatively charged proteins from plasma. Indeed, table 2 shows that the cationic pHDP-PEG polyplexes have a positive zeta-potential. Importantly, when pHP-PEG decationized polyplexes were incubated with human plasma for 1 h, only a slight change of the size distribution was observed, and the peak of the distribution remained unchanged. Consequently, crosslinked decationized polyplexes retained

their integrity in biological fluids, and did not show aggregation (mediated e.g. by plasma proteins). For example, almost no polyplexes with a diameter of >400 nm were detected which is in great contrast with the cationic polyplexes. In line with this, also after incubation the polyplexes for 48 h the size distribution only changed slightly, without any aggregation detected. A slight increase in size after 48 h probably occurs due to protein adsorption to the polyplexes as a consequence of loss of PEG density due to continuous hydrolysis of the ester bond linking PEG chains with HPMA-co-PDTEMA block. PEG is essential to stabilize nanoparticles, avoid aggregation and protein adsorption in blood. This is quite evident for cationic particles [12, 15, 16], but essential for anionic particles as well [49, 50].

The stability assessment is especially important for systemic administration of polyplexes. Firstly in terms of safety, cationic polymer-based systems, when administered intravenously lead to the formation of aggregates by interactions with negatively charged blood components. These aggregates can be retained in the lungs causing embolism and consequent death [12]. Other severe consequences comprise liver necrosis and as uncontrollable distribution and expression [10]. The assessment of the stability is also important to ensure the success of these systems when applied intravenously. In order to target tumors, polyplexes should also possess prolonged circulation and maintain a stable size in the order of few hundreds of nanometers to reach and extravasate in the tissue leaky tumor vasculature, via EPR effect [51-53]. Decationization of polyplexes complemented by the shielding properties of PEG, significantly improves the stability of polyplexes when compared to their cationic polyplexes and therefore increasing the chances to target tumors via EPR.

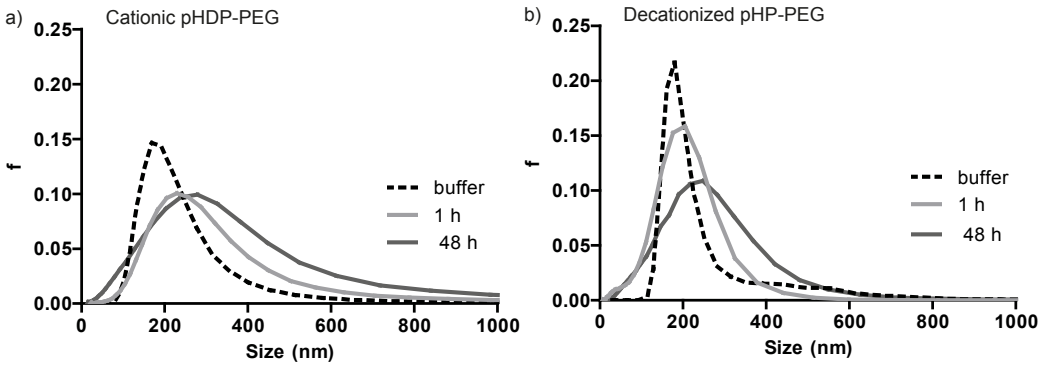

Figure 4. The size distribution of cationic pHDP-PEG (a) and decationized pHP-PEG (b) polyplexes as determined by fSPT after incubation in 90% (v/v) human plasma at 37 ºC for 1 h and 48 h. Size distribution was also determined in 20 mM HEPES pH 7.4.

3.4. *In vitro* and *in vivo* toxicity assessment

To assess the toxicity of the decationized pHP-PEG and cationic pHDP-PEG, the polymers were evaluated *in vitro* with HUVEC cells via MTT assay in an acute (24 h) and a long term toxicity test (Figure 5a) and *in vivo* with a zebrafish embryo model (Figures 5b and 5c) with different polymer concentrations (0.1 to 3 mg/mL). The cationic polymer b-PEI, a commonly used transfection agent, was used as a positive control for toxicity [37].

The *in vitro* toxicity was tested in HUVEC cells due their high sensitivity toward transfection agents [54]. The MTT test revealed that decationized pHP-PEG had no effect on the cell viability, in any of the concentrations tested, when incubated with the cells for 24 h. Only a slight decrease on the cell viability was found in case incubation was prolonged for 72 h. The *in vitro* evaluation of the cationic pHDP-PEG polymer showed that the polymer lead to decrease in cell viability with increasing concentrations, to a level of 70% cell viability for 3 mg/mL when tested for acute toxicity. For long term toxicity test (72 h incubation) the cytotoxic effects were even more pronounced and at 1 mg/mL already lead to decrease in cell viability to 20%. In the case of b-PEI extreme toxicity was observed, at the lowest concentration tested (0.1 mg/mL) b-PEI induced complete cell death in both acute and long terms *in vitro* toxicity test.

The zebrafish eggs were incubated with increasing polymer concentrations, and teratogenic effect and the mortality potential on the different zebrafish embryonic stages were monitored microscopically for a period of 72 h. The neutral polymer pHP-PEG showed no effect on the fish viability for any of the concentrations tested. Developmental defects and delayed hatching were observed only for the highest concentration tested (3 mg/mL). For the cationic polymer pHDP-PEG a significant decrease on zebrafish viability was observed at 3 mg/mL, resulting in 100% fish death at 72 h. Mortality was also detected at a very early stage of the development (1 out of 6) together with a slower heartbeat in the surviving ones. Furthermore, the cationic pHDP-PEG also interfered significantly in the embryonic development of the fishes. A decrease in the pigmentation was observed from a concentration of 0.3 mg/mL onwards, no hatching was observed at 48 h for 1 mg/mL and at 3 mg/mL all fish had a decreased heartbeat. In line with the *in vitro* test, b-PEI was again responsible for extreme toxicity, by inducing complete fish death at 0.1 mg/mL even at early stages of development.

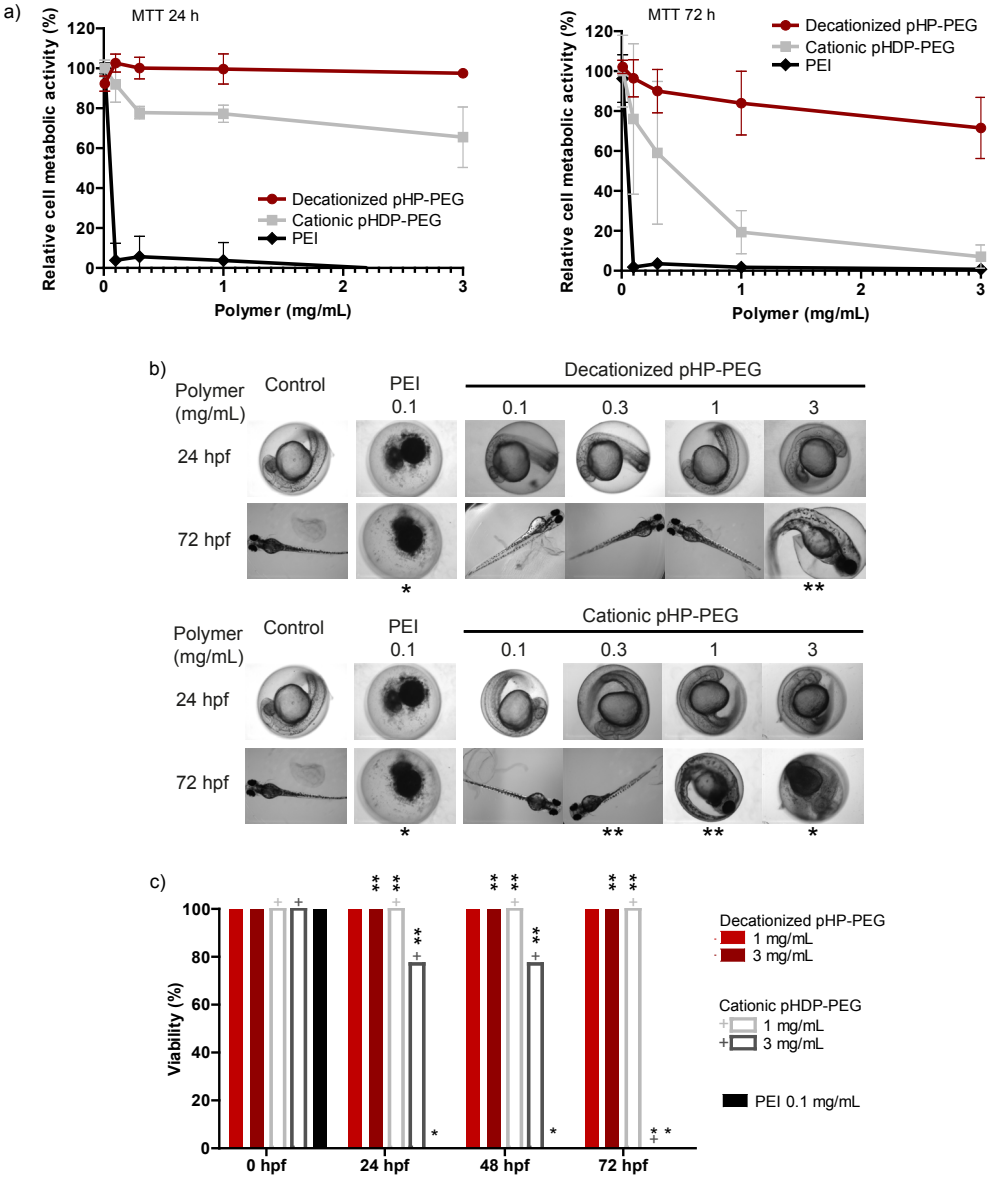

Figure 5. Safety evaluation of decationized polyplexes (a) HUVEC cell relative viability relative upon exposure for 24 h or 72 h to decationized pHP-PEG, cationic pHDP-PEG and b-PEI from 0.1 mg/mL to 3 mg/mL. Results are expressed as mean±SD (n=4). (b) Representative images of zebrafish embryo development upon exposure to decationized pHP-PEG and to cationic pHDP-PEG at concentrations ranging from 0.1–3 mg/mL. *significant mortality, **significant developmental defects (i.e. decreased pigmentation, delayed hatching ratio and slower heartbeat). (c) zebrafish survival upon exposure to decationized pHP-PEG and cationic pHDP-PEG polymers in comparison with bPEI (*100% mortality; n=6). hpf (hours post-fertilization).

Evident toxicity was induced by the biodegradable cationic pHDP-PEG polymer, particularly observed on long term (observed in HUVEC cells and zebrafish). Toxicity is obviously less than b-PEI, but by using a wide range of concentrations and exposure times we evidence that biodegradability is not sufficient for a completely safe gene delivery system. We demonstrate not only effects on cell and organism viability but also on the teratogenicity potential observed in zebrafish embryos at lower concentrations. In great contrast, a practically innocuous profile of the decationized pHP-PEG was observed in short and long terms *in vitro* and in the zebrafish assay. This contrast between decationized and cationic polymers proves the importance of developing gene delivery systems based on neutral polymers in order to build safe vectors.

3.5. *In vivo* biodistribution and tumor accumulation

Cy7-labeled pHP-PEG decationized and pHDP-PEG cationic polyplexes were intravenously injected into mice bearing subcutaneous A431 tumors, and their biodistribution and tumor accumulation were noninvasively monitored using 3D μCT-FMT. Hybrid μCT-FMT method allows the effective *in vivo* visualization of near-infrared (NIR) dye labeled nanomedicines, and the (semi-) quantification of their accumulation in tumors and healthy organs. By fusing and reconstructing 3D FMT data with μCT images, and by performing absorption pre-scans, a more accurate assignment of fluorescence signals to deep internal organs tissues can be performed [38, 55, 56]. Compared to the 2D FRI, 3D μCT-FMT is not limited to superficial visualization, animal sacrificing is not required.

In parallel with 3D μCT-FMT images, blood circulation kinetics was determined by 2D FRI signals of blood and urine collected at different time points p.i (Figure 6). Quantification of polyplex signals in blood showed that there was a very rapid decrease of the %ID for both cationic and decationized polyplexes which typical for polyplex systems when administered intravenously [15, 16, 22, 57, 58] (Figure 6a). Importantly, a significant higher blood circulation time was observed for decationized pHP-PEG polyplexes. Decationized polyplexes showed a higher signal in blood at all time points when compared to cationic pHDP-PEG. The elimination rate via kidneys was determined by detecting 2D FRI signals from urine (Figure 6b). High Cy7 %ID was detected in urine 15 min p.i. for both groups, followed by a rapid decrease 4 h p.i. Most likely, this was due to a rapid glomerular filtration of low M_w polymer fraction that is not built in the polyplexes. This fraction of polymers is the

same for both cationic and decationized polyplexes, as confirmed by the similar signals found for both polyplexes.

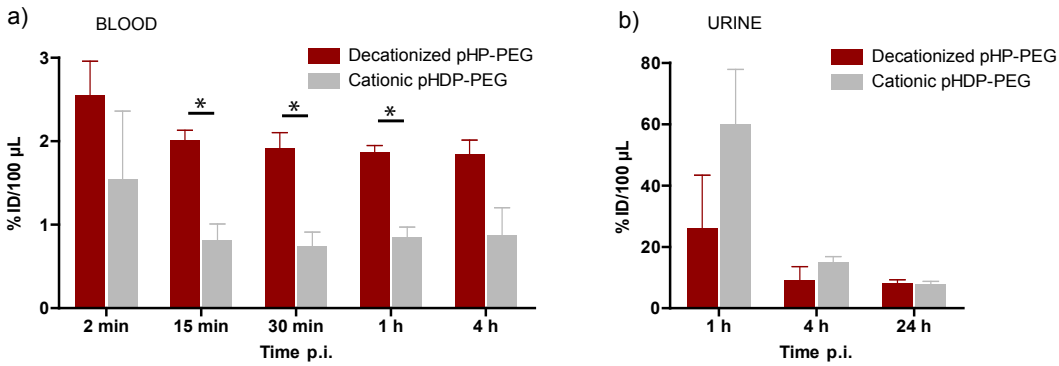

Figure 6. 2D FRI quantification as %ID (per 100 µl) of decationized pHP-PEG and cationic pHDP-PEG Cy7-labeled polyplexes signals in (a) blood and (b) urine at different time points p.i. Results are expressed as mean±SD (n=3). *p<0.01 (t-test).

Both polyplexes showed a high accumulation in healthy organs, mainly in liver and kidneys 15 min p.i. However, in the case of decationized polyplexes there was a rapid signal decrease at 4 h p.i. resulting in an apparent lower accumulation of decationized polyplexes in liver and kidneys, when compared to cationic polyplexes. Most likely decationized polyplexes were able to maintain a population of polyplexes in the circulation or rapidly accumulated in the different organs, but due to their improved ability to maintain small and stable size in biological fluids (Figure 4) together with their low unspecific uptake properties [33, 34], polyplexes can reenter the blood circulation and accumulate in tumor tissues. This behavior has been previously described for other nanoparticulate systems [59, 60].

The major organ of polyplex accumulation of polyplexes was the liver, which contains Kupffer cells as part of the mononuclear phagocyte system (MPS) which are responsible for phagocytic activity and rapid clearance of nanoparticles *in vivo* [60-62]. Liver accumulation is very critical for PEGylated polymer-DNA complexes [15, 22, 57]. The ability of decationized polyplexes to escape from liver and remain stable in circulation more efficiently determines their higher circulation *in vivo*. As hypothesized, PEG is not able to completely shield cationic particles, leading to unspecific uptake or opsonization, which in turn leads to decreased circulation time when compared to the decationized polyplexes.

Significant NIR signal was noticed in the bladder 15 min p.i. for both groups with similar degrees and with a rapid drop of signal 4 h p.i. The signal profiles are in line with the results determined by 2D FRI in urine and as quantified, the initial elimination into the bladder corresponds to 15-20 total %ID.

Accumulation in kidneys was also pronounced, with a tendency of higher accumulation of cationic polyplexes. Kidney accumulation has been previously found for polymeric vectors [57, 63, 64]. Kidney retention can be particularly critical for polycation-based systems. The nanoparticles within the kidney will have to pass through the glomerulus which is in close contact with glomerular basement membrane (GBM), a 300- to 350-nm-thick basal lamina rich in negatively charged proteoglycans, to which particles of around 100 nm can access [65]. Ultimately, particle retention in the GBM is driven by the surface charge, leading to cationic particles to be retained [66].

It is also important to point out that no significant lung deposition was observed for both systems. Lung capillaries are among the smallest blood vessels and sieving might occur in case aggregates are formed [60], which is normally associated with acute toxicity or off-targeting transfection [10, 12]. Our results demonstrate that both polyplexes do not induce acute aggregation *in vivo* in line with the results shown in Figure 4.

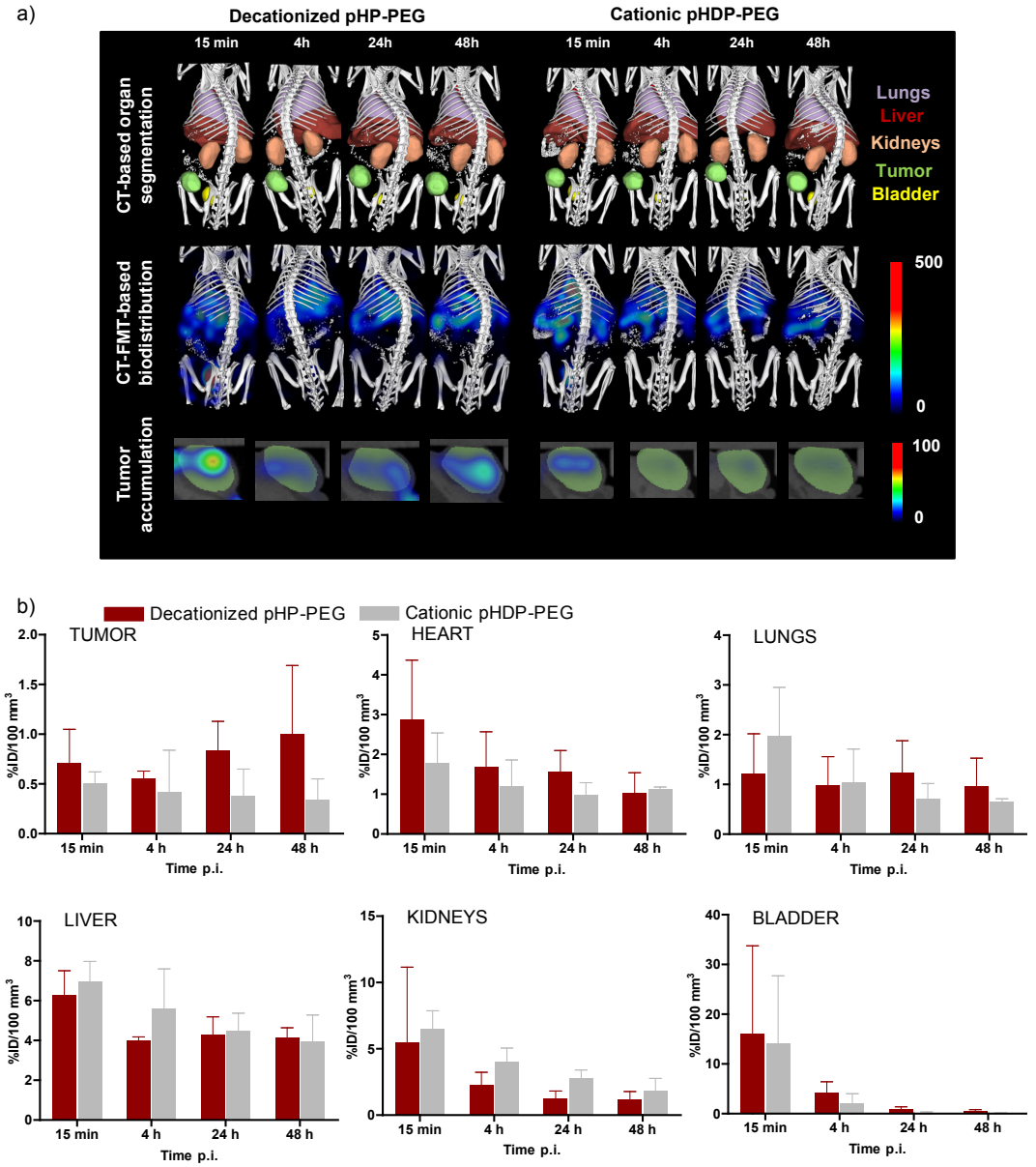

Figure 7. Noninvasive *in vivo* 3D CT-FMT imaging of the biodistribution and tumor accumulation of decationized pHP-PEG and cationic pHDP-PEG Cy7-labeled polyplexes. (a) Principle of 3D CT-FMT imaging: anatomical information obtained using μCT is used to assign the Cy7 signals coming from polyplexes to a specific organ or tissue of interest. The images were obtained at 15 min, 4 h, 24 h and 48 h p.i. and show Cy7 localization mainly in liver (red) and kidney (orange). Tumor accumulation was more prominent for decationized polyplexes. (b) Quantification of the tumor accumulation and biodistribution of Cy7-labeled decationized pHP-PEG and cationic pHDP-PEG polyplexes in tumors, liver, lungs, kidney, bladder and heart, expressed as %ID per 100 mm^3 tissue. Results are presented as mean±SD (n=3).

3.6. *Ex vivo* for probe accumulation and *in vivo* transfection

After the 3D μCT-FMT procedure at 48 p.i., mice were sacrificed and tumors, lungs, spleen, kidneys, heart skin, intestines and muscle were analyzed using 2D FRI (Figures 8a and b). The NIR signals from tumors and several physiologically relevant healthy organs (liver, spleen, lungs and kidneys) were quantified and compared for both Cy7-labeled decationized pHP-PEG and cationic pHDP-PEG polyplexes. 2D FRI quantification determined *ex vivo* supports and further validates the results of the 3D μCT-FMT analysis. In the case of 2D FRI measurements, a significantly higher accumulation in the tumors was observed for decationized polyplexes. As determined by 3D μCT-FMT, 3 times higher accumulation for decationized polyplexes was also found. The tendency of a lower accumulation in healthy organs was also observed for decationized polyplexes with 2D FRI. Similar accumulation in liver was observed for both polyplexes 48 p.i., but in the case of spleen and kidneys higher accumulation was observed for cationic polyplexes. The spleen, together with liver constitutes the MPS. In the spleen nanoparticles are sieved and subsequently taken up by macrophages or splenocytes [60, 61]. The apparent lower retention of decationized polyplexes in the spleen further demonstrates the advantages of decationized polyplexes.

Cryosections of tumors collected 48 p.i. were analyzed using fluorescence microscopy, to validate the *in vivo* and *ex vivo* Cy7-labeled polyplex accumulation results (Figures 8c and d). By quantifying the Cy7 signals on tumor sections of both groups, 2 times higher signal was observed for decationized polyplexes with statistically significance. Microscopy was also used to determine the *in vivo* tumor transfection potential of both decationized pHP-PEG and cationic pHDP-PEG polyplexes containing EGFP encoding pDNA (Figures 8c and d). The EGFP signal, which allows to infer on the transfection ability of polyplexes, was similar for both systems, even though significant differences were found in NIR tumor accumulation. Transfection requires polyplexes' (extensive) uptake by the target cells. The lower transfection ability of decationized polyplexes is therefore likely attributed to its low degree of unspecific uptake. We also showed that uptake can be triggered by the introduction of a targeting ligand at the surface of decationized polyplexes [33, 34]. Furthermore, the introduction of targeting ligands is important to accelerate the rate of cellular uptake of polyplexes and prevent premature reduction of disulfide crosslinks before cell entry due to the presence of secreted and cell membrane thiols [67]. Cationic polyplexes, in contrast, are known to be taken up extensively by electrostatic interaction with cell membrane anionic components [3, 68, 69].

The transfection ability of cationic pHDP-PEG polyplexes is in line with previous findings of pHPMA–DMAE to induce *in vivo* transfection in tumors [70].

It should be noticed that the ability of cationic polyplexes to transfect cells more efficiently has counterproductive effects because it also leads to an increased probability of off-targeting expression, especially when high accumulation is observed in liver, spleen and kidneys. Unwanted transfection in healthy organs has been previously observed particularly in liver and lungs [16, 22, 71]. In the recent years, several strategies have been developed to introduce target transfection with encouraging results [58, 63, 64, 72]. Decationized polyplexes can potentiate further specific transfection in tumors especially when a targeting ligand is introduced [34]. Furthermore, due to its low toxic and low teratogenic potential, decationized polyplexes are less limited to dose and repeated administration restrictions, resulting in a promising and attractive system for further optimization strategies and testing.

Future studies have to be focused on deeper evaluation of transfection ability of optimized formulations of decationized polyplexes. Optimization for a better *in vivo* performance can be done by using targeted systems or by optimizing the polymer structure, for example by determining the best PEG block molecular weight and density [73, 74] or by introduction of hydrophobic groups in the core of polyplexes groups into polyplexes [75]. In a next step, therapeutic genes should be used to determine the therapeutic potential of decationized polyplexes.

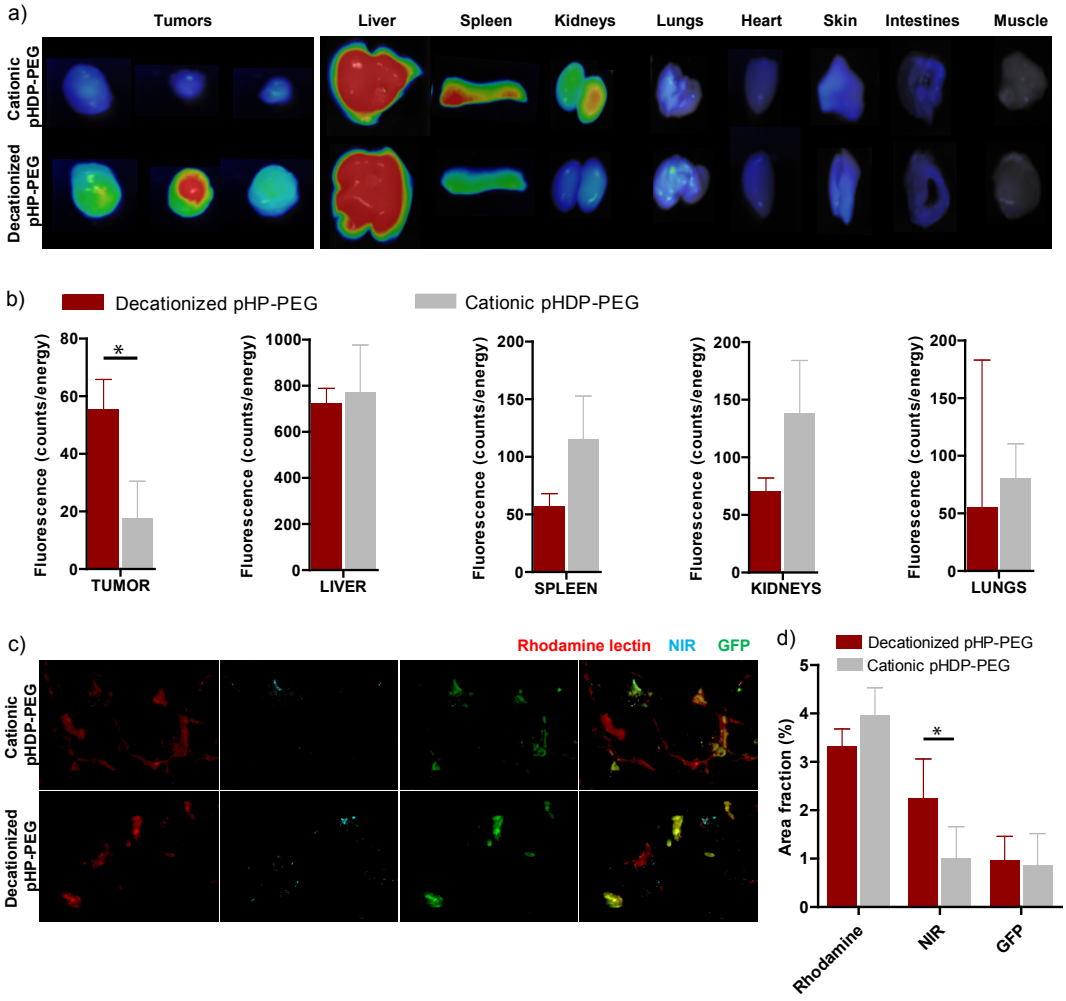

Figure 8. *Ex vivo* analysis. (a) Representative e*x vivo* 2D FRI assessment of the tumor accumulation and biodistribution of decationized pHP-PEG and cationic pHDP-PEG Cy7-labeled polyplexes at 48 h p.i. (b) Quantification of polyplex accumulation in tumors and healthy organs. Results are expressed as mean±SD (n=3). (c–d) Fluorescence microscopy imaging (c) and quantification (d) of decationized pHP-PEG and cationic pHDP-PEG Cy7-labeled polyplexes (blue) accumulating in tumors at 48 h p.i. and inducing EGFP expression (green). Blood vessels are labeled using rhodamine-lectin (red). Results are expressed as mean±SD (n=3). *p<0.05 (t-test).

4. CONCLUSION

Decationized polyplexes, unlike conventional polycationic polymeric gene delivery systems, are based on neutral polymers. In the present study, we demonstrate that the neutral polymer pHP-PEG when tested for toxicity *in vitro* with HUVEC cells showed a very good cytocompatibility in both acute and long term toxicity test. Furthermore, an *in vivo* zebrafish toxicity assay revealed that pHP-PEG did not induce fish mortality and, importantly, showed a much lower teratogenicity potential when compared with its cationic counterpart. This apparent safe polymer formed polyplexes with a high stability in biological fluids, as determined by fSPT, which validated its applicability *in vivo* applicability for systemic administration. Using noninvasive optical imaging (3D μCT-FMT) and complementary *ex vivo* analysis we demonstrated that by removing the cationic groups of polyplexes, we obtained a system with higher tumor accumulation, most likely due to their longer blood circulation and apparent decreased accumulation in healthy organs. *Ex vivo* analysis validated the optical imaging results and histology in tumor cryosections and showed that decationized polyplexes induced transgene expression *in vivo*.

The described strategy for preparing decationized polyplexes and the results reported are an important contribution to take into consideration to develop safer and more efficient non-viral gene delivery systems.

Acknowledgement

The authors gratefully acknowledge financial support by the Portuguese Foundation for Science and Technology (FCT) (grant SFRH/BD/47085/2008), by the German Academic Exchange Service (DAAD; 290084/2011-3), by the DFG (LA 2937/1-2), by the European Union (COST – Action TD1004), and by the European Research Council (ERC Starting Grant 309495: NeoNaNo).

References

[1] L.W. Seymour, A.J. Thrasher, Gene therapy matures in the clinic, Nat. Biotechnol., 30 (2012) 588-593.

[2] T. Wirth, N. Parker, S. Ylä-Herttuala, History of gene therapy, Gene, 525 (2013) 162-169.

[3] M.A. Mintzer, E.E. Simanek, Nonviral vectors for gene delivery, Chem. Rev., 109 (2008) 259-302.

[4] W. Li, F.C. Szoka, Jr., Lipid-based nanoparticles for nucleic acid delivery, Pharm. Res., 24 (2007) 438-449.

[5] J. Luten, C.F. van Nostrum, S.C. De Smedt, W.E. Hennink, Biodegradable polymers as non-viral carriers for plasmid DNA delivery, J. Control. Release, 126 (2008) 97-110.

[6] S.Y. Wong, J.M. Pelet, D. Putnam, Polymer systems for gene delivery—Past, present, and future, Progress in Polymer Science, 32 (2007) 799-837.

[7] E. Mastrobattista, M.A.E.M. van der Aa, W.E. Hennink, D.J.A. Crommelin, Artificial viruses: a nanotechnological approach to gene delivery, Nat. Rev. Drug Discov., 5 (2006) 115-121.

[8] A. Yousefi, G. Storm, R. Schiffelers, E. Mastrobattista, Trends in polymeric delivery of nucleic acids to tumors, J. Control. Release, 170 (2013) 209-218.

[9] P. Midoux, C. Pichon, J.-J. Yaouanc, P.-A. Jaffrès, Chemical vectors for gene delivery: a current review on polymers, peptides and lipids containing histidine or imidazole as nucleic acids carriers, Br. J. Pharmacol., 157 (2009) 166-178.

[10] P. Chollet, M.C. Favrot, A. Hurbin, J.-L. Coll, Side-effects of a systemic injection of linear polyethylenimine–DNA complexes, J. Gene Med., 4 (2002) 84-91.

[11] C.M. Ward, M.L. Read, L.W. Seymour, Systemic circulation of poly(L-lysine)/DNA vectors is influenced by polycation molecular weight and type of DNA: differential circulation in mice and rats and the implications for human gene therapy, Blood, 97 (2001) 2221-2229.

[12] M. Ogris, S. Brunner, S. Schuller, R. Kircheis, E. Wagner, PEGylated DNA/transferrin-PEI complexes: reduced interaction with blood components, extended circulation in blood and potential for systemic gene delivery, Gene Ther., 6 (1999) 595-605.

[13] R. Duncan, The dawning era of polymer therapeutics, Nat. Rev. Drug Discov., 2 (2003) 347-360.

[14] C.F. Jones, R.A. Campbell, A.E. Brooks, S. Assemi, S. Tadjiki, G. Thiagarajan, C. Mulcock, A.S. Weyrich, B.D. Brooks, H. Ghandehari, D.W. Grainger, Cationic PAMAM dendrimers aggressively initiate blood clot formation, ACS Nano, 6 (2012) 9900-9910.

[15] F.J. Verbaan, C. Oussoren, C.J. Snel, D.J.A. Crommelin, W.E. Hennink, G. Storm, Steric stabilization of poly(2-(dimethylamino)ethyl methacrylate)-based polyplexes mediates prolonged circulation and tumor targeting in mice, J. Gene Med., 6 (2004) 64-75.

[16] M. Harada-Shiba, K. Yamauchi, A. Harada, I. Takamisawa, K. Shimokado, K. Kataoka, Polyion complex micelles as vectors in gene therapy – pharmacokinetics and in vivo gene transfer, Gene Ther., 9 (2002) 407-414.

[17] M.H. Lee, Z. Yang, C.W. Lim, Y.H. Lee, S. Dongbang, C. Kang, J.S. Kim, Disulfide-cleavage-triggered chemosensors and their biological applications, Chem. Rev., 113 (2013) 5071-5109.

[18] F. Meng, W.E. Hennink, Z. Zhong, Reduction-sensitive polymers and bioconjugates for biomedical applications, Biomaterials, 30 (2009) 2180-2198.

[19] D.S. Manickam, J. Li, D.A. Putt, Q.-H. Zhou, C. Wu, L.H. Lash, D. Oupický, Effect of innate glutathione levels on activity of redox-responsive gene delivery vectors, J. Control.

Release, 141 (2010) 77-84.

[20] D. Oupický, R.C. Carlisle, L.W. Seymour, Triggered intracellular activation of disulfide crosslinked polyelectrolyte gene delivery complexes with extended systemic circulation in vivo, Gene Ther., 8 (2001) 713-724.

[21] Y. Vachutinsky, M. Oba, K. Miyata, S. Hiki, M.R. Kano, N. Nishiyama, H. Koyama, K. Miyazono, K. Kataoka, Antiangiogenic gene therapy of experimental pancreatic tumor by sFlt-1 plasmid DNA carried by RGD-modified crosslinked polyplex micelles, J. Control. Release, 149 (2011) 51-57.

[22] H.K. de Wolf, C.J. Snel, F.J. Verbaan, R.M. Schiffelers, W.E. Hennink, G. Storm, Effect of cationic carriers on the pharmacokinetics and tumor localization of nucleic acids after intravenous administration, Int. J. Pharm., 331 (2007) 167-175.

[23] D. Oupický, M. Ogris, K.A. Howard, P.R. Dash, K. Ulbrich, L.W. Seymour, Importance of lateral and steric stabilization of polyelectrolyte gene delivery vectors for extended systemic circulation, Mol. Ther., 5 (2002) 463-472.

[24] R.J. Fields, C.J. Cheng, E. Quijano, C. Weller, N. Kristofik, N. Duong, C. Hoimes, M.E. Egan, W.M. Saltzman, Surface modified poly(β amino ester)-containing nanoparticles for plasmid DNA delivery, J. Control. Release, 164 (2012) 41-48.

[25] D. Fischer, Y. Li, B. Ahlemeyer, J. Krieglstein, T. Kissel, In vitro cytotoxicity testing of polycations: influence of polymer structure on cell viability and hemolysis, Biomaterials, 24 (2003) 1121-1131.

[26] S.M. Moghimi, P. Symonds, J.C. Murray, A.C. Hunter, G. Debska, A. Szewczyk, A two-stage poly(ethylenimine)-mediated cytotoxicity: implications for gene transfer/therapy, Mol. Ther., 11 (2005) 990-995.

[27] S. Choksakulnimitr, S. Masuda, H. Tokuda, Y. Takakura, M. Hashida, In vitro cytotoxicity of macromolecules in different cell culture systems, J. Control. Release, 34 (1995) 233-241.

[28] C. Lonez, M. Vandenbranden, J.-M. Ruysschaert, Cationic lipids activate intracellular signaling pathways, Adv. Drug Deliv. Rev., 64 (2012) 1749-1758.

[29] W.T. Godbey, K.K. Wu, A.G. Mikos, Poly(ethylenimine)-mediated gene delivery affects endothelial cell function and viability, Biomaterials, 22 (2001) 471-480.

[30] K. Masago, K. Itaka, N. Nishiyama, U.-i. Chung, K. Kataoka, Gene delivery with biocompatible cationic polymer: Pharmacogenomic analysis on cell bioactivity, Biomaterials, 28 (2007) 5169-5175.

[31] O.M. Merkel, A. Beyerle, B.M. Beckmann, M. Zheng, R.K. Hartmann, T. Stöger, T.H. Kissel, Polymer-related off-target effects in non-viral siRNA delivery, Biomaterials, 32 (2011) 2388-2398.

[32] K. Regnström, E.G.E. Ragnarsson, M. Köping-Höggård, E. Torstensson, H. Nyblom, P. Artursson, PEI – a potent, but not harmless, mucosal immuno-stimulator of mixed T-helper cell response and FasL-mediated cell death in mice, Gene Ther., 10 (2003) 1575-1583.

[33] L. Novo, E.V.B. van Gaal, E. Mastrobattista, C.F. van Nostrum, W.E. Hennink, Decationized crosslinked polyplexes for redox-triggered gene delivery, J. Control. Release,

169 (2013) 246-256.

[34] L. Novo, E. Mastrobattista, C.F. van Nostrum, W.E. Hennink, Targeted decationized polyplexes for cell specific gene delivery, Bioconjug. Chem., 25 (2014) 802-812.

[35] H. Maeda, J. Wu, T. Sawa, Y. Matsumura, K. Hori, Tumor vascular permeability and the EPR effect in macromolecular therapeutics: a review, J. Control. Release, 65 (2000) 271-284.

[36] K. Braeckmans, K. Buyens, W. Bouquet, C. Vervaet, P. Joye, F. De Vos, L. Plawinski, L. Doeuvre, E. Angles-Cano, N.N. Sanders, J. Demeester, S.C. De Smedt, Sizing nanomatter in biological fluids by fluorescence single particle tracking, Nano Lett., 10 (2010) 4435-4442.

[37] L.Y. Rizzo, S.K. Golombek, M.E. Mertens, Y. Pan, D. Laaf, J. Broda, J. Jayapaul, D. Mockel, V. Subr, W.E. Hennink, G. Storm, U. Simon, W. Jahnen-Dechent, F. Kiessling, T. Lammers, In vivo nanotoxicity testing using the zebrafish embryo assay, J. Mater. Chem. B, 1 (2013) 3918-3925.

[38] S. Kunjachan, F. Gremse, B. Theek, P. Koczera, R. Pola, M. Pechar, T. Etrych, K. Ulbrich, G. Storm, F. Kiessling, T. Lammers, Noninvasive optical imaging of nanomedicine biodistribution, ACS Nano, 7 (2012) 252-262.

[39] A. Funhoff, C.F. van Nostrum, A. Janssen, M. Fens, D. Crommelin, W.E. Hennink, Polymer side-chain degradation as a tool to control the destabilization of polyplexes, Pharm. Res., 21 (2004) 170-176.

[40] D. Neradovic, C.F. van Nostrum, W.E. Hennink, Thermoresponsive polymeric micelles with controlled instability based on hydrolytically sensitive N-isopropylacrylamide copolymers, Macromolecules, 34 (2001) 7589-7591.

[41] M. Talelli, C.J.F. Rijcken, S. Oliveira, R. van der Meel, P.M.P. van Bergen en Henegouwen, T. Lammers, C.F. van Nostrum, G. Storm, W.E. Hennink, Nanobody – Shell functionalized thermosensitive core-crosslinked polymeric micelles for active drug targeting, J. Control. Release, 151 (2011) 183-192.

[42] E.V.B. van Gaal, R. van Eijk, R.S. Oosting, R.J. Kok, W.E. Hennink, D.J.A. Crommelin, E. Mastrobattista, How to screen non-viral gene delivery systems in vitro?, J. Control. Release, 154 (2011) 218-232.

[43] D.R. Grassetti, J.F. Murray, Determination of sulfhydryl groups with 2,2'- or 4,4'-dithiodipyridine, Arch. Biochem. Biophys., 119 (1967) 41-49.

[44] A.W. York, F. Huang, C.L. McCormick, Rational design of targeted cancer therapeutics through the multiconjugation of folate and cleavable siRNA to RAFT-synthesized (HPMA-s-APMA) copolymers, Biomacromolecules, 11 (2010) 505-514.

[45] J.-H. Ryu, R.T. Chacko, S. Jiwpanich, S. Bickerton, R.P. Babu, S. Thayumanavan, Self-cross-linked polymer nanogels: A versatile nanoscopic drug delivery platform, J. Am. Chem. Soc., 132 (2010) 17227-17235.

[46] G.T. Zugates, D.G. Anderson, S.R. Little, I.E.B. Lawhorn, R. Langer, Synthesis of poly(β-amino ester)s with thiol-reactive side chains for DNA delivery, J. Am. Chem. Soc., 128 (2006) 12726-12734.

[47] A. Schädlich, H. Caysa, T. Mueller, F. Tenambergen, C. Rose, A. Göpferich, J. Kuntsche, K. Mäder, Tumor accumulation of NIR fluorescent PEG–PLA nanoparticles: Impact of particle size and human xenograft tumor model, ACS Nano, 5 (2011) 8710-8720.

[48] V. Filipe, A. Hawe, W. Jiskoot, Critical evaluation of nanoparticle tracking analysis (NTA) by Nanosight for the measurement of nanoparticles and protein aggregates, Pharm. Res., 27 (2010) 796-810.

[49] C.D. Walkey, W.C.W. Chan, Understanding and controlling the interaction of nanomaterials with proteins in a physiological environment, Chem. Soc. Rev., 41 (2012) 2780-2799.

[50] G.R. Dakwar, E. Zagato, J. Delanghe, S. Hobel, A. Aigner, H. Denys, K. Braeckmans, W. Ceelen, S.C. De Smedt, K. Remaut, Colloidal stability of nano-sized particles in the peritoneal fluid: Towards optimizing drug delivery systems for intraperitoneal therapy, Acta Biomater., 10 (2014) 2965-2975.

[51] H. Maeda, Tumor-selective delivery of macromolecular drugs via the EPR effect: Background and future prospects, Bioconjug. Chem., 21 (2010) 797-802.

[52] J. Fang, H. Nakamura, H. Maeda, The EPR effect: Unique features of tumor blood vessels for drug delivery, factors involved, and limitations and augmentation of the effect, Adv. Drug Deliv. Rev., 63 (2011) 136-151.

[53] T. Lammers, F. Kiessling, W.E. Hennink, G. Storm, Drug targeting to tumors: Principles, pitfalls and (pre-) clinical progress, J. Control. Release, 161 (2012) 175-187.

[54] Y. Lee, K. Miyata, M. Oba, T. Ishii, S. Fukushima, M. Han, H. Koyama, N. Nishiyama, K. Kataoka, Charge-conversion ternary polyplex with endosome disruption moiety: A technique for efficient and safe gene delivery, Angew. Chem. Int. Ed. Engl., 47 (2008) 5163-5166.

[55] S. Kunjachan, R. Pola, F. Gremse, B. Theek, J. Ehling, D. Moeckel, B. Hermanns-Sachweh, M. Pechar, K. Ulbrich, W.E. Hennink, G. Storm, W. Lederle, F. Kiessling, T. Lammers, Passive versus active tumor targeting using RGD- and NGR-modified polymeric nanomedicines, Nano Lett., 14 (2014) 972-981.

[56] F. Gremse, B. Theek, S. Kunjachan, W. Lederle, A. Pardo, S. Barth, T. Lammers, U. Naumann, F. Kiessling, Absorption reconstruction improves biodistribution assessment of fluorescent nanoprobes using hybrid fluorescence-mediated tomography, Theranostics, 4 (2014) 960-971.

[57] T. Merdan, K. Kunath, H. Petersen, U. Bakowsky, K.H. Voigt, J. Kopecek, T. Kissel, PEGylation of poly(ethylene imine) affects stability of complexes with plasmid DNA under in vivo conditions in a dose-dependent manner after intravenous injection into mice, Bioconjug. Chem., 16 (2005) 785-792.

[58] Z. Ge, Q. Chen, K. Osada, X. Liu, T.A. Tockary, S. Uchida, A. Dirisala, T. Ishii, T. Nomoto, K. Toh, Y. Matsumoto, M. Oba, M.R. Kano, K. Itaka, K. Kataoka, Targeted gene delivery by polyplex micelles with crowded PEG palisade and cRGD moiety for systemic treatment of pancreatic tumors, Biomaterials, 35 (2014) 3416-3426.

[59] Y. Anraku, A. Kishimura, A. Kobayashi, M. Oba, K. Kataoka, Size-controlled long-circulating PICsome as a ruler to measure critical cut-off disposition size into normal and

tumor tissues, Chem. Commun., 47 (2011) 6054-6056.

[60] N. Bertrand, J.-C. Leroux, The journey of a drug-carrier in the body: An anatomo-physiological perspective, J. Control. Release, 161 (2012) 152-163.

[61] G. Storm, S.O. Belliot, T. Daemen, D.D. Lasic, Surface modification of nanoparticles to oppose uptake by the mononuclear phagocyte system, Adv. Drug Deliv. Rev., 17 (1995) 31-48.

[62] A. Schädlich, C. Rose, J. Kuntsche, H. Caysa, T. Mueller, A. Göpferich, K. Mäder, How stealthy are PEG-PLA nanoparticles? An NIR *in vivo* study combined with detailed size measurements, Pharm. Res., 28 (2011) 1995-2007.

[63] T. Nomoto, S. Fukushima, M. Kumagai, K. Machitani, Arnida, Y. Matsumoto, M. Oba, K. Miyata, K. Osada, N. Nishiyama, K. Kataoka, Three-layered polyplex micelle as a multifunctional nanocarrier platform for light-induced systemic gene transfer, Nat. Commun., 5 (2014).

[64] U. Lächelt, P. Kos, F.M. Mickler, A. Herrmann, E.E. Salcher, W. Rödl, N. Badgujar, C. Bräuchle, E. Wagner, Fine-tuning of proton sponges by precise diaminoethanes and histidines in pDNA polyplexes, Nanomedicine, 10 (2013) 35-44.

[65] C.H.J. Choi, J.E. Zuckerman, P. Webster, M.E. Davis, Targeting kidney mesangium by nanoparticles of defined size, Proc. Natl. Acad. Sci. U.S.A., 108 (2011) 6656-6661.

[66] J.E. Zuckerman, C.H.J. Choi, H. Han, M.E. Davis, Polycation-siRNA nanoparticles can disassemble at the kidney glomerular basement membrane, Proc. Natl. Acad. Sci. U.S.A., 109 (2012) 3137-3142.

[67] L. Brülisauer, G. Valentino, S. Morinaga, K. Cam, J. Thostrup Bukrinski, M.A. Gauthier, J.-C. Leroux, Bio-reduction of redox-sensitive albumin conjugates in FcRn-expressing cells, Angew. Chem. Int. Ed. Engl., 53 (2014) 8392-8396.

[68] K.A. Mislick, J.D. Baldeschwieler, Evidence for the role of proteoglycans in cation-mediated gene transfer, Proc. Natl. Acad. Sci. U.S.A., 93 (1996) 12349-12354.

[69] D. Vercauteren, J. Rejman, T.F. Martens, J. Demeester, S.C. De Smedt, K. Braeckmans, On the cellular processing of non-viral nanomedicines for nucleic acid delivery: Mechanisms and methods, J. Control. Release, 161 (2012) 566-581.

[70] H.K. de Wolf, J. Luten, C.J. Snel, G. Storm, W.E. Hennink, Biodegradable, cationic methacrylamide-based polymers for gene delivery to ovarian cancer cells in mice, Mol. Pharmaceutics, 5 (2008) 349-357.

[71] L. Wightman, R. Kircheis, V. Rössler, S. Carotta, R. Ruzicka, M. Kursa, E. Wagner, Different behavior of branched and linear polyethylenimine for gene delivery in vitro and in vivo, J. Gene Med., 3 (2001) 362-372.

[72] J. Zhou, J. Liu, C.J. Cheng, T.R. Patel, C.E. Weller, J.M. Piepmeier, Z. Jiang, W.M. Saltzman, Biodegradable poly(amine-co-ester) terpolymers for targeted gene delivery, Nat. Mater., 11 (2012) 82-90.

[73] Q. Yang, S.W. Jones, C.L. Parker, W.C. Zamboni, J.E. Bear, S.K. Lai, Evading immune cell uptake and clearance requires PEG grafting at densities substantially exceeding the minimum for brush conformation, Mol. Pharmaceutics, 11 (2014) 1250-1258.

[74] T.A. Tockary, K. Osada, Q. Chen, K. Machitani, A. Dirisala, S. Uchida, T. Nomoto, K. Toh, Y. Matsumoto, K. Itaka, K. Nitta, K. Nagayama, K. Kataoka, Tethered PEG crowdedness determining shape and blood circulation profile of polyplex micelle gene carriers, Macromolecules, 46 (2013) 6585-6592.

[75] C.E. Nelson, J.R. Kintzing, A. Hanna, J.M. Shannon, M.K. Gupta, C.L. Duvall, Balancing cationic and hydrophobic content of PEGylated siRNA polyplexes enhances endosome escape, stability, blood circulation time, and bioactivity in vivo, ACS Nano, 7 (2013) 8870-8880.

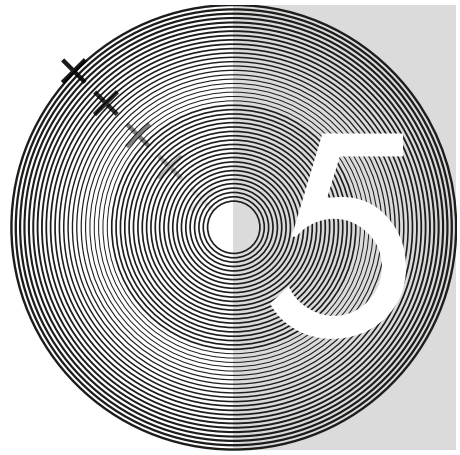

CHAPTER

Targeted decationized polyplexes for siRNA delivery

Luís Novo[a], Kaori M. Takeda[b], Tamara Petteta[a], George R. Dakwar[c], Joep B. van den Dikkenberg[a], Katrien Remaut[c], Kevin Braeckmans[c,d], Cornelus F. van Nostrum[a], Enrico Mastrobattista[a], Wim E. Hennink[a*]

[a]Department of Pharmaceutics, Utrecht Institute for Pharmaceutical Sciences, Utrecht University, 3584 CG Utrecht, The Netherlands

[b]Department of Materials Engineering, Graduate School of Engineering, The University of Tokyo, 7-3-1 Hongo, Bunkyo-ku, Tokyo 113-8656, Japan

[c]Laboratory for General Biochemistry and Physical Pharmacy, Faculty of Pharmacy, Ghent University, Ghent Research Group on Nanomedicines, Harelbekestraat 72, 9000 Ghent, Belgium

[d]Centre for Nano- and Biophotonics, Ghent University, Harelbekestraat 72, 9000 Ghent, Belgium

Submitted for publication

Abstract

The applicability of small interfering RNA (siRNA) in future therapies depends on the availability of safe and efficient carrier systems. Ideally, siRNA delivery requires a system that is stable in the circulation, but that upon specific uptake into target cells can rapidly release their cargo into the cytoplasm. Previously, we evaluated a novel generation of carrier systems ('decationized' polyplexes) for DNA delivery and it was shown that folate targeted decationized polyplexes had an excellent safety profile and showed intracellular triggered release upon cell specific uptake. Targeted decationized polyplexes consist of a core of disulfide crosslinked poly(hydroxypropyl methacrylamide) (pHPMA) stably entrapping nucleic acids and a shell of poly(ethylene glycol) (PEG) decorated with folate molecules. In the present study the applicability of folate targeted decationized polyplexes for siRNA delivery was evaluated. This required optimization of the carrier system particularly regarding the crosslink density of the core of the polyplexes. Stable nanosized siRNA decationized polyplexes were successfully prepared by optimizing the crosslink density of the core. Upon incubation in human plasma, a significant portion of siRNA remained entrapped in the decationized polyplexes as determined by fluorescence correlation spectroscopy (FCS). When tested in a folate receptor overexpressing cell line stably expressing luciferase, Skov3-luc, sequence specific gene silencing was observed. As expected, neither interference on the intrinsic luciferase expression nor on the cell metabolic activity (determined by XTT) was induced by the free-polymer or the siRNA polyplexes. In conclusion, targeted decationized polyplexes are safe and stable carriers that interact with the targeted cells and rapidly disassemble upon cell entry making them promising siRNA delivery systems.

KEYWORDS siRNA delivery, polymer, targeting, nanoparticle, biocompatibility

1. INTRODUCTION

The use of siRNA is currently explored as gene therapy strategy to treat several diseases, including viral infections, neurodegenerative disorders and cancer [1, 2]. siRNA therapies are based on the ability to induce efficient and specific gene

silencing to reduce or eliminate expression of any target protein of interest. siRNA is composed of a 20–23 double strand nucleic acid sequence. siRNA can be synthetically produced and, when introduced in the cytoplasm of the cells, it is incorporated into a protein complex, called the RNA-induced silencing complex (RISC). The siRNA activated RISC catalyzes the degradation of mRNA strands complementary to siRNA, blocking its translation into target proteins [3, 4].

siRNA is especially interesting, because when used as therapeutic nucleic acid, unlike DNA therapeutics, once released in the cytoplasm transport into the nucleus is not necessary to exert its pharmacological action. However, just like DNA, siRNA cannot penetrate cellular membranes by passive diffusion because of its high molecular weight and hydrophilic character. Furthermore, siRNA can be easily degraded by nucleases present in the bloodstream. Therefore, systemic administration of siRNA requires safe and efficient carrier systems.

Recently, several siRNA delivery systems based on polymers, lipids, peptides or proteins have been developed [4-6]. In general, delivery vehicles are based on polycations, which form nanoparticles with siRNA via electrostatic interactions, referred to as ‘polyplexes’. It has been observed in many studies that polycation-based complexes require modification of the carrier surface with a neutral and hydrophilic polymer (e.g. PEG) to shield their charge and minimize interactions with constituents present in extracellular fluids. Furthermore, introduction of PEG allows a more controllable polyplex preparation with higher colloidal stability [7, 8]. The surface decoration of polyplexes with PEG, however, does not avoid unfavorably biodistribution to healthy (nontarget) organs, particularly liver, spleen and kidneys, as well as premature dissociation of the polyplex resulting in release of free siRNA in circulation [9-13].

Because of the items mentioned above, efficient *in vivo* delivery of siRNA requires a system that is highly stable both in the circulation and extracellular milieu, while retaining the ability to readily dissociate and release the loaded siRNA within the cell [14-16]. This particular property can be potentially achieved by introduction of disulfide crosslinks in the core of siRNA polyplexes [17, 18]. Disulfide crosslinking stabilization of nanocarriers is particularly interesting because these particles are stable in in the bloodstream conditions, but prone to rapid cleavage in reducing conditions such as the intracellular environment [19].

Besides de severe effects induced at the systemic level (e.g. embolism or blood coagulation), the polycationic nature of the conventional systems leads to severe

toxicity at the cellular level as well [4, 20-22]. So far, significant improvements have been reported regarding avoidance of systemic toxicity/aggregation, however cellular toxicity of polycations can only be partially reduced (i.e. by the use of biodegradable polymers [23]). Polycations can affect the cells at many levels and they compromise the cell membrane integrity [24-26], interact with crucial cellular polyanions (i.e. cell receptors, enzymes, mRNA or genomic DNA) [27], interfere with cell expression profile [28-30] and activate oncogenes or apoptosis [25, 30, 31].

Given the insufficient *in vivo* stability of siRNA-polycation complexes as well as their poor biodistribution and their intrinsic toxicity, alternatives for polycations are urgently needed. Decationized polyplexes, based on noncharged and hydrophilic polymers, have been developed as interesting plasmid DNA (pDNA) gene delivery systems [32]. These polyplexes consist of a core of disulfide crosslinked pHPMA, in which pDNA is entrapped and are surrounded by a PEG shell. The formation and encapsulation of negatively charged nucleic acid molecules is firstly driven by electrostatic interactions using the transient presence of cationic charges in the polymer. After complex formation, followed by structure stabilization exploiting disulfide crosslinking, cationic charged side groups are removed by hydrolysis of labile groups that are linked via carbonate ester bonds to pHPMA backbone of the polymer. These decationized polyplexes showed a high and stable DNA loading, which is exclusively based on physical entrapment of the nucleic acid in the disulfide crosslinked core. Therefore, decationized polyplexes possess an intracellularly triggered release profile, by the specific cleavage of disulfide crosslinks on the intracellular reducing environment. Decationized polyplexes are based on neutral polymers which explains their excellent cytocompatibility and low teratogenicity as well as low mortality potential in a zebrafish toxicity assay [32, 33]. These particles also showed a low degree of unspecific uptake together with very high degree of cell specific uptake and transfection upon introduction a targeting ligand at the distal end of the PEG shell [34]. The preparation of folic acid (FA) targeted decationized polyplexes is particularly interesting because this small targeting molecule selectively binds with high affinity to its receptor, the folate receptor, which is overexpressed specifically in several tumor types, including metastatic forms [35]. Consequently, folate decorated nanomedicines have been developed for tumor targeting [36]. FA targeting has also demonstrated its feasibility for siRNA delivery to improve the specificity of gene silencing [37-39].

In the present study, the applicability of folate targeted decationized polyplexes

as platform for incorporation and delivery of siRNA, has been investigated. The applicability of decationized polyplexes for siRNA formulation and delivery required both polymer and particle preparation optimization. Given its size, <1/100 the length of plasmid DNA, and stiff backbone structure, siRNA has an inherently poor binding affinity for polycations, and consequently, siRNA complexation and retention is more challenging than pDNA [40]. In the present study we describe the optimization steps for the preparation of siRNA-loaded and decationized polyplexes, as well their stability and *in vitro* toxicity and gene silencing activity.

2. MATERIALS AND METHODS

2.1. Materials

Carbonic acid 2-dimethylamino-ethyl ester 1-methyl-2-(2-methacryloylamino)-ethyl ester (HPMA–DMAE) and *N*-[2-(2-pyridyldithio)]ethyl methacrylamide (PDTEMA) were synthesized as previously described [32]. Agarose multi-purpose was purchased from Roche Molecular Biochemicals (Mannheim, Germany). 6× DNA Loading Dye was purchased from Fermentas (St. Leon-Roth, Germany). SYBR Safe DNA gel stain, Lipofectamine 2000, folate free RPMI-1640 medium, Opti-MEM and dialyzed fetal bovine serum (FBS) were purchased from Life Technologies (Breda, The Netherlands). The Skov3-luc (human ovarian carcinoma cell line stably expressing firefly luciferase) cell line was obtained from Cell BioLabs (San Diego, USA). Luciferase assay kit was obtained from Promega (Leiden, The Netherlands). All other chemicals, reagents and media were obtained from Sigma-Aldrich (Zwijndrecht, The Netherlands).

The following buffer systems were used: 4-(2-hydroxyethyl)-1-piperazineethanesulfonic acid (HEPES) for buffering at pH 6.8–8.2; 3-[[1,3-dihydroxy-2-(hydroxymethyl)propan-2-yl]amino]propane-1-sulfonic acid (TAPS) for buffering solutions at pH 7.7-9.1; phosphate buffered saline, pH 7.4 (PBS) was obtained from B. Braun (Melsungen, Germany).

The siRNA sequences used as follows: Luciferase GL3 siRNA (anti-Luc siRNA, directed against luciferase) (ThermoScientific, Etten-Leur, The Netherlands), sense strand 5′-CUU ACG CUG AGU ACU UCG AdTdT-3′; Negative control LV2 (scramble siRNA), sense strand 5′-AUC GUA CGU ACC GUC GUA UdTdT-3′;

Alexa 647 labeled Negative Control LV2 at the 3′ end of the sense strand (kindly donated by Dr. Mastrobattista (Dept. Pharmaceutics, UU)).

2.2. Polymer synthesis

2.2.1. Synthesis of (FA-PEG)$_2$-ABCPA

The synthesis and characterization of folate-PEG (M_w 5000 Da) bi-functionalized azo-macronitiator ((FA-PEG)$_2$-ABCPA) was performed as previously described [34].

2.2.2. Synthesis of pHDP-PEG-FA

p(HPMA–DMAE-co-PDTEMA)-b-PEG-FA (pHDP-PEG-FA) was synthesized by free radical polymerization using (FA-PEG)$_2$-ABCPA as macroinitiator (Scheme 1). The polymer was synthesized using a HPMA–DMAE-to-initiator ratio (M/I) of 150 (mol/mol), using a feed ratio HPMA–DMAE/PDTEMA of 1/0.6 (mol/mol). The polymerization was carried at 70 ºC for 24 h in DMSO under an N_2 atmosphere, using 2.5 µmol macroinitiator and monomer concentration of 0.8 M. After polymerization, the product was precipitated in diethyl ether and collected by centrifugation, dialyzed against 5 mM NH_4Ac buffer pH 5.0 for 3 days at 4 °C (MWCO 6000-8000) and collected by freeze-drying. Unreacted FA-PEG present in the product was removed by precipitation in cold EtOH (5 mg/mL of solids) followed centrifugation. The pHDP-PEG-FA soluble in the EtOH supernatant was collected after EtOH evaporation, dissolution in water and freeze-drying.

2.2.3. Preparation of p(HPMA-co-PDTEMA)-b-PEG-FA

p(HPMA-co-PDTEMA)-b-PEG-FA (pHP-PEG-FA) was prepared by dissolving 5 mg of pHDP-PEG-FA in 2.5 mL 10 mM HEPES, 10 mM TAPS, pH 8.5 and incubated for 6 h at 37 ºC to hydrolyze the dimethylaminoethanol (DMAE) side groups [32]. After hydrolysis, the polymer was purified with a PD-10 desalting column following the supplier's protocol and collected by freeze-drying.

2.3. Polymer characterization

2.3.1. Gel permeation chromatography (GPC) characterization of the polymers

Analysis of the $(FA\text{-}PEG)_2$-ABCPA macroinitiator and pHDP-PEG-FA polymer was performed using a Waters System (Waters Associates Inc., Milford, MA) with refractive index (RI) and UV detection using two serial Plgel 5 µm MIXED-D columns (Polymer Laboratories) and DMF containing 10 mM LiCl as eluent. The flow rate was 1 mL/min and the temperature was 60 °C. UV detection of FA groups was done at 363 nm. The number average molecular weight (M_n), weight average molecular weight (M_w) and polydispersity (PDI, M_w/M_n) of pHDP PEG-FA was determined using a series of PEG calibration standards.

2.3.2. ^{1}H NMR characterization of the polymers

The copolymer composition was determined by ^{1}H NMR in DMSO-d6. The NMR spectrum was recorded on a 400 MHz Agilent 400-MR NMR spectrometer (Agilent Technologies, Santa Clara, USA). The copolymer composition and calculation of the number average molecular weight (M_n) was performed as previously described [32]. The ratio HPMA–DMAE/PDTEMA was determined by comparison of the integrals at δ 4.6 ppm (bs, $CH_2C\underline{H}CH_3O$, HPMA–DMAE) and the integral at δ8.5 ppm (bs, pyridyl group proton, PDTEMA) (∫δ4.6/∫δ8.5).

Number average molecular weight (M_n) of the polymer was determined according to equation (1):

$$M_n = (\int\delta 4.6 \times M_{HPMA–DMAE} + \int\delta 8.5 \times M_{PDTEMA})/(\int\delta 3.5/448) + 5441.4 \text{ (g/mol)} \quad (1)$$

where, ∫δ3.5, ∫δ4.6 and ∫δ8.5 are the integrals at 3.5, 4.6, and 8.5 ppm, respectively. $M_{HPMA–DMAE}$, M_{PDTEMA} are the molar masses of HPMA–DMAE and PDTEMA, respectively. The number of protons for the $FA\text{-}PEG_{5000}$ block, this is ∫δ3.5, was set to 448.

2.3.3. UV spectroscopy characterization

The quantification of the molarity of thiol reactive pyridyl disulfide (PDS) groups per weight of polymer was performed by UV spectroscopy on a Shimadzu UV-2450 UV/VIS spectrophotometer (‘s-Hertogenbosch, The Netherlands). pHDP-PEG-FA stock solutions of 1 mg/mL in 20 mM HEPES pH 7.4 containing 50 mM tris(2-

carboxyethyl)phosphine (TCEP) were prepared and after incubation for 1 h at 37 ºC, the UV absorbance at 343 nm was measured to determine the release of 2-mercaptopyridine [41]. Quantification was performed using a calibration curve with 2-mercaptopyridine standards.

2.4. Preparation of decationized polyplexes

The method previously described for the preparation of pDNA decationized polyplexes [32] was optimized for siRNA entrapment (Scheme 2). The amount of polymer added to complex siRNA was optimized on the basis of the N/P ratio (N, molarity protonable amines from polymer; P, molarity of negatively charged phosphates siRNA)). Polymer solutions of pHDP-PEG-FA (e.g. for N/P=8, 1 mg/mL polymer solution, 105 µL) were mixed with 210 µL siRNA (concentration 7500 nM, 210 µL) in 10 mM HEPES, 10 mM TAPS at pH 8.5 by vortexing.

After complexation, polyplexes were crosslinked by addition of a half molar equivalent of dithiothreitol (DTT) to PDS groups of the polymer, in order to induce self-crosslinking of the polyplexes for 1 h at pH 8.5 [42]. Alternatively, crosslinking was performed by addition of the dithiol 3,6-dioxa-1,8-octane-dithiol (DODT) corresponding with a molar equivalent of DODT thiol groups to PDS groups of the polymer.

After crosslinking, the cationic DMAE side groups were removed by hydrolysis by incubation of the polyplex dispersions at 37 °C and pH 8.5 for 6 h, to yield pHP-PEG-FA polyplexes [32]. Next, the pH of the dispersion was adjusted to pH 7.4 with 1M HCl and the ionic strength was adjusted to 150 mM with 1.5 M NaCl to diluting the polyplexes to a final siRNA concentration of 4000 nM. Depending on the application, the polyplex dispersions were further diluted with PBS (10 mM Na_2HPO_4/NaH_2PO_4, 140 mM NaCl, pH 7.4) or 20 mM HEPES pH 7.4. For comparative studies siRNA cationic pHDP-PEG-FA polyplexes were prepared by adjusting the pH to 7.4 with 1M HCl immediately after crosslinking.

For *in vitro* testing, the polyplex dispersions were purified by dialysis overnight against sterile PBS using SlideALyzer MINI Dialysis Devices 20K MWCO (Thermo Fisher Scientific).

2.5. Particle size and zeta potential determination

2.5.1. Dynamic light scattering (DLS)

The size of the polyplexes was measured with DLS on an ALV CGS-3 system (Malvern Instruments, Malvern, UK) equipped with a JDS Uniphase 22 mW He-Ne laser operating at 632.8 nm, an optical fiber-based detector, a digital LV/LSE-5003 correlator with temperature controller set at 25 °C or 37 °C. Measurements were performed in PBS at a final siRNA concentration of 500 nM.

2.5.2. Zeta potential

The zeta potential of the polyplexes was measured using a Malvern Zetasizer Nano-Z (Malvern Instruments, Malvern, UK) with universal ZEN 1002 'dip' cells and DTS (Nano) software (version 4.20) at 25 °C. Zeta potential measurements were performed of polyplex dispersions in 20 mM HEPES pH 7.4 at a siRNA concentration of 500 nM.

2.5.3. Nanoparticle tracking analysis (NTA)

Size distribution of the polyplexes was determined by NTA on a NanoSight LM10SH (NanoSight, Amesbury, United Kingdom), equipped with a sample chamber with a 532-nm laser. Using a siRNA polyplex concentration of 1 nM in PBS, videos of 160 s were taken and analyzed by NTA 2.0 image analysis software (NanoSight, Amesbury, UK). The detection threshold was set at 2 and the minimum track length at 10. The mode and mean size and SD values were reported by the NTA software.

2.5.4. Transmission electron microscopy (TEM)

The size and morphology of the polyplexes were analyzed using transmission electron microscopy (TEM, FEI Tecnai T10). A droplet of polyplex dispersion of at 1000 nM siRNA in 20 mM HEPES pH 7.4 was placed on a carbon coated copper. The samples were stained with 2% uranyl acetate. Size determination was done with Olympus MeasureIT software.

2.6. Gel Retardation Assay

Decationized pHP-PEG-FA and cationic pHDP-PEG-FA polyplexes were incubated for 2.5 h at 37 ºC in the absence or presence of 10 mM DTT (as reducing agent). Next, 15 µL (1000 nmol siRNA) of polyplex dispersion in PBS was mixed with 3 µL 6× DNA Loading Dye and the polyplexes were loaded into 2% agarose gel in Tris-acetate-EDTA (TAE) buffer stained with SYBR safe and run at 120 V for 30 min. The gel was analyzed by a Gel Doc™ XR+ system (BioRad Laboratories Inc., Hercules, CA) with Image Lab software.

2.7. Polyplex stability determined by fluorescence correlation spectroscopy (FCS)

siRNA release from the polyplexes during 2 h of incubation with 20 mM HEPES buffer pH 7.4 or in 90% human plasma following incubation at 37°C, was determined by FCS as previously described by Buyens et al. [43]. Briefly, FCS measurements were performed on free naked Alexa 647-siRNA (λ_{exc} = 594 nm, λ_{em} = 633 nm) and Alexa 647-siRNA encapsulated in decationized pHP-PEG polyplexes, on a C1si laser scanning confocal microscope (Nikon, Japan), equipped with a Time-Correlated Single Photon Counting (TCSPC) Data Acquisition module (Picoquant, Berlin, Germany), and water immersion objective lens (Plan Apo 60×, NA 1.2, collar rim correction, Nikon, Japan). During the measurements, the glass bottom 96-well plate (Grainer Bio-one, Frickenhausen, Germany) was covered with Adhesive Plates Seals (ThermoScientific, UK) to avoid evaporation of water. For each sample, fluorescence intensity fluctuations were recorded using Symphotime (Picoquant, Berlin, Germany), during 1 minute in triplicates. As the baseline fluorescence intensity of the fluorescence fluctuation profiles recorded by FCS is proportional to the concentration of free siRNA, the percentage of complexed and released siRNA can be calculated as described and validated by Buyens et al. [43].

2.8. Cell culture

Skov3-luc cells (folate receptor overexpressing cell line) were cultured in DMEM (4500 mg/L glucose) supplemented with antibiotics/antimycotics (penicillin, streptomycin sulphate, amphotericin B) and 10% FBS (Sigma-Aldrich). Cells were

maintained at 37 °C in a 5 % CO_2 humidified air atmosphere.

2.9. Gene silencing

Skov3-luc, folate overexpressing cell line, stably expressing firefly luciferase were seeded into 96-well plates (6000 cells per well). After 24 h, the medium was removed and replaced with folate-free RPMI 1640 supplemented with 10% dialyzed FBS, with or without 1 mM folic acid, containing siRNA polyplex dispersions at siRNA concentrations of 100, 250, 500 and 1000 nM (anti-Luc and scramble siRNA). The cells were incubated with siRNA polyplexes for 24 h at 37 ºC. Lipofectamine 2000 (Life Technologies) siRNA complexes were prepared according to the manufacturer's protocol and used as positive control for transfection [14], and PBS treated cells were used as negative control. Alternatively, pHP-PEG-FA free polymer (concentrations ranging from 0.001 to 1 mg/mL) was also incubated incubated with the cells for 24 h.

Luciferase cellular expression was measured 48 h after transfection. Cells were washed with 100 µL of cold PBS and lysed with 50 µL of lysis buffer (Reporter Lysis Buffer 5× (Promega), diluted in mQ H_2O). Cell lysis was completed by performing a freeze-thaw cycle after placing the cells for 1 h at -80 °C. Next, 20 µL of cell lysate was mixed with 100 µL of Luciferase Assay Reagent (Promega) and after 2 sec, luminescence was measured for 10 sec using a FLUOstar OPTIMA microplate, equipped with a luminescence light guide (BMG LabTech, Germany). The obtained luciferase is expressed as relative light units (RLU).

2.10. Toxicity

The effect of the decationized pHP-PEG-FA free polymer or pHP-PEG-FA siRNA polyplexes on the cell metabolic was determined by XTT. Free polymer (concentrations ranging from 0.001 to 1 mg/mL) or polyplexes (concentrations ranging from 100 nM to 1000 nM siRNA) were incubated with the Skov3-luc cells in 96-well plates (6000 cells per well) for 24 h with folate-free RPMI 1640 supplemented with 10% dialyzed FBS. XTT assay was performed 48 h after incubation of polymer and polyplexes with the cells.

The XTT assay was performed by incubating Skov3-luc cells for 1 h at 37 °C in a CO_2-incubator after addition of 50 µL per well of a freshly prepared XTT

solution (25 μM *N*-methyl dibenzopyrazine methylsulfate (PMS) and 1 mg/mL 2,3-bis(2-methoxy-4-nitro-5-sulfophenyl)-2H-tetrazolium-5-carboxanilide (XTT) in plain RPMI 1640 medium). The relative cell metabolic activity was calculated by normalizing the absorbance at 490 nm (reference wavelength of 655 nm) with the absorbance of buffer treated cells.

2.11. Statistical analysis

Statistical analyses were performed with the software GraphPad Prism 5 (GraphPad Software Inc., La Jolla, California, USA).

3. RESULTS & DISCUSSION

3.1. Polymer synthesis

FA functionalized polymer for the preparation of targeted decationized polyplexes was synthesized by free radical copolymerization of HPMA–DMAE with PDTEMA using the FA-PEG_{5000} bi-functionalized $(FA\text{-}PEG)_2$-ABCPA as macroinitiator (Scheme 1). The polymerization resulted in the formation of the block copolymer p(HPMA–DMAE-co-PDTEMA)-b-PEG-FA with a yield close to 50%. The characteristics of the synthesized polymer were established by ^1H NMR, GPC and UV spectroscopic analysis and are given in Table 1. Although both HPMA–DMAE and PDTEMA are both methacrylamide monomers, incorporation of PDTEMA was slightly lower than the feed composition, as previously observed [32]. The M_n calculated from ^1H NMR spectroscopic analysis (34.9 kDa) was close to that determined with GPC (39.7 kDa, PDI = 2.1). UV spectroscopy was used to determine incorporation of PDTEMA and 630±21 nmol PDTEMA monomer per mg of polymer was found.

The cationic HPMA–DMAE monomer was incorporated in the copolymer to allow electrostatically driven formation interaction of the polymer with siRNA to yield nanoparticulate polyplexes. The PDTEMA monomer contains the PDS functionality, which allows interchain disulfide crosslinking stabilization of the core of the polyplexes by thiol-disulfide exchange reaction. After stabilization, the labile DMAE cationic groups can be removed by hydrolysis to yield the decationized

polyplexes based on PEG-pHPMA [44]. The copolymer composition, in particular the HPMA–DMAE/PDTEMA molar ratio, ultimately determines the crosslinking density of the core of decationized polyplexes.

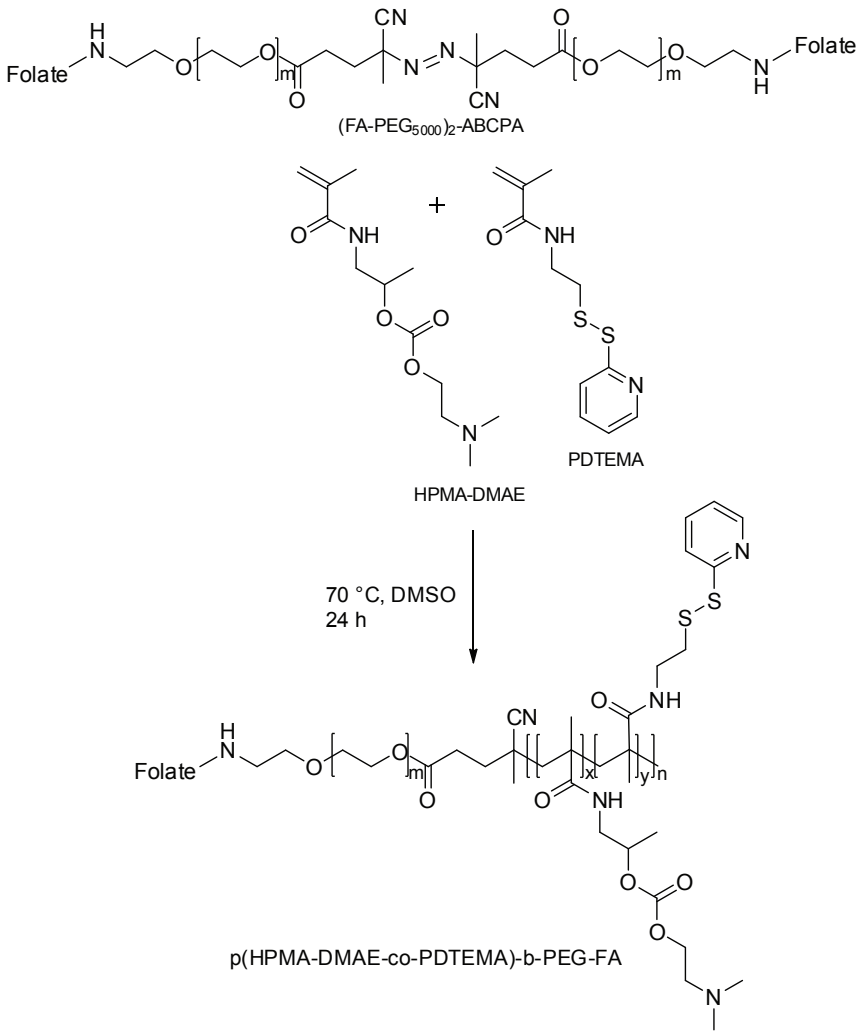

Scheme 1. Synthesis of p(HPMA–DMAE-co-PDTEMA)-b-PEG by free-radical polymerization of HPMA–DMAE, PDTEMA and using $(FA\text{-}PEG_{5000})_2$-ABCPA macroinitiator.

Table 1. p(HPMA–DMAE-co-PDTEMA)-b-PEG-FA characteristics determined by GPC, ^{1}H NMR, UV spectroscopic analysis.

GPC		NMR			UV
M_n (kDa)	PDI	M_n (kDa)	Feed HPMA–DMAE/PDTEMA	Copolymer HPMA–DMAE/PDTEMA	$nmol_{PDS}/mg_{polymer}$
39.7	2.1	34.9	1/0.6	1/0.4	630±21

3.2. Preparation and stability of decationized pHP-PEG-FA polyplexes loaded with siRNA

siRNA polyplexes based on pHP-PEG-FA were formed through a 3-step process in a similar process as described for the preparation of pDNA polyplexes [32, 34] (Scheme 2). The first step was the electrostatic complexation of the cationic block copolymer p(HPMA–DMAE-co-PDTEMA)-b-PEG-FA (pHDP-PEG-FA) with siRNA. The stabilization of the polyplexes was subsequently established via interchain disulfide crosslinking using DTT. The addition of half molar equivalents of DTT to PDS groups of the polymer, induced self-crosslinking of the polyplexes [42] to yield disulfide crosslinked cationic pHDP-PEG-FA polyplexes. p(HPMA-co-PDTEMA)-b-PEG-FA (pHP-PEG) decationized polyplexes were obtained by removal of the DMAE cationic side groups from cationic pHDP-PEG-FA polyplexes by hydrolysis of carbonate ester bond linking the DMAE side groups to the HPMA backbone at pH 8.5 for 6 h. It is aimed that after decationization, the loaded siRNA is retained in the pHPMA crosslinked core of the polyplexes which are surrounded by a PEG shell containing the FA targeting ligand.

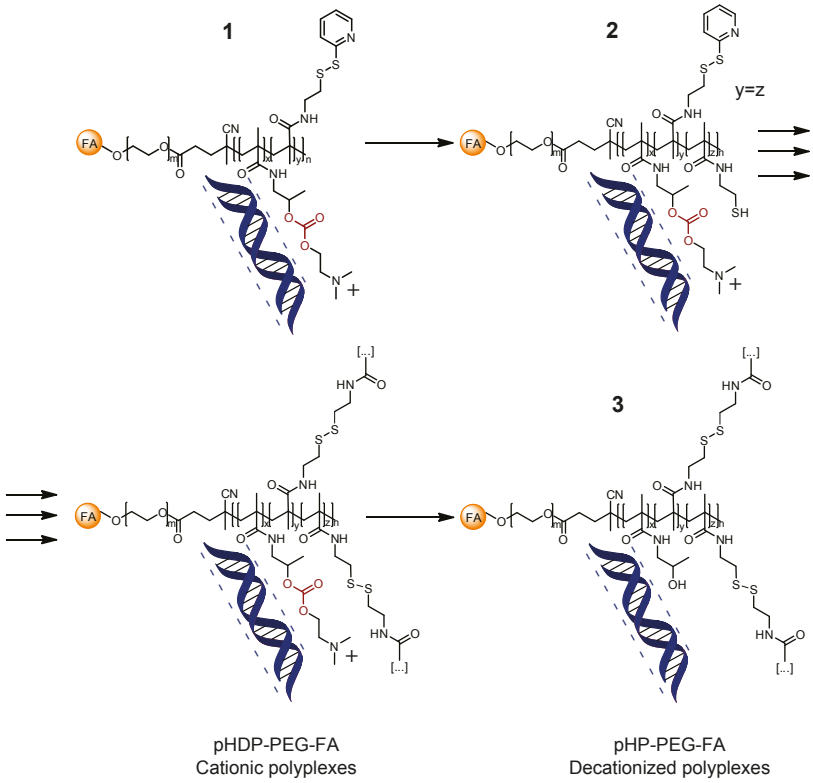

Scheme 2. 3-step preparation of interchain disulfide-crosslinked decationized polyplexes: 1. charge-driven condensation with nuclei acids; 2. stabilization through disulfide crosslinking by addition of half molar equivalents of DTT to PDS groups in the polymer; 3. decationization of cationic pHDP-PEG-FA polyplexes for 6 h at 37ºC and pH 8.5, resulting in decationized pHP-PEG-FA polyplexes (adapted from Novo et al. [32]).

Previously, decationized polyplexes have been optimized for entrapment of pDNA using pHDP-PEG with a HPMA–DMAE/PDTEMA ratio of 6.5/1 [32, 34]. Stabilization of the polyplexes via interchain disulfide crosslinking occurred using the short dithiol DODT by thiol-disulfide exchange reaction between the thiol groups from DODT and PDS groups in the polymer. To fully complex siRNA and form stable polyplexes with pHDP-PEG-FA (HPMA–DMAE/PDTEMA 6.5/1) an N/P=8 was used and the ability of decationized pHP-PEG-FA polyplexes to retain the entrapped siRNA was evaluated by a gel retardation assay (Figure 1). Decationized polyplexes were also incubated with 10 mM DTT (lane 2) to mimic the intracellular reducing environment [19, 45]. In this gel retardation assay, retained siRNA in the polyplexes is visible in the starting slot of the well whereas free or released siRNA

migrates towards the anode. As shown in Figure 1, pHP-PEG-FA polyplexes which were prepared at an HPMA–DMAE/PDTEMA ratio of 6.5/1 were not able to stably entrap siRNA after loss of cationic DMAE groups, even in the absence of 10 mM DTT (lane 1). Crosslinked pHDP-PEG-FA cationic polyplexes were also evaluated using the same assay and it was shown that both in the absence (lane 1) and presence of 10 mM DTT (lane 2) no free siRNA was detected which demonstrates that at preparation conditions of N/P=8 the formed complexes quantitatively retained the added siRNA.

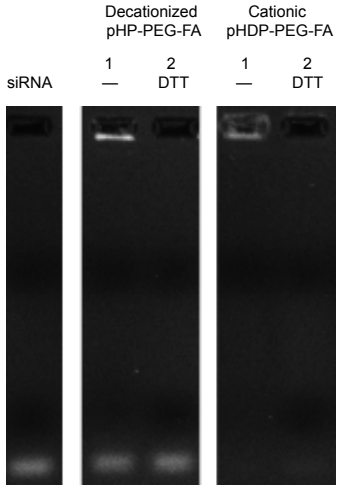

Figure 1. Agarose gel retardation assay of decationized pHP-PEG-FA and comparison with cationic pHDP-PEG-FA polyplexes: lane 1, untreated sample; lanes 2, sample treated with 10 mM DTT (control, free siRNA). Polyplexes were prepared using pHDP-PEG-FA with HPMA–DMAE/PDTEMA=6.5/1, N/P=8 and DODT as crosslinker.

These results point out the importance of considering the differences between pDNA and siRNA for optimization of siRNA decationized polyplexes. pDNA has a size between 3000-5000 bp but siRNA is composed of only 21 bp, which corresponds to 8 nm and <1/100 of pDNA length. [40, 46]. In addition, the rigidity of siRNA hampers its effective complexation with cationic polymers and adversely affects the stability of polyplexes [47]. Accordingly, effective retention of siRNA molecules in the core of decationized polyplexes required a more densely packed crosslinked core, when compared to pDNA-loaded decationized polyplexes. Therefore, in the present study pHDP-PEG-FA with HPMA–DMAE/PDTEMA ratio

of 2.5/1 was synthesized. A further increase of PDTEMA, a hydrophobic monomer, (HPMA–DMAE/PDTEMA 1.5/1) led to a reduced water solubility of the block copolymer. A good aqueous solubility is however essential for polyplex preparation, and this polymer was therefore not evaluated in this study.

Another aspect of crosslinking procedure that was important to take into consideration to obtain a more condensed crosslinked core of siRNA decationized polyplexes was the use of a so-called 'zero-length' crosslinking agent (DTT), which is a strong reducing agent, that can be used as alternative to the dithiol DODT. Therefore, decationized polyplexes were prepared using pHDP-PEG-FA with HPMA–DMAE/PDTEMA ratio of 2.5/1 and N/P=8 using both DTT and DODT as crosslinking agents and size distribution determination by NTA (Figure 2a) and gel retardation assay (Figure 2b) were performed. Size distribution of pHP-PEG-FA decationized polyplexes prepared with DODT as crosslinker showed a mean size of around 167±63 nm, whereas polyplexes prepared with DTT possessed an evident smaller mean size of 99±40 nm and narrower size distribution (Figure 2a). When polyplexes prepared with both methods were evaluated with a gel retardation assay (Figure 2b), significant differences in the retention behavior of polyplexes were observed. In the case of decationized polyplexes crosslinked with DODT, siRNA was not fully encapsulated and a high degree of free siRNA was detected (lane 1). In contrast, when decationized polyplexes were prepared using DTT as crosslinker, complete siRNA retention in the polyplexes was observed (lane 2). The loss of electrostatic interactions between the polymer and siRNA leads to hydration and slight swelling of the polyplex core, when the short DODT crosslinker is used. However, by using of a zero-length crosslinking agent such as DTT, swelling is reduced and a more condensed crosslinked core is obtained preventing leakage of siRNA.

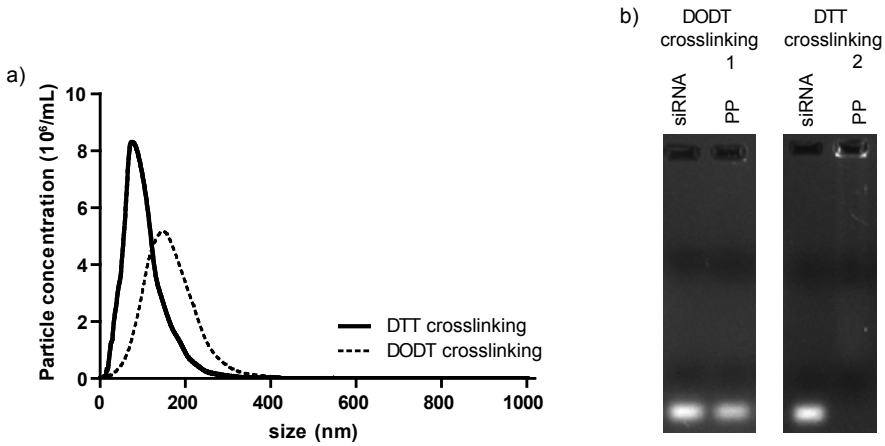

Figure 2. pHP-PEG-FA decationized polyplexes prepared using the dithiol DODT or DTT as crosslinking agents. (a) Polyplexes size distribution determined by NTA. (b) Agarose gel retardation assay: lane 1, DODT crosslinked polyplex (PP) untreated sample; lane 2, DTT crosslinked polyplex (PP) untreated sample (control, free siRNA). Polyplexes were prepared using pHDP-PEG-FA with HPMA–DMAE/PDTEMA=2.5/1 and N/P=8.

Decationized polyplexes are designed to stably entrap siRNA and simultaneously preserve the desired intracellular triggered release. This later property of decationized polyplexes using pHDP-PEG-FA with HPMA–DMAE/PDTEMA=2.5/1, N/P=8 and DTT as zero-length crosslinking agent was evaluated by a gel retardation assay (Figure 3) in the absence (lane 1) or presence of a reducing agent (10 mM DTT, lane 2). As demonstrated in Figure 3, decationized polyplexes completely entrapped siRNA when dispersed in PBS. However, when the polyplexes were incubated with 10 mM DTT for 2.5 hours (lane 2), mimicking the intracellular reducing environment [19, 45], disulfide crosslinks were cleaved and the polyplexes completely released the encapsulated siRNA. As control, crosslinked pHDP-PEG-FA cationic polyplexes were also studied, but no free siRNA was detected, both in the absence (lane 1) or presence of DTT (lane 2), since siRNA was still retained in the polyplexes by electrostatic interactions between the negatively charged siRNA and the cationic polymer. These results demonstrate that siRNA encapsulation in pHP-PEG-FA decationized polyplexes is mainly driven by physical entrapment and that in the presence of a reducing agent polyplexes release their siRNA loading.

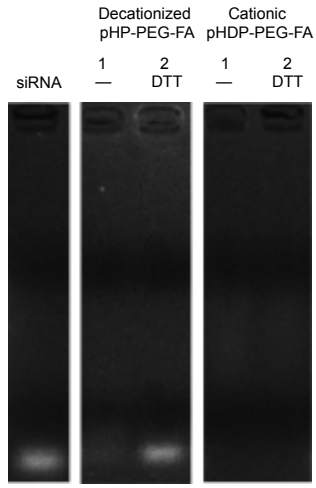

Figure 3. Agarose gel retardation assay of decationized pHP-PEG-FA and cationic pHDP-PEG-FA polyplexes: lane 1, untreated sample; lanes 2, sample treated with 10 mM DTT. Polyplexes were prepared using pHDP-PEG-FA with HPMA–DMAE/PDTEMA=2.5/1, N/P=8 and DTT to induce self-crosslinking.

The polyplexes prepared with pHDP-PEG-FA with HPMA–DMAE/PDTEMA=2.5/1, N/P=8 and DTT as zero-length crosslinking agent were further characterized and evaluated.

The particle size determined by DLS and zeta potential measurement results are shown in Table 2. The cationic pHDP-PEG-FA polyplexes formed at an N/P=8 yielded nanosized particles with a diameter of 126±2 nm and a positive zeta potential of +5.9±0.4 mV. After decationization, pHP-PEG-FA polyplexes had a size of 123±6 nm and a slightly negative zeta-potential of -2.6±0.1 mV. The decrease in zeta potential towards a slightly negative charge confirms the loss of the cationic DMAE groups [32] and retention of the negatively charged siRNA in the core. The similar sizes of both polyplexes proves that polyplex structure remains intact after decationization using a high crosslink density and the use of zero-length crosslinking (DTT).

Table 2. Particle z-average diameter (Z-avg) and polydispersity index (PDI) determined by DLS and zeta potential (ζ Pot) of cationic pHDP-PEG-FA and decationized pHP-PEG-FA polyplexes. Polyplexes were prepared with pHDP-PEG-FA with HPMA–DMAE/PDTEMA ratio of 2.5/1 at N/P=8. Results are expressed as mean±SD (n=3).

Polyplexes	DLS		Zetasizer
	Z-avg (nm)	PDI	ζ Pot (mV)
pHDP-PEG-FA	126±2	0.14±0.02	5.9±0.4
pHP-PEG-FA	124±2	0.12±0.02	-2.6±0.1

The size and shape of siRNA decationized pHP-PEG-FA polyplexes were also evaluated with TEM (Figure 4) and with this technique, small (~30 nm) and spherical particles were detected. A small population of more elongated structures can also be observed which are probably the result of inter-particle crosslinking. The discrepancy between DLS and electron microscopy in terms of measured size has been previously observed for PEGylated polyplexes and is most likely due to lack of uranyl acetate staining of the PEG corona [48]. Furthermore, in the case of DLS measurements, the presence of few larger particles in a sample has a great impact on the zaverage size, due to its sensitivity to large particles [49].

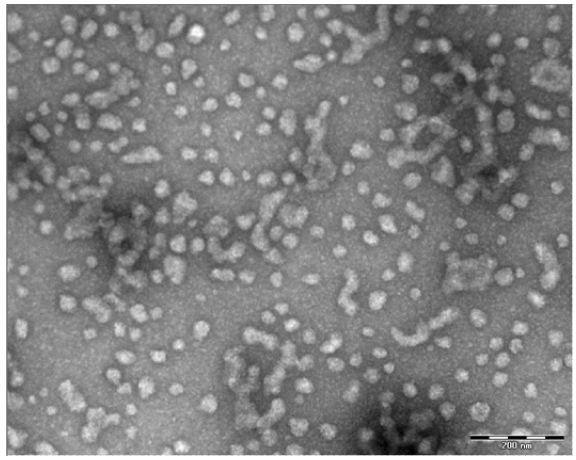

Figure 4. TEM images of decationized pHP-PEG-FA polyplexes prepared with pHDP-PEG-FA with HPMA–DMAE/PDTEMA ratio of 2.5/1 at N/P=8. Magnification 73000×. Scale bar 200 nm.

The size of siRNA decationized pHP-PEG-FA polyplexes was also analyzed by NTA (Figure 5). NTA analyzes simultaneously a set of individual particles in a suspension and gives information on the real size distribution of the sample, which cannot be obtained with DLS [49]. The mean size and size distribution

of decationized pHP-PEG-FA polyplexes was also compared with that of the cationic pHDP-PEG-FA polyplexes. In line with DLS data, the decationized and cationic polyplexes showed comparable average sizes (around 100 nm). The size distributions of both decationized and cationic polyplexes almost overlap (SD around 40 nm), demonstrating once more that the method to prepare siRNA decationized polyplexes using DTT as crosslinking agent leads to efficient stabilization of the nanoparticles. The stability of decationized polyplexes at physiological ionic strength and pH, was evaluated by incubation of the polyplexes for 24 h in PBS at 37 ºC, followed by NTA analysis. It was shown that after incubation, decationized polyplexes maintained their size distribution (Figure 5).

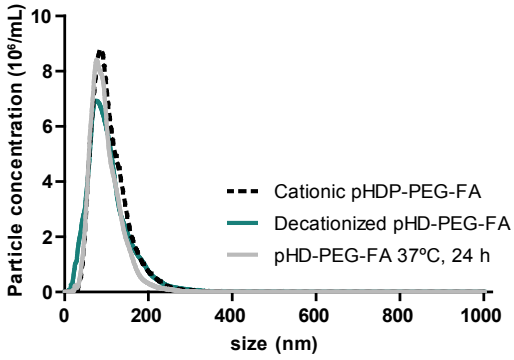

Figure 5. Cationic pHDP-PEG-FA and decationized pHP-PEG-FA siRNA (before and after incubation for 24 h at 37ºC in PBS) polyplexes size distribution determined by NTA. Polyplexes were prepared with pHDP-PEG-FA with HPMA–DMAE/PDTEMA ratio of 2.5/1 at N/P=8. For the x-axis you use only 0-400 nm. So please adjust this.

The stability in of decationized pHP-PEG-FA polyplexes in physiological ionic strength and pH, was further confirmed by continuous DLS measurement during incubation of the polyplexes for 24 h at 37 ºC in PBS (Figure 6). This figure shows that the polyplexes maintained a stable size of around 120 nm as well as a constant intensity of scattered light for 24 h. These results show that decationized polyplexes were very stable without particle swelling, disassembling or aggregation demonstrating their excellent colloidal stability.

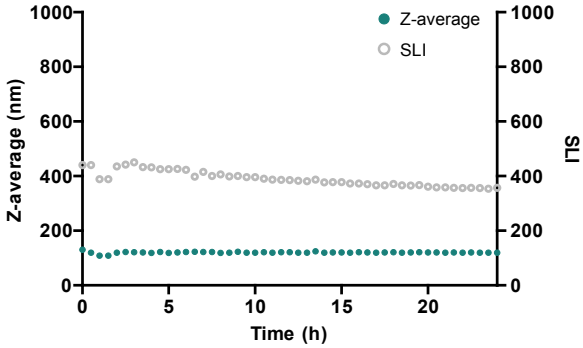

Figure 6. Particle size and scattered light intensity (SLI) of siRNA decationized pHP-PEG-FA polyplexes determined by DLS upon incubation in PBS at 37 °C for 24 h. Polyplexes were prepared with pHDP-PEG-FA with HPMA–DMAE/PDTEMA ratio of 2.5/1 at N/P=8.

3.3. Stability of decationized polyplexes in plasma

In vivo application of siRNA-loaded nanoparticles requires a high stability of the particles before reaching their target tissue. Often premature dissociation of siRNA from polyplexes occurs in the bloodstream or in the polyanion rich environment of the kidneys [9-12]. Thus, it is crucial to assess the stability of siRNA polyplexes in biological fluids to get insight into the *in vivo* potential of these nanomedicines. FCS is an important technique to evaluate the stability of fluorophore-labeled siRNA complexes in undiluted biological fluids [43, 50]. This technique is based on the measurement of fluorescence intensity fluctuations of labeled siRNA in the excitation volume of a confocal microscope. The average intensity of these fluctuations is proportional to free siRNA concentration. In the case of complexed siRNA, the average intensity is significantly decreased. The release of siRNA from polyplexes, will result in in the presence of free siRNA in the sample, which can be determined by analysis of average intensity of the fluorescence.

Decationized pHP-PEG-FA polyplexes loaded with Alexa 647 labeled siRNA were incubated in human plasma and the possible release of siRNA was studied with FCS for 2 h (Figure S1, Supporting Information). The amount of free siRNA was first evaluated in buffer, and analysis showed that less than 20% free siRNA in the polyplex dispersion was observed after decationization. When siRNA pHP-PEG-FA decationized polyplexes were incubated in plasma, a burst release of siRNA was detected (~60%). However, after this initial release the remaining siRNA remained entrapped in the polyplexes up to 2 h. Most likely, siRNA molecules

loosely entrapped in the polyplexes and located in the outer core of the polyplexes, dissociate from the polyplexes in the presence of plasma proteins. These siRNA molecules are probably kept in the polyplexes via weak hydrophobic interactions, in the compact core of siRNA polyplexes as previously observed for other polymer-siRNA complexes [11, 51]. These interactions are broken in the presence of plasma proteins leading to release of siRNA from the polyplexes. Due to siRNA small size and inability to control that crosslinks occur inter-chains (not intra-chains), complete retention inside the polyplexes of unmodified siRNA is very challenging even for crosslinked systems [18, 50]. Nevertheless, an important percentage of the total siRNA encapsulated remained in the decationized polyplexes to exert its gene silencing activity.

3.4 *In vitro* cytotoxicity and gene silencing activity of decationized pHP-PEG-FA polyplexes

pHP-PEG-FA decationized polyplexes were evaluated for cytotoxicity and gene silencing activity in the presence of serum using a folate receptor overexpressing cell line, that stably expresses firefly luciferase, Skov3-luc.

First the potential *in vitro* toxicity of free pHP-PEG-FA polymer was analyzed by incubating the cells with solutions with a wide range of polymer concentrations (from 0.001 to 1 mg/mL) (Figure S2, Supporting Information). Possible cytotoxic effects of free pHP-PEG-FA were evaluated by studying the interference on the intrinsic expression of luciferase by the cells (Figure S2a) and the by determining the interference on the cell metabolic activity determined by XTT assay (Figure S2b). Results showed that that up to 1 mg/mL neither interference on luciferase expression nor on the cell metabolic activity were detected demonstrating that the free polymer possesses a very good cytocompatibility.

The cytotoxicity was also evaluated for siRNA pHP-PEG-FA decationized polyplexes with the XTT assay (Figure S3, Supporting Information). Again, cell viability was maintained close to 100% even at high decationized polyplex concentrations (1000 nM siRNA, ~0.05 mg/mL pHP-PEG-FA). In line with previous findings, where high cytocompatibility was observed for pHP-PEG systems [32, 34], and the results of the present study show that the safety profile was preserved with increasing the crosslink density of polyplexes.

Transfection efficiency of targeted decationized pHP-PEG-FA polyplexes was

evaluated by their ability to induce luciferase gene silencing in Skov3-luc. Figure 7 shows that with increasing anti-Luc siRNA polyplex dose luciferase expression was reduced to 75%, at the highest concentration (1000 nM siRNA). In contrast, cells treated with polyplexes encapsulation scramble siRNA luciferase expression was kept close to 100% luciferase, up to 1000 nM siRNA (Figure 7a). These results suggest that the reduction of luciferase expression observed in cells treated with siRNA was due to sequence-specific gene silencing.

The targeting ability of pHP-PEG-FA polyplexes was evaluated by anti-Luc siRNA polyplexes in the presence of FA saturated medium. Indeed, almost no silencing was observed even at the highest doses (Figure 7b) and demonstrates the potential of cell-specific transfection of folate targeted decationized polyplexes that was also previously observed for pDNA polyplexes [34]. It should be noted that at the same siRNA dose, the decationized pHP-PEG-FA polyplexes possessed a lower silencing efficiency than the Lipofectamine siRNA formulation (Figure 7a). This high transfection activity of Lipofectamine has been previously found to occur due its highly degree of unspecific interaction with the transfected cells and its ability to later cluster in the cytoplasm [14]. It should also be noted that transfection protocol using Lipofectamine requires the absence of serum which blocks its applicability *in vivo*. Whereas the transfection of pHP-PEG-FA polyplexes were evaluated in the presence of serum. Further, folate-targeted nanoparticles interact with high affinity to the folate receptor of the cells and are internalized by receptor-mediated endocytosis. These folate-conjugates remain in ‘recycling’ endosomes or eventually escape into the cytoplasm [35, 36, 52]. For efficient nucleic acid delivery (DNA- or RNA-based), polyplexes which end up in endosomes require endosomal escape [53-59]. pHP-PEG-FA do not possess intrinsic endosomal escape functionalities which limits its efficiency at low concentrations [32].

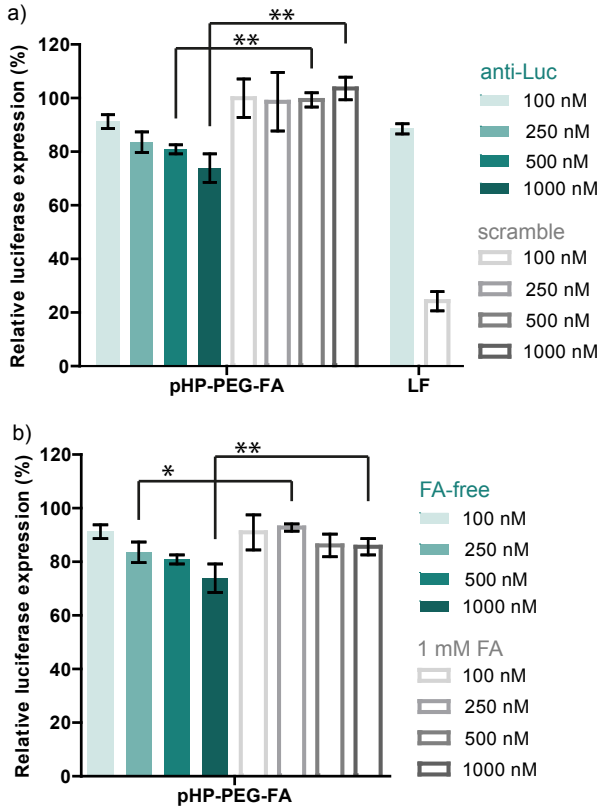

Figure 7. *In vitro* luciferase gene knockdown in Skov3-luc cells. Cell were treated with decationized pHP-PEG-FA polyplexe dispersions containing anti-luciferase siRNA or scramble siRNA of different concentrations (a) and pHP-PEG-FA polyplexes containing anti-luciferase siRNA in FA depleted medium and in FA saturated medium (1 mM) (b). Results were normalized to buffer treated samples and Lipofectamine 2000 (LF) was used as positive control for transfection (100 nM siRNA). Results are expressed as mean±SD (n=4). *p<0.05; **p<0.01 (t-test).

4. CONCLUSION

In this study, folate targeted decationized polyplexes for siRNA delivery were developed. Polymer structure and polyplex preparation protocols were optimized to efficiently entrap the 21 bp structure of siRNA into nanosized polyplexes based on neutral polymers. The major cause of siRNA entrapment was the presence of interchain disulfide crosslinks, which provides stability in extracellular environment and simultaneously allowing an intracellular triggered release. As determined by

FCS, even when incubated in human plasma, polyplexes retained a substantial part of their siRNA loading. siRNA decationized polyplexes tested *in vitro* with Skvo3-luc, a folate receptor overexpressing cell line stably expressing luciferase, showed sequence specific gene silencing without detected cytotoxicity.

siRNA decationized polyplexes are ~100-120 nm in diameter with slightly negative zeta potential which is the optimal feature to reduce off-target accumulation and retention upon systemic administration, particularly in the kidney. In addition, their safety profile, ability to retain part of the encapsulated siRNA in plasma, capacity to interact with the targeted cells and disassemble upon cell entry make pHP-PEG-FA decationized polyplexes a promising platform for siRNA delivery.

ACKNOWLEDGMENT

L. Novo was financially supported by Fundação para a Ciência e a Tecnologia (FCT), the Portuguese Foundation for Science and Technology, grant SFRH/BD/47085/2008. K.M. Takeda was financially by the Japanese Materials Education program for the future leaders in Research, Industry, and Technology (MERIT).

APPENDIX A. SUPPORTING INFORMATION

Supplementary Figures S1-S3 can be found in Supporting Information

References

[1] A. Daka, D. Peer, RNAi-based nanomedicines for targeted personalized therapy, Adv. Drug Deliv. Rev., 64 (2012) 1508-1521.

[2] M. Videira, A. Arranja, D. Rafael, R. Gaspar, Preclinical development of siRNA therapeutics: Towards the match between fundamental science and engineered systems, Nanomedicine, 10 (2014) 689-702.

[3] G.J. Hannon, RNA interference, Nature, 418 (2002) 244-251.

[4] K.A. Whitehead, R. Langer, D.G. Anderson, Knocking down barriers: advances in siRNA delivery, Nat. Rev. Drug Discov., 8 (2009) 129-138.

[5] Y.-K. Oh, T.G. Park, siRNA delivery systems for cancer treatment, Adv. Drug Deliv. Rev., 61 (2009) 850-862.

[6] M.E. Davis, The First targeted delivery of siRNA in humans via a self-assembling, cyclodextrin polymer-based nanoparticle: From concept to clinic, Mol. Pharmaceutics, 6 (2009) 659-668.

[7] A. Sato, S.W. Choi, M. Hirai, A. Yamayoshi, R. Moriyama, T. Yamano, M. Takagi, A. Kano, A. Shimamoto, A. Maruyama, Polymer brush-stabilized polyplex for a siRNA carrier with long circulatory half-life, J. Control. Release, 122 (2007) 209-216.

[8] S. Mao, M. Neu, O. Germershaus, O. Merkel, J. Sitterberg, U. Bakowsky, T. Kissel, Influence of polyethylene glycol chain length on the physicochemical and biological roperties of poly(ethylene imine)-graft-poly(ethylene glycol) block copolymer/siRNA polyplexes, Bioconjug. Chem., 17 (2006) 1209-1218.

[9] H.K. de Wolf, C.J. Snel, F.J. Verbaan, R.M. Schiffelers, W.E. Hennink, G. Storm, Effect of cationic carriers on the pharmacokinetics and tumor localization of nucleic acids after intravenous administration, Int. J. Pharm., 331 (2007) 167-175.

[10] J.E. Zuckerman, C.H.J. Choi, H. Han, M.E. Davis, Polycation-siRNA nanoparticles can disassemble at the kidney glomerular basement membrane, Proc. Natl. Acad. Sci. U.S.A., 109 (2012) 3137-3142.

[11] C.E. Nelson, J.R. Kintzing, A. Hanna, J.M. Shannon, M.K. Gupta, C.L. Duvall, Balancing cationic and hydrophobic content of PEGylated siRNA polyplexes enhances endosome escape, stability, blood circulation time, and bioactivity in vivo, ACS Nano, 7 (2013) 8870-8880.

[12] B. Naeye, H. Deschout, V. Caveliers, B. Descamps, K. Braeckmans, C. Vanhove, J. Demeester, T. Lahoutte, S.C. De Smedt, K. Raemdonck, In vivo disassembly of IV administered siRNA matrix nanoparticles at the renal filtration barrier, Biomaterials, 34 (2013) 2350-2358.

[13] O.M. Merkel, D. Librizzi, A. Pfestroff, T. Schurrat, M. Béhé, T. Kissel, In vivo SPECT and real-time gamma camera imaging of biodistribution and pharmacokinetics of siRNA delivery using an optimized radiolabeling and purification procedure, Bioconjug. Chem., 20 (2008) 174-182.

[14] A. Kwok, S.L. Hart, Comparative structural and functional studies of nanoparticle formulations for DNA and siRNA delivery, Nanomedicine, 7 (2011) 210-219.

[15] D.S. Manickam, J. Li, D.A. Putt, Q.-H. Zhou, C. Wu, L.H. Lash, D. Oupický, Effect of innate glutathione levels on activity of redox-responsive gene delivery vectors, J. Control. Release, 141 (2010) 77-84.

[16] M. Breunig, C. Hozsa, U. Lungwitz, K. Watanabe, I. Umeda, H. Kato, A. Goepferich, Mechanistic investigation of poly(ethylene imine)-based siRNA delivery: Disulfide bonds boost intracellular release of the cargo, J. Control. Release, 130 (2008) 57-63.

[17] S. Matsumoto, R.J. Christie, N. Nishiyama, K. Miyata, A. Ishii, M. Oba, H. Koyama, Y. Yamasaki, K. Kataoka, Environment-responsive block copolymer micelles with a disulfide cross-linked core for enhanced siRNA delivery, Biomacromolecules, 10 (2008) 119-127.

[18] R.J. Christie, Y. Matsumoto, K. Miyata, T. Nomoto, S. Fukushima, K. Osada, J. Halnaut, F. Pittella, H.J. Kim, N. Nishiyama, K. Kataoka, Targeted polymeric micelles for siRNA treatment of experimental cancer by intravenous injection, ACS Nano, 6 (2012) 5174-5189.

[19] F. Meng, W.E. Hennink, Z. Zhong, Reduction-sensitive polymers and bioconjugates for biomedical applications, Biomaterials, 30 (2009) 2180-2198.

[20] H. Lv, S. Zhang, B. Wang, S. Cui, J. Yan, Toxicity of cationic lipids and cationic polymers in gene delivery, J. Control. Release, 114 (2006) 100-109.

[21] R. Duncan, The dawning era of polymer therapeutics, Nat. Rev. Drug Discov., 2 (2003) 347-360.

[22] C.F. Jones, R.A. Campbell, A.E. Brooks, S. Assemi, S. Tadjiki, G. Thiagarajan, C. Mulcock, A.S. Weyrich, B.D. Brooks, H. Ghandehari, D.W. Grainger, Cationic PAMAM dendrimers aggressively initiate blood clot formation, ACS Nano, 6 (2012) 9900-9910.

[23] J. Luten, C.F. van Nostrum, S.C. De Smedt, W.E. Hennink, Biodegradable polymers as non-viral carriers for plasmid DNA delivery, J. Control. Release, 126 (2008) 97-110.

[24] D. Fischer, Y. Li, B. Ahlemeyer, J. Krieglstein, T. Kissel, In vitro cytotoxicity testing of polycations: influence of polymer structure on cell viability and hemolysis, Biomaterials, 24 (2003) 1121-1131.

[25] S.M. Moghimi, P. Symonds, J.C. Murray, A.C. Hunter, G. Debska, A. Szewczyk, A two-stage poly(ethylenimine)-mediated cytotoxicity: implications for gene transfer/therapy, Mol. Ther., 11 (2005) 990-995.

[26] S. Choksakulnimitr, S. Masuda, H. Tokuda, Y. Takakura, M. Hashida, In vitro cytotoxicity of macromolecules in different cell culture systems, J. Control. Release, 34 (1995) 233-241.

[27] C. Lonez, M. Vandenbranden, J.-M. Ruysschaert, Cationic lipids activate intracellular signaling pathways, Adv. Drug Deliv. Rev., 64 (2012) 1749-1758.

[28] W.T. Godbey, K.K. Wu, A.G. Mikos, Poly(ethylenimine)-mediated gene delivery affects endothelial cell function and viability, Biomaterials, 22 (2001) 471-480.

[29] K. Masago, K. Itaka, N. Nishiyama, U.-i. Chung, K. Kataoka, Gene delivery with biocompatible cationic polymer: Pharmacogenomic analysis on cell bioactivity, Biomaterials, 28 (2007) 5169-5175.

[30] O.M. Merkel, A. Beyerle, B.M. Beckmann, M. Zheng, R.K. Hartmann, T. Stöger, T.H. Kissel, Polymer-related off-target effects in non-viral siRNA delivery, Biomaterials, 32 (2011) 2388-2398.

[31] K. Regnström, E.G.E. Ragnarsson, M. Köping-Höggård, E. Torstensson, H. Nyblom, P. Artursson, PEI – a potent, but not harmless, mucosal immuno-stimulator of mixed T-helper cell response and FasL-mediated cell death in mice, Gene Ther., 10 (2003) 1575-1583.

[32] L. Novo, E.V.B. van Gaal, E. Mastrobattista, C.F. van Nostrum, W.E. Hennink, Decationized crosslinked polyplexes for redox-triggered gene delivery, J. Control. Release, 169 (2013) 246-256.

[33] L. Novo, L.Y. Rizzo, S.K. Golombek, G.R. Dakwar, B. Lou, W. Jahnen-Dechent, K. Remaut, E. Mastrobattista, C.F. van Nostrum, F. Kiessling, K. Braeckmans, T. Lammers, W.E. Hennink, Decationized polyplexes as stable and safe carrier systems for improved biodistribution in systemic gene therapy, Manuscript submitted for publication, (2014).

[34] L. Novo, E. Mastrobattista, C.F. van Nostrum, W.E. Hennink, Targeted decationized polyplexes for cell specific gene delivery, Bioconjug. Chem., 25 (2014) 802-812.

[35] A.R. Hilgenbrink, P.S. Low, Folate receptor-mediated drug targeting: From therapeutics to diagnostics, J. Pharm. Sci., 94 (2005) 2135-2146.

[36] Y. Lu, P.S. Low, Folate-mediated delivery of macromolecular anticancer therapeutic agents, Adv. Drug Deliv. Rev., 64, Supplement (2012) 342-352.

[37] D.S.W. Benoit, S. Srinivasan, A.D. Shubin, P.S. Stayton, Synthesis of Folate-Functionalized RAFT Polymers for Targeted siRNA Delivery, Biomacromolecules, 12 (2011) 2708-2714.

[38] C. Dohmen, D. Edinger, T. Fröhlich, L. Schreiner, U. Lächelt, C. Troiber, J. Rädler, P. Hadwiger, H.-P. Vornlocher, E. Wagner, Nanosized multifunctional polyplexes for receptor-mediated siRNA delivery, ACS Nano, 6 (2012) 5198-5208.

[39] C. Dohmen, T. Frohlich, U. Lachelt, I. Rohl, H.-P. Vornlocher, P. Hadwiger, E. Wagner, Defined folate-PEG-siRNA conjugates for receptor-specific gene silencing, Mol. Ther. Nucleic Acids, 1 (2012) e7.

[40] C. Scholz, E. Wagner, Therapeutic plasmid DNA versus siRNA delivery: Common and different tasks for synthetic carriers, J. Control. Release, 161 (2012) 554-565.

[41] D.R. Grassetti, J.F. Murray, Determination of sulfhydryl groups with 2,2'- or 4,4'-dithiodipyridine, Arch. Biochem. Biophys., 119 (1967) 41-49.

[42] J.-H. Ryu, R.T. Chacko, S. Jiwpanich, S. Bickerton, R.P. Babu, S. Thayumanavan, Self-cross-linked polymer nanogels: A versatile nanoscopic drug delivery platform, J. Am. Chem. Soc., 132 (2010) 17227-17235.

[43] K. Buyens, B. Lucas, K. Raemdonck, K. Braeckmans, J. Vercammen, J. Hendrix, Y. Engelborghs, S.C. De Smedt, N.N. Sanders, A fast and sensitive method for measuring the integrity of siRNA-carrier complexes in full human serum, J. Control. Release, 126 (2008) 67-76.

[44] A. Funhoff, C.F. van Nostrum, A. Janssen, M. Fens, D. Crommelin, W.E. Hennink, Polymer side-chain degradation as a tool to control the destabilization of polyplexes, Pharm. Res., 21 (2004) 170-176.

[45] M.H. Lee, Z. Yang, C.W. Lim, Y.H. Lee, S. Dongbang, C. Kang, J.S. Kim, Disulfide-cleavage-triggered chemosensors and their biological applications, Chem. Rev., 113 (2013) 5071-5109.

[46] E. Wagner, Polymers for siRNA delivery: Ispired by viruses to be targeted, dynamic, and precise, Acc. Chem. Res., 45 (2011) 1005-1013.

[47] S.-Y. Lee, M.S. Huh, S. Lee, S.J. Lee, H. Chung, J.H. Park, Y.-K. Oh, K. Choi, K. Kim, I.C. Kwon, Stability and cellular uptake of polymerized siRNA (poly-siRNA)/polyethylenimine (PEI) complexes for efficient gene silencing, J. Control. Release, 141 (2010) 339-346.

[48] M. Harada-Shiba, K. Yamauchi, A. Harada, I. Takamisawa, K. Shimokado, K. Kataoka, Polyion complex micelles as vectors in gene therapy – pharmacokinetics and in vivo gene transfer, Gene Ther., 9 (2002) 407-414.

[49] V. Filipe, A. Hawe, W. Jiskoot, Critical evaluation of nanoparticle tracking analysis (NTA) by Nanosight for the measurement of nanoparticles and protein aggregates, Pharm. Res., 27 (2010) 796-810.

[50] C. Troiber, J.C. Kasper, S. Milani, M. Scheible, I. Martin, F. Schaubhut, S. Küchler, J. Rädler, F.C. Simmel, W. Friess, E. Wagner, Comparison of four different particle sizing methods for siRNA polyplex characterization, Eur. J. Pharm. Biopharm., 84 (2013) 255-264.

[51] R.J. Christie, K. Miyata, Y. Matsumoto, T. Nomoto, D. Menasco, T.C. Lai, M. Pennisi, K. Osada, S. Fukushima, N. Nishiyama, Y. Yamasaki, K. Kataoka, Effect of polymer structure on micelles formed between siRNA and cationic block copolymer comprising thiols and amidines, Biomacromolecules, 12 (2011) 3174-3185.

[52] X. Zhao, H. Li, R.J. Lee, Targeted drug delivery via folate receptors, Expert Opin. Drug Deliv., 5 (2008) 309-319.

[53] M.A. Mintzer, E.E. Simanek, Nonviral vectors for gene delivery, Chem. Rev., 109 (2008) 259-302.

[54] M.A.E.M. Aa, U.S. Huth, S.Y. Häfele, R. Schubert, R.S. Oosting, E. Mastrobattista, W.E. Hennink, R. Peschka-Süss, G.A. Koning, D.J.A. Crommelin, Cellular uptake of cationic polymer-DNA complexes via caveolae plays a pivotal role in gene transfection in COS-7 cells, Pharm. Res., 24 (2007) 1590-1598.

[55] Z. Yang, G. Sahay, S. Sriadibhatla, A.V. Kabanov, Amphiphilic block copolymers enhance cellular uptake and nuclear entry of polyplex-delivered DNA, Bioconjug. Chem., 19 (2008) 1987-1994.

[56] D. Vercauteren, J. Rejman, T.F. Martens, J. Demeester, S.C. De Smedt, K. Braeckmans, On the cellular processing of non-viral nanomedicines for nucleic acid delivery: Mechanisms and methods, J. Control. Release, 161 (2012) 566-581.

[57] M. Meyer, A. Philipp, R. Oskuee, C. Schmidt, E. Wagner, Breathing life into polycations: Functionalization with pH-responsive endosomolytic peptides and polyethylene glycol enables siRNA delivery, J. Am. Chem. Soc., 130 (2008) 3272-3273.

[58] M. Meyer, C. Dohmen, A. Philipp, D. Kiener, G. Maiwald, C. Scheu, M. Ogris, E. Wagner, Synthesis and biological evaluation of a bioresponsive and endosomolytic siRNA−polymer conjugate, Mol. Pharmaceutics, 6 (2009) 752-762.

[59] S.S. Yu, C.M. Lau, W.J. Barham, H.M. Onishko, C.E. Nelson, H. Li, C.A. Smith, F.E. Yull, C.L. Duvall, T.D. Giorgio, Macrophage-specific RNA interference targeting via “Click”, mannosylated polymeric micelles, Mol. Pharmaceutics, 10 (2013) 975-987.

APPENDIX A

SUPPORTING INFORMATION

Supporting figures

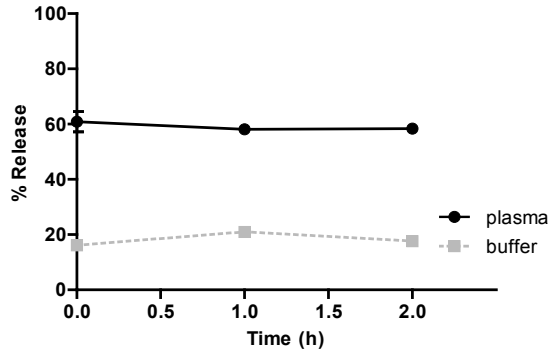

Figure S1. Time dependent siRNA released from decationized pHP-PEG-FA polyplexes when incubated in human plasma or 20 mM HEPES buffer pH 7.4, as measured by FCS. Results are expressed as mean±SD (n=3).

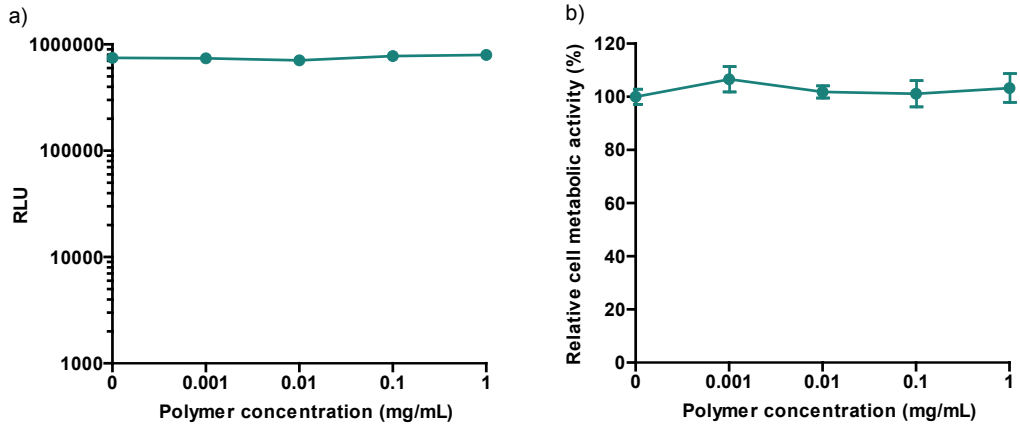

Figure S2. Luciferase expression (a) and relative metabolic activity determined by XTT (b) of Skov3-luc cells upon treatment decationized pHP-PEG-FA polymer at different concentrations. XTT results were normalized to buffer treated samples. Results are expressed as mean±SD (n=5).

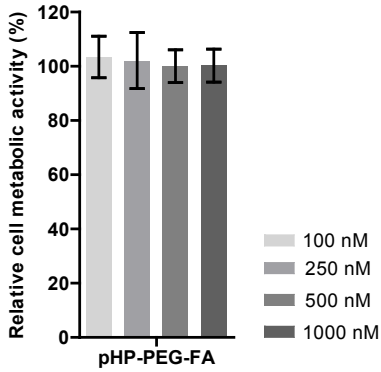

Figure S3. Relative metabolic activity determined by XTT of Skov3-luc cells upon treatment decationized pHP-PEG-FA polyplexes at different concentrations. Results were normalized to buffer treated samples. Results are expressed as mean±SD (n=5).

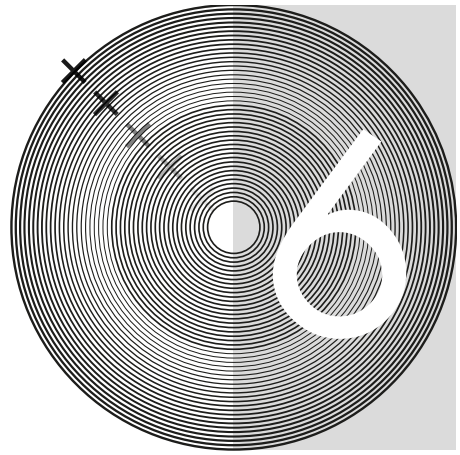

CHAPTER

Development and evaluation of strategies for targeted decationized polyplexes with endosomal escaping functionalities

Luís Novo, Yang Shi, Enrico Mastrobattista, Cornelus F. van Nostrum, Wim E. Hennink*

Abstract

Decationized polyplexes have demonstrated their potential as polymeric vectors for DNA delivery. These systems consist of a core of disulfide crosslinked poly(hydroxypropyl methacrylamide) (pHPMA) stably entrapping plasmid DNA (pDNA) and a shell of poly(ethylene glycol) (PEG). Decationized polyplexes are based on neutral hydrophilic polymers and have demonstrated important features among which an excellent safety profile and intracellular triggered release pDNA. Moreover when these polyplexes were decorated with folic acid (FA) as targeting ligand on the PEG shell, cell specific uptake and transfection was achieved, and finally, they showed improved *in vivo* blood circulation half-life and tumor accumulation upon systemic administration. Nevertheless, *in vitro* studies have shown that decationized polyplexes require further optimization, since they possess low transfection activity, most likely due to lack of endosomal escaping ability. In this chapter, 2 different strategies to introduce endosomal escaping functionalities aiming for improvement of the transfection efficiency were evaluated. The first strategy encompasses incorporation of imidazole groups that have buffering capacity at endosomal pH. The second approach comprises the functionalization of decationized polyplexes with the endosomolytic peptide INF7. From *in vitro* transfection studies we however concluded that unfortunately both strategies did not lead to significant improvements of their transfection activity. Evaluation of the cytotoxicity of the functionalized decationized polyplexes demonstrated that both strategies do not introduce significant changes in the excellent safety profile. Further studies to determine the optimal polymer architecture are therefore necessary to exploit the full transfection potential of decationzed polyplexes.

KEYWORDS gene delivery, polymer, targeting, nanoparticle, endosomal escape

1. INTRODUCTION

Decationized polyplexes have been developed to overcome some of the major issues related to conventional polycationic vectors for gene delivery. A major challenge of polycationic vectors has been the accomplishment of long blood circulation and the desired biodistribution for effective targeted delivery.

Incorporation of PEG into polycation-based systems effectively avoids the unwanted formation of aggregates and reduces protein binding *in vivo*, which leads to improved circulation kinetics and tumor accumulation [1-3]. However, formation of pDNA/polycation particles requires an excess of polycations, meaning that in the formulations some free polymer is present, and additionally, PEG shielding is not sufficient to completely avoid unspecific cell binding in highly vascularized organs and consequent suboptimal *in vivo* biodistribution and blood circulation half-lives [4, 5]. Another hurdle arises from polycation inherent toxicity by compromising the cell physically and inducing critical changes at the biomolecular level [6-8].

Decationized polyplexes [9, 10], unlike conventional polycationic systems, are based on neutral hydrophilic polymers. Structurally they consist of a core of disulfide-crosslinked pHPMA, in which pDNA is entrapped, and a PEG shell, which can be decorated with targeting ligands. The innovation of this system relies on the transient presence of cationic charge to complex DNA for the formation of polyplexes. When polyplexes are stabilized by interchain disulfide crosslinking, the cationic groups are subsequently removed by hydrolysis ('decationization'), and the neutral polymer based vector is formed. The interchain disulfide crosslinking strategy to stabilize the polyplex structure provides an intracellularly triggered release mechanism for the entrapped pDNA. This mechanism relies on the fact that disulfide crosslinks are stable in the bloodstream, avoiding unwanted premature disassembly of the polyplexes in the circulation, but can be rapidly cleaved in the intracellular reducing environment [11-13]. Decationized polyplexes have demonstrated unique features, when compared to their cationic precursors. As shown in this thesis, the systems showed excellent safety profile (chapters 2, 3 and 4), cell specific uptake and transfection when decorated with folate as targeting ligand on the PEG shell (chapter 3), and finally showed improved *in vivo* blood circulation half-life and tumor accumulation upon systemic administration (chapter 4).

Even though the advantages of decationized polyplexes are obvious, both untargeted and folate targeted decationized polyplexes possess low transfection efficiency *in vitro* [9, 10] and required the use of chloroquine, a well-known agent to promote endosomal escape of non-viral delivery systems [14, 15], to induce noticeable transfection. Endosomal escape is particularly critical for effective transfection, because upon cellular uptake polyplexes can be trapped in the endosomes and need to be released into the cytoplasm before lysosomal digestion occurs or before the transfection cargo is being disposed of by the cells via

exocytosis [16-20].

One proposed mechanism for endosomal release of polyplexes is the “proton sponge effect” [21]. Proton sponge is achieved when polymers that are used for the formation of polyplexes, possess buffering capacity within the pH endosome pH that ranges from pH 7 to 5. Polymers with buffering capacity become strongly protonated in endosomes when the pH drops from 7 to 5 which is accompanied with the influx of chloride anions increasing the ion concentration in the endosome. Consequently, due to osmotic pressure, water influx occurs resulting in rupture of the endosome [21, 22]. The proton sponge hypothesis is however still controversial [7] or may not be generally applicable [23]. But it should be mentioned that transfection activity is often observed for polymeric vectors that have buffering capacity in the pH range mentioned above [24]. An interesting design to introduce buffering capacity in decationized polyplexes is the corporation of histidine or histidine-like groups in the polyplexes. The imidazole ring of histidine is a weak base with pKa of 6-6.5 and introduction of imidazole functionalities in polyplexes can potentially introduce buffering capacity within the endosomal pH range while being close to neutral at physiological pH [25, 26]. Indeed, several studies have shown that introduction of histidine or imidazole functional groups into polymeric vectors significantly improve their endosomal buffering capacity as well as the efficiency of endosomal escape and transfection activity while having reduced cytotoxicity [26-29].

Another approach to improve endosomal escape comprises the use of endosomolytic peptides. Several peptides have been identified as capable of improving polyplex endosomal escape ability such histidine-rich variant of HA-2 (H5WYG) and other histidine rich peptides, the pH-responsive KALA peptide, the bee venom derived peptide (melittin), or the sHGP peptide derived from the endodomain of HIV gp41 [28, 30-32]. Particularly, the N-terminal segment of the HA-2 subunit of the haemagglutinin of the influenza virus, the INF7 peptide, is potentially suitable to functionalize the decationized polyplexes without significantly changing the safety profile of decationized polyplexes. The INF7 acidic peptide, is especially interesting because is highly lytic at endosomal pH (pH 5.5) but not at physiological pH (pH 7.4) [33]. Furthermore, modification of polymeric vectors with INF7 has demonstrated result in improved transfection efficiency [34-36].

The main goal of this study was to improve the transfection activity of folate targeted decationzed polyplexes. We evaluated the introduction of functionalities

for improved endosomal escape by incorporation of imidazole groups and the INF7 peptide in decationized polyplexes.

2. MATERIALS AND METHODS

2.1. Materials

Carbonic acid 2-dimethylamino-ethyl ester 1-methyl-2-(2-methacryloylamino)-ethyl ester (HPMA–DMAE) and *N*-[2-(2-pyridyldithio)]ethyl methacrylamide (PDTEMA) were synthesized as previously described [9]. pCMV_Luc plasmid, encoding for firefly luciferase, with human cytomegalovirus promoter (CMV), was amplified with competent *E. coli* DH5α and purified with NucleoBond® (Macherey-Nagel, Bioke, Leiden, The Netherlands). pCMV_Luc was purchased from the Plasmid Factory (Bielefeld, Germany). Agarose Multi-purpose was purchased from Roche Molecular Biochemicals (Mannheim, Germany). Exgen 500 (22 kDa, l-PEI) and 6× DNA Loading Dye were purchased from Fermentas (St. Leon-Roth, Germany). Folate free RPMI-1640 medium and dialyzed fetal bovine serum (FBS) were purchased from Life Technologies (Breda, The Netherlands). KB cells (Mouth epidermal carcinoma cells) were obtained from the American Type Culture Collection (ATCC) (Maryland, USA). Luciferase assay kit was obtained from Promega (Leiden, The Netherlands). Micro BCA Protein Assay kits was purchased from Thermo Fisher Scientific (Etten-Leur, The Netherlands). All other chemicals, reagents and media were obtained from Sigma-Aldrich (Zwijndrecht, The Netherlands).

The following buffer systems were used: 4-(2-hydroxyethyl)-1-piperazineethanesulfonic acid (HEPES) for buffering at pH 6.8–8.2; 3-[[1,3-dihydroxy-2-(hydroxymethyl)propan-2-yl]amino]propane-1-sulfonic acid (TAPS) for buffering solutions at pH 7.7-9.1.

Influenza peptide (INF7, sequence GLFEAIEGFIENGWEGMIDGWYGC) was synthesized by Genescript (Piscataway, USA). Cysteine-modified melittin peptide (Mel) (CIGA VLKV LTTG LPAL ISWI KRKR QQ, all-(D) configuration [37]) was also synthesized by Genscript, (Piscataway, USA).

2.2. Monomer synthesis

2.2.1. Synthesis of N-(2-(1H-imidazol-4-yl)ethyl)methacrylamide (abbreviated as Histamine methacrylamide, HisMA)

Histamine dihydrochloride (3.312 g, 18 mmol, 1 eq) was dissolved in 7.2 mL 5 M NaOH (2 eq) aqueous solution in a 3-necked round bottomed flask. Subsequently 7.2 mL DCM was added to the flask to yield a two phase system and 5 mg hydroquinone monomethylether was added to prevent premature polymerization. This 2 phase system was cooled to 0 ºC and, while under vigorous stirring, 7.2 mL of 2.5 M methacryloyl chloride solution in DCM (1.76 mL, 18 mmol, 1 eq) and 7.2 mL of 2.5 M NaOH were simultaneously added in order to keep the aqueous phase at pH 8-10 (Scheme 1). The methacryloyl chloride and NaOH solutions were added dropwise over a period of 30 min. Next, the reaction mixture was stirred overnight at room temperature. Afterwards, the crude product, present at the interphase of the water/DCM phases, was collected by decantation, dissolved in methanol and dried over $MgSO_4$. Subsequently, $MgSO_4$ was removed by filtration and the solvent was removed by rotary evaporation.

The obtained crude product (2.19 g) was purified by flash column chromatography (VersaPak® Silica Cartridge 40×75 mm) as follows. The crude product was dissolved in 5 mL acetone/methanol 90/10 (v/v) and then applied onto the column (pre-equilibrated with the same eluent). The purification was performed by isocratic elution using acetone/methanol 90/10 (v/v) as eluent. The fractions containing HisMA and HisMA with some traces of impurities (monitored by TLC) were pooled and the solvent was removed by rotary evaporation. Further purification was done by recrystallization in acetone; the product was dissolved in a minimal volume of warm acetone and the solution was cooled to -20 ºC, resulting in crystallization of HisMA. The solvent containing impurities was discarded and the product was washed with cold acetone. After removal of the traces of acetone, white crystals where obtained. (Yield: 1.050 g, 5.84 mmol, 32%). The identity of HisMA was assessed by NMR analysis: ^{1}H NMR (400 MHz, MeOD-d4): δ (ppm) 1.92 (s, 3H), 2.82 (t, 2H), 3.48 (t, 2H), 5.36 (s, 1H), 5.67 (s, 1H), 6.86 (m, 1H), 7.60 (s, 1H).

2.2. Polymer synthesis

2.2.1. Synthesis of (FA-PEG)$_2$-ABCPA

The synthesis and characterization of the FA-PEG (M_w 5000 Da) bi-functionalized 4,4′-azobis(4-cyanovaleric acid) (ABCPA) ((FA-PEG)$_2$-ABCPA) macronitiator was performed as previously described [10].

2.2.2. Synthesis of pHDP-PEG-FA

p(HPMA–DMAE-co-PDTEMA)-b-PEG-FA (pHDP-PEG-FA) was synthesized by free radical polymerization using (FA-PEG)$_2$-ABCPA as macroinitiator (Scheme 2a). The polymer was synthesized using a monomer-to-initiator ratio (M/I) of 220 (mol/mol) and a feed ratio HPMA–DMAE/PDTEMA of 1/0.2 (mol/mol). The polymerization was carried at 70 ºC for 24 h in DMSO under an N_2 atmosphere, using 2.5 µmol macroinitiator and a monomer concentration of 0.8 M. After polymerization, the product was precipitated in diethyl ether and collected by centrifugation. Next, the pellet was dried from remaining ether in a vaccum oven overnight, dissolved in 5 mM NH_4Ac buffer pH 5.0, dialyzed against the same buffer for 3 days at 4 °C (MWCO 6000-8000) and collected by freeze-drying. Unreacted FA-PEG present in the product was removed by precipitation in cold EtOH (5 mg/mL of solids) followed by centrifugation. The pHDP-PEG-FA soluble in the EtOH supernatant was collected after EtOH evaporation, dissolution in water and freeze-drying.

2.2.3. Synthesis of pHDP-His-PEG-FA

p(HPMA–DMAE-co-PDTEMA-co-HisMA)-b-PEG-FA (pHDP-His-PEG-FA) was also synthesized using the (FA-PEG)$_2$-ABCPA macroinitiator (Scheme 2b). The polymer was synthesized using an M/I of 240 (mol/mol), and a feed ratio HPMA–DMAE/PDTEMA/HisMA of 1/0.2/0.2 (mol/mol). Polymerization conditions and purification were as described in section 2.2.2 for pHDP-PEG-FA.

2.2.4. Synthesis of pHis

Poly(histamine methacrylamide) (abbreviated as pHis) was synthesized by free radical polymerization using azobisisobutyronitrile (AIBN) as initiator (Scheme 2c).

The polymer was synthesized using 2.5 μmol AIBN, monomer concentration of 1 M and M/I of 100 (mol/mol). The polymerization was carried at 70 ºC for 24 h in 2 mL DMSO under an N_2 atmosphere. The polymer was purified by dialysis against acetic acid solution pH ~4 for 3 days at 4 °C (MWCO 6000-8000) and collected by freeze-drying.

2.2.5. Synthesis of pHDP-INF7-PEG-FA

p(HPMA–DMAE-co-PDTEMA-co-INF7)-b-PEG-FA (pHP-INF7-PEG-FA) was prepared by dissolving 3.5 mg of p(HPMA–DMAE-co-PDTEMA)-b-PEG-FA (1 μmol pyridyl disulfide (PDS) groups) in 400 μL N_2 purged DMF containing 1 μmol triethylamine. Next, 1.3 mg INF7-SH peptide (Mw 2694 g/mol; 0.5 μmol) dissolved in 2 mL N_2 purged DMF was slowly added to the polymer solution. The reaction was monitored for 6 h using UV spectroscopy by determining the relative UV absorbance at 343 nm of the released 2-mercaptopyridine from the reacted PDS groups via thiol-disulfide exchange reaction with the thiol group of the terminal cysteine of the INF7 peptide [38]. pHP-INF7-PEG-FA was purified by dialysis against 5 mM NH_4Ac buffer pH 5.0 for 3 days at 4 °C (MWCO 25000) and collected by freeze-drying.

2.3. Polymer characterization

2.3.1. Gel permeation chromatography (GPC) characterization of the polymers

The polymers (pHDP-PEG-FA, pHDP-His-PEG-FA and pHDP-INF7-PEG-FA) were analyzed by GPC using a Waters System (Waters Associates Inc., Milford, MA) with refractive index (RI) and UV detection using two serial Plgel 5 μm MIXED-D columns (Polymer Laboratories) and DMF containing 10 mM LiCl as eluent. The flow rate was 1 mL/min and the temperature was 60 °C. UV detection at 363 nm for FA and 280 nm for PDS groups and INF7 peptide was used. The number average molecular weight (M_n), weight average molecular weight (M_w) and polydispersity index (PDI, M_w/M_n) of pHDP-PEG-FA, pHDP-His-PEG-FA and pHDP-INF7-PEG-FA were determined using a series of PEG calibration standards.

pHis was analyzed by Viscotek-GPCmax (Viscotek, Oss, The Netherlands) light scattering/viscosimetric detection system using two Ultrahydrogel 1000 7.8×300 mm in series with Ultrahydrogel 6×40 guard column and 0.3 M NaAc pH 4.4 as

eluent as previously described [10, 39]. The flow rate was 0.7 mL/min and the temperature was 30 °C. OmniSEC software was used to calculate M_n, M_w and PDI by integrating data from RI, viscosity detector and laser photometer (λ = 670 nm) (right (90°) and low (7°) angle light scattering). PEO (M_n=18.1 kDa, M_w=18.9 kDa, Malvern (Worcestershire, UK)) was used for calibration.

2.3.2. ^{1}H NMR characterization of the polymers

The compositions of pHDP-PEG-FA and pHDP-His-PEG-FA as well their M_n's were determined by ^{1}H NMR in DMSO-d6. NMR spectra were recorded on a 400 MHz Agilent 400-MR NMR spectrometer (Agilent Technologies, Santa Clara, USA). The ratio HPMA–DMAE/PDTEMA/HisMA incorporated in the polymer was determined by comparison of the integrals at δ 4.6 ppm (bs, $CH_2C\underline{H}CH_3O$, HPMA–DMAE), the integral at δ8.5 ppm (bs, pyridyl group proton, PDTEMA) and the integral at δ6.8 (bs, imidazole group proton, HisMA) (∫δ4.6/∫δ8.5/δ6.8).

The number average molecular weight (M_n) of pHDP-PEG-FA and pHDP-His-PEG-FA was determined according to equation (1):

$$M_n = (\int\delta 4.6 \times M_{HPMA–DMAE} + \int\delta 8.5 \times M_{PDTEMA} + \int\delta 6.8 \times M_{HisMA})/(\int\delta 3.5/448) + 5441.4 \text{ (g/mol)} \quad (1)$$

where, ∫δ3.5, ∫δ4.6, ∫δ8.5 and ∫δ6.8 are the integrals at 3.5, 4.6, 8.5 and 6.8 ppm, respectively. $M_{HPMA–DMAE}$, M_{PDTEMA} and M_{HisMA} are the molar masses of HPMA–DMAE, PDTEMA and HisMA, respectively. The number of protons for the FA-PEG_{5000} block (M_n 5441.4 g/mol) (∫δ3.5) was set at 448.

2.3.3. UV spectroscopic characterization of the polymers

The quantification of the molarity of thiol reactive PDS groups per weight of pHDP-PEG-FA pHDP-His-PEG-FA and pHDP-INF7-PEG-FA was performed by UV spectroscopy using a Shimadzu UV-2450 UV/VIS spectrophotometer (‘s-Hertogenbosch, The Netherlands). Stock solutions of polymer of 1 mg/mL in 20 mM HEPES pH 7.4 also containing 50 mM tris(2-carboxyethyl)phosphine (TCEP) were prepared. After incubation for 1 h at 37 ºC the UV absorbance of the formed 2-mercaptopyridine was measured at 343 nm [38]. Quantification was performed using a calibration curve of 2-mercaptopyridine standards.

2.3.4. Polymer acid-base titration

The buffering capacity of the HisMA containing polymers was determined by acid-base titration. pHis and pHDP-His-PEG-FA were dissolved in 5 mL 150 mM NaCl aqueous solution to a final 10 mM His concentration. The pH of the solution was lowered to 2.0 with 1 M HCl. Next, the solution was titrated by stepwise addition with 10 µL of 0.1 M NaOH under continuous stirring. After each addition the pH of the solution was measured till the pH was 12.

The buffering capacity (BC) of gene delivery polymers is normally defined as the percentage of amine groups that become protonated when the pH drops pH 7.4 to 5.0. From the acid-base titration curves BC was calculated as previously described [40], from equation (2)

$$BC = \frac{\Delta n_{NaOH}}{n_N} \times 100\ (\%) \qquad (2)$$

where, Δ_{NaOH} is the number of moles of added of NaOH required to bring the solution from pH 5.0 to pH 7.4 and n_N is the total number of moles of protonable amines in the polymer.

2.4. Polyplex preparation

2.4.1. pHis based polyplexes

Polymer solutions of pHis (70 µL) were added to 140 µL pDNA solution in 20 mM HEPES pH 5.5 and immediately vortexed. Polyplexes were prepared at His/P ratio (His, molarity of HisMA groups from polymer; P, molarity of negatively charged phosphates from pDNA) from 1 to 16. For example, to prepare polyplexes with His/P ratio of 2 and final pDNA concentration of 50 µg/mL, 0.24 mg/mL pHis solution was mixed with 75 µg/mL pDNA solution. When desired, the pH of the solutions was adjusted to pH 7.4 by addition of 1 M NaOH and the ionic strength was adjusted to 150 mM using 1.5 M NaCl.

2.4.2. pHDP-PEG-FA, pHDP-His-PEG-FA and pHDP-INF7-PEG-FA based decationized polyplexes

The preparation of decationized polyplexes was done according to the method previously described (Scheme 3) [9, 10]. Briefly, to prepare polyplexes with N/P ratio 4 (N, molarity of protonable amines of the polymer from HPMA–DMAE; P, molarity

of negatively charged phosphates from pDNA) and final pDNA concentration of 50 µg/mL, 70 µL of polymer solutions of pHDP-PEG-FA (0.93 mg/mL), pHDP-His-PEG-FA (0.97 mg/mL) or pHDP-INF7-PEG-FA (1.45 mg/mL) were mixed by vortexing with 140 µL pDNA solution (75 µg/mL) in 10 mM HEPES also containing 10 mM TAPS pH 8.5 at room temperature. After complexation, interchain disulfide crosslinking of the polyplexes was induced by addition of the dithiol 3,6-dioxa-1,8-octane-dithiol (DODT) at a molar equivalent of DODT thiol groups to PDS groups of the polymer. Polyplex dispersions were incubated for 1 h at pH 8.5. After the crosslinking step, the cationic dimethylaminoethanol (DMAE) side groups were removed by hydrolysis at 37 °C and pH 8.5 for 6 h [9], resulting in pHP-PEG-FA, pHP-His-PEG-FA or pHDP-INF7-PEG-FA decationized polyplexes, derived from the cationic precursors pHDP-PEG-FA, pHDP-His-PEG-FA and pHDP-INF7-PEG-FA, respectively. Next, the pH of the dispersions was adjusted with 1M HCl to pH 7.4 and the ionic strength was adjusted to 150 mM with NaCl.

2.4.3. pHDP-PEG-FA/pHis based decationized polyplexes

Decationized polyplexes based on blends of the block copolymer pHDP-PEG-FA and pHis were prepared essentially as described for decationized polyplexes based on pHDP-PEG-FA only, with some small changes. To prepare polyplexes with an N/(His)/P ratio of 4/2, 70 µL of polymer solution of a mixture of pHDP-PEG-FA (0.93 mg/mL) and pHis (0.24 mg/mL) was mixed by vortexing with 140 µL pDNA solution in 10 mM HEPES also containing 10 mM TAPS pH 5.5 at room temperature. After complexation, DODT was added to the polyplex dispersion and the pH was raised to pH 7.1 with 1 M NaOH and the dispersions were incubated for 1 h to allow polyplex crosslinking. Next, the pH was raised to pH 8.5 with 1 M NaOH and decationization procedure was performed as described in section 2.4.2 to yield pHP-PEG-FA/pHis decationized polyplexes.

2.5. Polyplex characterization

2.5.1. Size determination

The size of the polyplexes was measured by dynamic light scattering (DLS) using an ALV CGS-3 system (Malvern Instruments, Malvern, UK) equipped with a JDS Uniphase 22 mW He-Ne laser operating at 632.8 nm, an optical fiber-based

detector, a digital LV/LSE-5003 correlator with temperature controller set at 25 °C. Measurements were performed in buffers containing 150 mM NaCl (20 mM HEPES at pH 5.5 or 7.4) at a final pDNA polyplex concentration of 20 µg/mL.

2.5.2. Zeta potential determination

Zeta potential of the polyplexes was determined using a Malvern Zetasizer Nano-Z (Malvern Instruments, Malvern, UK) with universal ZEN 1002 'dip' cells and DTS (Nano) software (version 4.20) at 25 °C. Zeta-potential measurements were performed in 20 mM HEPES at pH 5.5 or 7.4 at a final pDNA polyplex concentration of 20 µg/mL.

2.5.3. Gel Retardation Assay

Polyplex dispersions (20 µL) in HEPES buffered saline (HBS; 20 mM HEPES, 130 mM NaCl, pH 7.4) (at 20 µg/mL polyplex pDNA concentration) were mixed with 4 µL 6× DNA Loading Dye and loaded into 0.8% agarose gel in Tris-acetate-EDTA (TAE) buffer pH 8 containing 0.5 µg/mL ethidium bromide and run at 120 V for 50 min. pDNA was detected using a Gel Doc™ XR+ system (BioRad Laboratories Inc., Hercules, CA) with Image Lab software.

2.6. Cell culture

Human mouth epidermal carcinoma KB cells (folate receptor overexpressing cell line) were cultured in Minimum Essential Medium (MEM) supplemented with 10% FBS (Sigma-Aldrich) and antibiotics/antimycotics (penicillin, streptomycin sulphate, amphotericin B). Cells were maintained at 37 °C in a 5 % CO_2 humidified air atmosphere.

2.7. *In vitro* transfection

The transfection efficiency of the different polyplex formulations was determined by luciferase assay following the protocol and recommendations of van Gaal et al. [41]. KB cells were seeded into 96-well plates at a density of 10,000 cells per well 24 h prior to transfection. Before transfection, cell culture medium was replaced by

100 µL folate-free RPMI 1640 supplemented with 12.5 % dialyzed FBS. Polyplex formulations of 25 µL containing 0.25 µg (10 µg/mL), 1 µg (40 µg/mL) or 3 µg (120 µg/mL) of pDNA were added to the cells. Polyplexes based on Exgen 500 at 10 µg/mL and N/P=6, prepared according to the manufacturer's protocol, were used as positive control for transfection [41]. After 24 h incubation at 37 °C, 5% CO_2 in a humidified atmosphere, the medium was replaced by MEM with 10% FBS and incubated for additional 24 h.

Luciferase expression was measured 48 h after transfection. In short, medium was removed and the cells were washed with 100 µL of cold phosphate buffered saline (PBS). Next, using 50 µL of Reporter Lysis Buffer (Promega), the cells were lysed by a freeze-thaw cycle after keeping the cells 1 h at -80 °C. The luminescence was measured by mixing 10 µL of cell lysate with 50 µL of Luciferase Assay Reagent (Promega) and detecting luminescence for 10 sec, 2 sec after addition of assay reagent. Measurements were performed using a FLUOstar OPTIMA microplate, equipped with a luminescence light guide (BMG LabTech, Germany). The concentration of protein in the lysates was determined by the Micro BCA Protein Assay Reagent Kit (Thermo Fisher Scientific) to normalize luciferase activity as relative light units (RLU) per mg total cellular protein.

2.8. *In vitro* toxicity

Possible cytotoxicity of the polyplexes was analyzed using the XTT assay which determines the cellular metabolic activity. The XTT assay was performed in parallel with transfection experiments using essentially the same protocol as described in section 2.7. As positive control for toxicity polyplexes based on branched polyethyleneimine (b-PEI 25 kDa) were used [8, 42] at 10, 40 and 120 µg/mL and N/P=6 and prepared as previously described [43]. Forty eight h after transfection, 50 µL of a freshly prepared XTT solution (25 µM *N*-methyl dibenzopyrazine methylsulfate (PMS) and 1 mg/mL 2,3-bis(2-methoxy-4-nitro-5-sulfophenyl)-2H-tetrazolium-5-carboxanilide (XTT) in plain RPMI 1640 medium) was added to 100 µL cell medium in each well. The cells were subsequently incubated for 1 h at 37 °C in a 5 % CO_2 humidified air atmosphere. Next, absorbance was measured at 490 nm with a reference wavelength of 655 nm. Cell viability is expressed as relative metabolic activity normalized against buffer treated cells.

3. RESULTS AND DISCUSSION

3.1. Synthesis of His containing polymers

To obtain polymers with imidazole functional groups via free radical polymerization, HisMA, a methacrylamide monomer, was synthesized. The reaction route consisted of the methacrylation of histamine in a two-phase system of chloroform and an aqueous solution of NaOH (Scheme 1). The product was obtained in a yield of 32 % and very good purity as evidenced from the ^{1}H NMR spectrum (Figure 1).

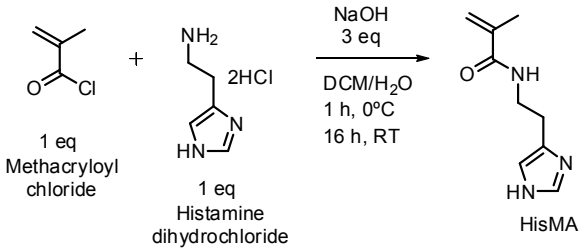

Scheme 1. Synthesis of HisMA from the reaction between methacryloyl chloride and histamine in a two-phase system.

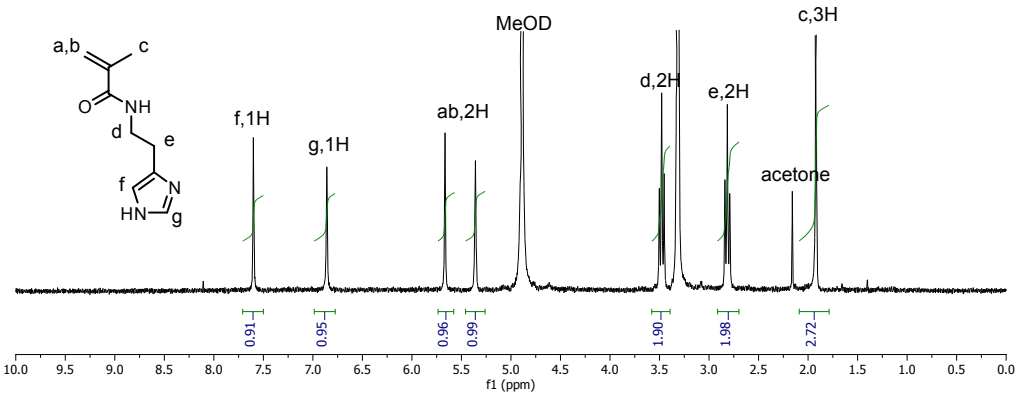

Figure 1. ^{1}H NMR spectrum of HisMA in MeOD-d4.

The folic acid functionalized polymer p(HPMA–DMAE-co-PDTEMA)-b-PEG-FA (pHDP-PEG-FA) was synthesized by free radical copolymerization of HPMA–

DMAE with PDTEMA using the FA-PEG_{5000} bi-functionalized azo macroinitiator, $(FA-PEG)_2$-ABCPA, as previously described (Scheme 2a) [10]. Introduction of imidazole buffering functionality in the block copolymer was established by introducing HisMA in the co-polymerization mixture to yield p(HPMA–DMAE-co-PDTEMA-co-HisMA)-b-PEG-FA (pHDP-His-PEG-FA). pHDP-PEG-FA and pHDP-His-PEG-FA polymers were obtained with a yield of 50-60%. ^{1}H NMR, GPC and UV spectroscopy were used to characterize the synthesized polymers (Table 1). The results show that the copolymer composition (HPMA–DMAE/PDTEMA 1/0.13-0.14; NMR analysis) was close to that of the feed, in agreement with earlier findings [9, 10]. It was found that the HisMA molar fraction in pHDP-His-PEG-FA was 2 times higher than that of the feed which points to a higher reactivity of this monomer than HPMA–DMAE and PDTEMA in radical polymerization. The M_n calculated by ^{1}H NMR spectroscopic analysis for pHDP-PEG-FA (46.9 kDa) was close to the determined M_n by GPC (39.4 kDa, PDI = 2.3). Also for pHDP-His-PEG-FA the M_n calculated by ^{1}H NMR (56.9 KDa) was close to that as determined by GPC (57.4 kDa, PDI = 2.2). Furthermore, UV spectroscopy showed that 276±28 nmol PDS groups per mg of pHDP-PEG-FA and 221±33 nmol/mg of PDS groups per mg of pHDP-His-PEG-FA were present in the copolymers. Poly(histamine methacrylamide) (pHis) was synthesized, using AIBN as initiator. The polymer was obtained in a 95% yield and the M_n as determined by aqueous GPC was 70.0 kDa (PDI = 1.6, dn/dc = 0.199 mL/g).

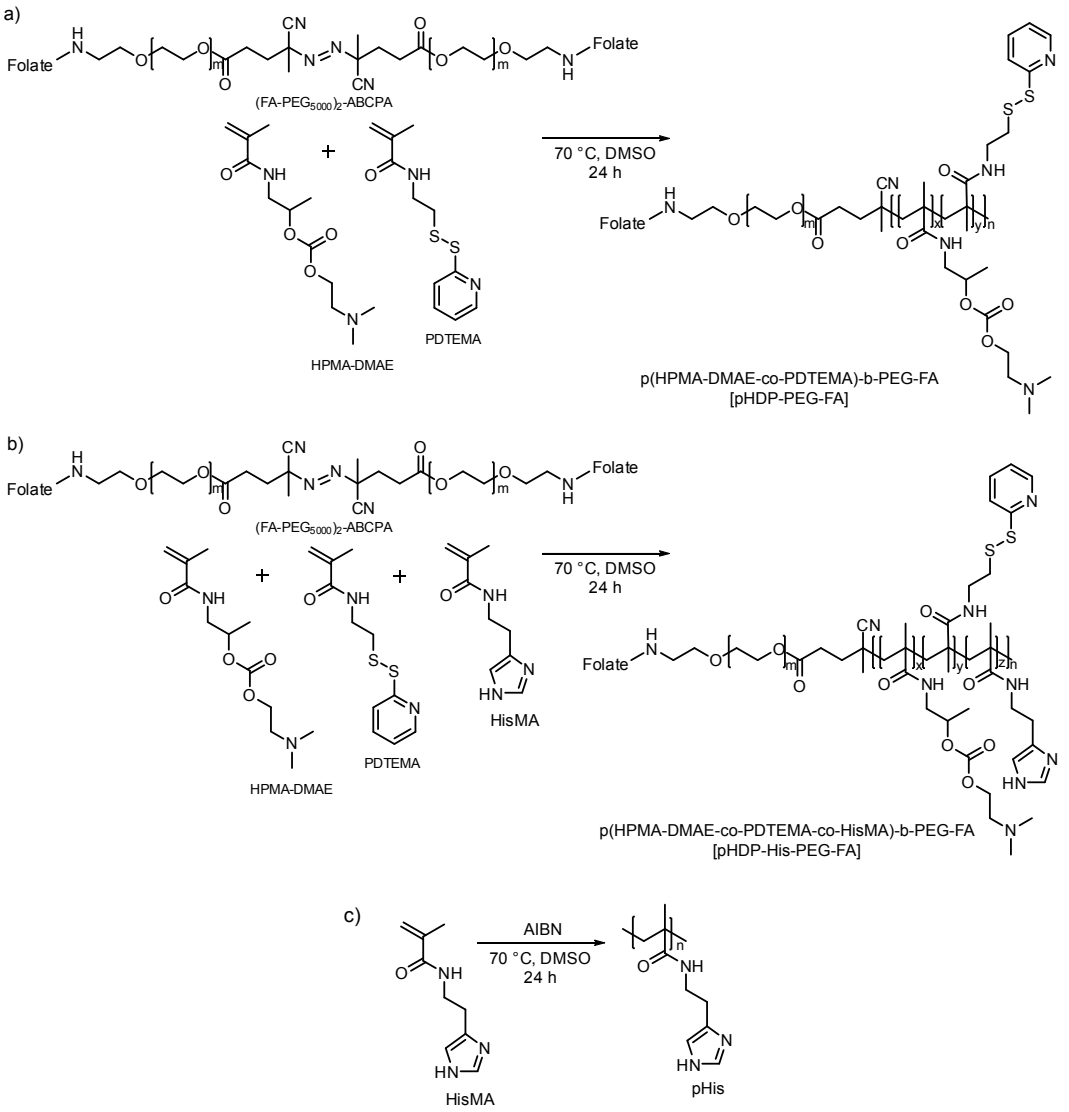

Scheme 2. Synthesis of pHDP-PEG-FA by free radical copolymerization of HPMA–DMAE and PDTEMA using $(FA\text{-}PEG_{5000})_2$-ABCPA as macroinitiator to yield (a). Synthesis of pHDP-His-PEG-FA by free radical copolymerization HPMA–DMAE, PDTEMA and HisMA using $(FA\text{-}PEG_{5000})_2$-ABCPA as macroinitiator (b). c) Free radical polymerization of HisMA using AIBN as initiator to yield pHis.

3.2. Synthesis of INF7 peptide containing polymers

FA targeted decationized polyplexes were functionalized with the endosomolytic peptide INF7 via disulfide covalent linkage to trigger endosomal escape of the

decationized polyplexes. In order to functionalize pHDP-PEG with INF7, the peptide's C-terminal cysteine was reacted with part of the PDS groups (feed ratio SH-INF7/PDS of 0.5) of pHDP-PEG-FA via thiol-disulfide exchange reaction in N_2-purged DMF using triethylamine as catalyst (Scheme 3). The reaction, performed in anhydrous DMF, was preferred over reaction in aqueous solutions to avoid hydrolysis of the labile DMAE cationic groups, since thiol-disulfide exchange reaction requires basic conditions. The kinetics of reaction was followed by detecting the release of 2-mercaptopyridine upon reaction of the PDS groups with the thiolated IN7 peptide, and it was observed that within 1 h the reaction was almost completed, with close to 50% PDS groups reacted with the peptide. Next, the polymer was purified by dialysis and characterized (Table 1). GPC analysis revealed that pHDP-INF7-PEG-FA, when compared to pHDP-PEG-FA, showed an increase in M_w from 107.8 kDa to 121.5 kDa. Also, a decrease in the molarity of PDS groups per weight of polymer from 276±28 nmol/mg of polymer to 101±17 nmol/mg of polymer was observed. Coupling INF7 peptide to approximately 50% of PDS groups of pHDP-PEG-FA led to a theoretical increase in M_n of the polymer to 61.4 kDa and resulted in a decrease to 133 nmol PDS/mg polymer, which was close to the experimental value.

Table 1. Polymer characteristics as determined by GPC, ^{1}H NMR and UV spectroscopy.

	GPC		NMR		NMR	UV
Polymer	M_w; M_n (kDa)	PDI	M_n (kDa)	Feed HPMA–DMAE/PDTEMA/HisMA	Polymer HPMA–DMAE/PDTEMA/HisMA	$nmol_{PDS}/mg_{polymer}$
pHDP-PEG-FA	107.9; 46.9	2.3	39.4	1/0.20/0	1/0.14/0	276±28
pHDP-His-PEG-FA	126.3; 57.4	2.2	56.9	1/0.2/0.2	1/0.13/0.38	221± 33
pHis	105.9; 70.0	1.5	N.A	N.A.	N.A..	N.A.
pHDP-INF7-PEG-FA	121.5; 45.0	2.7	N.A.	N.A.	N.A.	101±16

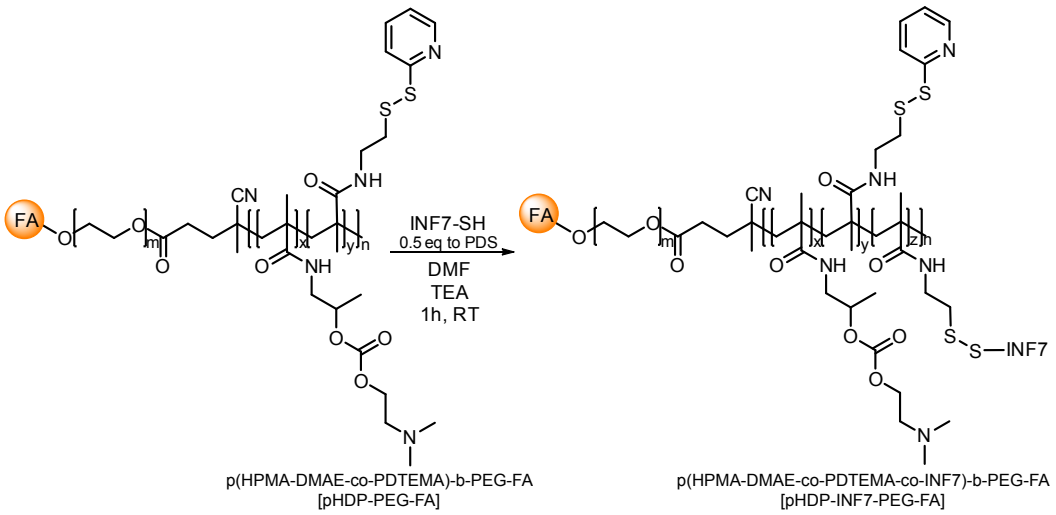

Scheme 3. Synthesis of pHDP-INF7-PEG-FA by thiol-disulfide exchange reaction between INF7-SH peptide and PDS groups of pHDP-PEG-FA.

3.3. Buffering capacity of pHis and pHDP-His-PEG-FA

It has been shown in previous publications that imidazole containing polymers have buffering capacity in the endosomal pH range (7.4-5.0) [27-29, 44, 45]. The buffering capacity was determined by acid-base titration of pHis and pHDP-His-PEG-FA (Figure 2). Figure 2a shows that the buffering capacity of the synthesized pHis between pH 7.4 and 5 was 33% and the polymer displayed a pKa of around 6.5, which in line with previously characterized imidazole functionalized polymers [26, 44]. The buffering capacity per HisMA monomer was more than 2 times higher than that of PEI [46]. The buffering capacity of the HisMA group in pHis was not significantly different from that in the block copolymer pHDP-His-PEG-FA (Figure 2b).

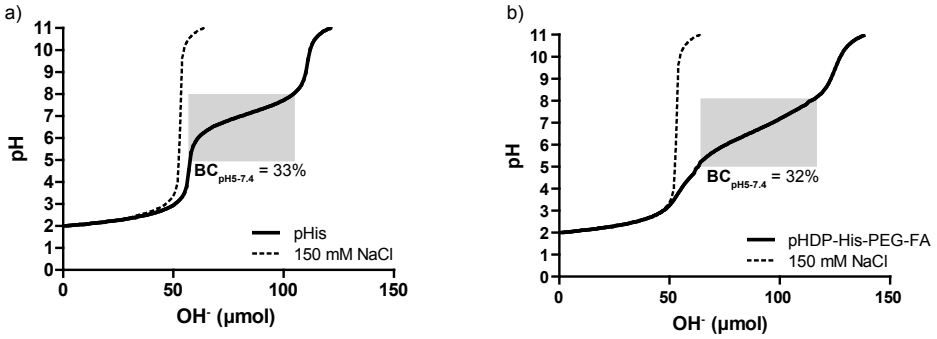

Figure 2. Acid-base titration curve of pHis (a) and pHDP-His-PEG-FA (b) (10 mM His groups) with 0.1 M NaOH in 150 mM NaCl aqueous solution.

3.4. Polyplex forming behavior of pHis

Since the pKa of pHis is around 6.5, the pDNA complexation behavior of this polymer is strongly dependent on the pH used for complexation. At pH 7.4 not only the charge density of pHis is relatively low, but also its water solubility is compromised [47]. So preparation of polyplexes based on pHis requires complexation at a pH where the charge density of the polymer is high. Therefore, the ability of pHis to form polyplexes was studied by preparing the polyplexes at pH 5.5 with variable molar ratio between HisMA and negatively charged phosphates from pDNA (His/P ratio) (Figure 3). Upon formation of the polyplexes at pH 5.5, the pH was increased to pH 7.4 and the change in the polyplex properties was determined. It was observed that small (~70 nm) positively charged polyplexes (zeta potential ~+30 mV) at pH 5.5 and at His/P of 2 were formed (Figure 3a and 3b). When the pH of polyplex dispersion was subsequently raised to pH 7.4, drastic changes in the particle properties were observed. An His/P of 8 was necessary to maintain positively charged polyplexes (+7 mV) without tendency to aggregate, however, the size of the polyplexes increased from 55 nm to 250 nm (Figure 3b). As determined by the acid-base titration (Figure 2), at pH 7.4 the polymer has a low charge density (only ~1 out of ten nitrogens of the imidazole group is protonated) which directly negatively influences the electrostatic complexation ability of this polymer, leading to particle swelling and/or aggregation at low His/P. In a gel retardation assay (Figure 3c), this is confirmed and an excess of polymer (His/P of 6) was necessary to fully retain pDNA upon incubation of polyplexes at pH 7.4 and 150 mM NaCl. It should be noticed that at lower His/P ratio (2 and 4), a high degree of retention was observed and polyplexes were still detected by DLS even though

polyplexes were negatively charged (<-20 mV). Most likely, the complexes pDNA and polymer are hold together by hydrophobic or hydrogen bond interactions which are possible when both polymer and pDNA are in close proximity [48].

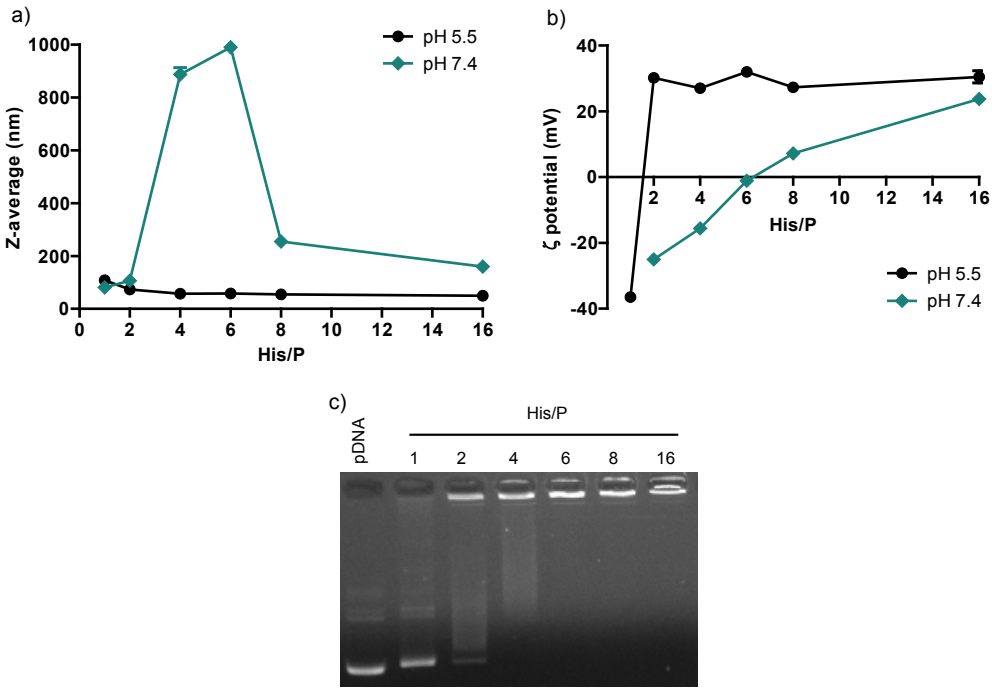

Figure 3. Complexation behavior of pHis and pDNA. Size (z-average) (a) and zeta potential (b) as function of His/P ratio of polyplexes initially prepared at pH 5.5 and measured at pH 5.5 or 7.4 (containing 150 mM NaCl for DLS measurements). Agarose gel retardation assay of pHis polyplexes prepared at pH 5.5 and run at pH 7.4 and 150 mM NaCl.

3.4. Decationized polyplex design and preparation

The main goal of our study was to improve the endosomal escape of FA targeted decationized polyplexes to result in better transfection activity, while maintaining their safety profile. Therefore, imidazole groups with buffering capacity in the endosomal pH range were introduced in the polymers and functionalization with a peptide having endosomolytic activity was investigated.

The preparation of FA targeted decationized polyplexes was done according to the previously described method [9, 10] (Scheme 4). In short, the preparation followed a 3-step process and started with electrostatic complexation between

the cationic block copolymer p(HPMA–DMAE-co-PDTEMA)-b-PEG-FA (pHDP-PEG-FA) with negatively charged pDNA at optimal N/P ratio of 4. Next, interchain disulfide crosslinking of the polyplexes was performed via thiol-disulfide exchange by addition of DODT dithiol at a molar equivalent of thiol groups from DODT and the PDS groups of the PDTEMA in the polymer block of the polyplex core. Finally, decationized (p(HPMA-co-PDTEMA)-b-PEG-FA (pHP-PEG-FA) polyplexes were obtained, by removal of the DMAE cationic groups from the pHDP-PEG-FA cationic polyplexes after hydrolysis of the carbonate ester bonds linking the DMAE groups to the pHPMA backbone at pH 8.5 for 6 h.

The preparation of decationized polyplexes using p(HPMA–DMAE-co-PDTEMA-co-His)-b-PEG-FA (pHDP-His-PEG-FA) cationic block copolymer yielded pHP-His-PEG-FA decationized polyplexes. The preparation of polyplexes at N/P of 4, occurred at a simultaneous His/P of 2.

A second approach for the incorporation of His functionalities in the decationized polyplexes consisted of the incorporation of pHis homopolymer in the core of decationized polyplexes. In order to prepare such polyplexes, pDNA was co-complexed with pHDP-PEG-FA and pHis at pH 5.5. This pH of complexation was required, as pointed out above, to ensure high charge density and water solubility of pHis. Polyplexes were prepared by addition of pHDP-PEG-FA at an N/P of 4 and pHis at a His/P ratio of 2 which is required for full complexation of pDNA at pH 5.5. After complexation, the pH was increased stepwise in the presence of DODT to crosslink the polyplexes and finally decationized to yield pHP-PEG-FA/pHis decationized polyplexes.

The preparation of decationized polyplexes functionalized with the endosomolytic peptide INF7 started with complexing pDNA and the INF7-functionalized pHDP-PEG-FA, p(HPMA–DMAE-co-PDTEMA-co-INF7)-b-PEG-FA (pHDP-INF7-PEG-FA), at N/P of 4. After complexation the dithiol, DODT, was added for interchain disulfide crosslinking, followed by the described decationization process to yield pHDP-INF7-PEG-FA decationized polyplexes. The PDS groups present as side chains in the core of the polyplexes are highly reactive with thiol groups through a disulfide exchange reaction [49-51] and sequential reaction with thiols is feasible [52]. During crosslinking equimolar conditions of crosslinker thiols and PDS groups were used, which decreases the possibility of undesired reactions with disulfides that link the INF7 peptide to the polymer backbone. The importance of disulfide bridges to link INF7 peptide to the polymers forming decationized polyplexes is related to

the fact that disulfides can be cleaved in the reductive cell environment allowing the release of the peptide intracellularly, which is essential for its endosomolytic activity. INF7 exerts its endosomolytic activity when localized intracellularly in its free form [36] and functionalization of polymeric vectors with using disulfide linkages has previously shown its usefulness in improving polyplex transfection efficiency [34, 35, 53].

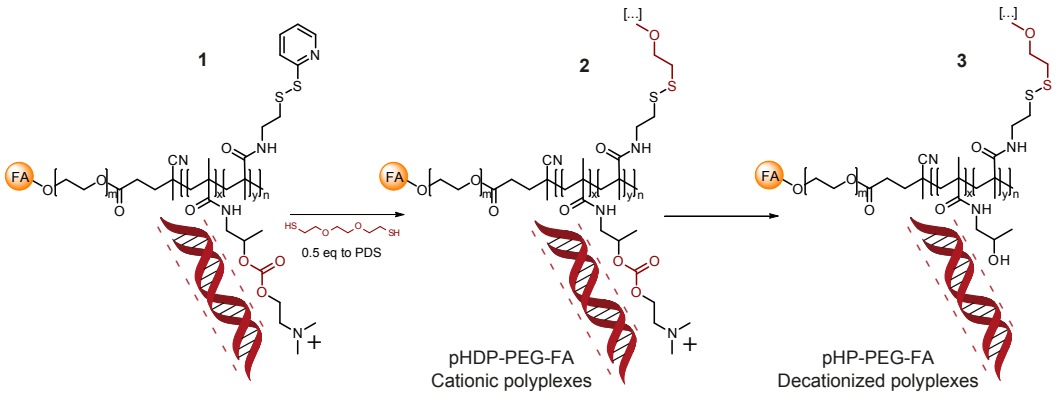

Scheme 4. General approach for the preparation of FA targeted interchain disulfide-crosslinked decationized polyplexes through a 3-step process: 1. charge-driven condensation of pHDP-PEG-FA cationic polymer with pDNA; 2. stabilization through disulfide crosslinking; 3. decationization of cationic pHDP-PEG-FA polyplexes, yielding decationized pHP-PEG-FA polyplexes (adapted from [9]).

The prepared polyplexes were evaluated for size by DLS and by zeta potential measurements (Table 2). pHP-PEG-FA decationized polyplexes prepared at an N/P of 4 showed a diameter of 139±5 nm and a zeta potential of -10±2 mV, as also previously observed [10]. The negative zeta potential of FA decorated decationized polyplexes is due to the encapsulation of negatively charged pDNA in the core of the polyplexes based on a noncharged polymer (pHPMA) and the presence of negative FA groups at the surface of the polyplex. pHP-His-PEG-FA decationized polyplexes also prepared at an N/P of 4 and an His/P of 2 were significantly smaller (80±3 nm) than those based on pHP-PEG-FA (139±5 nm). Introduction of HisMA in the core of the polyplexes thus resulted in the formation of more condensed polyplexes, most likely due to the higher hydrophobicity of the core of polyplexes, since polyplexes where formed at pH 8.5 at which the imidazole groups of HisMA are virtually uncharged resulting in a hydrophobic polymer. The zeta potential of -8±2 mV for pHP-His-PEG-FA decationized polyplexes was close

to that of pHP-PEG-FA polyplexes, demonstrating a low degree of protonation of His groups at pH 7.4 due to their pKa of 6.5. Co-complexation of pHDP-PEG-FA and pHis at N/His/P ratio of 4/2 to prepare pHP-PEG-FA/pHis polyplexes resulted in polyplexes with a diameter of 151±7 nm and a zeta potential of -7±1 mV, which shows that initial complexation at pH 5.5 followed by crosslinking at pH 7.1 and decationization at pH 8.5 allowed the preparation of decationzed polyplexes with similar properties as those based on pHP-PEG-FA. The relative small size and the fact that no aggregation was not observed for pHP-PEG-FA/pHis polyplexes most likely gives an indication that pHis is not free in the polyplex dispersion.

Preparation of pHP-INF7-PEG-FA decationized polyplexes at N/P of 4 resulted in polyplexes with diameter of 162±8 nm and a zeta potential of -13±3 mV. These polyplexes had a slightly greater size when compared to pHP-PEG-FA decationized polyplexes (139±5 nm). Nevertheless, grafting of the acidic peptide to pHDP-PEG-FA did not significantly affect the DNA complexation behavior of this polymer and nanosized decationized polyplexes were still obtained.

Table 2. Particle z-average diameter (Z-avg) and polydispersity index (PDI) determined by DLS, and particle zeta potential (ζ Pot), of decationized polyplexes. Results are expressed as mean±SD (n=3).

Polyplexes	N/(His)/P	DLS		Zetasizer
		Z-ave (nm)	PDI	ζ Pot (mV)
pHP-PEG-FA	4	139±5	0.16±0.01	-10±2
pHP-His-PEG-FA	4/(2)	80±3	0.11±0.01	-8±2
pHP-PEG-FA+pHis	4/(2)	151±7	0.21±0.03	-7±1
pHP-INF7-PEG-FA	4	162±8	0.19±0.02	-13±3

3.5. *In vitro* transfection and cytotoxicity

Transfection activity and cytotoxicity of the folate targeted decationized polyplexes containing pDNA encoding for firefly luciferase were evaluated using polyplexes prepared at an N/P=4 and a pDNA dose of 0.25, 1 and 3 μg per well. The transfection activity of the different FA targeted decationized polyplexes was evaluated in the presence of serum and absence of folic acid using KB cells which overexpress the folate receptor [54]. As positive control, ExGen 500 (l-PEI) based polyplexes at their optimal formulation (N/P=6, 10 μg/mL, 0.25 μg pDNA per well) were used [41]. b-PEI based polyplexes formulated at N/P=6 were used as positive control for toxicity [8, 42].

Firstly, decationized polyplexes based on pHP-His-PEG-FA or on pHP-PEG-FA/pHis block copolymer/homopolymer were evaluated for transfection activity as function of pDNA concentration using His/P ratio of 2 (Figure 4a). The efficiency was compared to that of pHP-PEG-FA polyplexes and polyplexes based on pHis (His/P of 2). Figure 4a shows that transfection activity of pHP-His-PEG-FA polyplexes was low and equal to that of polyplexes lacking imidazole buffering groups. In contrast, when KB cells were incubated with pHis based polyplexes prepared at a His/P ratio of 2, at a pDNA dose of 1 μg/well of pDNA significant luciferase expression was observed (close to ExGen level). Figure 3 shows that pHis polyplexes prepared at His/P ratio of 2 had a rather high size and poor DNA condensation capability. Most likely, in contrast to the stabilized decationized polyplexes, such polyplexes tend to aggregate and aggregation is known to contribute to high transfection efficiency *in vitro* [41]. Cytotoxicity evaluation as function of polyplex concentration (Figure 4d) revealed that introduction of His functionalities in decationized polyplexes did not interfere on the cell metabolic activity as determined by the XTT assay, even at the highest dose tested where b-PEI based polyplexes induced complete cell death. The good cytocompatibility of histidine or imidazole functionalized systems has been previously observed [26-28]. The protonation profile of the imidazole group in HisMA is particularly important, since only small percentage of imidazole groups are protonated at physiological pH [26] meaning that histidine- or imidazole-based polymers have a low charge density and are thus close to neutral at that pH. Another important aspect of the protonation behavior of pHP-His-PEG-FA and pHis (pKa 6.5) is their ability to buffer the upper endosomal pH range (pH 6–7.4). For safety reasons endosomal escape is preferred early in the endosomal pathway [44], since disruption of late endosomal/lysosomal compartments leads to protease leakage into the cytosol which can trigger apoptosis [7].

Decationized polyplexes functionalized with the endosomolytic peptide INF7, pHP-INF7-PEG-FA, were also evaluated for transfection activity as function of polyplex concentration (Figure 4b). The results show that luciferase expression was very low upon incubation of the cells with these INF7 functionalized polyplexes. Previous studies have demonstrated that functionalization of polymeric vectors with INF7 using disulfide linkages lead to improved transfection efficiency likely by inducing endosomal escape [34, 35, 53]. Such approach has been previously demonstrated to be successful for pHPMA–DMAE pDNA formulations [34], but required polyplexes prepared at high N/P ratios. Increasing N/P ratios for complex formation of decationized polyplexes can lead to increasing INF7 peptide

concentration in the formulation at a fixed pDNA dose. Figure 4c shows that at a fixed pDNA dose and with increasing the N/P to 16 a slight increase in transfection efficiency was observed for pHP-INF7-PEG-FA polyplexes, in contrast to pHP-PEG-FA polyplexes (while both polyplexes did not interfere on the relative cellular protein content). However, the observed luciferase expression was more than 2 orders of magnitude lower than ExGen at its optimal formulation, meaning that significant improvements of the transfection efficiency are still required. Cytotoxicity evaluation of pHP-INF7-PEG-FA polyplexes as function of polyplex concentration (Figure 4d) showed that the introduction of INF7 in the decationized polyplexes did not affect the cell viability in the range of doses tested. The ability of INF7 peptide to be highly lytic at endosomal pH, and not at physiological pH contributes to its safety [33]. Modification of decationized polyplexes with the membrane lytic peptide melittin was also evaluated (Figure S1, Supporting Information). The melittin peptide is highly lytic and can significantly improve transfection efficiency of polyplexes, however, its use requires careful optimization of the degree of functionalization of polyplexes and/or functionalization of its lysines with acid-reversible protecting groups, otherwise significant toxicity might be observed [37, 55]. Functionalization of pHP-PEG-FA with melittin using the same degree of functionalization of INF7 containing polyplexes, induced almost complete cell death upon incubation of the cells with a polyplex dose of 1 μg pDNA (Figure S1, Supporting Information). Due to the significant cell death no conclusions could be drawn weather melittin peptide can realistically be used to yield more efficient decationzed polyplexes.

In contrast to other polymeric gene delivery systems, introduction of compounds in the polyplexes with buffering capacity in the endosomal pH range or endosomolytic peptides did not result in a significant increase in transfection efficiency. Transfection efficiency of polymeric vectors with endosomal escaping ability might be strongly influenced by the polymer architecture as well as the degree of functionalization, either by groups with buffering capacity or by endosomolytic peptides [28, 44, 45, 55-57]. Tuning further the buffering capacity and pKa of polymers used for polyplexes preparation might have substantial effect on the transfection activity [58], as e.g. demonstrated by methylation of imidazole groups of poly(L-histidine) [59]. Establishment of the optimal polymer architecture used for decationized polyplexes can lead to more efficient transfection. Nevertheless, to understand the true requirements of decationized polyplexes, studying their intracellular trafficking is also essential. For example, polyplexes decorated with FA can be internalized through a caveolar pathway, and the formed caveolae are primarily pH-neutral

organelles which do not necessary lead to lysosomal trafficking [7]. Such route would most likely hamper the mechanism of action of imidazole containing polymers [44]. Chloroquine, which has been shown to improve transfection efficiency of decationized polyplexes, has an apparent broader mechanism of action, acting not only on endosomes but can also interact with pDNA altering its physico-chemical properties [15]. Introduction of a functionalization that mimics the mechanism of action of chloroquine [60] is an important alternative approaches to be considered.

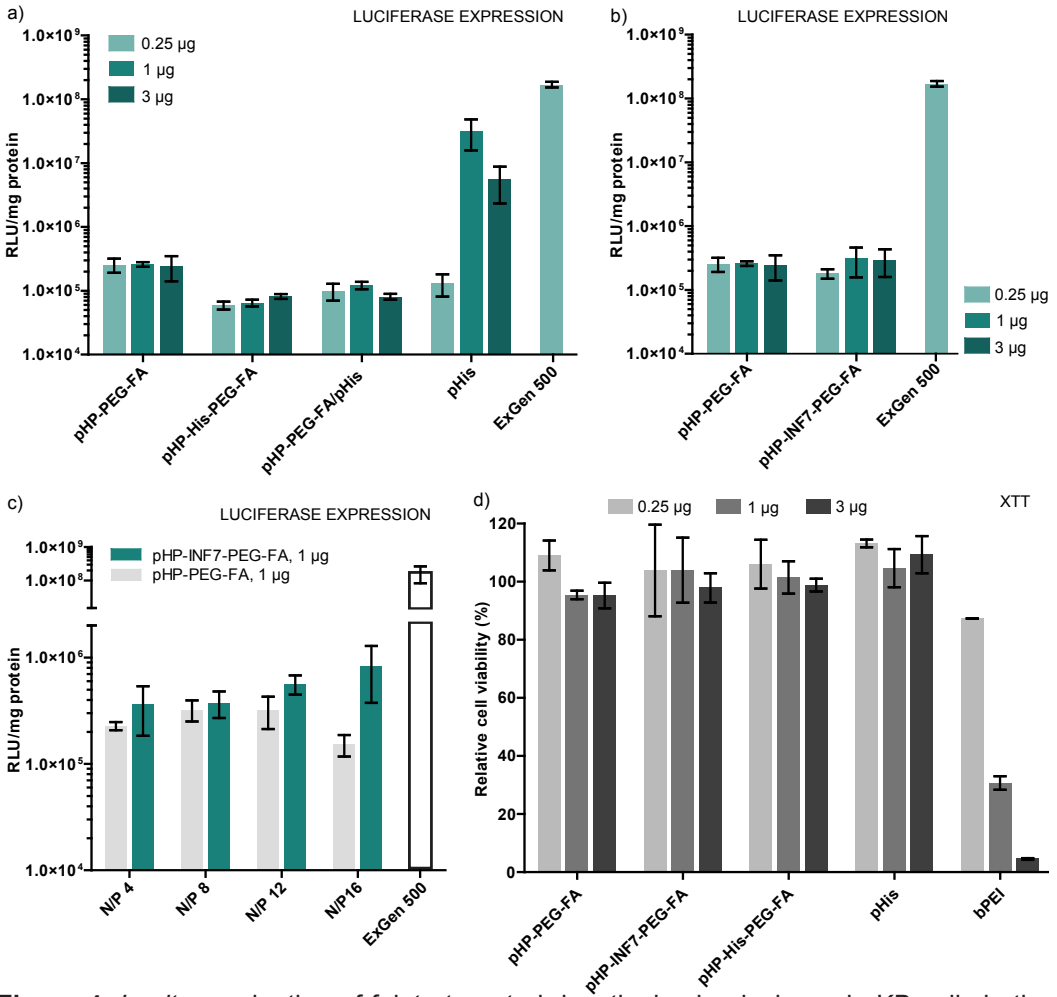

Figure 4. *In vitro* evaluation of folate targeted decationized polyplexes in KB cells in the presence of 10% FBS. Effect of pDNA dose (0.25, 1 and 3 µg of pDNA/well) on luciferase transgene expression by pHP-PEG-FA, pHP-His-PEG-FA, pHP-PEG-FA/pHis and pHis polyplexes (N/P=4, (His)/P=2) (a). Effect of pDNA dose (0.25, 1 and 3 µg of pDNA/well) (b) and N/P for complexation (1 µg of pDNA/well) (c) on luciferase transgene expression by pHP-PEG-FA and pHP-INF7-PEG-FA. Effect of pDNA dose (0.25, 1 and 3 µg of pDNA/well) on cell viability upon treatment with decationized polyplexes (N/P=4, (His)/P=2) (d). Results are expressed as mean±SD (n = 3).

4. CONCLUSION

Different copolymers were synthesized to prepare folate targeted decationized polyplexes with possible endosomal escaping functionalities. The pHis and pHDP-His-PEG-FA polymers with imidazole functionalities allowed buffering ability of these polymers at endosomal pH. However, folate targeted decationized polyplexes based on pHP-His-PEG-FA and pHP-PEG-FA/pHis, when evaluated for transfection efficiency in KB cells overexpressing FA receptor, did not show a significant improvement of transfection activity for both polyplexes. Functionalization of folate targeted decationized polyplexes with the endosomolytic peptide INF7 resulted only in a slight increase of transfection with increasing polymer-peptide concentration, yet below the levels required for an effective system.

Understanding the intracellular trafficking of decationized polyplexes and optimization of the polymer architecture and properties should be performed to increase transfection efficiency of this system.

ACKNOWLEDGMENT

L. Novo was financially supported by Fundação para a Ciência e a Tecnologia (FCT), the Portuguese Foundation for Science and Technology, grant SFRH/BD/47085/2008.

APPENDIX A. SUPPORTING INFORMATION

Supplementary Method S1 and Figure S1 can be found in Supporting Information.

References

[1] F.J. Verbaan, C. Oussoren, C.J. Snel, D.J.A. Crommelin, W.E. Hennink, G. Storm, Steric stabilization of poly(2-(dimethylamino)ethyl methacrylate)-based polyplexes mediates prolonged circulation and tumor targeting in mice, J. Gene Med., 6 (2004) 64-75.

[2] M. Ogris, S. Brunner, S. Schuller, R. Kircheis, E. Wagner, PEGylated DNA/transferrin-PEI complexes: reduced interaction with blood components, extended circulation in blood and potential for systemic gene delivery, Gene Ther., 6 (1999) 595-605.

[3] M. Harada-Shiba, K. Yamauchi, A. Harada, I. Takamisawa, K. Shimokado, K. Kataoka, Polyion complex micelles as vectors in gene therapy – pharmacokinetics and in vivo gene transfer, Gene Ther., 9 (2002) 407-414.

[4] H.K. de Wolf, C.J. Snel, F.J. Verbaan, R.M. Schiffelers, W.E. Hennink, G. Storm, Effect

of cationic carriers on the pharmacokinetics and tumor localization of nucleic acids after intravenous administration, Int. J. Pharm., 331 (2007) 167-175.

[5] D. Oupický, M. Ogris, K.A. Howard, P.R. Dash, K. Ulbrich, L.W. Seymour, Importance of lateral and steric stabilization of polyelectrolyte gene delivery vectors for extended systemic circulation, Mol. Ther., 5 (2002) 463-472.

[6] R. Duncan, The dawning era of polymer therapeutics, Nat. Rev. Drug Discov., 2 (2003) 347-360.

[7] L. Parhamifar, A.K. Larsen, A.C. Hunter, T.L. Andresen, S.M. Moghimi, Polycation cytotoxicity: a delicate matter for nucleic acid therapy-focus on polyethylenimine, Soft Matter, 6 (2010) 4001-4009.

[8] O.M. Merkel, A. Beyerle, B.M. Beckmann, M. Zheng, R.K. Hartmann, T. Stöger, T.H. Kissel, Polymer-related off-target effects in non-viral siRNA delivery, Biomaterials, 32 (2011) 2388-2398.

[9] L. Novo, E.V.B. van Gaal, E. Mastrobattista, C.F. van Nostrum, W.E. Hennink, Decationized crosslinked polyplexes for redox-triggered gene delivery, J. Control. Release, 169 (2013) 246-256.

[10] L. Novo, E. Mastrobattista, C.F. van Nostrum, W.E. Hennink, Targeted decationized polyplexes for cell specific gene delivery, Bioconjug. Chem., 25 (2014) 802-812.

[11] M.H. Lee, Z. Yang, C.W. Lim, Y.H. Lee, S. Dongbang, C. Kang, J.S. Kim, Disulfide-cleavage-triggered chemosensors and their biological applications, Chem. Rev., 113 (2013) 5071-5109.

[12] F. Meng, W.E. Hennink, Z. Zhong, Reduction-sensitive polymers and bioconjugates for biomedical applications, Biomaterials, 30 (2009) 2180-2198.

[13] D.S. Manickam, J. Li, D.A. Putt, Q.-H. Zhou, C. Wu, L.H. Lash, D. Oupický, Effect of innate glutathione levels on activity of redox-responsive gene delivery vectors, J. Control. Release, 141 (2010) 77-84.

[14] M.A. Wolfert, L.W. Seymour, Chloroquine and amphipathic peptide helices show synergistic transfection in vitro, Gene Ther., 5 (1998) 409-414.

[15] J. Cheng, R. Zeidan, S. Mishra, A. Liu, S.H. Pun, R.P. Kulkarni, G.S. Jensen, N.C. Bellocq, M.E. Davis, Structure−function correlation of chloroquine and analogues as transgene expression enhancers in nonviral gene delivery, J. Med. Chem., 49 (2006) 6522-6531.

[16] M.A. Mintzer, E.E. Simanek, Nonviral vectors for gene delivery, Chem. Rev., 109 (2008) 259-302.

[17] M.A.E.M. Aa, U.S. Huth, S.Y. Häfele, R. Schubert, R.S. Oosting, E. Mastrobattista, W.E. Hennink, R. Peschka-Süss, G.A. Koning, D.J.A. Crommelin, Cellular uptake of cationic polymer-DNA complexes via caveolae plays a pivotal role in gene transfection in COS-7 cells, Pharm. Res., 24 (2007) 1590-1598.

[18] Z. Yang, G. Sahay, S. Sriadibhatla, A.V. Kabanov, Amphiphilic block copolymers enhance cellular uptake and nuclear entry of polyplex-delivered DNA, Bioconjug. Chem., 19 (2008) 1987-1994.

[19] D. Vercauteren, J. Rejman, T.F. Martens, J. Demeester, S.C. De Smedt, K. Braeckmans, On the cellular processing of non-viral nanomedicines for nucleic acid delivery: Mechanisms and methods, J. Control. Release, 161 (2012) 566-581.

[20] Y. Wang, L. Huang, A window onto siRNA delivery, Nat. Biotechnol., 31 (2013) 611-612.

[21] O. Boussif, F. Lezoualc'h, M.A. Zanta, M.D. Mergny, D. Scherman, B. Demeneix, J.P. Behr, A versatile vector for gene and oligonucleotide transfer into cells in culture and in vivo: polyethylenimine, Proc. Natl. Acad. Sci. U.S.A., 92 (1995) 7297-7301.

[22] A. Akinc, M. Thomas, A.M. Klibanov, R. Langer, Exploring polyethylenimine-mediated DNA transfection and the proton sponge hypothesis, J. Gene Med., 7 (2005) 657-663.

[23] A.M. Funhoff, C.F. van Nostrum, G.A. Koning, N.M.E. Schuurmans-Nieuwenbroek, D.J.A. Crommelin, W.E. Hennink, Endosomal escape of polymeric gene delivery complexes is not always enhanced by polymers buffering at low pH, Biomacromolecules, 5 (2003) 32-39.

[24] W.-C. Tseng, T.-Y. Fang, L.-Y. Su, C.-H. Tang, Dependence of transgene expression and the relative buffering capacity of dextran-grafted polyethylenimine, Mol. Pharmaceutics, 2 (2005) 224-232.

[25] C. Pichon, C. Gonçalves, P. Midoux, Histidine-rich peptides and polymers for nucleic acids delivery, Adv. Drug Deliv. Rev., 53 (2001) 75-94.

[26] D. Putnam, C.A. Gentry, D.W. Pack, R. Langer, Polymer-based gene delivery with low cytotoxicity by a unique balance of side-chain termini, Proc. Natl. Acad. Sci. U.S.A., 98 (2001) 1200-1205.

[27] S. Luo, R. Cheng, F. Meng, T.G. Park, Z. Zhong, Water soluble poly(histamine acrylamide) with superior buffer capacity mediates efficient and nontoxic in vitro gene transfection, J. Polym. Sci. A Polym. Chem., 49 (2011) 3366-3373.

[28] M.L. Read, S. Singh, Z. Ahmed, M. Stevenson, S.S. Briggs, D. Oupický, L.B. Barrett, R. Spice, M. Kendall, M. Berry, J.A. Preece, A. Logan, L.W. Seymour, A versatile reducible polycation-based system for efficient delivery of a broad range of nucleic acids, Nucleic Acids Res., 33 (2005) e86.

[29] K.-L. Chang, Y. Higuchi, S. Kawakami, F. Yamashita, M. Hashida, Efficient gene transfection by histidine-modified chitosan through enhancement of endosomal escape, Bioconjug. Chem., 21 (2010) 1087-1095.

[30] A. Aied, U. Greiser, A. Pandit, W. Wang, Polymer gene delivery: overcoming the obstacles, Drug Discovery Today, 18 (2013) 1090-1098.

[31] J. Hoyer, I. Neundorf, Peptide vectors for the nonviral delivery of nucleic acids, Acc. Chem. Res., 45 (2012) 1048-1056.

[32] J.G. Schellinger, J.A. Pahang, J. Shi, S.H. Pun, Block copolymers containing a hydrophobic domain of membrane-lytic peptides form micellar structures and are effective gene delivery agents, ACS Macro Lett., 2 (2013) 725-730.

[33] C. Plank, B. Oberhauser, K. Mechtler, C. Koch, E. Wagner, The influence of endosome-disruptive peptides on gene transfer using synthetic virus-like gene transfer systems, J. Biol. Chem., 269 (1994) 12918-12924.

[34] A.M. Funhoff, C.F. van Nostrum, M.C. Lok, J.A.W. Kruijtzer, D.J.A. Crommelin, W.E. Hennink, Cationic polymethacrylates with covalently linked membrane destabilizing peptides as gene delivery vectors, J. Control. Release, 101 (2005) 233-246.

[35] D. Finsinger, J.S. Remy, P. Erbacher, C. Koch, C. Plank, Protective copolymers for nonviral gene vectors: synthesis, vector characterization and application in gene delivery, Gene Ther., 7 (2000) 1183-1192.

[36] C. Dohmen, D. Edinger, T. Fröhlich, L. Schreiner, U. Lächelt, C. Troiber, J. Rädler, P. Hadwiger, H.-P. Vornlocher, E. Wagner, Nanosized multifunctional polyplexes for receptor-mediated siRNA delivery, ACS Nano, 6 (2012) 5198-5208.

[37] M. Meyer, A. Philipp, R. Oskuee, C. Schmidt, E. Wagner, Breathing life into polycations: Functionalization with pH-responsive endosomolytic peptides and polyethylene glycol enables siRNA delivery, J. Am. Chem. Soc., 130 (2008) 3272-3273.

[38] D.R. Grassetti, J.F. Murray, Determination of sulfhydryl groups with 2,2'- or 4,4'-dithiodipyridine, Arch. Biochem. Biophys., 119 (1967) 41-49.

[39] X. Jiang, A. van der Horst, M. van Steenbergen, N. Akeroyd, C. van Nostrum, P. Schoenmakers, W. Hennink, Molar-mass characterization of cationic polymers for gene delivery by aqueous size-exclusion chromatography, Pharm. Res., 23 (2006) 595-603.

[40] Z. Zhong, J. Feijen, M.C. Lok, W.E. Hennink, L.V. Christensen, J.W. Yockman, Y.-H. Kim, S.W. Kim, Low molecular weight linear polyethylenimine-b-poly(ethylene glycol)-b-polyethylenimine triblock copolymers: Synthesis, characterization, and in vitro gene transfer properties, Biomacromolecules, 6 (2005) 3440-3448.

[41] E.V.B. van Gaal, R. van Eijk, R.S. Oosting, R.J. Kok, W.E. Hennink, D.J.A. Crommelin, E. Mastrobattista, How to screen non-viral gene delivery systems in vitro?, J. Control. Release, 154 (2011) 218-232.

[42] S.M. Moghimi, P. Symonds, J.C. Murray, A.C. Hunter, G. Debska, A. Szewczyk, A two-stage poly(ethylenimine)-mediated cytotoxicity: implications for gene transfer/therapy, Mol. Ther., 11 (2005) 990-995.

[43] J.W. Wiseman, C.A. Goddard, D. McLelland, W.H. Colledge, A comparison of linear and branched polyethylenimine (PEI) with DCChol/DOPE liposomes for gene delivery to epithelial cells in vitro and in vivo, Gene Ther., 10 (2003) 1654-1662.

[44] J. Shi, J.G. Schellinger, R.N. Johnson, J.L. Choi, B. Chou, E.L. Anghel, S.H. Pun, Influence of histidine incorporation on buffer capacity and gene transfection efficiency of HPMA-co-oligolysine brush polymers, Biomacromolecules, 14 (2013) 1961-1970.

[45] U. Lächelt, P. Kos, F.M. Mickler, A. Herrmann, E.E. Salcher, W. Rödl, N. Badgujar, C. Bräuchle, E. Wagner, Fine-tuning of proton sponges by precise diaminoethanes and histidines in pDNA polyplexes, Nanomedicine, (2013).

[46] I. Richard, M. Thibault, G. De Crescenzo, M.D. Buschmann, M. Lavertu, Ionization behavior of chitosan and chitosan–DNA polyplexes indicate that chitosan has a similar capability to induce a proton-sponge effect as PEI, Biomacromolecules, 14 (2013) 1732-1740.

[47] E.S. Lee, K. Na, Y.H. Bae, Super pH-sensitive multifunctional polymeric micelle, Nano Lett., 5 (2005) 325-329.

[48] R.J. Christie, K. Miyata, Y. Matsumoto, T. Nomoto, D. Menasco, T.C. Lai, M. Pennisi, K. Osada, S. Fukushima, N. Nishiyama, Y. Yamasaki, K. Kataoka, Effect of polymer structure on micelles formed between siRNA and cationic block copolymer comprising thiols and amidines, Biomacromolecules, 12 (2011) 3174-3185.

[49] G.T. Zugates, D.G. Anderson, S.R. Little, I.E.B. Lawhorn, R. Langer, Synthesis of poly(β-amino ester)s with thiol-reactive side chains for DNA delivery, J. Am. Chem. Soc., 128 (2006) 12726-12734.

[50] M.H. Stenzel, Bioconjugation using thiols: Old chemistry rediscovered to connect polymers with nature's building blocks, ACS Macro Lett., 2 (2012) 14-18.

[51] L. Wong, C. Boyer, Z. Jia, H.M. Zareie, T.P. Davis, V. Bulmus, Synthesis of versatile thiol-reactive polymer scaffolds via RAFT polymerization, Biomacromolecules, 9 (2008) 1934-1944.

[52] J.-H. Ryu, S. Jiwpanich, R. Chacko, S. Bickerton, S. Thayumanavan, Surface-functionalizable polymer nanogels with facile hydrophobic guest encapsulation capabilities, J. Am. Chem. Soc., 132 (2010) 8246-8247.

[53] C. Dohmen, T. Frohlich, U. Lachelt, I. Rohl, H.-P. Vornlocher, P. Hadwiger, E. Wagner, Defined folate-PEG-siRNA conjugates for receptor-specific gene silencing, Mol. Ther. Nucleic Acids, 1 (2012) e7.

[54] K.A. Mislick, J.D. Baldeschwieler, J.F. Kayyem, T.J. Meade, Transfection of folate-polylysine DNA complexes: Evidence for lysosomal delivery, Bioconjug. Chem., 6 (1995) 512-515.

[55] J.G. Schellinger, J.A. Pahang, R.N. Johnson, D.S.H. Chu, D.L. Sellers, D.O. Maris, A.J. Convertine, P.S. Stayton, P.J. Horner, S.H. Pun, Melittin-grafted HPMA-oligolysine based copolymers for gene delivery, Biomaterials, 34 (2013) 2318-2326.

[56] H. Wei, L.R. Volpatti, D.L. Sellers, D.O. Maris, I.W. Andrews, A.S. Hemphill, L.W. Chan, D.S.H. Chu, P.J. Horner, S.H. Pun, Dual responsive, stabilized nanoparticles for efficient in vivo plasmid delivery, Angew. Chem. Int. Ed. Engl., 52 (2013) 5377-5381.

[57] H. Uchida, K. Miyata, M. Oba, T. Ishii, T. Suma, K. Itaka, N. Nishiyama, K. Kataoka, Odd–even effect of repeating aminoethylene units in the side chain of N-substituted polyaspartamides on gene transfection profiles, J. Am. Chem. Soc., 133 (2011) 15524-15532.

[58] S.A. Chew, M.C. Hacker, A. Saraf, R.M. Raphael, F.K. Kasper, A.G. Mikos, Altering amine basicities in biodegradable branched polycationic polymers for nonviral gene delivery, Biomacromolecules, 11 (2010) 600-609.

[59] S. Asayama, T. Kumagai, H. Kawakami, Synthesis and characterization of methylated poly(L-histidine) to control the stability of its siRNA polyion complexes for RNAi, Bioconjug. Chem., 23 (2012) 1437-1442.

[60] S.E. Andaloussi, T. Lehto, I. Mager, K. Rosenthal-Aizman, Oprea, II, O.E. Simonson, H. Sork, K. Ezzat, D.M. Copolovici, K. Kurrikoff, J.R. Viola, E.M. Zaghloul, R. Sillard, H.J. Johansson, F. Said Hassane, P. Guterstam, J. Suhorutsenko, P.M. Moreno, N. Oskolkov, J. Halldin, U. Tedebark, A. Metspalu, B. Lebleu, J. Lehtio, C.I. Smith, U. Langel, Design of a peptide-based vector, PepFect6, for efficient delivery of siRNA in cell culture and

systemically in vivo, Nucleic Acids Res., 39 (2011) 3972-3987.

APPENDIX A.

SUPPORTING INFORMATION

Methods

S1. Melittin functionalized pHP-PEG-FA decationized polyplexes (pHP-PEG-FA/Mel)

The preparation of decationized polyplexes functionalized with *melittin* was essentially done according to the described method in section 2.4.2 with, small changes. In order to prepare polyplexes with N/P ratio 4 and final pDNA concentration of 50 µg/mL, 70 µL of polymer solutions of pHDP-PEG-FA (0.93 mg/mL), was mixed by vortexing with 140 µL pDNA solution (75 µg/mL) in 10 mM HEPES also containing 10 mM TAPS pH 8.5 at room temperature. Next, the polyplexes were crosslinked with DODT, using half molar equivalent of DODT thiol groups to PDS groups of the polymer. Polyplex dispersions were incubated for 1 h at pH 8.5. After crosslinking, 9 nmol cysteine-modified melittin peptide (Mel), dissolved in N_2 purged HBS buffer (1 mg/mL), was added to the polyplex dispersion in order to react with the remaining 50% PDS groups via thiol-disulfide exchange reaction. After 1 h at room temperature, polyplexes where decationized and prepared for testing as described in section 2.4.2.

Supporting Figures

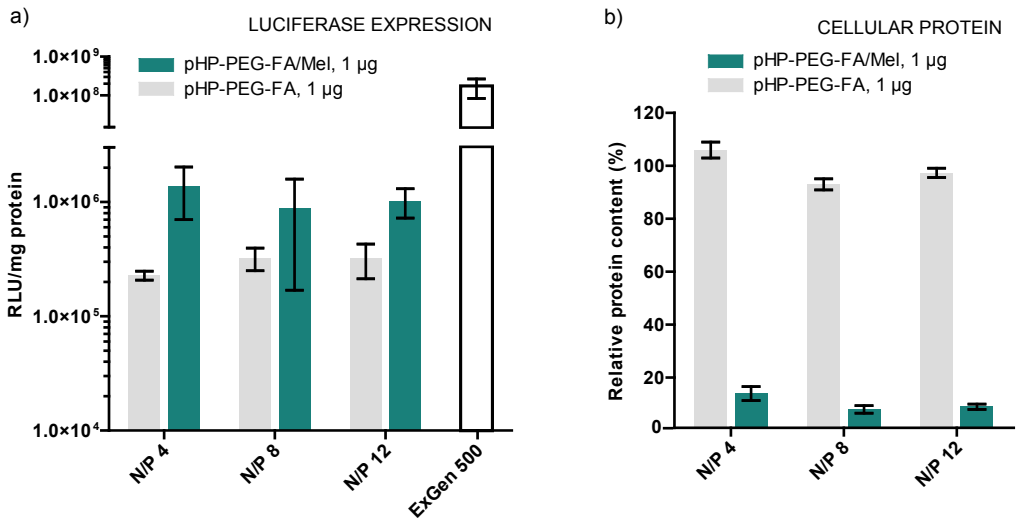

Figure S1. *In vitro* evaluation of folate targeted decationized polyplexes in KB cells in the presence of 10% FBS. Effect of functionalization of pHP-PEG-FA decationized polyplexes with melittin peptide (pHP-PEG-FA/Mel) and N/P for complexation (1 µg of pDNA/well) on luciferase transgene expression (a) or on the relative cell viability given by the relative protein content determined by µBCA assay (b). Results are expressed as mean±SD (n = 3).

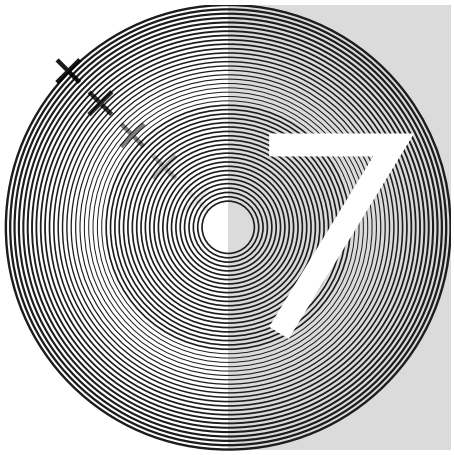

CHAPTER 7

Summary and perspectives

1. SUMMARY

Gene therapy holds great promise for the treatment or prevention of intractable diseases. The great majority of gene therapy modalities require the use of a safe and efficient gene delivery vectors. Due to their natural ability to introduce foreign DNA into cells, viral vectors have been mainly used in gene therapy clinical applications so far. However, the serious safety risks associated with viral vectors (e.g. massive immune reactions, possible insertional mutagenesis) have increasingly directed the focus of gene delivery vector development to nonviral vectors. Within the nonviral vectors, polymers are of special interest due to their chemical and structural flexibility, meaning that upon optimization polymeric systems can exhibit desired functional properties. Consequently, polymeric vectors can be used as potential safer alternatives to viral vectors for a great variety of gene therapy applications.

In **Chapter 1** a general introduction of gene therapy is given. This chapter describes the current applications and modalities of gene therapy as well as the identified barriers for successful clinical application of gene therapy using polymeric vectors. Conventional polymeric gene delivery systems are based on cationic polymers, which can form nanosized particles with nucleic acids by electrostatic interactions. However, the clinical applicability of these systems is significantly restricted due to their high toxicity mainly due the cationic nature of the polymers, leading to intolerable cellular toxicity. Furthermore, targeted therapies using systemic administration require long-circulating systems. However, polyplexes preparation requires the use of an excess of cationic charges, which significantly hampers the *in vivo* circulation half-life, limiting the accumulation in the target site. Current strategies have been focusing on the stabilization of polycationic vectors by shielding the polyplexes with hydrophilic polymers such as PEG, which have resulted in the prevention of the most catastrophic events from cationic polyplex instability. Nevertheless, i*n vivo* efficiency primary requirement is polyplex accumulation into target tissues, and the improvements on circulation half-lives given by PEG stabilization are still inadequate, which limits efficient target accumulation.

Given the problems associated with the use of polycationic systems for targeted gene therapy in **Chapter 2** we described a method to prepare a novel class of polymeric gene delivery systems, the **decationized polyplexes**, which unlike conventional polyplexes, are based on neutral polymers. Decationized polyplexes were prepared by the transient presence cationic groups coupled

to the polymer backbone to allow electrostatic driven condensation with pDNA. After condensation polyplexes were stabilized by interchain disulfide crosslinking and finally the unnecessary labile cationic groups were removed by hydrolysis (**decationization**), yielding neutral polymer-based polyplexes with intracellularly triggered DNA release without adversely affecting the high DNA loading capacity of the conventional cationic systems. The structure of decationized polyplexes consists of a core of disulfide crosslinked poly(hydroxypropyl methacrylamide) (pHPMA), in which pDNA is entrapped, and a shell of poly(ethylene glycol) (PEG). The formed polyplexes had a size of ~120 nm and a slightly negative zeta-potential (~-5mV) together with very good colloidal stability. The expected ability of polyplexes to exclusively disassemble intracellularly was demonstrated by forced introduction of the polyplexes into the cytosol of HeLa cells by electroporation, which resulted in a high level of expression of the reporter gene. Additionally, the excellent safety profile of decationized polyplexes showed no interference on the cellular cell viability (given by neutral red assay) or metabolic activity (given by XTT assay) as well as and no induced membrane destabilization (determined by LDH assay) at any of the doses tested. Furthermore, decationized polyplexes, due to lack of cationic charge, showed a low degree of non-specific uptake, which is an important property to achieve highly specific for targeted therapies.

In order to demonstrate the importance of the latter property, in **Chapter 3** folate targeted disulfide crosslinked decationized polyplexes were developed. The strategy for the preparation of targeted decationized polyplexes consisted of incorporating the folate molecule in the PEG end of the cationic block copolymer used for the preparation of the cationic precursor of decationzed polyplexes. This strategy allowed the direct preparation of decationized polyplexes decorated with folate molecules exposed on the PEG shell with similar biophysical properties as the untargeted system. *In vitro* evaluation of folate targeted decationized polyplexes in folate receptor overexpressing cell lines (HeLa and OVCAR-3) showed significantly higher cellular uptake of folate targeted decationized polyplexes, when compared to their non-targeted counterparts. On the contrary, for a cell line (A549) that did not express the folate receptor similar uptake was observed for both targeted and non-targeted decationized polyplexes. As expected, in the case of the cationic polyplexes (disulfide crosslinked polyplexes without decationization), a high degree of nonspecific uptake was observed in all cell lines tested. Transfection studies using OVCAR-3 cells showed higher transfection efficiency for folate-targeted polyplexes. Furthermore, when the medium was saturated with free folic acid, transfection of

folate targeted decationized polyplexes was almost completely blocked, meaning that transfection is mainly driven by receptor mediated endocytosis.

The high degree of nonspecific uptake of polycationic systems contributes to their short *in vivo* circulation half-lives, as well as high degree of undesired accumulation in off-target tissues for systemic applications. The use of decationized polyplexes *in vivo*, with demonstrated low degree of non-specific uptake *in vitro*, was hypothesized to possess improved *in vivo* circulation half-lives, biodistribution and safety profile. This hypothesis was demonstrated in **Chapter 4.** Firstly, the *in vivo* applicability of decationized polyplexes for systemic administration was evaluated by determining the stability of Cy5-labeled decationzed polyplexes in human plasma using fluorescence single particle tracking (fSPT), in which a stable size distribution was observed for 48 h. The safety profile of decationized polyplexes was determined by incubation of the free polymers that form the decationized polyplexes with HUVEC cells, and MTT assay showed excellent cytocompatibility of the neutral polymers. The safety of the polymers was further demonstrated by an *in vivo* zebrafish assay, where a remarkable low teratogenicity and mortality profile was found for the neutral polymer, in great contrast with its cationic counterpart. Near-infrared (NIR) dye-labeled polyplexes were finally evaluated for their biodistribution and tumor accumulation by noninvasive optical imaging when administered systemically in A431 tumor bearing mice. Decationized polyplexes exhibited an increased circulation time and higher tumor accumulation, when compared to their cationic precursors. Furthermore, histological analysis of tumors sections showed that decationized polyplexes were able to induced reporter transgene expression *in vivo*.

The clear advantages given by decationized polyplexes, such as safety, stability, improved *in vivo* circulation half-life as well as the ability to specifically interact with target cells and rapidly disassemble and release their cargo upon cell uptake are important properties not only for pDNA therapies, but also for siRNA or mRNA gene therapy modalities as well. Consequently in **Chapter 5** we expanded the applicability of decationized polyplexes for siRNA delivery. Given the fact that siRNA has <1/100 the length of pDNA, and stiff backbone structure, siRNA complexation and retention in decationized polyplexes required optimization of the carrier system, particularly the crosslink density of the core of the polyplexes. By increasing the crosslinking density of polyplexes stable nanosized folate targeted decationized polyplexes encapsulating siRNA were successfully prepared. Stability evaluation in human plasma by fluorescence correlation spectroscopy (FCS)

demonstrated that even upon incubation in biological fluids, a significant fraction of siRNA remained stability entrapped in the decationized polyplexes. When evaluated *in vitro* in a folate receptor overexpressing cell line stably expressing luciferase, Skov3-luc, a dose-dependent sequence specific gene silencing was observed. Importantly, introduction of higher crosslink density in the decationized polyplexes has not influenced their safety profile. Even though further optimization of decationized polyplexes is required we have demonstrated their potential application as a platform for the different nucleic acid therapies.

One of the most important aspects to optimize in the decationized polyplexes is their efficiency. *In vitro* studies (Chapters 2, 3 and 5) have shown that decationized polyplexes alone possess low transfection efficiency, most likely due to lack of endosomal escaping ability. In **Chapter 6** we describe 2 different strategies to introduce endosomal escaping functionalities to improve efficiency without significantly compromising the safety profile of folate targeted decationized polyplexes: incorporation in the polyplexes of imidazole groups with buffering capacity at endosomal pH; and functionalization of decationized polyplexes with the endosomolytic peptide INF7. Both strategies did not result however in significant improvements of the *in vitro* transfection efficiency of folate targeted decationized polyplexes. Cytotoxicity evaluation by XTT assay revealed both strategies for functionalization of decationized polyplexes did not introduce significant changes of their safety profile. Results showed that optimization of decationized polyplexes or exploration of other 'endosomal escape' strategies must be tested to improve the transfection efficiency of decationzed polyplexes.

2. FUTURE PERSPECTIVES

2.1. Towards efficient decationzed polyplexes

A major concern for applicability of decationized polyplexes is related to their efficiency. In Chapter 6 it was shown that introduction of functional groups in the polyplexes with buffering capacity in the endosomal pH range or endosomolytic peptides did not result in a significant improvement of their transfection efficiency. It is known that transfection efficiency of polymeric vectors with endosomal escaping is strongly influenced by the polymer architecture [1-5]. For example, multi-block alignment of the different functionalities might be an important option to improve

transfection efficiency [6, 7]. The chemical and structural flexibility of polymeric systems allows, in principle, the preparation of desired architectures in a well-defined manner.

Other strategies to improve polyplex endosomal escape of decationized polyplexes without significantly affecting their safety profile is the incorporation of pH sensitive polyacids [8], that can be finely tuned to possess membrane disrupting ability at endosomal pH. Given the fact that decationized polyplexes have shown improved transfection in the presence of chloroquine, incorporation of peptides functionalized with derivatives of chloroquine [9] or direct incorporation of chloroquine analogs into de polymer can potentially improve transfection efficiency of decationized polyplexes, allowing the applicability of the chloroquine principle for *in vivo* applications.

One of the reasons for efficient *in vitro* transfection of certain cationic polymers is due to their membrane disruptive properties, which can be directly direct involved on the nuclear the nuclear localization of DNA, meaning that polycations may also be capable of disrupting the nuclear envelope [10]. In order to decationized polyplexes maintain their safety profile they must lack the ability to disrupt membranes at physiological pH, which could lead to severe cellular toxicity. However, incorporating nuclear transport functionalities into decationized polyplexes, to allow transport of pDNA into the nucleus seems essential to improve their transfection efficiency. For example, histones [11], short peptide sequences [12] or the trisaccharide maltotriose [13], could be easily incorporated or covalently linked to into decationized polyplexes to improve nuclear localization without changing their safety profile as previously observed for other nonviral vectors that have used these strategies.

Incorporation of PEG into polyplexes has demonstrated enormous advantages for *in vivo* stability of polyplexes. Simultaneously, PEGylation has shown to directly hamper transfection efficiency PEGyated nanoparticles. Therefore the preparation of polyplexes with detachable PEG has led to significant improvements on the transfection efficiency of polyplexes when compared to their counterparts with non-detachable PEG. The use of acid labile linkers [14-16] for PEG detachment inside the endosomes, and disulfide linkers [17-19] for detachment upon cell entry, have resulted on several orders of magnitude higher transfection degree both *in vitro* and *in vivo*.

Decationized polyplexes have demonstrated their potential for siRNA delivery. However, in Chapter 5, complete siRNA retention in the polyplexes when exposed to human plasma was not achieved. Structural design improvements of decationized polyplexes could be introduced to allow complete siRNA retention, for example by using core-shell interface crosslinking. Furthermore, for full of siRNA retention, strategies can be directed to siRNA itself, by multimerization of siRNA via disulfide linkages [20, 21] or by preparation of polymer-siRNA [22] and endosomolytic peptide-siRNA conjugates [23]. Such strategies can improve not only the siRNA retention but the silencing efficiency as well.

2.2. Further improvement on the *in vivo* performance

The *in vivo* evaluation of decationized polyplexes in Chapter 4 have demonstrated that removal of cationic charges from polyplex systems, indeed results in improved circulation half-life and biodistribution. Given the safety profile of decationized polyplexes, follow-up studies should be performed focusing on increasing doses and transgene expression kinetics, as well as exploring the *in vivo* performance of decationized polyplexes decorated with the desired targeting ligands [24]. The chemical flexibility of decationized polyplexes potentially allows a straightforward polymer functionalization before (Chapter 3) and after (Chapter 4 and 6) polymerization, which can be chosen depending on the chemical stability of the functionality.

Nevertheless, structural optimization might be required for further improvements on *in vivo* performance of decationized polyplexes. The i*n vivo* performance of nanoparticles is strongly dependent on PEG molecular weight and density [25, 26]. Optimization of such parameters, is essential to maximize the decationized polyplex circulation half-life and *in vivo* performance.

Another possible structural optimization consists in increasing the hydrophobicity of the core of polyplexes. It was found that introduction of hydrophobic groups into polyplexes did not only increase the stability but also resulted in a substantial increase of the circulation half-life [27]. Introduction of the hydrophobic monomer butyl methacrylate (BMA) has the additional advantage to also give tuned pH-dependent membrane disruptive behavior for endosomal escape to polyplexes.

2.3. Integration with other technologies

Gene therapies without homeostasis disruption might require highly specific spatiotemporal controllable systems. The use of pDNA incorporating specific promoters allows the selective transcription in tissues or different cancer cell types. In the case of RNA therapeutics such specificity cannot be generated, unless shRNA approach is used. Other promoters allow temporal control upon external stimuli, this is the case of heat-inducible promoter heat shock protein promoter (HSP70) [28, 29].

In order to provide decationized polyplexes with spatiotemporal control over transgene expression, an interesting approach would require the integration of iron oxide (IO) magnetic nanoparticles. Such approach could be achieved by grafting the polymer into IO magnetic nanoparticles to form polyplexes [30]. The superparamagnetic properties of IO are used as magnetic resonance imaging (MRI) contrast allowing for noninvasive *in situ* monitoring of polyplex accumulation [31]. However, from a therapeutic point of view IO nanoparticles can also be used to generate a heat inducible gene expression system [32]. IO nanoparticles absorb energy and generate heat in response to an alternating magnetic field (AMF). Magnetic fields, unlike most of external stimuli, can penetrate deeply into tissues, and AMF applicators can be used to control gene expression by heating IO nanoparticles *in vivo* [32]. Hyperthermia alone can be used to induce cell death, however, depending on the treatment such effect might undesirable. In that case, hyperthermia can be used to control and generate gene expression without tissue damage [33]. Furthermore, heating of magnetic nanoparticles can be used to permeabilize endosomes and lysosomes [34], which can directly assist in endosomal escape of decationized polyplexes and generate spaciotemporal control over RNA therapeutics as well.

2.4. Critical perspective and conclusion

Gene therapy is now considered a field of research with great promises but little clinical progress. Particularly, safety issues of both viral and non-viral vectors have hampered the clinical progress of gene delivery. In this thesis we describe a new polymeric gene delivery system which aims to overcome most of the safety concerns of polymeric gene delivery systems and at the same time introduce improvements on the *in vivo* performance for targeted gene therapies for both

DNA and RNA therapies.

Our results have shown that there are still several aspects that can be optimized in the decationized polyplexes. However, it should be noted that gene therapy research field is highly multidisciplinary area where progress is dependent not only on the development of safe and efficient gene delivery carriers but also on progresses of cellular and molecular biology, chemistry, medicine and technology. Indeed important advances have been obtained also in those areas. Strategies like engineering pDNA to possess long-term expression have already been identified and evaluated [35]. Polymers can now be synthesized with well-defined structures and architectures [36, 37]. Polyplexes with several functionalities can now be prepared in automated systems with very high reproducibility [38]. Microfluidic systems for have been developed to better reproduce the *in vivo* conditions that nanoparticles face for a better translation into *in vivo* [39]. Integrating the best technologies available is very challenging, but future research should make efforts to integrate the most recent advances in the different disciplines to really understand where we stand now in the field of gene therapy.

The truth might be that the realization of the classical gene therapy concept by substituting a defective gene to achieve a complete permanent cure might still be far, however, the use of gene therapy as alternative or in synergy with conventional treatments may be a future reality [40, 41], for example, despite of all the barriers for efficient polymeric gene delivery, some promising systems have already proven their *in vivo* therapeutic efficacy upon systemic administration [42-44]. Hopefully, an increasing number of innovative systems with added therapeutic benefit will be reported, including systems integrating the decationzed polyplex concept.

References

[1] J. Shi, J.G. Schellinger, R.N. Johnson, J.L. Choi, B. Chou, E.L. Anghel, S.H. Pun, Influence of histidine incorporation on buffer capacity and gene transfection efficiency of HPMA-co-oligolysine brush polymers, Biomacromolecules, 14 (2013) 1961-1970.

[2] H. Wei, L.R. Volpatti, D.L. Sellers, D.O. Maris, I.W. Andrews, A.S. Hemphill, L.W. Chan, D.S.H. Chu, P.J. Horner, S.H. Pun, Dual responsive, stabilized nanoparticles for efficient in vivo plasmid delivery, Angew. Chem. Int. Ed. Engl., 52 (2013) 5377-5381.

[3] U. Lächelt, P. Kos, F.M. Mickler, A. Herrmann, E.E. Salcher, W. Rödl, N. Badgujar, C. Bräuchle, E. Wagner, Fine-tuning of proton sponges by precise diaminoethanes and histidines in pDNA polyplexes, Nanomedicine, (2013).

[4] H. Uchida, K. Miyata, M. Oba, T. Ishii, T. Suma, K. Itaka, N. Nishiyama, K. Kataoka, Odd–even effect of repeating aminoethylene units in the side chain of N-substituted polyaspartamides on gene transfection profiles, J. Am. Chem. Soc., 133 (2011) 15524-15532.

[5] M.L. Read, S. Singh, Z. Ahmed, M. Stevenson, S.S. Briggs, D. Oupický, L.B. Barrett, R. Spice, M. Kendall, M. Berry, J.A. Preece, A. Logan, L.W. Seymour, A versatile reducible polycation-based system for efficient delivery of a broad range of nucleic acids, Nucleic Acids Res., 33 (2005) e86.

[6] S. Fukushima, K. Miyata, N. Nishiyama, N. Kanayama, Y. Yamasaki, K. Kataoka, PEGylated polyplex micelles from triblock catiomers with spatially ordered layering of condensed pDNA and buffering units for enhanced intracellular gene delivery, J. Am. Chem. Soc., 127 (2005) 2810-2811.

[7] K. Miyata, M. Oba, M. Kano, S. Fukushima, Y. Vachutinsky, M. Han, H. Koyama, K. Miyazono, N. Nishiyama, K. Kataoka, Polyplex micelles from triblock copolymers composed of tandemly aligned segments with biocompatible, endosomal escaping, and DNA-condensing functions for systemic gene delivery to pancreatic tumor tissue, Pharm. Res., 25 (2008) 2924-2936.

[8] B.B. Lundy, A. Convertine, M. Miteva, P.S. Stayton, Neutral polymeric micelles for RNA delivery, Bioconjug. Chem., 24 (2013) 398-407.

[9] S.E. Andaloussi, T. Lehto, I. Mager, K. Rosenthal-Aizman, Oprea, II, O.E. Simonson, H. Sork, K. Ezzat, D.M. Copolovici, K. Kurrikoff, J.R. Viola, E.M. Zaghloul, R. Sillard, H.J. Johansson, F. Said Hassane, P. Guterstam, J. Suhorutsenko, P.M. Moreno, N. Oskolkov, J. Halldin, U. Tedebark, A. Metspalu, B. Lebleu, J. Lehtio, C.I. Smith, U. Langel, Design of a peptide-based vector, PepFect6, for efficient delivery of siRNA in cell culture and systemically in vivo, Nucleic Acids Res., 39 (2011) 3972-3987.

[10] G. Grandinetti, A.E. Smith, T.M. Reineke, Membrane and nuclear permeabilization by polymeric pDNA vehicles: Efficient method for gene delivery or mechanism of cytotoxicity?, Mol. Pharmaceutics, 9 (2011) 523-538.

[11] K.M. Wagstaff, D.J. Glover, D.J. Tremethick, D.A. Jans, Histone-mediated transduction as an efficient means for gene delivery, Mol. Ther., 15 (2007) 721-731.

[12] W.-J. Yi, J. Yang, C. Li, H.-Y. Wang, C.-W. Liu, L. Tao, S.-X. Cheng, R.-X. Zhuo, X.-Z. Zhang, Enhanced nuclear import and transfection efficiency of TAT peptide-based gene delivery systems modified by additional nuclear localization signals, Bioconjug. Chem., 23 (2011) 125-134.

[13] H. Akita, T. Masuda, T. Nishio, K. Niikura, K. Ijiro, H. Harashima, Improving in vivo hepatic transfection activity by controlling intracellular trafficking: The function of GALA and maltotriose, Mol. Pharmaceutics, 8 (2011) 1436-1442.

[14] V. Knorr, L. Allmendinger, G.F. Walker, F.F. Paintner, E. Wagner, An acetal-based PEGylation reagent for pH-sensitive shielding of DNA polyplexes, Bioconjug. Chem., 18 (2007) 1218-1225.

[15] C. Fella, G.F. Walker, M. Ogris, E. Wagner, Amine-reactive pyridylhydrazone-based PEG reagents for pH-reversible PEI polyplex shielding, Eur. J. Pharm. Sci., 34 (2008) 309-320.

[16] G.F. Walker, C. Fella, J. Pelisek, J. Fahrmeir, S. Boeckle, M. Ogris, E. Wagner, Toward synthetic viruses: endosomal pH-triggered deshielding of targeted polyplexes greatly enhances gene transfer in vitro and in vivo, Mol. Ther., 11 (2005) 418-425.

[17] C. Zhu, M. Zheng, F. Meng, F.M. Mickler, N. Ruthardt, X. Zhu, Z. Zhong, Reversibly shielded DNA polyplexes based on bioreducible PDMAEMA-SS-PEG-SS-PDMAEMA triblock copolymers mediate markedly enhanced nonviral gene transfection, Biomacromolecules, 13 (2012) 769-778.

[18] M. Kumagai, S. Shimoda, R. Wakabayashi, Y. Kunisawa, T. Ishii, K. Osada, K. Itaka, N. Nishiyama, K. Kataoka, K. Nakano, Effective transgene expression without toxicity by intraperitoneal administration of PEG-detachable polyplex micelles in mice with peritoneal dissemination, J. Control. Release, 160 (2012) 542-551.

[19] S. Takae, K. Miyata, M. Oba, T. Ishii, N. Nishiyama, K. Itaka, Y. Yamasaki, H. Koyama, K. Kataoka, PEG-detachable polyplex micelles based on disulfide-linked block catiomers as bioresponsive nonviral gene vectors, J. Am. Chem. Soc., 130 (2008) 6001-6009.

[20] S.-Y. Lee, M.S. Huh, S. Lee, S.J. Lee, H. Chung, J.H. Park, Y.-K. Oh, K. Choi, K. Kim, I.C. Kwon, Stability and cellular uptake of polymerized siRNA (poly-siRNA)/polyethylenimine (PEI) complexes for efficient gene silencing, J. Control. Release, 141 (2010) 339-346.

[21] H. Mok, S.H. Lee, J.W. Park, T.G. Park, Multimeric small interfering ribonucleic acid for highly efficient sequence-specific gene silencing, Nat. Mater., 9 (2010) 272-278.

[22] H. Takemoto, A. Ishii, K. Miyata, M. Nakanishi, M. Oba, T. Ishii, Y. Yamasaki, N. Nishiyama, K. Kataoka, Polyion complex stability and gene silencing efficiency with a siRNA-grafted polymer delivery system, Biomaterials, 31 (2010) 8097-8105.

[23] C. Dohmen, D. Edinger, T. Fröhlich, L. Schreiner, U. Lächelt, C. Troiber, J. Rädler, P. Hadwiger, H.-P. Vornlocher, E. Wagner, Nanosized multifunctional polyplexes for receptor-mediated siRNA delivery, ACS Nano, 6 (2012) 5198-5208.

[24] S.Y. Wong, J.M. Pelet, D. Putnam, Polymer systems for gene delivery—Past, present, and future, Progress in Polymer Science, 32 (2007) 799-837.

[25] Q. Yang, S.W. Jones, C.L. Parker, W.C. Zamboni, J.E. Bear, S.K. Lai, Evading immune cell uptake and clearance requires PEG grafting at densities substantially exceeding the minimum for brush conformation, Mol. Pharmaceutics, 11 (2014) 1250-1258.

[26] T.A. Tockary, K. Osada, Q. Chen, K. Machitani, A. Dirisala, S. Uchida, T. Nomoto, K. Toh, Y. Matsumoto, K. Itaka, K. Nitta, K. Nagayama, K. Kataoka, Tethered PEG crowdedness determining shape and blood circulation profile of polyplex micelle gene carriers, Macromolecules, 46 (2013) 6585-6592.

[27] C.E. Nelson, J.R. Kintzing, A. Hanna, J.M. Shannon, M.K. Gupta, C.L. Duvall, Balancing cationic and hydrophobic content of PEGylated siRNA polyplexes enhances endosome escape, stability, blood circulation time, and bioactivity in vivo, ACS Nano, 7 (2013) 8870-8880.

[28] E.V.B. van Gaal, W.E. Hennink, D.J.A. Crommelin, E. Mastrobattista, Plasmid engineering for controlled and sustained gene expression for nonviral gene therapy, Pharm. Res., 23 (2006) 1053-1074.

[29] Q. Huang, J.K. Hu, F. Lohr, L. Zhang, R. Braun, J. Lanzen, J.B. Little, M.W. Dewhirst, C.-Y. Li, Heat-induced gene expression as a novel targeted cancer gene therapy strategy, Cancer Res., 60 (2000) 3435-3439.

[30] F.M. Kievit, O. Veiseh, C. Fang, N. Bhattarai, D. Lee, R.G. Ellenbogen, M. Zhang, Chlorotoxin labeled magnetic nanovectors for targeted gene delivery to glioma, ACS Nano, 4 (2010) 4587-4594.

[31] N. Hijnen, S. Langereis, H. Grüll, Magnetic resonance guided high-intensity focused ultrasound for image-guided temperature-induced drug delivery, Adv. Drug Deliv. Rev., 72 (2014) 65-81.

[32] M. Yamaguchi, A. Ito, A. Ono, Y. Kawabe, M. Kamihira, Heat-inducible gene expression system by applying alternating magnetic field to magnetic nanoparticles, ACS Synth. Biol, 3 (2013) 273-279.

[33] R. Deckers, B. Quesson, J. Arsaut, S. Eimer, F. Couillaud, C.T.W. Moonen, Image-guided, noninvasive, spatiotemporal control of gene expression, Proc. Natl. Acad. Sci. U.S.A., 106 (2009) 1175-1180.

[34] M. Domenech, I. Marrero-Berrios, M. Torres-Lugo, C. Rinaldi, Lysosomal membrane permeabilization by targeted magnetic nanoparticles in alternating magnetic fields, ACS Nano, 7 (2013) 5091-5101.

[35] D.J. Glover, H.J. Lipps, D.A. Jans, Towards safe, non-viral therapeutic gene expression in humans, Nat. Rev. Genet., 6 (2005) 299-310.

[36] M. Ahmed, R. Narain, Progress of RAFT based polymers in gene delivery, Progress in Polymer Science, 38 (2013) 767-790.

[37] E. Wagner, Polymers for siRNA delivery: Inspired by viruses to be targeted, dynamic, and precise, Acc. Chem. Res., 45 (2011) 1005-1013.

[38] H. Wang, K. Liu, K.-J. Chen, Y. Lu, S. Wang, W.-Y. Lin, F. Guo, K.-i. Kamei, Y.-C. Chen, M. Ohashi, M. Wang, M.A. Garcia, X.-Z. Zhao, C.K.F. Shen, H.-R. Tseng, A rapid pathway toward a superb gene delivery system: Programming structural and functional diversity into a supramolecular nanoparticle library, ACS Nano, 4 (2010) 6235-6243.

[39] P.M. Valencia, O.C. Farokhzad, R. Karnik, R. Langer, Microfluidic technologies for accelerating the clinical translation of nanoparticles, Nat Nano, 7 (2012) 623-629.

[40] J. Li, Y. Wang, Y. Zhu, D. Oupický, Recent advances in delivery of drug–nucleic acid combinations for cancer treatment, J. Control. Release, 172 (2013) 589-600.

[41] S.L. Ginn, I.E. Alexander, M.L. Edelstein, M.R. Abedi, J. Wixon, Gene therapy clinical trials worldwide to 2012 – an update, J. Gene Med., 15 (2013) 65-77.

[42] Q. Chen, K. Osada, T. Ishii, M. Oba, S. Uchida, T.A. Tockary, T. Endo, Z. Ge, H. Kinoh, M.R. Kano, K. Itaka, K. Kataoka, Homo-catiomer integration into PEGylated polyplex micelle from block-catiomer for systemic anti-angiogenic gene therapy for fibrotic pancreatic tumors, Biomaterials, 33 (2012) 4722-4730.

[43] J. Zhou, J. Liu, C.J. Cheng, T.R. Patel, C.E. Weller, J.M. Piepmeier, Z. Jiang, W.M. Saltzman, Biodegradable poly(amine-co-ester) terpolymers for targeted gene delivery, Nat. Mater., 11 (2012) 82-90.

[44] R.J. Christie, Y. Matsumoto, K. Miyata, T. Nomoto, S. Fukushima, K. Osada, J. Halnaut, F. Pittella, H.J. Kim, N. Nishiyama, K. Kataoka, Targeted polymeric micelles for siRNA treatment of experimental cancer by intravenous injection, ACS Nano, 6 (2012) 5174-5189.

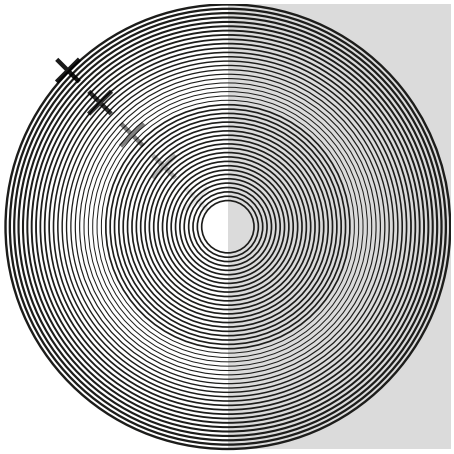

APPENDICES

NEDERLANDSE SAMENVATTING

Gentherapie is een veelbelovende toepassing voor de behandeling of preventie van slecht te behandelen ziekten. De meeste vormen van gentherapie vereisen het gebruik van veilige en efficiënte vectoren voor de genafgifte. Voor klinische toepassingen zijn tot op heden voornamelijk virale vectoren gebruikt, vanwege hun natuurlijke vermogen om vreemd DNA in cellen te introduceren. Deze virale vectoren gaan echter gepaard met ernstige bijwerkingen (bijvoorbeeld sterke immuunreacties en mogelijke insertiemutagenese), waardoor de focus steeds meer verschuift naar niet-virale vectoren voor genafgifte. Binnen de niet-virale vectoren zijn polymeren in het bijzonder interessant vanwege hun chemische en structurele flexibiliteit, waardoor polymeersystemen na optimalisatie de gewenste functionele eigenschappen kunnen vertonen. Polymeer gebaseerde vectoren kunnen daarom gebruikt worden als mogelijk veiliger alternatief voor veel verschillende toepassingen van gentherapie.

In **hoofdstuk 1** wordt een algemene introductie in gentherapie gegeven. Dit hoofdstuk beschrijft de huidige toepassingen en vormen van gentherapie, als ook de bekende obstakels voor de succesvolle klinische toepassing via polymere vectoren. De conventionele polymere genafgiftesystemen zijn gebaseerd op kationogene polymeren, welke nanodeeltjes vormen met nucleïnezuren door middel van elektrostatische interacties. De klinische toepasbaarheid van deze systemen is echter aanzienlijk beperkt door de hoge toxiciteit, die voornamelijk voortkomt uit de hoge mate van cellulaire toxiciteit vanwege de kationogene aard van de polymeren. Daarnaast zijn systemen nodig die lang circuleren in de bloedbaan voor gerichte therapie na systemische toediening. Om polyplexen te maken is echter een overmaat van kationogene ladingen nodig. Dit leidt tot een beduidend lagere *in vivo* circulatie-halfwaardetijd, waardoor de accumulatie in het doelweefsel beperkt is. Momenteel focust men zich vooral op het stabiliseren van de polykationogene vectoren door het afschermen van de polyplexen met hydrofiele polymeren zoals polyethyleenglycol (PEG). Dit heeft geresulteerd in het verminderen van de meest rampzalige gevolgen van instabiliteit van kationogene polyplexen. Desalniettemin zijn de verbeteringen in de circulatie-halfwaardetijd door PEG-stabilisatie nog steeds onvoldoende, waardoor de efficiënte accumulatie in het doelweefsel beperkt wordt.

Vanwege de problemen die verbonden zijn aan het gebruik van polykationogene

systemen voor gerichte genafgifte, beschrijven wij in **hoofdstuk 2** een methode om een nieuwe klasse van polymere genafgiftesystemen te creëren. Dit zijn de **gedekationiseerde polyplexen**, die in tegenstelling tot conventionele polyplexen gebaseerd zijn op neutrale polymeren. Gedekationiseerde polyplexen werden bereid met behulp van polymeren voorzien van kationogene groepen waardoor elektrostatisch gedreven condensatie met pDNA mogelijk was. Na condensatie werden de polyplexen gestabiliseerd door disulfidebruggen tussen de ketens aan te brengen. Tot slot werden de kationogene groepen verwijderd via hydrolyse (‘**dekationisatie’**), waarna polyplexen van neutrale polymeren overbleven die getriggerde intracellulaire DNA-afgifte vertonen zonder de hoge DNA laadcapaciteit van de conventionele kationogene systemen te verlagen. De structuur van gedekationiseerde polyplexen bestaat uit een kern van poly(hydroxypropyl methacrylamide) (pHPMA), aan elkaar verbonden via disulfide bruggen, waarin het pDNA ingesloten zit, en een schil van PEG. De gevormde polyplexen hadden een grote van ~ 120 nm, een geringe negatieve zeta-potentiaal (~ -5 mV) en een zeer goede kolloïdale stabiliteit. Het verwachte vermogen van de polyplexen om uitsluitend intracellulair uiteen te vallen werd aangetoond door het geforceerd inbrengen van de polyplexen in het cytoplasma van HeLA cellen door elektroporatie, wat resulteerde in een hoge mate van expressie van het reporter gen. Daarnaast hadden de gedekationiseerde polyplexen in alle geteste doseringen geen negatieve invloed op de overleving van de cellen (neutral red assay), noch op de metabole activiteit (XTT assay), en ze induceerden ook geen membraan destabilisatie (bepaald via LDH assay). Het gebrek aan kationogene ladingen leidde bovendien tot weinig niet-specifieke opname, een belangrijke eigenschap voor het bereiken van zeer specifiek gerichte therapie.

Om te laten zien hoe belangrijk deze laatstgenoemde eigenschap is, werden in **hoofdstuk 3** gedekationiseerde polyplexen met disulfide bruggen gemaakt en voorzien van folaatgroepen voor doelgerichte therapie. De folaatgroepen werden gekoppeld aan de PEG-uiteinden van de kationogene blokcopolymeren die gebruikt werden voor de bereiding van de kationogene precursor van de gedekationiseerde polyplexen. Deze methode maakte de directe bereiding mogelijk van gedekationiseerde polyplexen met folaatmoleculen op de PEG schil die dezelfde biofysische eigenschappen vertoonden als het niet-doelgerichte systeem. Tijdens *in vitro* experimenten met de folaatgerichte gedekationiseerde polyplexen in cellijnen met overexpressie van de folaatreceptor (HeLA en OVCAR-3) werden deze deeltjes significant meer opgenomen door de cellen dan

hun niet-gerichte tegenhangers. Daarentegen vertoonden de gerichte en niet-doelgerichte systemen dezelfde opname in een cellijn (A549) die de folaatreceptor niet bezit. Zoals verwacht werd in alle cellijnen een hoge mate van niet-specifieke opname waargenomen voor de kationogene polyplexen (d.w.z. polyplexen met disulfide verbindingen zonder dekationisatie). Verder is de transfectie bestudeerd in OVCAR-3 cellen. Hierbij vertoonden folaatgefunctionaliseerde polyplexen een efficiëntere transfectie. Bovendien werd de transfectie van gedekationiseerde folaat-polyplexen bijna volledig geremd wanneer het medium was verzadigd met vrij foliumzuur, wat betekent dat de transfectie voornamelijk een gevolg is van receptorgemedieerde endocytose.

De hoge mate van niet-specifieke opname van de polykationogene systemen resulteert in een relatief korte *in vivo* circulatie-halfwaardetijd en in veel ongewenste accumulatie in andere weefsels dan het doelweefsel. Gedekationiseerde polyplexen daarentegen vertoonden *in vitro* een lage mate van niet-specifieke opname. Daarom was de hypothese dat deze deeltjes *in vivo* een betere circulatie-halfwaardetijd en biodistributie zouden vertonen en daarnaast ook een beter veiligheidsprofiel. Deze hypothese werd gedemonstreerd in **hoofdstuk 4**. Ten eerste werd de toepasbaarheid van gedekationiseerde polyplexen voor systemische toediening *in vivo* geëvalueerd. Dit werd gedaan door bepaling van de stabiliteit van Cy5-gelabelde gedekationiseerde polyplexen in humaan plasma via *fluorescence single particle tracking* (fSPT). Hierbij werd een stabiele verdeling van de deeltjesgrootte gezien gedurende 48 uur. Verder werd het veiligheidsprofiel van de gedekationiseerde polyplexen vastgesteld door HUVEC-cellen te incuberen met de vrije polymeren die deze polyplexen vormen. Een MTT assay liet zien dat de neutrale polymeren een uitstekende celcompatibiliteit vertonen. Vervolgens werd de veiligheid van de polymeren ook aangetoond in een *in vivo* test in zebravissen, waar een opmerkelijk lage teratogeniciteit en mortaliteit werden gevonden voor het neutrale polymeer, dit in sterke tegenstelling tot zijn kationogene tegenhanger. Tot slot werd via niet-invasieve optische beeldvorming gekeken naar de biodistributie en tumor accumulatie van nabij-infrarood (NIR) gelabelde polyplexen na systemische toediening in muizen met A431 tumoren. De gedekationiseerde polyplexen vertoonden een langere circulatietijd en meer tumoraccumulatie in vergelijking met hun kationogene precursors. Bovendien bleek uit histologische analyse van de tumorsecties dat de gedekationiseerde polyplexen *in vivo* de expressie van een reportergen induceerden.

De gedekationiseerde polyplexen hebben duidelijk voordelen zoals veiligheid,

stabiliteit en verbeterde *in vivo* circulatie-halfwaardetijd, als ook het vermogen tot specifieke interacties met doelcellen en het feit dat ze bij opname in cellen snel uiteenvallen en hun ingesloten pDNA afgeven. Dit zijn niet alleen belangrijke eigenschappen voor pDNA therapie, maar ook voor gentherapie met siRNA of mRNA. Daarom onderzochten we de toepasbaarheid van gedekationiseerde polyplexen in **hoofdstuk 5** uit voor afgifte van siRNA. siRNA heeft een lengte die 1/100 kleiner is dan die van pDNA en heeft daarnaast een starre hoofdketen. Daarom is voor complexvorming met siRNA en retentie in gedekationiseerde polyplexen een optimalisatie van dit afgiftesysteem nodig, in het bijzonder de dichtheid van het netwerk in de kern van de polyplexen. Door het aantal netwerkverbindingen te verhogen, werden stabiele, met siRNA beladen nanodeeltjes vervaardigd van folaatgefunctionaliseerde gedekationiseerde polyplexen. Evaluatie van de stabiliteit in humaan plasma met behulp van 'fluorescentie correlatie microscopie' (FCS) toonde aan dat zelfs na incubatie in biologische vloeistoffen een aanzienlijk deel van het siRNA stabiel ingesloten bleef in de gedekationiseerde polyplexen. Tijdens *in vitro* studies in een cellijn met overexpressie van de folaatreceptor en stabiele luciferase expressie (Skov3-luc) werd een dosisafhankelijke sequentie-specifieke gen-inactivering waargenomen. Het is belangrijk op te merken dat de verhoging van de netwerkdichtheid geen invloed had op het veiligheidsprofiel. Ook al is verdere optimalisatie van de gedekationiseerde polyplexen nodig, we hebben aangetoond dat ze potentie hebben te dienen als platform voor verschillende vormen van nucleïnezuurtherapie.

De efficiëntie van gedekationiseerde polplexen moet nog worden geoptimaliseerd. *In vitro* studies (hoofdstuk 2, 3 en 5) toonden aan dat gedekationiseerde polyplexen als zodanig weinig efficiënt zijn, waarschijnlijk doordat de deeltjes in onvoldoende mate uit endosomen ontsnappen. In **hoofdstuk 6** beschrijven wij twee verschillende strategieën met als doel om ontsnapping uit de endosomen te bewerkstelligen, en daarmee de efficiëntie van gedekationiseerde polyplexen te verbeteren zonder het veiligheidsprofiel teveel aan te tasten. De eerste strategie is introductie van imidazoolgroepen in de polyplexen, met een buffer capaciteit bij endosomale pH; de tweede is de functionalisatie van gedekationiseerde polyplexen met het endosomolytische INF7-peptide. Beide methoden resulteerden echter niet in significante verbeteringen van de *in vitro* transfectie-efficiëntie van gedekationiseerde folaat-polyplexen. De cytotoxiciteit werd onderzocht met een XTT assay en voor beide strategieën werden geen significante veranderingen in het veiligheidsprofiel gezien. Deze resultaten maken duidelijk dat optimalisatie

van de gedekationiseerde polyplexen en het verkennen van andere strategieën voor endomosale ontsnapping nog moeten worden onderzocht om de transfectie-efficiëntie van gedekationiseerde polyplexen te verbeteren.

LIST OF ABBREVIATIONS

%ID	% of injected dose
2-MEA	2-mercaptoethylamine hydrochloride
2-MP	2-mercaptopyridine
ABCPA	4,4'-azobis(4-cyanovaleric acid)
ACN	acetonitrile
AIBN	azobisisobutyronitrile
AIDS	acquired immunodeficiency syndrome
AMF	alternating magnetic field
APC	allophycocyanin
APMA	*N*-(3-aminopropyl)methacrylamide hydrochloride
ATCC	American Type Culture Collection
BMA	butyl methacrylate
bp	base pairs
b-PEI	branched polyethylenimine
CDI	1,1'-carbonyldiimidazole
CMV	human cytomegalovirus promoter
Cy5-NHS	Cyanine5 NHS ester
Cy7-NHS	Cyanine7 NHS ester
DCC	N,N'-dicyclohexylcarbodiimide
DCM	dichloromethane
DCU	dicyclohexylurea
DLS	dynamic light scattering
DMAE	dimethylaminoethanol
DMAP	4-dimethylaminopyridine
DMEM	Dulbecco's modified Eagle's medium
DMF	dimethylformamide
DMSO	dimethyl sulfoxide
DODT	3,6-dioxa-1,8-octane-dithiol
DPTS	4-(dimethylamino)pyridinium 4-toluenesulfonate
E3	Endopan 3
EDTA	ethylenediaminetetraacetic acid
EGFP	enhanced green fluorescent protein
EPR	enhanced permeation and retention
EtOAc	ethylacetate
EtOH	ethanol
FA	folic acid

FBS	fetal bovine serum
FCS	fluorescence correlation spectroscopy
FITC	fluorescein isothiocyanate
FMT	fluorescence molecular tomography
FR	folate receptor
FRI	fluorescence reflectance imaging
fSPT	fluorescence single particle tracking
GBM	glomerular basement membrane
GDEPT	gene-directed enzyme pro-drug therapy
GPC	gel permeation chromatography
HA	Influenza haemagglutinin
HBS	HEPES buffered saline
HER2	human epidermal growth factor receptor 2
HisMA	*N*-(2-(1H-imidazol-4-yl)ethyl)methacrylamide
HIV	human immunodeficiency virus
HPMA–DMAE	carbonic acid 2-dimethylamino-ethyl ester 1-methyl-2-(2-methacryloyl-amino)-ethyl ester
HPMAm	*N*-(2-Hydroxypropyl)methacrylamide
hpf	hours post-fertilization
HSP70	heat shock protein promoter 70
IO	iron oxide
LDH	lactate dehydrogenase
l-PEI	linear polyethylenimine
Mel	cysteine-modified melittin peptide
MEM	minimum essential medium
miRNA	microRNA
Mn	number average molecular weight
MP	multi-purpose
MPS	mononuclear phagocyte system
MRI	magnetic resonance imaging
MTT	3-(4,5-dimethylthiazol-2-yl)-2,5-diphenyltetrazolium bromide
Mw	weight average molecular weight
MWCO	molecular weight cut-off
NaOAc	sodium acetate
NH4Ac	ammonium acetate
NHS	*N*-hydroxysuccinimide
NIR	near-infrared
NIR	near infrared
NLS	nuclear localization signal

NMR	nuclear magnetic resonance
NTA	nanoparticle tracking analysis
p.i.	post-injection
PAsp(DET)	poly(*N*-(*N*-(2-aminoethyl)-2-aminoethyl)aspartamide)
PBA	phosphate buffered albumin
PBS	phosphate buffered saline
PDI	polydispersity index
pDNA	plasmid DNA
PDS	pyridyl disulfide
PDTEA•HCl	2-(Pyridyldithio)-Ethylamine Hydrochloride
PDTEMA	*N*-[2-(2-pyridyldithio)]ethyl methacrylamide
PEG	poly(ethylene glycol)
PEI	polyethylenimine
PEO	poly(ethylene oxide)
pHis	poly(histamine methacrylamide)
pHPMA	poly(hydroxypropyl methacrylamide)
PMS	N-methyl dibenzopyrazine methylsulfate
RGD	arginylglycylaspartic acid
RISC	RNA-induced silencing complex
RLU	relative light units
RNAi	RNA interference
RO	reverse osmosis
ROI	region of interest
RPMI	Roswell Park Memorial Institute
SCID	severe combined immunodeficiency
shRNA	short hairpin RNA
siRNA	small interfering RNA
TAE	tris-acetate-EDTA
TAPS	3-[[1,3-dihydroxy-2-(hydroxymethyl)propan-2-yl]amino]propane-1-sulfonic acid
t-Boc	di-tert-butyl dicarbonate
TCEP	tris(2-carboxyethyl)phosphine
TFA	trifluoroacetic acid
THF	tetrahydrofuran
TLC	thin layer chromatography
TNBSA	(2,4,6-trinitrobenzene sulfonic acid)
TNBSA	trinitrobenzene sulfonic acid
Tris	tris(hydroxymethyl)aminomethane
UPLC	ultra high performance liquid chromatography

XTT	2,3-bis(2-methoxy-4-nitro-5-sulfophenyl)-2H-tetrazolium-5-carboxanilide
µCT	micro-computed tomography

ACKNOWLEDGEMENT

No one achieves anything alone and this thesis would not be possible without the contributions so many of you have made. And that's why I would like to express my deepest gratitude to my colleagues, staff and supervisors with whom I spent over four years doing my research. I would like to thank you for all your constant help, support and for sharing your knowledge and ideas with me. Particularly, I would to thank Prof. Wim Hennink for giving me the opportunity to conduct my PhD at the Department of Pharmaceutics and for always trusting me and guiding me with an exceptional dedication. Also, I would like to thank my co-promotors, Dr. René van Nostrum and Dr. Enrico Mastrobattista, who have really helped me with finding out the solutions to overcome many challenges I had to face during my project. I cannot forget to mention the great collaborators I had the privilege to work with. In particular, I would like to mention my great collaboration with RWTH Aachen University, Twan Lammers, Larissa Rizzo and Susanne Golombek, as well as with Ghent University, Kevin Braeckmans and George Dakwar. Their work has decisively contributed to the success of my research project. My special thanks to the Master's students, Mariam, Tamara and Kaori, whose hard work and dedication helped to make this project a success.

When I picture myself at the time I arrived to the Netherlands, I can say that I have grown a lot personally and professionally, but my greatest achievement, the one I am the most proud of, is the number of friends I have made at the Department. You have helped me to feel like a part of a family that I could always count on.

Nothing would be possible without you (literally). Thank you for helping me going through the toughest times, making me feel respected and important. I am proud of meeting so many intelligent, kind, good people and, most importantly, people who had an incredible patience for me.

To all of you "obrigado"!

Luís

CURRICULUM VITAE

Luís Filipe Lima Novo was born on 16th of May, 1985 in Viana do Castelo, Portugal. After finishing his secondary education, in 2003, he was admitted at University of Minho for Integrated Master in Biomedical Engineering. During his 5-year Master's program he was awarded with the Scholar Merit Award for the best Biomedical Engineering student of his year, twice. His Master's research project was performed at Katholieke Universiteit Leuven, Belgium, where his work has contributed to 4 publications. In 2008, his Master thesis was awarded with magna cum laude by Katholieke Universiteit Leuven. Just after the graduation, he started his academic career – first, working at Katholieke Universiteit Leuven and later on at Warsaw Technical University, Poland. In 2009, Luís won a prestigious 'Doctoral Degree grant' from The Portuguese Foundation of Science and Technology (FCT), funding his PhD research at the Department of Pharmaceutical Sciences at Utrecht University, the Netherlands. Under the supervision of Prof. dr. Ir. W.E. Hennink, Luís focused his research on developing new polymeric gene delivery formulations and the results of this work are described in this thesis. The PhD thesis entitled "Decationized Polyplexes for Targeted Gene Delivery: from carrier design to in vivo evaluation" was defended on 20th of October, 2014.

LIST OF PUBLICATIONS

L. Novo, E.V.B. van Gaal, E. Mastrobattista, C.F. van Nostrum, W.E. Hennink, Decationized crosslinked polyplexes for redox-triggered gene delivery, J. Control. Release, 169 (2013) 246-256.

Y. Shi, M.J. van Steenbergen, E.A. Teunissen, **L. Novo**, S. Gradmann, M. Baldus, C.F. van Nostrum, W.E. Hennink, Π–Π Stacking increases the stability and loading capacity of thermosensitive polymeric micelles for chemotherapeutic drugs, Biomacromolecules, 14 (2013) 1826-1837.

L. Novo, E. Mastrobattista, C.F. van Nostrum, W.E. Hennink, Targeted decationized polyplexes for cell specific gene delivery, Bioconjug. Chem., 25 (2014) 802-812.

L. Novo, L.Y. Rizzo, S.K. Golombek, G.R. Dakwar, B. Lou, W. Jahnen-Dechent, K. Remaut, E. Mastrobattista, C.F. van Nostrum, F. Kiessling, K. Braeckmans, T. Lammers, W.E. Hennink, Decationized polyplexes as stable and safe carrier systems for improved biodistribution in systemic gene therapy, J. Control. Release, In Press (2014).

L. Novo, K.M. Takeda, T. Petteta, G.R. Dakwar, J.B. van den Dikkenberg, K. Remaut, K. Braeckmans, C.F.v. Nostrum, E. Mastrobattista, W.E. Hennink, Targeted decationized polyplexes for siRNA delivery, Submitted for publication (2014).

L. Novo, E. Mastrobattista, C.F. van Nostrum, T. Lammers, W.E. Hennink, Decationized polyplexes for gene delivery, Submitted for publication (2014).